

UNIVERSITY OF SOUTHAMPTON

FACULTY OF NATURAL AND ENVIRONMENTAL SCIENCES

School of Chemistry

Synthesis of polyfluorinated carbohydrates

by

Lucas Gilbert Quiquempoix

Thesis for the degree of Doctor of Philosophy

September 2018

UNIVERSITY OF SOUTHAMPTON

ABSTRACT

FACULTY OF NATURAL AND ENVIRONMENTAL SCIENCES

Chemistry

Thesis for the degree of Doctor of Philosophy

SYNTHESIS OF POLYFLUORINATED CARBOHYDRATES

Lucas Gilbert Quiquempoix

The impact of deoxyfluorination on fundamental properties of carbohydrates is a large topic of investigation in our group. More precisely, the insertion of polyfluorinated motifs has shown to alter lipophilicity, transport rates across red blood cells, and binding to certain receptors. As large quantities of fluorinated analogues are required for the study of these properties, as well as for other ongoing synthetic projects, convenient syntheses of polyfluorinated carbohydrates on large scale are currently being investigated. This thesis describes the successful synthesis of previously reported 2,3,4-trideoxy-2,3,4-trifluoro-D-glucopyranose and 2,3-dideoxy-2,2,3,3-tetrafluoro-D-glucopyranose.

Regarding the synthesis of the 2,3,4-trifluoroglucose, two different synthetic routes were investigated, both of which starting with the conversion of the commercial and cheap levoglucosan into its trifluorinated counterpart, then subjected to an anomeric hydrolysis procedure developed in our group which afforded the open form of the sugar.

The synthesis of 2,2,3,3-tetrafluoroglucose was achieved *via* a fluorinated building block approach relying on an intermolecular coupling reaction between D-glyceraldehyde acetonide and the 4-bromo-2,2,3,3-tetrafluorobutene. As this reaction turned out to be the most problematic when repeated in our group, extensive efforts were devoted to its optimization, this include investigation under flash flow conditions, as well as the utilization of a different protected derivative of D-glyceraldehyde.

This thesis also reports the study of intramolecular hydrogen bond (H-bond) interactions in a series levoglucosan derivatives, some of which involve fluorine atoms as H-bond acceptor. Ultimately, this study brought additional evidence of the ability of C-F bonds to compete with better H-bond acceptors such as an oxygen atom.

Table of Contents

Table of Contents	i
Table of Tables	ix
Table of Figures	xi
Academic Thesis: Declaration Of Authorship	xiiiv
Acknowledgements	xvii
Definitions and Abbreviations.....	xviix
Chapter 1: Introduction	1
1.1 Fluorinated carbohydrates: background	1
1.1.1 Carbohydrates.....	1
1.1.2 Fluorination of carbohydrates: a strategy to increase the binding affinity.	3
1.2 Influence of fluorination on adjacent functional groups.....	5
1.3 Intramolecular OH...F bonding: Background	6
1.3.1 Hydrogen bond: Definition and characteristics	6
1.3.2 Study of intramolecular OH...F interactions in solution <i>via</i> proton NMR ...	7
1.3.3 Intramolecular hydrogen bonding in fluorinated derivatives of carbohydrates	8
1.3.4 Aims and objectives	11
1.4 Fluorine NMR exchange spectroscopy of fluorinated carbohydrates transport across red blood cell membranes.....	12
1.4.1 Background	12
1.4.2 Limitations of the method	14
1.4.3 Development of an improved NMR protocol: objectives.....	15
Chapter 2: Study of intramolecular hydrogen bonds in levoglucosan derivatives ..	17
2.1 Target molecules and strategy of synthesis	17
2.2 Synthesis of 2-deoxy-, 2-deoxy-3-fluoro-, and -2,3-difluoro levoglucosan	18
2.3 Attempted synthesis of 2-deoxy-2,2-difluoro levoglucosan	19
2.4 Synthesis of 2- <i>O</i> -methoxy levoglucosan.....	20
2.5 Analysis of the target compounds	20

2.5.1	Sample preparation	20
2.5.2	Description of the C4–OH intramolecular interactions	21
2.5.3	Description of the C3–OH intramolecular interactions	23
2.5.4	Conclusions	24
Chapter 3:	Synthesis of 2,3,4-trideoxy-2,3,4-trifluoro-D-glucopyranose	25
3.1	Objectives	25
3.2	Previous syntheses of 2,3,4-trifluoro-D-glucopyranose	25
3.2.1	Synthesis from D-glyceraldehyde acetonide.....	25
3.2.2	Synthesis from butynediol	27
3.3	New strategy for the synthesis of 2,3,4-trifluoro-D-glucopyranose.....	29
3.3.1	Retrosynthetic overview.....	29
3.3.2	Retentive deoxofluorination on levoglucosan derivatives.....	30
3.4	New synthesis of 2,3,4-trifluoro-D-glucopyranose.....	31
3.4.1	Synthesis of 2,3,4-trifluoro levoglucosan <i>via</i> C3 fluorination of 2,4-difluoro levoglucosan and levoallosan	31
3.4.1.1	Synthesis of 2,4-difluoro-levoglucosan	31
3.4.1.2	Attempted C3 fluorination <i>via</i> deoxofluorination of 2,4-difluoro levoglucosan.....	36
3.4.1.3	Attempted C3 fluorination <i>via</i> triflate displacement on a 2,4- difluoro levoallosan derivatives	38
3.4.1.4	Deoxofluorination of 2,4-difluoro levoallosan	40
3.4.2	Synthesis of 2,3,4-trifluoro levoglucosan <i>via</i> the Sarda synthesis	43
3.4.2.1	Synthesis of the Černý epoxide	43
3.4.2.2	Synthesis of 2,3,4-trifluoro levoglucosan.....	44
3.4.3	Anomeric hydrolysis of the mixture 2,3,4-trifluoro levogluco and - galactosan	46
3.4.4	Anomeric hydrolysis of 2,3,4-trifluoro levoglucosan	47
3.5	Structural analysis	47
3.5.1	Study of intramolecular H-bonds in 2,4-difluoro allosan	47
3.5.2	Crystal structure of fluoro levoglucosan derivatives.....	49

3.5.3	Conformational and configurational analysis of 2,3,4-trifluoro-D-glucopyranose	49
3.6	Summary	51
Chapter 4:	Synthesis of 2,3-dideoxy-2,2,3,3-tetrafluoro-D-glucopyranose	55
4.1	Previous syntheses of 2,2,3,3-tetrafluoro-D-glucopyranose	55
4.1.1	Enantioselective syntheses proposed by the Linclau group	55
4.1.2	Diastereoselective synthesis proposed by the Konno group	57
4.2	Objectives	58
4.3	The upscaling of the Konno synthesis	59
4.4	Modifications of the Konno synthesis	61
4.4.1	Ley's aldehyde as substitute to D-glyceraldehyde acetonide	61
4.4.1.1	Synthesis of Ley's aldehyde	61
4.4.1.2	Coupling between bromo-tetrafluorobutene and Ley's aldehyde ..	62
4.4.2	Improved separation of the diastereoisomers	64
4.5	Summary	66
Chapter 5:	Introduction to alkyllithium mediated coupling under micro-flow conditions	69
5.1	Alkyllithium mediated coupling under batch conditions: scope and limitations ..	69
5.2	Alkyllithium mediated coupling under micro-flow conditions: Background	70
5.2.1	Description of micro-flow reactors	70
5.2.2	Multi-reactor setup and alkyllithium mediated couplings	71
5.2.3	Micro-flow reactor: properties and benefits	72
5.2.3.1	Micro-tube reactors	72
5.2.3.2	Micro-mixers	72
5.2.3.3	Optimisation of batch processes	73
5.3	Perfluoroalkylation under micro-flow conditions	74
5.3.1	Generation of perfluoroalkyllithium in the presence of electrophiles	74
5.3.2	Generation of perfluoroalkyllithium in the absence of electrophiles	76

Chapter 6:	Coupling between bromo-tetrafluorobutene and Ley's aldehyde under micro-flow conditions.....	79
6.1	Formation of the lithiated intermediate in the presence of Ley's aldehyde	79
6.1.1	Investigation of Yoshida's coupling conditions	79
6.1.2	Investigation of Konno's coupling conditions.....	82
6.1.3	Investigation of conditions involving a reduced excess of MeLi	84
6.1.4	Investigation of adapted conditions involving reduced excesses of Ley's aldehyde	86
6.1.5	Conclusions	87
6.2	Formation of the lithiated intermediate in the absence of Ley's aldehyde.....	88
6.2.1	Investigation of Yoshida's coupling conditions	89
6.2.2	Investigation of conditions promoting the formation of tetrafluorobutene lithium on large quantities.....	91
6.2.3	Investigation of conditions involving a different alkyl lithium reagent	94
6.2.4	Conclusion.....	96
6.3	Large scale synthesis of 4,6- <i>O</i> -benzylidene-2,2,3,3-tetrafluoro- <i>D</i> -glucose and galactose.....	97
Chapter 7:	Experimental.....	101
7.1	General conditions	101
7.2	Study of intramolecular hydrogen bonding in levoglucosan derivatives.....	102
7.2.1	Characterisation data of 1,6-Anhydro-2-deoxy-2-fluoro- β - <i>D</i> -glucopyranoside (1.26)	102
7.2.2	Characterisation data of 1,6-anhydro-2,4-dideoxy-2,4-difluoro- β - <i>D</i> -glucopyranoside (1.32)	102
7.2.3	1,6-Anhydro-2,3-dideoxy-2,3-difluoro- β - <i>D</i> -glucopyranoside (1.27).....	103
7.2.4	1,6-Anhydro-2-deoxy- β - <i>D</i> -arabino-hexopyranoside (1.28)	104
7.2.5	1,6-Anhydro-2,3-dideoxy-3-fluoro- β - <i>D</i> -arabino-hexopyranoside (1.29).	104
7.2.6	Attempted synthesis of 2-deoxy-2,2-difluoro levoglucosan (1.30).....	105
7.2.6.1	1,6-Anhydro-4- <i>O</i> -benzyl-2- <i>O</i> -(<i>p</i> -methoxybenzyl)- β - <i>D</i> -glucopyranoside (2.5).....	105

7.2.6.2	3- <i>O</i> -Acetyl-1,6-anhydro-4- <i>O</i> -benzyl-2- <i>O</i> -(<i>p</i> -methoxybenzyl)- β -D-glucopyranoside (2.8)	106
7.2.6.3	3- <i>O</i> -Acetyl-1,6-anhydro-4- <i>O</i> -benzyl- β -D-glucopyranoside (2.9)	107
7.2.6.4	3- <i>O</i> -Acetyl-1,6-anhydro-4- <i>O</i> -benzyl- β -D-arabino-hexopyranos-2-uloside (2.4)	107
7.2.6.5	3- <i>O</i> -Acetyl-2,6-anhydro-4- <i>O</i> -benzyl-2-fluoro-D-mannopyranosyl fluorides (2.10/2.11)	108
7.2.7	Synthesis of 2- <i>O</i> -methoxy levoglucosan	109
7.2.7.1	1,6-Anhydro-3,4-di- <i>O</i> -benzyl-2- <i>O</i> -(<i>p</i> -methoxybenzyl)- β -D-glucopyranoside (2.15)	109
7.2.7.2	1,6-Anhydro-3,4-di- <i>O</i> -benzyl- β -D-glucopyranoside (2.16)	110
7.2.7.3	1,6-Anhydro-3,4-di- <i>O</i> -benzyl-2- <i>O</i> -methyl- β -D-glucopyranoside (2.7)	110
7.2.7.4	1,6-Anhydro-2- <i>O</i> -methyl- β -D-glucopyranoside (1.31).....	111
7.2.8	Experimental procedure for sample preparation	112
7.3	Synthesis of 2,3,4-trideoxy,2,3,4-trifluoro-D-glucopyranose.....	112
7.3.1	Synthesis of trifluoro levoglucosan <i>via</i> deoxofluorination of 2,4-dideoxy-2,4-difluoro levoglucosan.....	112
7.3.1.1	1,6:3,4-Dianhydro-2- <i>O</i> - <i>p</i> -tolylsulfonyl- β -D-galactopyranoside (3.34)	112
7.3.1.2	1,6-Anhydro-2,4-dideoxy-2,4-difluoro- β -D-glucopyranoside (1.32) synthesised from tosyl epoxide 3.34	113
7.3.1.3	1,6-Anhydro-2,4-di- <i>O</i> - <i>p</i> -tolylsulfonyl- β -D-glucopyranoside (3.33) .	114
7.3.1.4	1,6-Anhydro-2,4-dideoxy-2,4-difluoro- β -D-glucopyranoside (1.32) synthesised from 2,4-di- <i>O</i> -tosyl levoglucosan 3.33	114
7.3.2	Synthesis of trifluoro levoglucosan <i>via</i> triflate displacement on 2,4-dideoxy-2,4-difluoro 3- <i>O</i> -(trifluoromethanesulfonyl) levoallosan	115
7.3.2.1	Oxidation of 2,4-difluoro levoglucosan (1.32).....	115
7.3.2.2	Reduction of the mixture 3.43/3.44	115
7.3.2.3	1,6-Anhydro-2,4-dideoxy-2,4-difluoro-3- <i>O</i> -(trifluoromethanesulfonyl)- β -D-allopyranoside (3.42)	117

7.3.3	Synthesis of trifluoro levoglucosan <i>via</i> deoxofluorination of 2,4-dideoxy-2,4-difluoro levoallosan	118
7.3.3.1	1,6-Anhydro-2,3,4-trideoxy-2,3,4-trifluoro- β -D-glucopyranoside (3.26)	118
7.3.4	Synthesis of trifluoro levoglucosan <i>via</i> the Sarda synthesis.....	119
7.3.4.1	1,6-Anhydro-4-O-benzyl-2-O- <i>p</i> -tolylsulfonyl- β -D-glucopyranoside (3.47)	119
7.3.4.2	1,6:2,3-Dianhydro-4-O-benzyl- β -D-mannopyranoside (2.6)	120
7.3.4.3	1,6-Anhydro-4-O-benzyl-2-deoxy-2-fluoro- β -D-glucopyranoside (3.28)	120
7.3.4.4	1,6-Anhydro-4-O-benzyl-2,3-dideoxy-2,3-difluoro- β -D-glucopyranoside (2.1).....	121
7.3.4.5	1,6-Anhydro-2,3-dideoxy-2,3-difluoro- β -D-glucopyranoside (1.27)	122
7.3.4.6	1,6-Anhydro-2,3-dideoxy-2,3-difluoro-4-O-(trifluoromethanesulfonyl)- β -D-glucopyranoside (3.48).....	122
7.3.4.7	1,6-Anhydro-4-O-benzoyl-2,3-dideoxy-2,3-difluoro- β -D-galactopyranoside (3.49).....	123
7.3.4.8	1,6-Anhydro-2,3-dideoxy-2,3-difluoro- β -D-galactopyranoside (3.50)	124
7.3.4.9	Deoxofluorination of 1,6-Anhydro-2,3-dideoxy-2,3-difluoro- β -D-galactopyranoside (3.50).....	124
7.4	Anomeric hydrolysis of the mixture 2,3,4-trideoxy-2,3,4-trifluoro levogluco and -galactosan.....	126
7.5	Synthesis of 2,3-dideoxy-2,2,3,3-tetrafluoro-D-glucopyranose	129
7.5.1	The upscaling of Konno's synthesis	129
7.5.1.1	(2R)-2,3-O-isopropylidene-D-glyceraldehyde (4.16)	129
7.5.1.2	Alkyl lithium mediated coupling between 4-bromo-3,3,4,4-tetrafluoro-but-1-ene (4.16) and D-glyceraldehyde acetonide (3.1)	129
7.5.1.3	(2R,3R)-4,4,5,5-tetrafluoro-6-hepten-1,2,3-triol (4.19)	131
7.5.1.4	(2R,3S)-4,4,5,5-tetrafluoro-6-hepten-1,2,3-triol (4.20)	132

7.5.1.5	2,3-dideoxy-2,2,3,3-tetrafluoro-D-glucopyranose (1.40)	132
7.5.1.6	2,3-dideoxy-2,2,3,3-tetrafluoro-D-galactopyranose (4.1)	133
7.5.2	Modifications of the Konno synthesis.....	134
7.5.2.1	(2R,5R,6R)-5,6-dimethoxy-5,6-dimethyl-1,4-dioxane-2-carbaldehyde (4.24).....	134
7.5.2.2	Akylolithium mediated coupling between 4-bromo-3,3,4,4- tetrafluoro-but-1-ene (4.16) and Ley's aldehyde (4.24)	135
7.5.2.3	Deprotection of the coupling adduct mixture 4.27/4.28	136
7.5.2.4	Ozonolysis of the triol mixture 4.19/4.20.....	137
7.5.2.5	Separation of tetrafluoro glucose (1.40) and galactose (4.1)	137
7.5.2.6	Deprotection of 4,6-O-benzylidene-tetrafluoroglucose (4.29)	139

Bibliography 141

Table of Tables

Table 3.1: Difluorination of tosyl epoxide 3.34	32
Table 3.2: Difluorination of 2,4-ditosyl levoglucosan 3.33	35
Table 3.3: Deoxofluorination of 2,4-difluoro levoglucosan 1.32	36
Table 3.4: Deoxofluorination of 2,4-difluoro levoallosan 3.45	41
Table 3.5: Deoxyfluorination of 2,3-difluoro levogalactosan 3.50	45
Table 4.1: Intermolecular coupling between aldehyde 3.1 and 4.16	60
Table 4.2: Intermolecular coupling between aldehyde 4.24 and 4.16	62

Table of Figures

Figure 1.1: Sugar binding pocket of a periplasmic protein with glucose 1.1 as substrate ⁴	1
Figure 1.2: Representation of hydrophobic patches on glucose 1.1 and galactose 1.2	2
Figure 1.3: Binding pocket of the <i>E. coli</i> galactose transport protein, with glucose substrate 1.1 shown in yellow, aromatic residues in blue, and polar residues in red ⁷	2
Figure 1.4: Activities of thrombin inhibitors (left), crystal structure of 1.3 in the thrombin D pocket (right).	3
Figure 1.5: Inhibition study of glycogen phosphorylase	4
Figure 1.6: Relative transport rate of hexafluorohexopyranose 1.6 across the RBC membrane..	4
Figure 1.7: UDP-galactofuranose 1.6 and its tetrafluorinated analogue 1.7	5
Figure 1.8: The effect of fluorination on pK _a s	5
Figure 1.9: Relative H-bond acidities (pK _{AH}) of conformationally locked cyclohexanol derivatives	6
Figure 1.10: ¹ J(OH,F) coupling constants measured in CDCl ₃ for the cage molecule 1.14 and the γ-fluoropropanol 1.15	7
Figure 1.11: Intramolecular O—H···F—C bond in the myo-inositol derivatives 1.16 and 1.17	8
Figure 1.12: Intramolecular H-bonds in 4-fluoro levoglucosan derivatives 1.18 to 1.21	8
Figure 1.13: Hyperconjugation between the C4—F and C3—O bonds	9
Figure 1.14: Intramolecular H-bonds in fluorinated-α-D-hexopyranosides 1.22 to 1.25	10
Figure 1.15: Levoglucosan derivatives considered for ¹ H NMR analysis	11
Figure 1.16: ¹⁹ F NMR spectrum of 3-fluoro-glucose 1.33 in red blood cells suspension ³⁸	12
Figure 1.17: Relative transport rates of monofluorinated glucose derivatives across the erythrocytes membrane	12
Figure 1.18: ¹⁹ F NMR spectrum of 2-deoxy-2-fluoro-glucose 1.34 in RBC suspension	13

Figure 1.19: Relative transport rates of polyfluorinated glucose derivatives across the erythrocytes membrane	14
Figure 1.20: Polyfluorinated analogues of D-glucose considered for investigation	16
Figure 2.1: ^1H NMR analysis of 1.26 in CDCl_3 (12 mM).....	21
Figure 2.2: Intramolecular C4–OH...F–C2 bonds in levoglucosan derivatives 1.26 to 1.31 in CDCl_3	22
Figure 2.3: Comparison of the O–H...F interactions in 1.19 and 1.26	23
Figure 2.4: Intramolecular C3–OH...O ₆ bonds in levoglucosan derivatives in CDCl_3	23
Figure 3.1: Trifluoro glucose 1.37	25
Figure 3.2: Impact of hyperconjugation on C4–OTs ₄ and C2–OTs ₂ bonds (lengths exaggerated).....	32
Figure 3.3: Electrostatic clashes between the –C–F bonds in 3.43 and approaching hydrides... ..	39
Figure 3.4: $^{19}\text{F}[^1\text{H}]$ NMR spectrum recorded for 2,3,4-trideoxy-2,3,4-trifluoro levoglucosan 3.26	42
Figure 3.5: X-ray crystallographic analysis of 2,3,4-trifluoro-levoglucosan 3.26	42
Figure 3.6: $^{19}\text{F}[^1\text{H}]$ NMR spectrum of the mixture 3.26/3.51 , details of trifluoro levogalactosan 3.51	45
Figure 3.7: ^1H and $^1\text{H}[^{19}\text{F}]$ NMR spectra recorded for 2,4-difluoro allosan 3.45	48
Figure 3.8: Effect of the bond polarisation of C5–C6 and C1–O on the H-accepting abilities of F ₂ and F ₄ in 3.45 (hyperconjugation).....	48
Figure 3.9: X-ray crystallographic analysis of 2,4-difluoro-allosan 3.45	49
Figure 3.10: X-ray crystallographic analysis of the fluorinated derivatives of levoglucosan 3.48 , 3.49 , and 3.50	49
Figure 3.11: X-ray crystallographic analysis of trifluoro glucose 1.37 and galactose 3.56	50
Figure 3.12: $^1\text{H}[^{19}\text{F}]$ NMR spectrum of trifluoro glucose 1.37 in CDCl_3	50
Figure 3.13: $^1\text{H}[^{19}\text{F}]$ NMR spectrum of trifluoro glucose 3.56 in acetone- <i>d</i> ₆	51
Figure 4.1: Tetrafluoro glucose 1.40 and galactose 4.1	55
Figure 4.2: Potential substitute of D-glyceraldehyde acetonide 3.1 as chiral building block	61

Table of Figures

Figure 5.1: Micro-tube reactor ($\approx 100 \text{ cm} < L < 200 \text{ cm}$) used as pre-cooling loop (left), stainless steel micro-tube reactor (L highly variable) used as reactor (right)	72
Figure 5.2: T-shaped and hexagonal micro-mixers, front view (left) and top view (right)	73
Figure 6.1: Potential side products formed in R1	96

Academic Thesis: Declaration of Authorship

I, Lucas Gilbert Quiquempoix

declare that this thesis and the work presented in it are my own and has been generated by me as the result of my own original research.

Synthesis of polyfluorinated carbohydrates

I confirm that:

1. This work was done wholly or mainly while in candidature for a research degree at this University;
2. Where any part of this thesis has previously been submitted for a degree or any other qualification at this University or any other institution, this has been clearly stated;
3. Where I have consulted the published work of others, this is always clearly attributed;
4. Where I have quoted from the work of others, the source is always given. With the exception of such quotations, this thesis is entirely my own work;
5. I have acknowledged all main sources of help;
6. Where the thesis is based on work done by myself jointly with others, I have made clear exactly what was done by others and what I have contributed myself;
7. Parts of this work have been published as: Quiquempoix, L.; Bogdan, E.; Wells, N.; Le Questel, J.-Y.; Graton, J.; Linclau, B. *Molecules* **2017**, *22*, 518.

Signed:

Date:

Acknowledgements

First of all, I would like to thank Prof Bruno Linclau for giving me the opportunity to do my PhD within his group during the last three years. His full commitment, guidance, and enthusiasm have been much appreciated over these years.

I would like to thank all the members of the Linclau group, past and present for their help and the good time we spent together inside and outside the lab. This includes in no particular order Gemma, Zhong, Bichette, Florent, Guillaume, Gert-Jan “Jean-jean” Hoffman, Bjeff, Rachel, J.B, R.K, Rob “the bro” szpera, Simon, Hannah, Diego, Mariana, David, and all the people I forgot to mention here. A special thanks go to Clément who helped me when I started in the lab.

I am also grateful to all the people from the other research groups for always being helpful and for the good moments we shared. Special thanks go to Victor “Totor” Lethuillier, Shamin, Thomas, Josh, Jess, Mike, Joe, Kathleen, Alex, Debacker.

I don’t forget all the staff from the chemistry department without whom this PhD would not have been possible, in particular Neil for performing the numerous NMR analyses I requested, John and Julie for running all the MS analyses, Mark Light for providing the X-ray structures, and also Keith and Mark for running the stores and for the nice chats we had together.

I would also like to say a massive thank to all my friends from Rouen for the quality time we spent together, mostly in festival, and for always being supportive.

Last but not least, I’d like to thank my family and my girlfriend Lolita for their unfailing support throughout these last years. Finally, I’d like to dedicate this thesis to my parents who have always encouraged me to pursue my goals and, most importantly, to always be curious about new knowledge, new experiences, and other cultures.

Definitions and Abbreviations

Alk-Li	Alkyl lithium
aq.	Aqueous
Ac	Acetate
Bn	Benzyl
BDA	Butane-2,3-diacetal
CSD	Cambridge Structural Database
DAST	Diethylaminosulfur trifluoride
DCM	Dichloromethane
DDQ	Dichlorodicyanoquinone
DMF	Dimethylformamide
DMS	Dimethyl sulfide
DMSO	Dimethylsulphoxide
<i>dr</i>	diastereomeric ratio
E ⁺	Electrophile
equiv.	Equivalent
EXSY	Exchange Spectroscopy
FDG	Fluoro Deoxy Glucose
GC	Gas chromatography
GLUT1	GLucose Transporter 1
H-bond	Hydrogen bond
HPLC	High Performance Liquid Chromatography
<i>K_d</i>	Dissociation constant
<i>K_i</i>	Inhibition constant (M)
M1, M2	Micromixer
Me	Methyl
NfF	Nonafluorobutanesulfonyl Fluoride
NMR	Nuclear Magnetic Resonance
Ph	Phenyl
P1, P2, P3	Micro-tube reactor (pre-cooling loop)
PDB	Protein Data Bank
p <i>K_{AH}</i>	Hydrogen-bond acidity
PMB	<i>p</i> -Methoxybenzyl

Definitions and Abbreviations

R1, R2	Micro-tube reactor (reactor)
RBC	Red Blood Cell
Rf	Retention factor
rt	Room temperature
STD	Saturation Transfer Difference
TBAT	Tetrabutylammonium triphenyldifluorosilicate
TCCA	Trichloroisocyanuric acid
TEMPO	2,2,6,6-Tetramethylpiperidin-1-yl) oxyl
THF	Tetrahydrofuran
TLC	Thin Layer Chromatography
t^{R1}	Residence time in R1
Ts	Tosyl
TsOH	<i>p</i> -Toluenesulfonic acid
UDP	Uridine Diphosphate

Chapter 1: Introduction

1.1 Fluorinated carbohydrates: background

1.1.1 Carbohydrates

Carbohydrates play a key role in a broad range of important biological processes. As part of glycoconjugates such as glycolipids and glycoproteins, found on the cell surfaces, they are involved in various recognition events including infection, inflammation and immune response.^{1,2} Given that many diseases arise from the malfunctioning of these processes, their understanding as well as the ability to interfere with them is of great pharmaceutical interest. In this context, the development of inhibitors targeting enzymes involved in glycoconjugate biosynthesis, such as glycosyltransferases, is a promising strategy to develop new therapeutic tools.³

Structural analyses of carbohydrate-protein complexes through X-ray diffraction revealed that hydrogen bond (H-bond) interactions constitute the main interaction between the two binding partners. As illustrated below with the crystal structure of D-glucose **1.1** in complex with a periplasmic binding protein (**Figure 1.1**),⁴ each hydroxyl from a carbohydrate is involved in multiple H-bonds with polar protein residues, acting simultaneously as both donor and acceptor, this ultimately resulting in the formation of a H-bond network ensuring the stability of the carbohydrate-protein complexes.

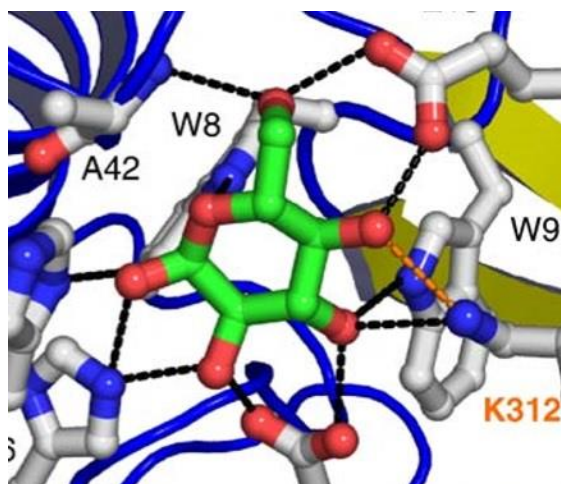


Figure 1.1: Sugar binding pocket of a periplasmic binding protein with glucose **1.1** as substrate⁴

Owing to the highly directional character of H-bonds, and given that stereochemically defined hydroxyl groups are engaged, interactions of carbohydrates with protein receptors can be very specific.⁵ However, due to the strong competition arising from the aqueous solvent (biological

medium), the formation of these sugar-protein H-bonds does not generally constitute a sufficient energetic contribution to drive forward the binding event.^{1,2}

Even though highly hydrophilic, carbohydrate exhibit small hydrophobic patches constituting of C-H bonds, described below for glucose **1.1** and galactose **1.2** (**Figure 1.2**), which are typically found to interact with aromatic moieties within binding pockets.⁶

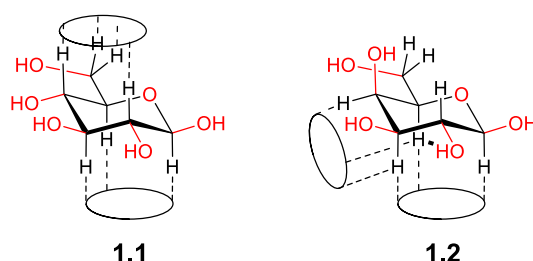


Figure 1.2: Representation of hydrophobic patches on glucose **1.1** and galactose **1.2**

This is clearly evidenced in the crystal structure obtained for the *E. coli* galactose transport protein in which glucose **1.1** is stacked in between an aromatic tryptophan and a phenylalanine residue (**Figure 1.3**).⁷

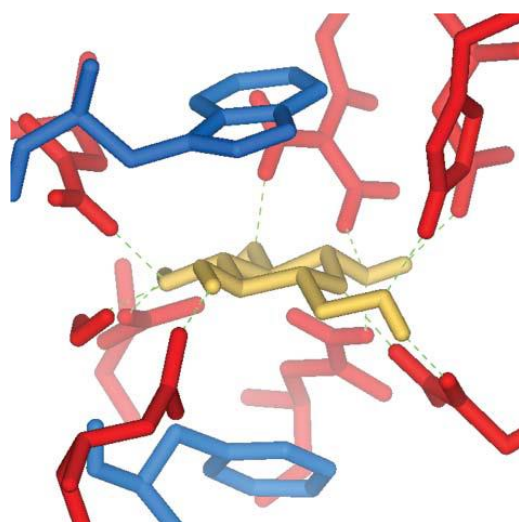


Figure 1.3: Binding pocket of the *E. coli* galactose transport protein, with glucose substrate **1.1** shown in yellow, aromatic residues in blue, and polar residues in red⁷

Before binding, these hydrophobic patches cause energetically unfavourable situations where water molecules are trapped at the interface between the hydrophobic surfaces from both binding partners. Ultimately, these “unstable” water molecule are desolvated from both the ligand and the receptor upon binding, thus leading to a beneficial decrease of the free energy of binding which constitutes the main driving force of the carbohydrate-protein complex formation.⁸ Nevertheless, altogether, carbohydrates usually display low affinity toward their protein receptors (dissociation constant K_D within micromolar to the millimolar range).^{1,2}

1.1.2 Fluorination of carbohydrates: a strategy to increase the binding affinity

Fluorination of bioactive compounds is now a well-established strategy in the design of new drugs as the introduction of this small but very electronegative atom impacts a multitude of chemical and physical properties. For instance, substitution of hydrogens or other functional groups by fluorine has been shown to alter the lipophilicity as well as the conformational bias of a molecule, this potentially resulting in an improvement of the biological and/or pharmacological properties.⁹ Currently, it has been estimated that 30-40% of agrochemicals and 25% of pharmaceuticals on the market contain at least one fluorine atom.¹⁰ It is also quite remarkable that in 2008, a third of the top 30 best-selling pharmaceutical products in the US were at least monofluorinated.¹¹

Regarding carbohydrates, substitution of one or several hydroxyls by fluorinated motifs exhibiting large hydrophobic areas constitutes a sensible strategy to extend the scarce C-H hydrophobic patches found on these molecules, and hence to promote their binding through increased desolvation energies.^{12,13} Also, owing to their high polarisation, -C-F bonds were found to accommodate attractive dipole-dipole interactions with certain protein residues, thereby providing an additional energy gain favourable to the binding event. The existence of such interactions was first evidenced by Diederich and co-workers with the crystal structure of inhibitor **1.3** in complex with thrombin (**Figure 1.4**),^{14,15} in which the close contacts between the aromatic -C-F bond from **1.3** and an a H-C_α-C=O moiety indicated $\delta^+C-F^{\delta-}\cdots\delta^+H-C_{\alpha}^{\delta-}$ and $\delta^+C-F^{\delta-}\cdots\delta^+C=O^{\delta-}$ interactions. Alongside the increased hydrophobicity of the aromatic ring resulting from the fluorination (decreased polarizability), the latter were deemed responsible for the increased affinity of **1.3** toward the thrombin receptor, with respect to the non-fluorinated inhibitor **1.4**, accounting for the fivefold increased inhibition potency of the former compared to the latter.

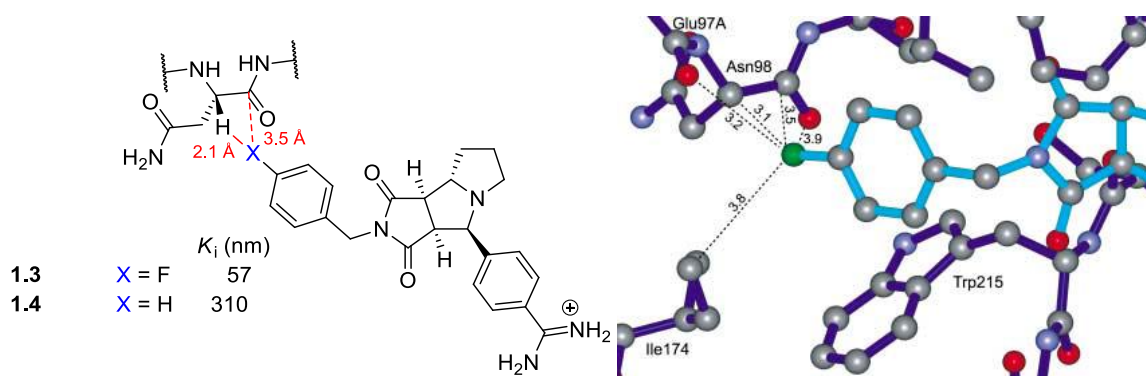


Figure 1.4: Activities of thrombin inhibitors (left), crystal structure of **1.3** in the thrombin D pocket (right).

Subsequently, an extensive study of the protein data bank conducted by the same group revealed that similar F \cdots C=O and F \cdots CN interactions could be observed in numerous crystallographic structures of protein-ligand complexes.^{16,17}

In 1998, DiMagno and co-workers proposed a new approach for increasing protein-carbohydrate affinity via sugar-ring polyfluorination, coined 'polar hydrophobicity'. It was proposed that the larger hydrophobic desolvation and the potential formation of polar interactions with protein residues, both resulting from the insertion of fluorinated motifs on carbohydrate backbones, would cause to considerably enhance sugar binding affinity.^{18,19}

One of the first examples illustrating this concept was published in 1986 by Withers and co-workers who, while investigating mono and difluorinated monosaccharides as inhibitors of glycogen phosphorylase, found that the C1 and C2 difluorinated glucose **1.5** exhibited a remarkably increased affinity (lower K_i) compared to glucose **1.1**, and this was observed for both anomers.^{20,21}

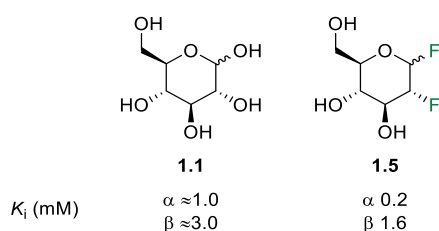


Figure 1.5: Inhibition study of glycogen phosphorylase

Although not invoked by the authors, a reason for such increased affinity was the apparition of a larger hydrophobic domain that promoted the binding through hydrophobic desolvation. Also, both C-F bonds could potentially have been involved in attractive dipole-dipole or dipole charge interactions.

In 1998, the transport study of hexafluorohexopyranose **1.6** across the red blood cell membrane, conducted by DiMagno and co-workers, revealed that **1.6** was conveyed 10 times faster than the normal glucose, and this despite the loss of stereochemical information (**Figure 1.6**).¹⁸

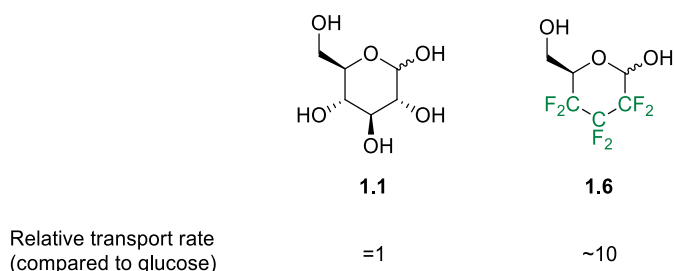


Figure 1.6: Relative transport rate of hexafluorohexopyranose **1.6** across the RBC membrane

Several control experiments were conducted to evidence that the faster transport was due to an enhanced binding of **1.6** toward the glucose transporter protein GLUT1 rather than *via* its diffusion through the membrane, facilitated by its increased hydrophobicity. These included an experiment conducted at 25 °C instead of 37 °C, for which the complete interruption of the transport was observed, while a diffusion mechanism would have been only slightly affected. Also, addition of D-

glucose **1.1** or phloretin, a known inhibitor of glucose efflux, both resulted in an impaired transfer. Hence, based on these results, O'Hagan and co-workers inferred that the faster transport rate of the hexafluorinated glucose **1.6** resulted from an enhanced binding to GLUT1, itself resulting from the presence of an hexafluorinated motif on the carbohydrate backbone (polar hydrophobicity).

More recently, saturation transfer difference (STD) NMR experiments conducted within our group revealed that uridine diphosphate (UDP)-tetrafluoro-galactofuranose **1.7** exhibits a higher affinity for UDP-galactopyranose mutase than natural UDP-galactofuranose **1.6** (**Figure 1.7**),²² once again evidencing the potential of polar hydrophobicity in the context of improving carbohydrate-protein affinity.

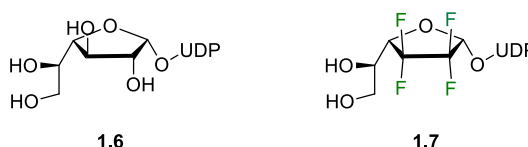


Figure 1.7: UDP-galactofuranose **1.6** and its tetrafluorinated analogue **1.7**

1.2 Influence of fluorination on adjacent functional groups

Owing to its strong electronegativity, fluorine has a marked impact on both Brønsted acidities and basicities of the neighbouring functional groups.²³ For example, a decrease in pKa of more than three units is observed from ethanol **1.8** to tetrafluoropropanol **1.9** and trifluoroethanol **1.10** (**Figure 1.8**).²⁴ This is of great significance as modification of pKa has shown to alter the binding affinity and bioavailability of certain biologically active compounds.⁹

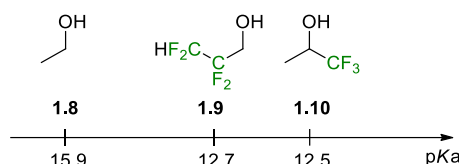


Figure 1.8: The effect of fluorination on pKas

Recently, our group investigated the impact of fluorination on the hydrogen bond acidity of conformationally locked cyclohexanol derivatives using FTIR equilibria measurements.²⁵ Contrary to what was assumed in the literature at that time, it appeared that the inductive effect of fluorine was not the only factor to impact the H-bond acidity, and that the relative configuration and the position of the inserted fluorine with regards to the neighbouring H-bond donors had to also be carefully considered. For example, the *cis*-1,3-diaxial fluorohydrin **1.11** and the 1,2-fluorohydrin **1.12** showed a decreased H-bond acidity compared to their non-fluorinated counterpart **1.13**, with **1.11** having virtually lost its capacity to act as an H-bond donor (**Figure 1.9**). As evidenced by the

NMR data collected for these compounds, this was due to intramolecular C–F⋯H–O interactions competing with the formation of intermolecular H-bonds, hence impeding the H-bond acidity.

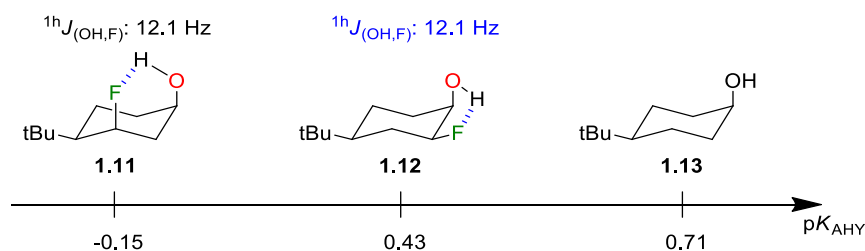


Figure 1.9: Relative H-bond acidities (pK_{AHY}) of conformationally locked cyclohexanol derivatives

These results demonstrated that OH⋯F H-bonds can significantly influence intermolecular H-bond properties of functional groups. Hence, given the importance of both inter- and intramolecular hydrogen bonding regarding the binding of ligands to receptors,²⁶ the study of these weak interactions, and the factors that influence them, is of interest.

1.3 Intramolecular OH⋯F bonding: Background

1.3.1 Hydrogen bond: Definition and characteristics

According to a recent IUPAC definition,^{27,28} a hydrogen bond (H-bond) can be described as an attractive interaction between a hydrogen from a molecular fragment X–H, called donor, in which X and H are covalently bonded and X is more electronegative than H, and an acceptor which usually is an anion (Y) or an electron rich molecular fragment (Z–Y) containing a lone pair or a π bond system. Formation of such X–H⋯Y–Z bond typically results in a lengthening of the X–H bond observable *via* a red shift in the infrared X–H stretching frequency, and/or a pronounced deshielding of the NMR X–H proton (donor fragment). Finally, it is noteworthy that H-bond interactions are generally characterised by a X–H⋯F angle comprised in between 110° and 180°. The closer the angle is to 180°, the stronger the H-bond is.

Although fluorine displays favourable characteristics to act as a H-bond acceptor, such as a high electronegativity and the presence of three lone pairs, it is also characterised by a low polarizability and a low proton affinity which, when covalently bonded to a carbon atom, make it a poor H-bond acceptor compared to other heteroatoms (nitrogen, oxygen, etc.).¹⁵ Indeed, after inspections of the Cambridge Structural Database (CSD), Dunitz and Taylor found that only 0.6% of the crystal structure analysed presented a X–H⋯F–C geometry propitious to the formation of H-bond (X = O, N), namely a H⋯F distance inferior to 2.3 Å and a X–H⋯F angle superior to 90°. ²⁹ However, this proportion rises up to 10% in the Protein Data Bank (PDB),³⁰ which tends to demonstrate that these interactions play a non-negligible role in the binding of ligand to protein receptors. Besides, recent

experimental IR and NMR studies as well as computational evidences corroborated the existence these weak $X-H\cdots F-C$ interactions, both in an intermolecular and intramolecular fashion.³¹

1.3.2 Study of intramolecular $OH\cdots F$ interactions in solution *via* proton NMR

Owing to the poor H-bond accepting capacity of organofluorines, both intra- and intermolecular $H\cdots F$ bonds are readily disrupted in presence of better acceptors (oxygen, nitrogen). Hence, NMR study of these interactions are conducted in apolar aprotic solvents such as deuterated chloroform ($CDCl_3$) or toluene (toluene-*d*8). Also, to avoid the formation of intermolecular H-bond between different substrate molecules, potentially disruptive for intramolecular $O-H\cdots F-C$ interactions, sample concentrations have to be kept relatively low (preferably ≤ 0.20 mM).

Besides inducing a de-shielding of the proton signal corresponding to the hydroxyl donor, H-bonds involving C-F bond as acceptor are further evidenced by a “through space” coupling $^1J(OH, F)$ through the $H\cdots F$ bond. Being proportional to the H-bond strength, this coupling constant can be quite large, as in the cage system **1.14** where both O-H and C-F are locked in a geometry forcing an intramolecular interaction (**Figure 1.10**).³² For more flexible substrates such as the acyclic fluorohydrin **1.15**, this value can be quite small, and is related to the population of intramolecular hydrogen bonding conformations.³³

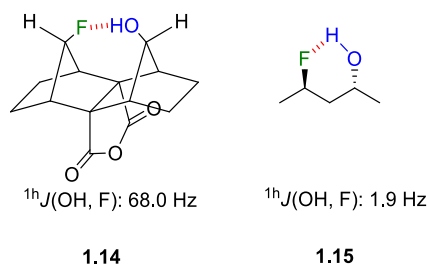


Figure 1.10: $^1J(OH, F)$ coupling constants measured in $CDCl_3$ for the cage molecule **1.14** and the γ -fluoropropanol **1.15**

Alternatively, the defined orientation of an hydroxyl group and hence its involvement in an H-bond interactions can be evidenced through the vicinal $^3J(H, OH)$ coupling which, unlike for a freely rotating hydroxyl, should adopt large (> 5.0 Hz) or small (≤ 3.0 Hz) values.³⁴ Thanks to a Karplus type equation developed by Fraser and co-workers,³⁵ the $^3J(H, OH)$ value measured can be correlated with a $H-C-O-H$ dihedral angle ($\theta_{H-C-O-H}$), thus giving an additional insight on the geometry of the H-bond studied. For example, besides the through space coupling $^1J(OH, F)$, the intramolecular $O-H\cdots F-C$ bonds in the *myo*-inositol derivatives **1.16** and **1.17** are also evidenced by the $^3J(H, OH)$ value of about 8.0 Hz (**Figure 1.11**), which indicates a torsion angle of *circa* 140° , corresponding to the geometry shown below with the hydroxyl pointing directly toward the fluorine atom.^{36,37}

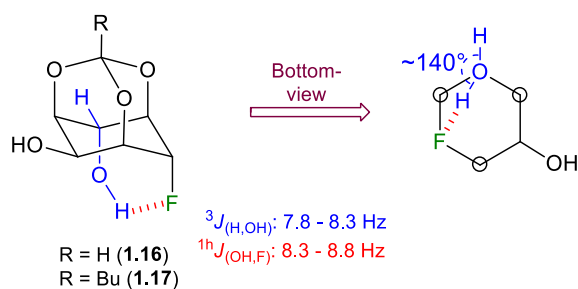


Figure 1.11: Intramolecular O–H···F–C bond in the myo-inositol derivatives **1.16** and **1.17**

1.3.3 Intramolecular hydrogen bonding in fluorinated derivatives of carbohydrates

In 2007, a ^1H NMR study of 4-fluorinated derivatives of levoglucosan in CDCl_3 conducted by Bernet and Vasella revealed the existence of bifurcated intramolecular H-bonds involving the C2 hydroxyl (C2–OH) as donor, and both the C4 fluorine (C4–F) and the endocyclic oxygen (O_5) as acceptors (**Figure 1.12**).

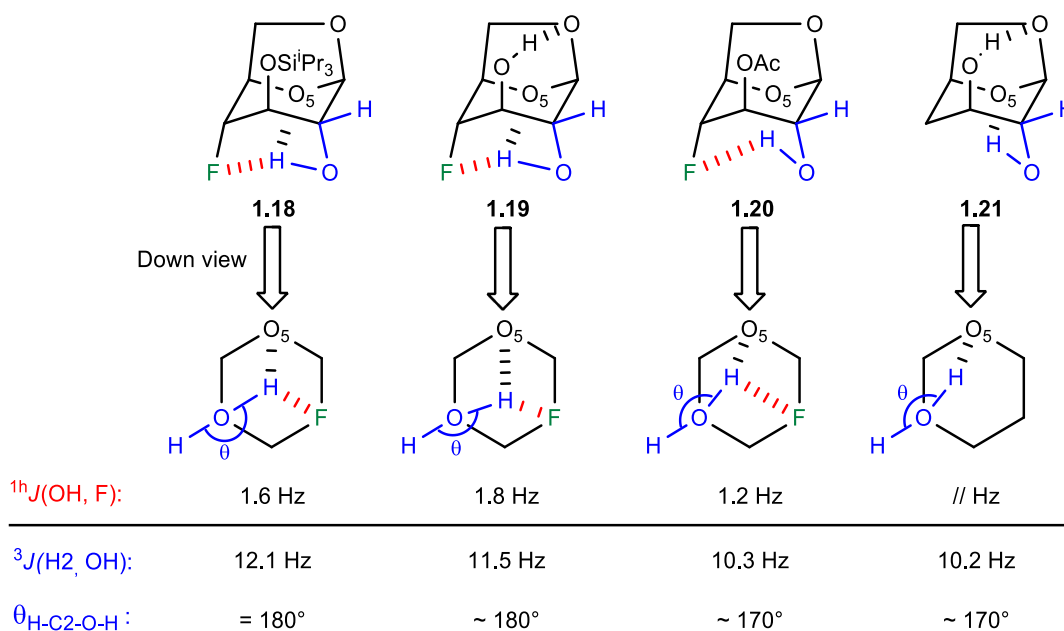


Figure 1.12: Intramolecular H-bonds in 4-deoxy-4-fluoro levoglucosan derivatives **1.18** to **1.21**

These trivalent interactions were evidenced by a through space coupling $^1hJ(\text{OH}, \text{F})$, as well as a $^3J(\text{H}_2, \text{OH})$ value of 10–12 Hz ($150^\circ \leq \theta_{\text{H-C2-O-H}} \leq 180^\circ$), indicating that the C2–OH proton was positioned in between C4–F and O_5 rather than pointing directly toward one of these two acceptors, as it would be the case for a divalent interaction.

For compound **1.18**, the $^3J(\text{H}_2, \text{OH})$ value of 12.1 Hz indicated a symmetrical geometry in which the C2–OH proton was roughly equidistant from C4–F and O_5 . As evidenced by the $^1hJ(\text{OH}, \text{F})$ coupling observed on the C2–OH signal (1.6 Hz), this was due to C4–F competing as H-bond acceptor with O_5 . Regarding **1.19**, the larger $^1hJ(\text{OH}, \text{F})$ value of 1.8 Hz suggested a shorter OH···F distance than in

1.18 and hence a stronger C2–OH...F–C4 interaction. Given the $^3J(\text{H2}, \text{OH})$ of 11.5 Hz, this corresponded to a situation where the C2–OH proton pointed slightly toward C4–F, hence indicating that this one was a better H-bond acceptor than O₅. This was explained by the electron donating effect of the partially deprotonated antiperiplanar hydroxyl, which by increasing the electron density in C4–F, enhanced its H-accepting capacities. In contrast, a minimal $^1J(\text{OH}, \text{F})$ coupling of 1.2 Hz was observed for **1.20**, which according to the $^3J(\text{H2}, \text{OH})$ of 10.3 Hz corresponded to a geometry in which the C2–OH proton points directly toward the endocyclic oxygen, as for the 4-deoxy levoglucosan derivatives **1.21**. The poor H-accepting capacity of C4–F was attributed to the antiperiplanar acetate group, which owing to its strong withdrawing effect decreased the electronic density in C4–F to the point that it barely competed as H-bond acceptor. As illustrated below (**Figure 1.13**), the strong influence of the C3 antiperiplanar substituent on the electronic density in C4–F can be explained through the optimal overlap between the bonding and anti-bonding orbitals of the C4–F and C3–O bonds ($\sigma_{\text{C3-O}}$, $\sigma^*_{\text{C3-O}}$, $\sigma_{\text{C4-F}}$, $\sigma^*_{\text{C4-F}}$), strongly promoting the electronic transfers through hyperconjugation.

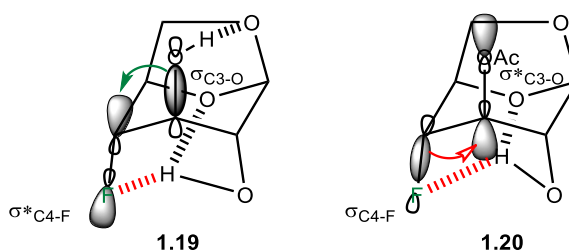


Figure 1.13: Hyperconjugation between the C4–F and C3–O bonds

In 2013, Bernet and Gouverneur reported similar bifurcated H-bonds in fluorinated derivatives of α -D-hexopyranosides (**Figure 1.14**). As for the 4-fluorinated levoglucosan derivatives, the combined analysis of both the through space $^1J(\text{OH}, \text{F})$ and the geminal $^3J(\text{H2}, \text{OH})$ couplings enabled to determine the geometry of the bifurcated H-bond, and hence to estimate the strength of the C2–OH...F–C4 interaction.

With a $^1J(\text{OH}, \text{F})$ of 9.1 Hz and a $^3J(\text{H2}, \text{OH})$ of 12.1 Hz, compound **1.22** exhibited a symmetric bifurcated H-bond, meaning that the C2–OH proton was roughly equidistant from the axial C4–F and O₅. Regarding compound **1.23**, an epimer of **1.22** exhibiting a C3 axial hydroxyl, the slightly higher $^1J(\text{OH}, \text{F})$ of 9.8 Hz, as well as the $^3J(\text{H2}, \text{OH})$ of 11.7 Hz, suggested a geometry in which the C2–OH proton pointed slightly toward C4–F, hence implying that the latter was a better H-bond acceptor than O₅. At the contrary, compound **1.24** for which the axial C3–OH was protected as an acetate showed a considerably reduced $^1J(\text{OH}, \text{F})$ value (5.7 Hz), indicating a much weaker O–H...F–C interaction than in compound **1.23**. According to the $^3J(\text{H2}, \text{OH})$ of 10.5 Hz, this corresponded to a geometry in which the C2–OH proton pointed directly toward O₅, and hence suggesting a H-bond

exclusively to the latter. Such imprecision was due to the presence of a polar substituent decreasing the $^3J(\text{H2}, \text{OH})$ coupling, not taken into consideration in the Karplus equation of Fraser and co-workers.³⁵ The sharp degradation of the H-accepting capacities of C4–F observed between compound **1.23** and **1.24** was once again rationalised by the C3 antiperiplanar substituent, strongly influencing the electronic density in the C4–F bond (*cf* **Figure 1.13**). Analysis of compound **1.25**, for which a CF₂ moiety was installed at C4, revealed a $^1J(\text{OH}, \text{F})$ value below 1.5 Hz witnessing of an extremely weak OH \cdots F interaction, also evidenced by the $^3J(\text{H2}, \text{OH})$ of 9.7 Hz indicating a geometry with the C2–OH proton pointing directly toward O₅. Comparison of these results with those obtained with **1.22**, for which C4–F competed favourably with O₅, clearly indicated that CHF is a better acceptor than CF₂. To explain this, the authors invoked a reduced electronic density in the axial C4–F of the CF₂ moiety, most presumably induced by the strong inductive effect of the geminal fluorine, which ultimately led to decreased H-accepting capacities. However, the influence of other changing parameters in the molecule were not excluded.

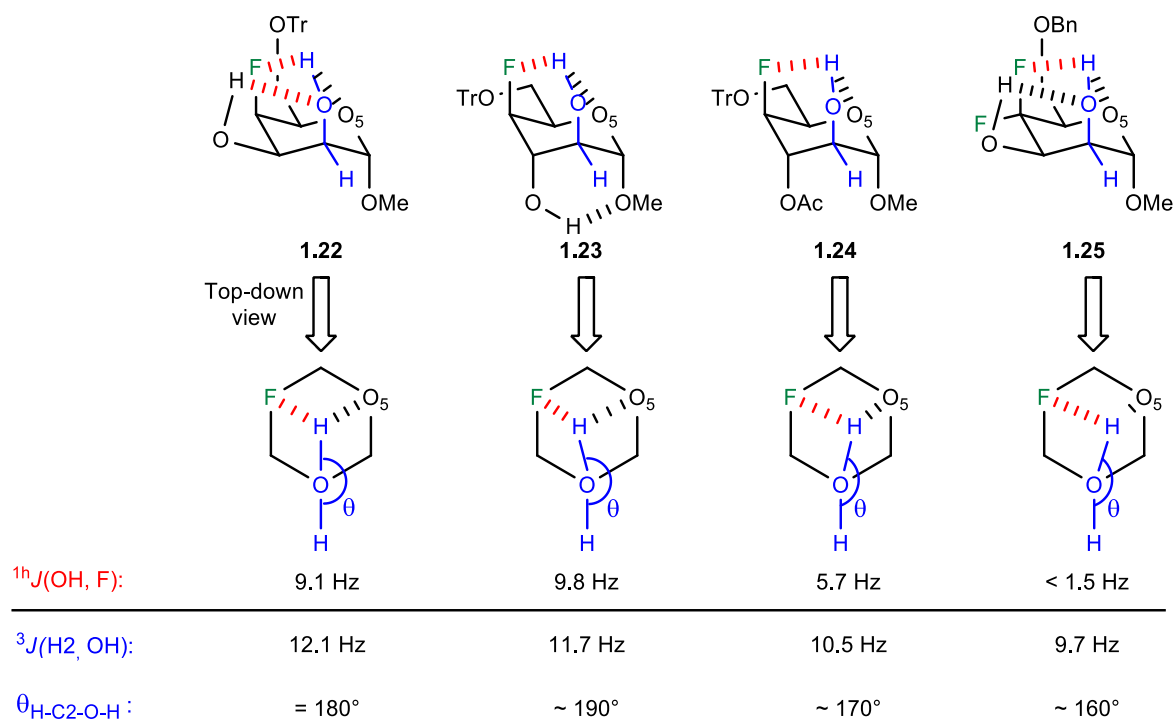


Figure 1.14: Intramolecular H-bonds in fluorinated- α -D-hexopyranosides **1.22** to **1.25**

It is noteworthy that these C2–OH \cdots F–C4 interactions were gradually replaced by intermolecular H-bonds to the solvent when increasing its polarity (CDCl₃, CD₃CN, THF-*d*8, acetone-*d*6 and DMSO-*d*6). Remarkably, the bifurcated H-bonds observed in compound **1.22** were only partially disrupted in acetone, as evidenced by the $^1J(\text{OH}, \text{F})$ of 5.2 Hz (not shown, 9.1 Hz in CDCl₃), this suggesting that the intramolecular OH \cdots F were not as weak as depicted in the literature.

To summarise, both these ^1H NMR studies emphasised the importance of intramolecular $\text{O}-\text{H}\cdots\text{F}-\text{C}$ interactions in fluorinated derivatives of carbohydrates, when in apolar medium. More importantly, these studies brought strong evidences that organofluorines could compete favourably as H-bond acceptor with other heteroatoms, like in this case with oxygen. Ultimately, these observations strongly suggest that the validity of the conclusion drawn by Dunitz and Taylor regarding the inability of organofluorines to act as H-bonds acceptors were restricted to the solid state,²⁹ and also that organofluoro compounds may act as H-bond acceptor in apolar environments such as protein hydrophobic pockets.

1.3.4 Aims and objectives

Recently, various synthetic projects conducted in our group have generated a range of levoglucosan derivatives amongst which the 2-deoxy-2-fluoro compounds **1.26** and **1.27** (**Figure 1.15**), presenting geometries favourable to the formation of a bifurcated H-bond between the C4 hydroxyl as donor (C4–OH), and both the C2 fluorine (C2–F) and the endocyclic oxygen (O_5) as competing acceptors. Hence, to expand the study of intramolecular $\text{OH}\cdots\text{F}$ bonds in levoglucosan type structure started by Bernet and Vasella,³⁴ detailed ^1H NMR analysis of these substrates in CDCl_3 was envisioned.

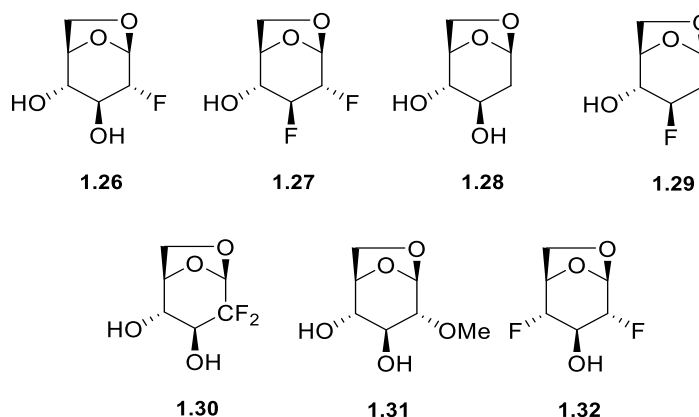


Figure 1.15: Levoglucosan derivatives considered for ^1H NMR analysis

To better appreciate the perturbation of the divalent $\text{C4}-\text{OH}\cdots\text{O}_5$ bond induced by the insertion of a C2 fluorine, substrates **1.28** and **1.29** in which no competing H-bond acceptor was present at C2 were also analysed. Additionally, study of compound **1.30** and **1.31** was envisioned to compare the H-accepting capacity of a $-\text{CHF}$ with both $-\text{CF}_2$ and $-\text{CHOMe}$ moieties. Regarding compounds **1.26**, **1.28**, **1.30**, and **1.31**, study of the substituent effects on the $\text{C3}-\text{OH}\cdots\text{O}_6$ intramolecular H-bond was also envisaged. In this context, substrate **1.32** was included in the list of compounds to analyse.

1.4 Fluorine NMR exchange spectroscopy of fluorinated carbohydrates transport across red blood cell membranes

1.4.1 Background

When analysed by fluorine NMR (^{19}F NMR) in the presence of red blood cells (RBC), fluorinated carbohydrates exhibit four distinct resonances corresponding to the intra- and extra-cellular populations of both anomers, as illustrated below with the example of 3-deoxy-3-fluoro-glucose **1.33** (3FDG) (Figure 1.16).³⁸

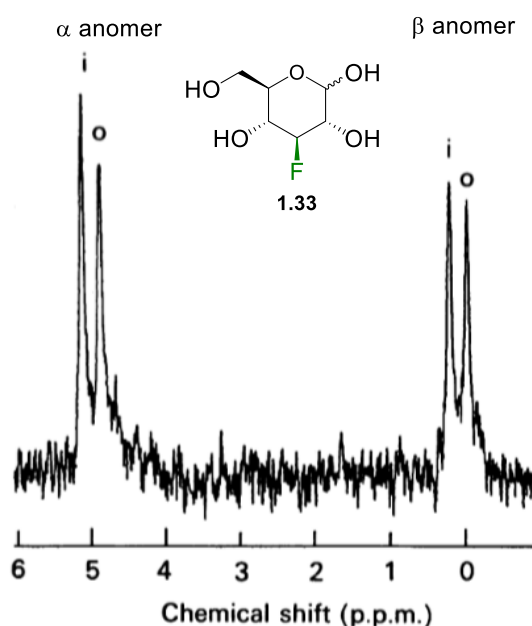


Figure 1.16: ^{19}F NMR spectrum of 3-deoxy-3-fluoro-glucose **1.33** in red blood cells suspension³⁸

Owing to this fortuitous feature referred to as “split peak effect”, the transport rate of fluorinated carbohydrates across the RBC membrane can be determined *via* basic NMR magnetization-transfer experiments, and this for each anomer. Using one-dimensional exchange spectroscopy (1D-EXSY), Potts and co-workers determined that the anomers of 3FDG **1.33** were transported at similar rates compared to the anomers of D-glucose **1.1** (Figure 1.17).^{38,39}

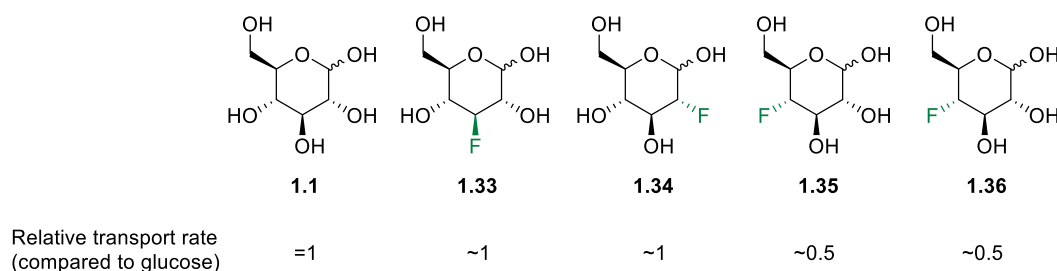


Figure 1.17: Relative transport rates of monofluorinated glucose derivatives across the erythrocytes membrane

Then, London and co-workers investigated the transport rates of -2, -3, -4, -6-deoxyfluoro analogues **1.33** to **1.36** via two-dimensional EXSY experiments (2D-EXSY).⁴⁰ This technic produced spectra such as the one shown below, obtained for 2FDG (**Figure 1.18**), on which the transmembrane exchange is clearly evidenced by the cross peaks observed between the signals corresponding to the intra- and extra-cellular populations, and from which the exchange rate are determined. It must also be noted that no cross peaks are observable corresponding to the α - β transition, indicating that mutarotation is completely negligible at the mixing time selected for this experiment (400 ms).

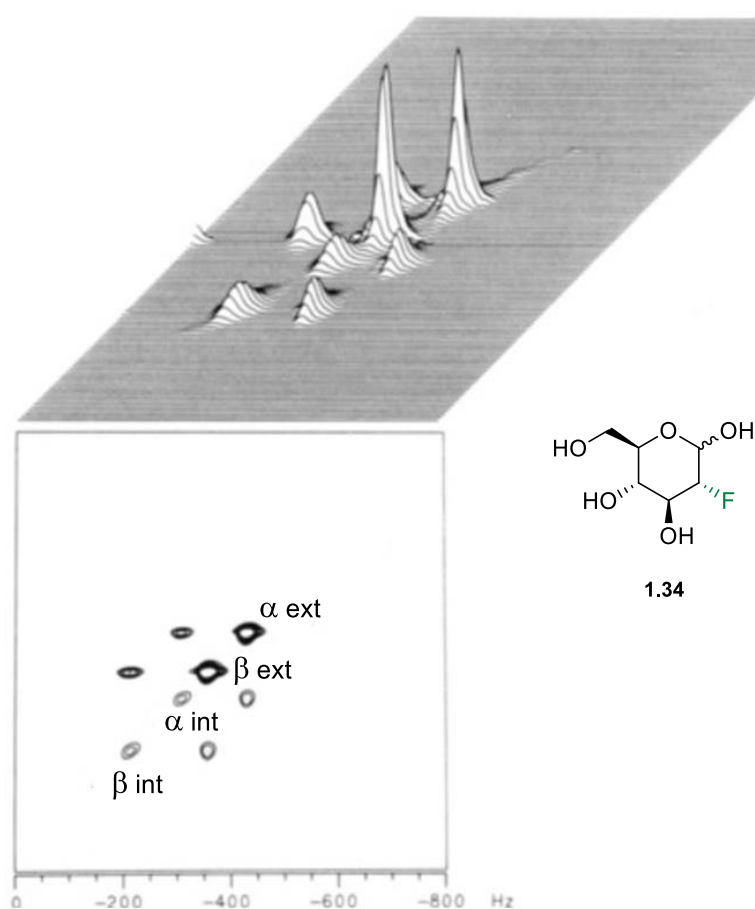


Figure 1.18: ^{19}F NMR spectrum of 2-deoxy-2-fluoro-glucose **1.34** in RBC suspension

As detailed on the previous page (**Figure 1.17**), it was found that 2FDG **1.34** was transported roughly at the same speed as 3FDG **1.33** and glucose **1.1**, while 4FDG **1.35** and 6FDG **1.36** were conveyed twice as slow. Also, like for D-glucose **1.1**, the α -anomers of all these monofluorinated sugars were transported faster compared to the β -anomers.

Using similar 2D-EXSY NMR experiments, DiMagno and co-workers investigated the transport rate of hexafluorohexopyranose **1.6** which, as mentioned previously, appeared to be 10 times faster than for D-glucose **1.1** (**Figure 1.19**).¹⁸ Such results were quite surprising as they suggested an enhanced binding of hexafluorinated glucose **1.6** toward GLUT1, despite the loss of stereochemical

information at C2, C3 and C4. Besides, the importance of the stereochemistry had been demonstrated with the example of D-galactose **1.39**, which was transported 10 times slower than D-glucose **1.1**. However, as mentioned previously in this chapter (*cf* section **1.1.2**), DiMagno and co-workers attributed the increased transport rate of **1.6** to its enhanced binding to GLUT1.

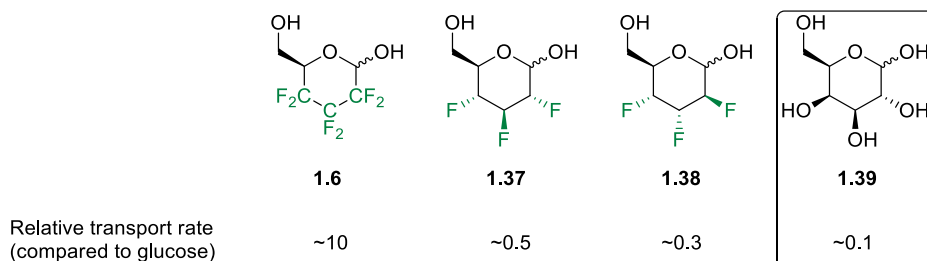


Figure 1.19: Relative transport rates of polyfluorinated glucose derivatives across the erythrocytes membrane

Also using 2D-EXSY NMR experiments, O'Hagan and co-workers examined the transport rate of both trifluoro glucose **1.37** and altrose **1.38**.⁴¹ Even though the glucose stereochemical information was respected in **1.37**, its transport rate was roughly halved compared to normal glucose **1.1**. The altrose analogue **1.38** was found to cross the membrane at around 30% of the rate of **1.1**, implying that the GLUT1 could distinguish the different stereogenicity associated with the C-F bonds. Also, it is noteworthy that for both **1.37** and **1.38** the α anomer was transported faster than the β , thus suggesting that GLUT1 was able to recognise the stereochemistry at the anomeric centre despite the presence of fluorinated motifs.

1.4.2 Limitations of the method

After looking through the experimental sections corresponding to the transport experiments described in the previous section, it was realised that little attention was paid to the metabolic and structural (shape) stability of the RBC over the analysis time. Indeed, the 2D-EXSY experiments required for polyfluorinated substrates given the overlap of the fluorine signals in the 1D spectrum frequently take several hours to acquire, this is often too long for RBCs to retain their normal shape and thus their transport capacities.

Also, concerning the 2D-EXSY-NMR analysis of polyfluorinated carbohydrates, it was believed that due to the strong scalar couplings between neighbouring fluorine atoms, the relationship linking cross peak volume, mixing time, and chemical-exchange rate constants, was compromised. It was believed that this was not addressed in the previous studies. Hence, owing to the loss of structural stability of the RBC over analysis, as well as the complications arising from ^{19}F - ^{19}F scalar couplings,

it was presumed that the transport rate measured for the hexafluorinated glucose **1.6** and both trifluoro glucose **1.37** and altrose **1.38** may not be entirely accurate.

Finally, it must be noted that the relative transport rates given for the fluoro sugars presented in the previous section were obtained by comparing their apparent efflux rates with the one of D-glucose **1.1**. However, the apparent efflux rates being kinetic parameters dependent on the concentration of substrates, it is difficult to correlate them with an enhanced or decreased binding affinity toward GLUT1 (compared to glucose). Therefore, the statement that the hexafluorinated glucose **1.6** is transported faster than glucose **1.1** owing to a better binding to GLUT1 appeared a bit premature.

1.4.3 Development of an improved NMR protocol: objectives

In partnership with Pr. Philip Kuchel's group, expert in the field of membrane transport study *via* NMR spectroscopy, an improved NMR protocol was designed that could address the problems mentioned in the previous section. This adapted method involved the introduction of inosine in the sample analysed, a purine nucleoside enabling the RCB to conserve their structural integrity over extended period of times, and which is not transported by the GLUT1 carrier. Also, a new reprocessing method of the 2D-EXSY-NMR spectra using a density matrix was elaborated, *via* which the perturbation caused by the strong F-F couplings could be circumvented. More importantly, this new method gives access to the specificity constant (k_{cat}/K_M), which unlike the apparent efflux rate is concentration independent (within reason), and can be correlated to the fluorosugar-GLUT1 affinity.⁴²

Using this new method, we decided to re-investigate the transport rate of all the monofluorinated derivatives of glucose **1.33** to **1.36**, as well as the trifluoro **1.37** and hexafluoro **1.6** glucose. Ultimately, this may lead to a reinterpretation of the results obtained *via* the contemporary transport experiments, but more importantly of the seminal results reported by DiMagno and O'Hagan. If it can be confirmed that polyfluorination leads to an enhanced interaction with GLUT1 protein, then this will be of direct and significant importance to the glycosciences. In order to investigate the impact of the nature and the position on the carbohydrate backbone of the fluorinated motif on the gain in binding affinity, the scope of substrates to analyse was extended to various polyfluorinated derivatives of glucose (**Figure 1.20**).

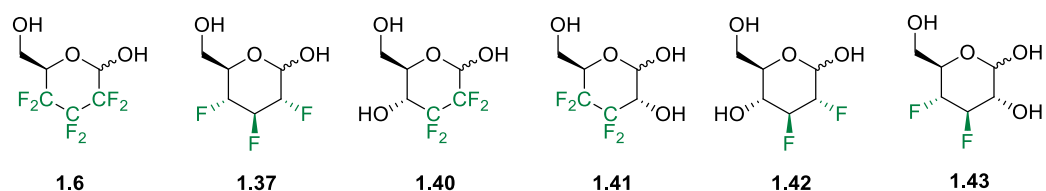


Figure 1.20: Polyfluorinated analogues of D-glucose considered for investigation

To access the specificity constant of each couple sugar-GLUT1, this method requires measuring of the apparent efflux rate constants of the fluoro sugar studied at several different concentrations. Hence, large quantities of the polyfluorinated sugars shown above were required (± 150 mg). My aim was to synthesise the 2,3,4-trideoxy-2,3,4-trifluoro-D-glucopyranose **1.37**, and 2,3-dideoxy-2,2,3,3-tetrafluoro-D-glucopyranose **1.40**, in sufficient quantities for the transport experiments.

Chapter 2: Study of intramolecular hydrogen bonds in levoglucosan derivatives

2.1 Target molecules and strategy of synthesis

As a reminder, the seven levoglucosan derivatives shown below were considered for ^1H NMR analysis in CDCl_3 (**Figure 1.15**).

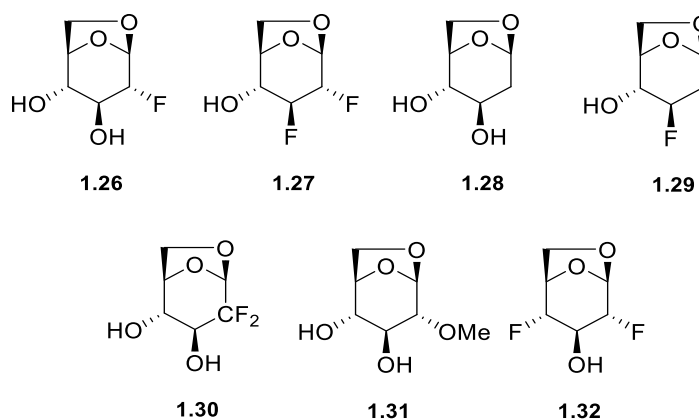
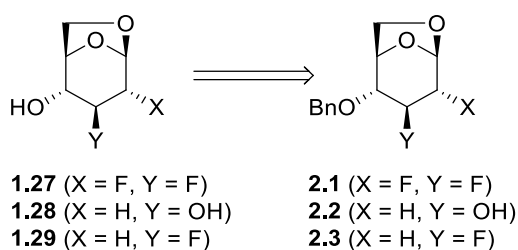


Figure 1.15: Levoglucosan derivatives considered for ^1H NMR analysis

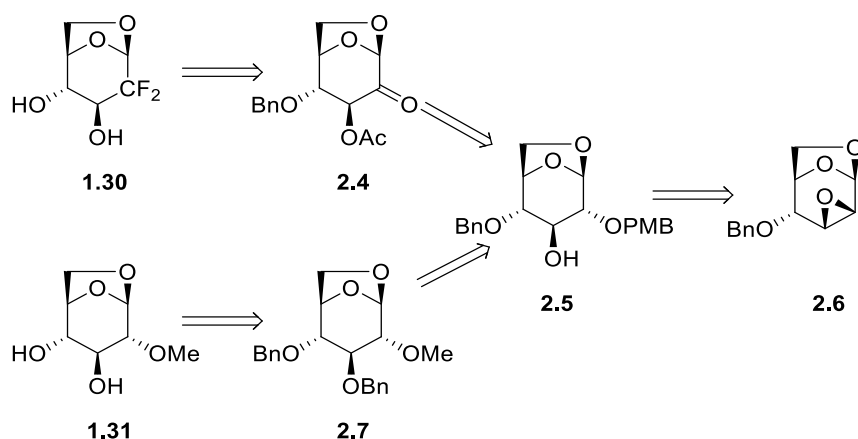
Apart from the 2-fluoro and the 2,4-difluoro levoglucosan derivatives **1.26** and **1.32**, which were available at the beginning of this project, the synthesis of the other targets was envisioned from levoglucosan derivatives generated during the syntheses of 2,3-dideoxy-2,3-difluoro **1.42** and 2,3-dideoxy-3-fluoro-D-glucopyranose (not shown), to which I contributed.⁴³

As detailed below (**Scheme 2.1**), 2,3-difluoro levoglucosan **1.27**, previously synthesised in our lab, as well as the 2-deoxy and 2-deoxy-3-fluoro levoglucosans **1.28** and **1.29** were readily accessible *via* hydrogenolysis of their 4-*O*-benzylated counterparts **2.1**, **2.2**, and **2.3**.



Scheme 2.1: Envisioned synthesis of compounds **1.27** to **1.29** from their 4-*O*-benzylated counterparts **2.1** to **2.3**

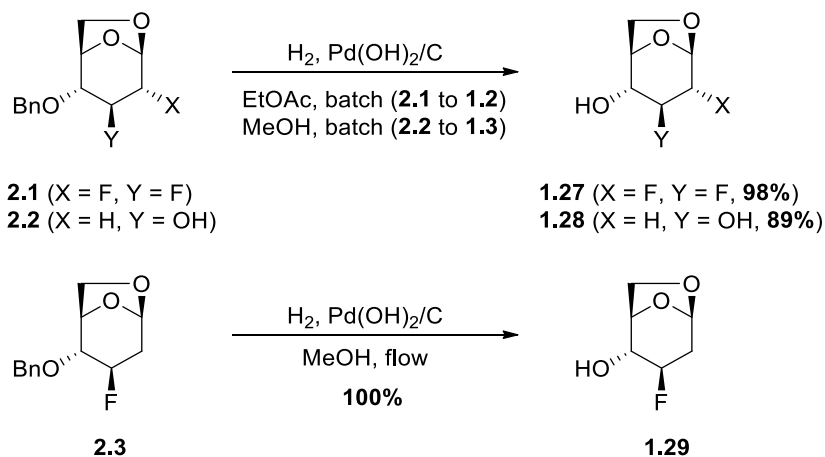
Synthesis of 2,2-difluoro levoglucosan **1.30** was envisioned *via* deoxofluorination of the 2-keto derivative **2.4**, prepared in 3 steps from 4-*O*-benzyl-2-*O*-(*p*-methoxybenzyl) (OPMB) levoglucosan **2.5** (Scheme 2.2). The latter resulting from the regioselective opening of the Černý epoxide **2.6** with *para*-methoxy benzyl alcoholate. The synthesis of 2-*O*-methoxy levoglucosan **1.31** was envisaged *via* hydrogenolysis of its 3,4-di-*O*-benzylated counterpart **2.7**, accessible in 3 steps from intermediate **2.5**.



Scheme 2.2: Retrosynthetic approach of 2-deoxy-2,2-difluoro levoglucosan **1.30** and 3-*O*-methoxy levoglucosan **1.31**

2.2 Synthesis of 2-deoxy-, 2-deoxy-3-fluoro-, and -2,3-difluoro levoglucosan

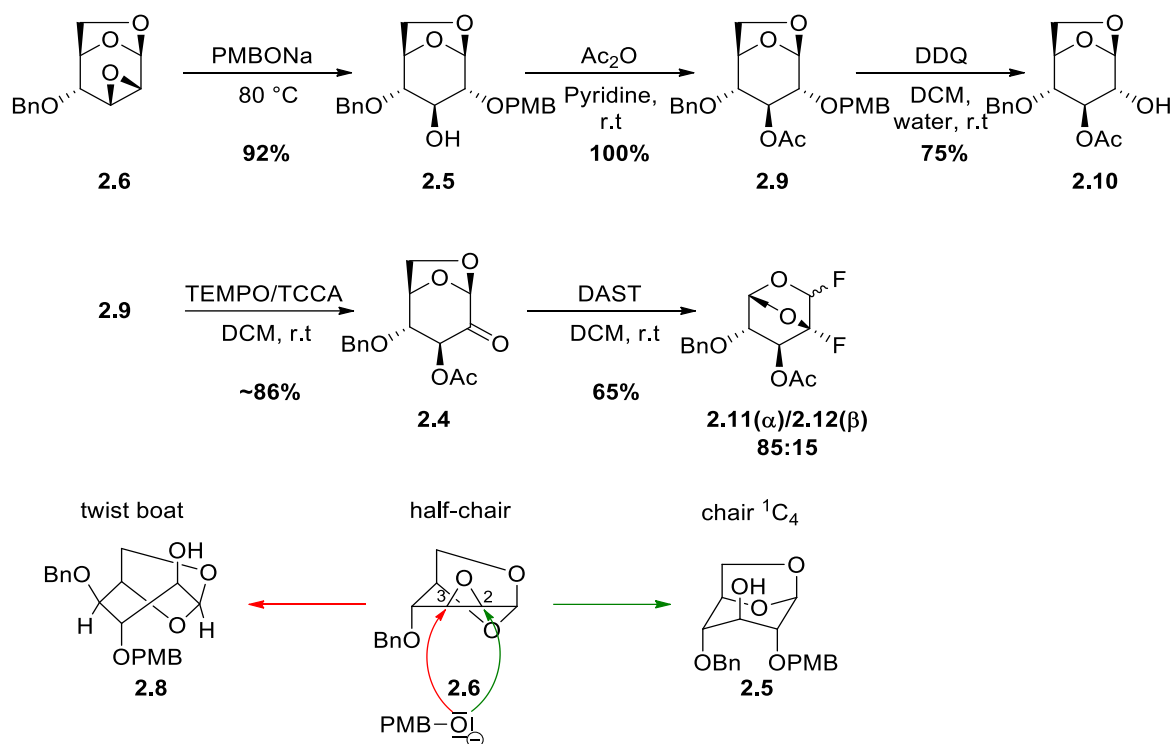
Pleasingly, hydrogenolysis of the 4-*O*-benzylated intermediates **2.1** and **2.2** using Pearlman's catalyst ($\text{Pd}(\text{OH})_2/\text{C}$) under batch conditions afforded the desired **1.27** and **1.28** in excellent yields (Scheme 2.3). Debenzylation of compound **2.3** was performed under flow conditions using a H-cube reactor fitted with a cartridge containing immobilised Pearlman's catalyst, which afforded target compound **1.29** in a quantitative yield.



Scheme 2.3: Hydrogenolysis of the levoglucosan derivatives **2.1** to **2.3**

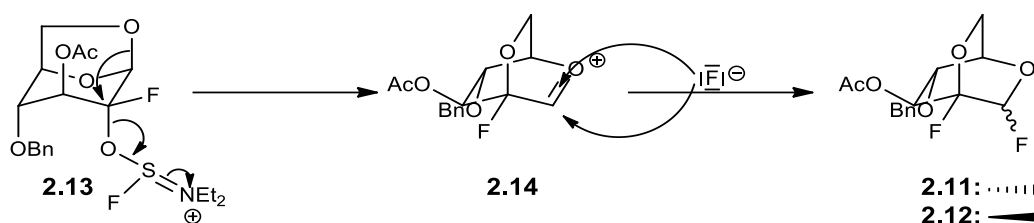
2.3 Attempted synthesis of 2-deoxy-2,2-difluoro levoglucosan **1.30**

Synthesis of 2-deoxy-2,2-difluoro levoglucosan **1.30** started by the reaction between the Černý epoxide **2.6** and sodium *p*-methoxy benzyl alcoholate, which produced exclusively the 2,4-protected levoglucosan **2.5** resulting from the C2 opening (92% yield, **Scheme 2.4**). Owing to its highly unstable twist boat conformation, compound **2.8** arising from the C3 opening of epoxide **2.6** was never observed (*cf* half chair transition state, Fürst-Plattner rule). The C3 hydroxyl in **2.5** was then acetylated to quantitatively afford the fully protected levoglucosan **2.9**. Subsequent treatment with dichlorodicyanoquinone (DDQ) enabled selective cleavage of the PMB protecting group to yield compound **2.10** (75%), which was subjected to oxidation conditions involving (2,2,6,6-tetramethylpiperidin-1-yl) oxyl (TEMPO), and trichloroisocyanuric acid (TCCA) as co-oxidant. The 2-keto derivative **2.4** was thus obtained containing only few impurities after workup, which was used in the next step without further purification (yield \approx 86%).



Scheme 2.4: Attempted synthesis of 2-deoxy-2,2-difluoro levoglucosan **1.30**

Then, difluorination of **2.4** with diethylaminosulfur trifluoride (DAST) afforded exclusively an inseparable α/β mixture of 2,6-anhydro mannosyl fluoride derivatives **2.11/2.12** (ratio 85:15, 65% yield). The obtention of both alpha and beta anomers indicates the formation of an oxonium intermediate **2.14**, presumably occurring from intermediate **2.13** in which the antiperiplanar relationship between the C1–O6 bond and the C2–O bond of the -OSFNEt₂ leaving group enable the C1→C2 migration of the anhydro bridge (**Scheme 2.5**).

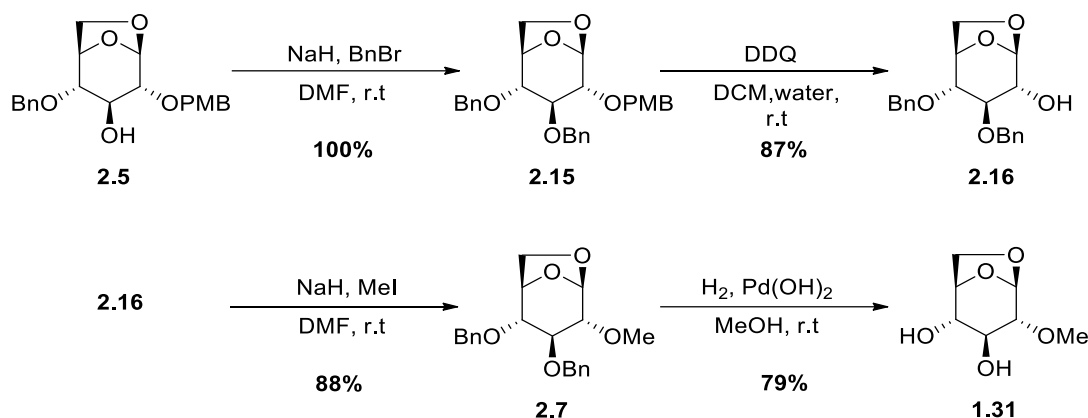


Scheme 2.5: Proposed mechanism for the 1,6-anhydro bridge migration leading to mannosyl fluorides **2.11** and **2.12**

Subsequent literature research revealed that similar rearrangements had been observed by Karban and co-workers while investigating the deoxofluorination of levoglucosan derivatives exhibiting a C2 axial hydroxyl.⁴⁴

2.4 Synthesis of 2-*O*-methoxy levoglucosan

Starting from compound **2.5**, benzylation afforded the fully protected levoglucosan **2.15** in a quantitative yield, from which the PMB group was cleaved using DDQ to give the 2,4-di-*O*-benzyl levoglucosan **2.16** (87% yield, **Scheme 2.6**). Treatment of the latter with methyl iodide (MeI) and NaH then enabled installation of the C2 methyl ether, thus giving access to compound **2.7** in a 88% yield. To finish, the benzyl ethers were removed under hydrogenolysis conditions with Pearlman's catalyst which afforded 2-*O*-methoxy levoglucosan **1.31** in a high yield (79%).



Scheme 2.6: Synthesis of 2-*O*-methoxy levoglucosan **1.31**

2.5 Analysis of the target compounds

2.5.1 Sample preparation

Prior to analysis, each of the target compounds were carefully chromatographed to clear any traces of impurities, and rigorously dried under high vacuum to remove all traces of organic solvents which

could have interfered with the intramolecular OH...F bonds. Once prepared, the CDCl₃ solutions containing the target compounds (7-19 mM) were further dried with 3 Å activated molecular sieves to suppress water-solute interactions, also highly disruptive for intramolecular OH...F bonds. This produced spectra such as the one recorded for the 2-fluoro levoglucosan derivatives **1.26** with no or few traces of water or polar solvents (**Figure 2.1**), from which both $^3J(\text{H}, \text{OH})$ and $^1J(\text{OH}, \text{F})$ values necessary to the description of the intramolecular H-bond interactions were obtained.

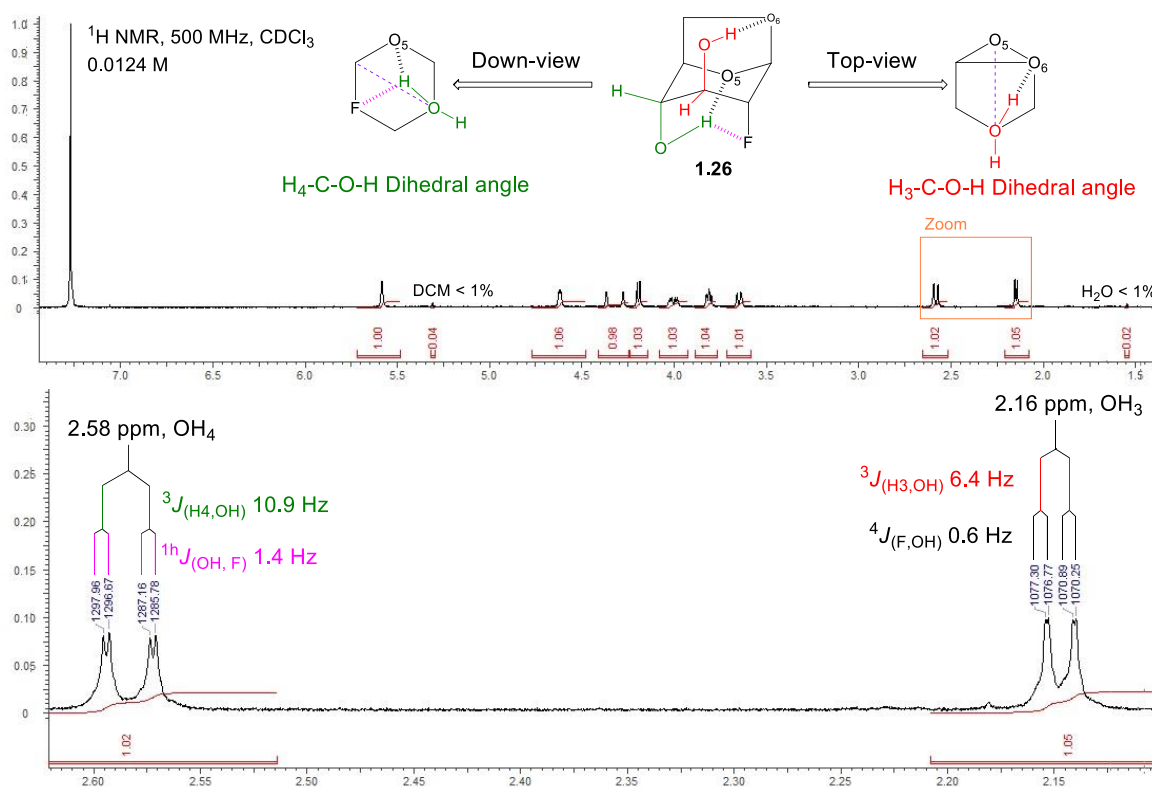


Figure 2.1: ^1H NMR analysis of **1.26** in CDCl₃ (12 mM)

It must however be noted that a control experiment in which a 7.5 mM solution of **1.26** was spiked with 1 equiv. of H₂O showed no change in the $^3J(\text{H4}, \text{OH})$ and $^1J(\text{OH}, \text{F})$ values, suggesting once again that the intramolecular OH...F interactions were not as weak as suggested in the literature, at least, not in the substrates investigated.

2.5.2 Description of the C4–OH intramolecular interactions

To facilitate comparison between the different compounds, the $^1J(\text{OH}, \text{F})$ and $^3J(\text{H4}, \text{OH})$ values recorded for each compound investigated are summarised in the figure next page (**Figure 2.2**).

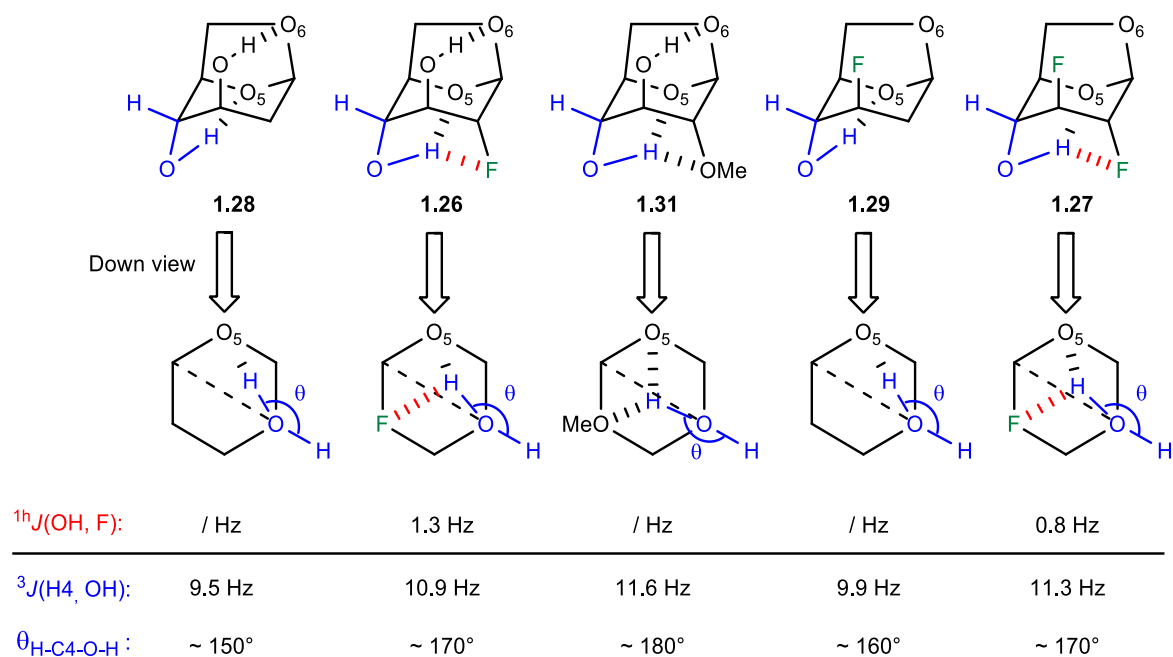


Figure 2.2: Intramolecular C4–OH...F–C2 bonds in levoglucosan derivatives **1.26** to **1.31** in CDCl_3

For compound **1.28**, bearing no competing acceptor at C2, the $^3J(\text{H4}, \text{OH})$ value of 9.5 Hz illustrated a geometry in which the C4–OH proton pointed directly towards O_5 , consistent with the divalent C4–OH... O_5 interaction expected for this compound. For compound **1.26**, with an axial fluorine at C2, the increased $^3J(\text{H4}, \text{OH})$ value of 10.9 Hz indicated a longer C4–OH... O_5 distance implying a bifurcated H-bond with C2–F as a competing acceptor. This was also evidenced by the $^1J(\text{OH}, \text{F})$ coupling, which given its low value of 1.3 Hz suggested a geometry with the C4–OH proton pointing toward the O_5 (weak OH...F interaction). It is interesting to note that no $^1J(\text{OH}, \text{F})$ coupling could be observed on **1.26** when previously analysed by Widmalm and co-workers.⁴⁵ Analysis of compound **1.31**, presenting an axial C2 methoxy group, revealed a further increased $^3J(\text{H4}, \text{OH})$ value of 11.6 Hz indicative of a *quasi*-symmetric bifurcated H-bond, resulting from a further lengthening of the C4–OH... O_5 distance. Given the strong accepting capacities of methoxy groups, it was assumed that C2–OMe was a better acceptor than O_5 and hence that the $^3J(\text{H4}, \text{OH})$ value of 11.6 Hz corresponded to a $\theta_{\text{H-C3-O-H}}$ dihedral angle of different sign, corresponding to a geometry with the C4–OH proton pointing slightly toward C2–OMe.

As expected, compound **1.29** exhibited a $^3J(\text{H4}, \text{OH})$ value below 10 Hz indicative of a divalent C4–OH... O_5 interaction, coherent given the absence of acceptor at C2. Concerning compound **1.27**, in which a fluorine was incorporated at C2, the increased $^3J(\text{H4}, \text{OH})$ value of 11.3 Hz attested of a bifurcated H-bond involving C2–F and O_5 acceptors, further evidenced by the $^1J(\text{OH}, \text{F})$ of 0.8 Hz. The latter also indicated a OH...F bond significantly weaker than in **1.26**, this presumably due to the decreased H-accepting capacities of C2–F entailed by the strong electro-withdrawing effect of C3–F (*cf* **Figure 1.13**). However, as indicated by the $^3J(\text{H4}, \text{OH})$ value of 11.3 Hz corresponding to an almost symmetrical bifurcated H-bond, this weak OH...F interaction seemed to be defined by a

shorter OH...F distance than in **1.26**. As mentioned by Bernet and Vasella, such incoherence could be due to perturbations caused by the polar substituent surroundings C4–OH, not taken into consideration in the Karplus equation of Fraser, that could have altered the vicinal $^3J(\text{H4}, \text{OH})$ coupling.³⁴

It is noteworthy that the decreased $^1J(\text{OH}, \text{F})$ value recorded for 2-fluoro levoglucosan **1.26** (1.3 Hz) compared to **1.19** (1.8 Hz), analysed by Bernet and co-workers, indicated a weakened O–H...F interaction (**Figure 2.3**). This was attributed to a decreased electronic density in the C2–F bond compared to the C4–F bond, resulting from the polarisation of the C1–O₆ bond (hyperconjugation, *cf* **Figure 1.13**)

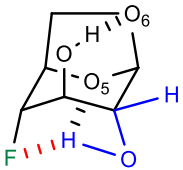
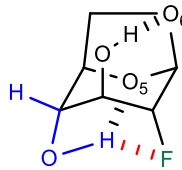
		
	1.19	1.26
$^1J(\text{OH}, \text{F})$:	1.8 Hz	1.3 Hz
$^3J(\text{H}_4, \text{OH})$:	11.5 Hz	10.9 Hz
$\theta_{\text{H-C-O-H}}$:	$\sim 180^\circ$	$\sim 170^\circ$

Figure 2.3: Comparison of the O–H...F interactions in **1.19** and **1.26**

2.5.3 Description of the C3–OH intramolecular interactions

The different $^3J(\text{H3}, \text{OH})$ values recorded for each compound investigated are summarised in the figure below (**Figure 2.4**).

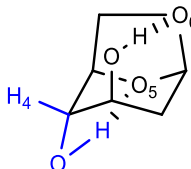
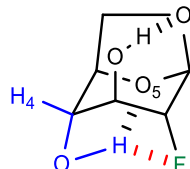
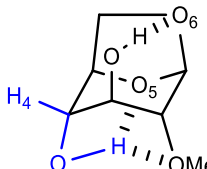
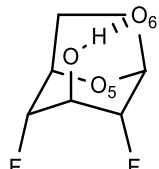
				
1.28	1.26	1.31	1.32	
$^3J(\text{H4}, \text{OH})$:	7.6 Hz	6.4 Hz	7.7 Hz	6.1 Hz

Figure 2.4: Intramolecular C3–OH...O₆ bonds in levoglucosan derivatives in CDCl₃

For all these compounds, the C3–OH groups are engaged in intramolecular H-bonds with O₆, resulting in $\theta_{\text{H-C3-O-H}}$ dihedral angles around 140–150°. As a consequence, the experimental coupling constants $^3J(\text{H3}, \text{OH})$ observed were significantly lower than the $^3J(\text{H4}, \text{OH})$, with values close to 8.0 Hz for compounds **1.28** and **1.31**. Interestingly, for the two deoxofluorinated derivatives **1.26** and **1.32**, further decreased $^3J(\text{H3}, \text{OH})$ values around 6.0 Hz were observed despite the fact their $\theta_{\text{H-C3-O-H}}$

O-H angles were not expected to be different to those exhibited by **1.28** and **1.31**. Once again, this could have been attributed to the presence of polar substituents surrounding the C3-OH, not considered in the Karplus equation of Fraser, decreasing the vicinal couplings $^3J(\text{H3}, \text{OH})$.

2.5.4 Conclusions

Our results complement and augment the conclusions drawn by Bernet and co-workers, that the weak intramolecular $\text{OH}\cdots\text{F}$ interactions can perturb stronger $\text{OH}\cdots\text{O}$ interactions. Also, the comparison between 2-fluoro-levoglucosan **1.26** and 4-levoglucosan **1.19** once more stressed out the impact of the neighbouring substituent on the H-accepting capacities of C-F bonds (*cf* **Figure 2.3**)

Chapter 3: Synthesis of 2,3,4-trideoxy-2,3,4-trifluoro-D-glucopyranose

3.1 Objectives

The main aim of this project was to synthesis 2,3,4-trideoxy-2,3,4-trifluoro-D-glucopyranose **1.37**, here further referred to as trifluoro glucose (**Figure 3.1**), on a sufficient quantity to conduct the EXSY experiments necessary to determine its exchange rate across the RBC membranes (± 150 mg, cf section **1.4.3**).

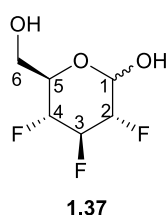


Figure 3.1: Trifluoro glucose **1.37**

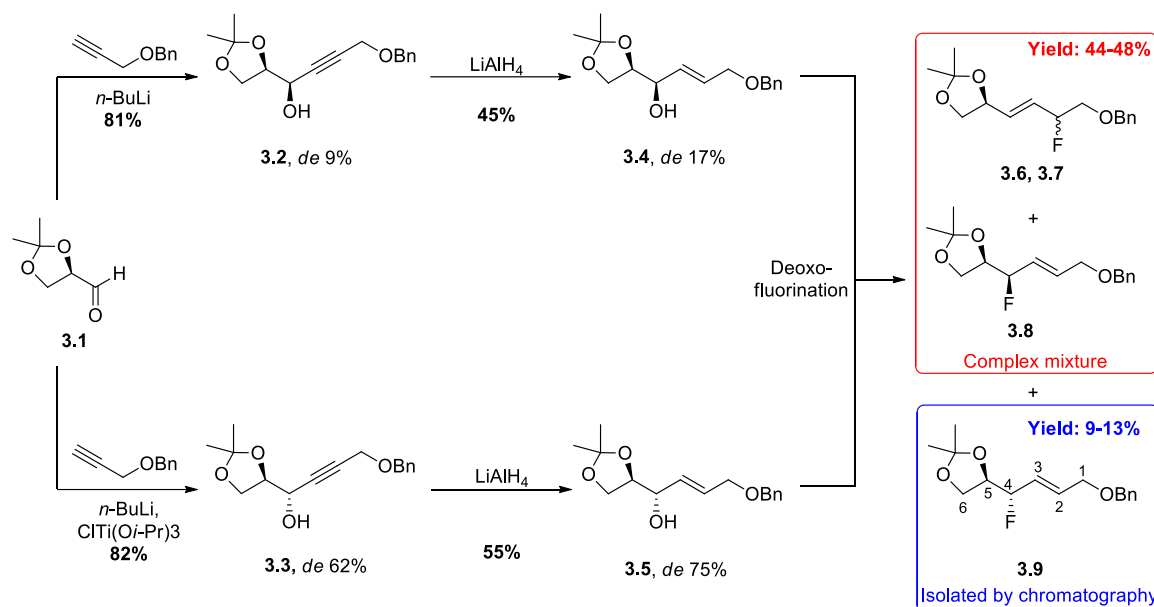
3.2 Previous syntheses of 2,3,4-trifluoro-D-glucopyranose

3.2.1 Synthesis from D-glyceraldehyde acetonide

The first synthesis of trifluoro glucose **1.37** was achieved by O'Hagan and co-workers starting from the advanced intermediate **3.9**, a compound isolated while investigating the deoxofluorination of the allylic alcohol mixtures **3.4** and **3.5** (**Scheme 3.1**).^{46,41} To facilitate the description of the synthesis, the carbons of the precursors are numbered according to their future position on the target sugar (see compound **1.37**).

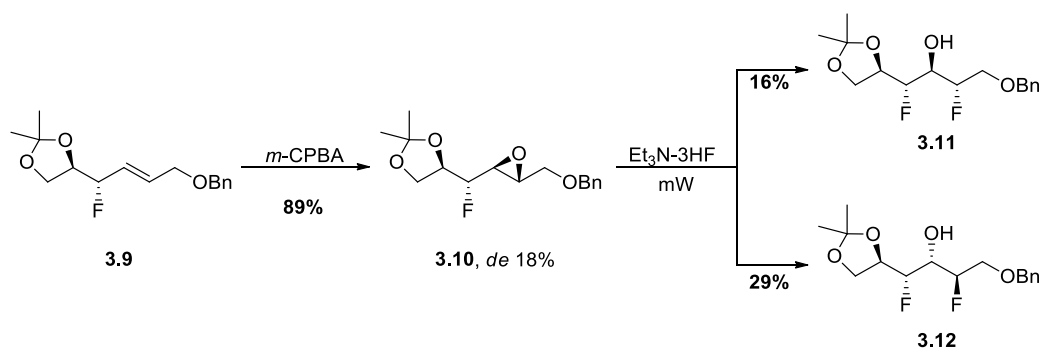
The first step toward the synthesis of the alcohol mixture **3.4** and **3.5** consisted in a reductive coupling between aldehyde **3.1** and benzyl propargyl ether. When performed under chelation-control conditions, the coupling occurred with a poor selectivity toward the *syn*-diastereoisomer **3.2** (*de* 9%). Similar conditions involving triisopropoxytitanium chloride seemed to disfavour the lithium chelation and afforded the *anti*-diastereoisomer **3.3** in a relatively high diastereomeric excess (*de* 62%). Propargylic reduction then exclusively led to the (*E*)-allylic alcohol mixture **3.4** and **3.5**, which were next treated with various deoxofluorinating reagents among which DAST, Deoxo-Fluor and TFEDMA. After reaction, several regio- and diastereoisomers were identified, among which the α -fluoroalkenes **3.8** and **3.9** resulting from the deoxofluorination of the C4 hydroxyl, and the α -fluoroalkenes **3.6** and **3.7** for which the fluorine insertion occurred at C2 after migration of

double bond.⁴⁷ This led O'Hagan and co-workers to propose the formation of a carbocation intermediate during reaction, and hence at the presence of a significant S_N1 type component of the deoxyfluorination mechanism.⁴⁷ While none of the conditions attempted could afford the α -fluoroalkene **3.9** in a decent yield, it was the only product which could be isolated pure by column chromatography.



Scheme 3.1: Synthesis of α -fluoroalkene **3.9** from D-glyceraldehyde acetonide **3.1**

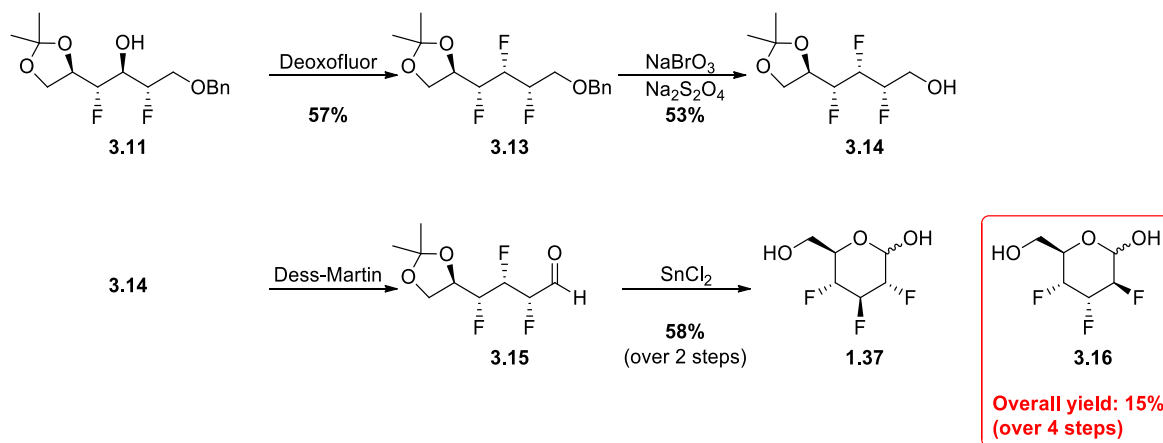
From α -fluoroalkene **3.9**, O'Hagan and co-workers then designed a synthesis giving access to the trifluoroglucose **1.37** and altrose **3.16** (Schemes 3.2 and 3.3).⁴¹



Scheme 3.2: Synthesis of 1,3-difluorohydrins **3.11** and **3.12** from α -fluoroalkene **3.9**

In the first step, fluoroalkene **3.9** was oxidised using *meta*-chloroperoxybenzoic acid (*m*-CPBA) to give epoxide **3.10** (*de* 18%), which upon treatment with triethylamine trifluoride ($\text{Et}_3\text{N}\cdot 3\text{HF}$) was regioselectively opened at C2 to give a mixture of 1,3-difluorohydrins **3.11** and **3.12**, which were separated by column chromatography.

To complete the synthesis of trifluoro glucose **1.37** (**Scheme 3.3**), 1,3-difluorohydrin **3.11** was first treated with deoxofluor to generate the trifluorinated derivatives **3.13**, then subjected to mild oxidative conditions which enabled cleavage of the benzyl ether and afforded fluorohydrin **3.14**.⁴⁸ The primary hydroxyl thus revealed was then oxidised into the corresponding aldehyde **3.15** which, due to its low stability, was directly engaged in the last step consisting of the acetonide cleavage. Once deprotected, the C5 hydroxyl then spontaneously reacted with the aldehyde to yield the 2,3,4-trifluoro glucose as its pyranose form **1.37**. Following the exact same 4 steps sequence, 1,3-difluorohydrin **3.12** was converted into the 2,3,4-trifluoro altrose **3.16**.



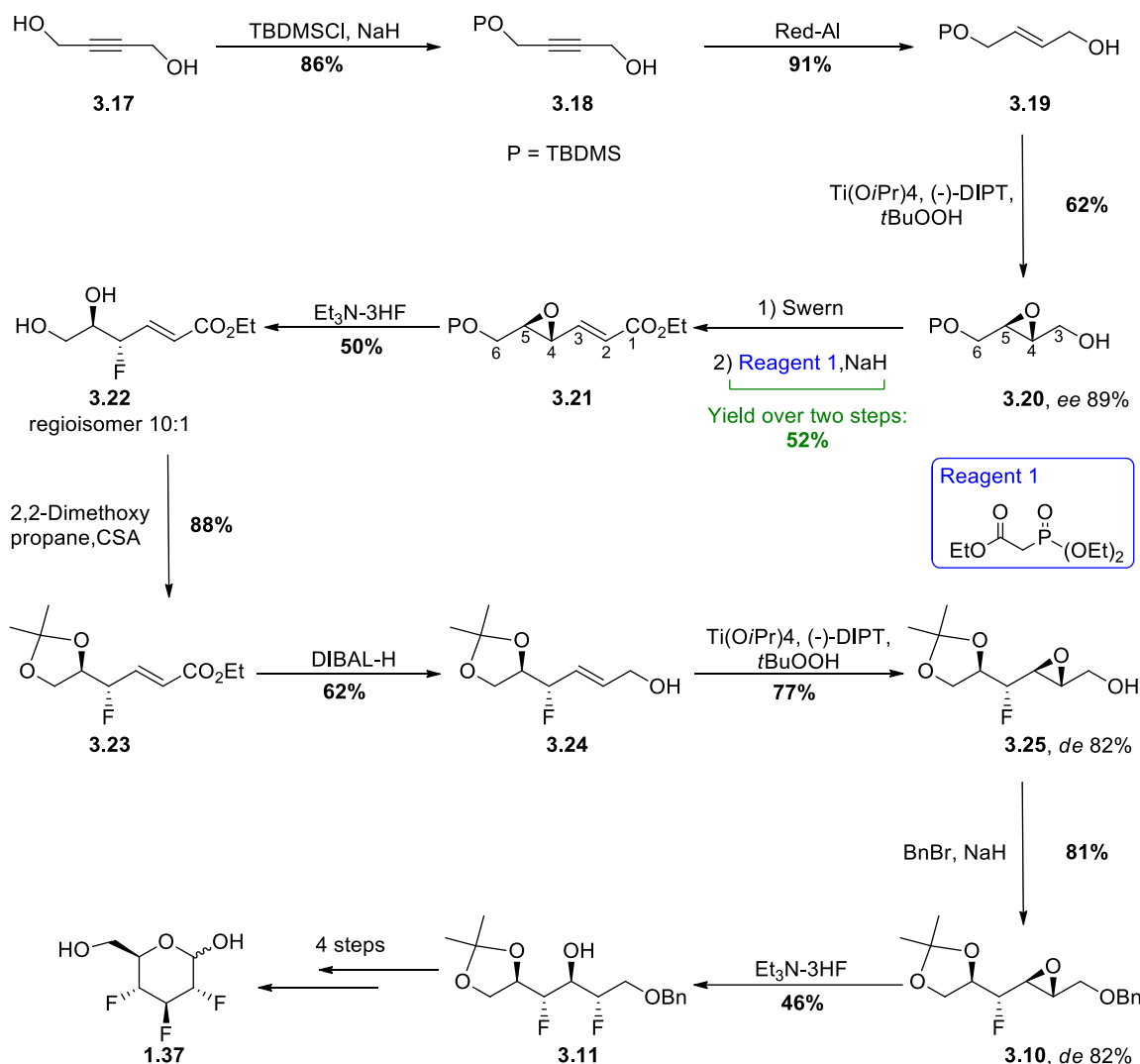
Scheme 3.3: Synthesis of trifluoro glucose **3.16** from 1,3-difluorohydrins **3.11**

Even if quite innovative in the landscape of fluorosugar synthesis, this route was deemed too lengthy and presented too many low yielding steps to be suitable for the synthesis of trifluoro glucose **1.37** on a hundred milligram scale. It is clear at first sight that insertion of the C2 and C4 fluorine atoms, respectively effected through deoxofluorination of the allyl alcohols mixtures **3.3/3.5** and opening of epoxide **3.10**, constitute the main weakness of this synthesis. Also, besides being low yielding, all the steps necessary to the conversion of epoxide **3.10** into trifluoro glucose **1.37** are only described in small scales (100 mg or less).

3.2.2 Synthesis from butynediol

A few years later, a second synthesis of trifluoro glucose **1.37** was published by O'Hagan and co-workers (**Scheme 3.4**).⁴⁹ This alternative synthesis started by the conversion of the commercial butynediol **3.17** into the monosilylated species **3.18**, on which the alkyne function was reduced using Red-al to give exclusively the *trans*-allylic alcohol **3.19**. Subsequently, asymmetric epoxidation following Sharpless conditions afforded the desired epoxide **3.20** in a good enantiomeric excess (89%). Following oxidation of the C3 hydroxyl into the corresponding aldehyde, compound **3.20** was engaged in a Horner-Wadsworth-Emmons olefination enabling installation of the C1 and C2 carbons, upon which the α,β -unsaturated ester **3.21** was obtained. In the next step, treatment with Et_3N -

3HF allowed both cleavage of the tert-butyldimethylsilyl ether and C4 selective insertion of fluorine, hence affording almost exclusively regioisomer **3.22**. Acetonide protection of the terminal diol followed by reduction of the ester function using diisobutylaluminium hydride (DIBAL-H) then gave access to the allyl alcohol **3.24**, which following Sharpless asymmetric epoxidation was converted into the desired epoxide **3.25** (*de* 82%). At this stage, the C1 hydroxyl was protected as a benzyl ether to give compound **3.10**, then treated with Et₃N-3HF to yield the 1,3-difluorohydrin **3.11**, which ultimately was converted into trifluoro glucose **1.37** as described in the previous synthesis (**Scheme 3.3**).



Scheme 3.4: Synthesis of trifluoro glucose **1.37** from butynediol **3.17**

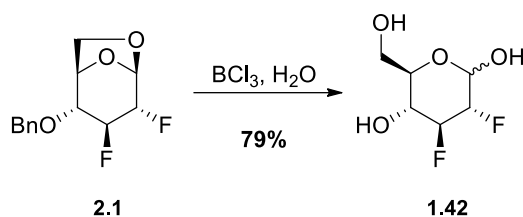
By proceeding through the selective opening of epoxide **3.21** with Et₃N-3HF, reported in a 50% yield, the low yielding deoxofluorination step (13%) previously required to insert the C4 fluorine could be avoided. Also, insertion of the C2 fluorine *via* selective opening of epoxide **3.10** could be significantly improved by generating the epoxide substrate in an asymmetric fashion (*de* 82%). However, despite these ameliorations, this alternative synthetic route was five steps longer than

the previous one, and resulted in a similar efficiency (overall yield $\approx 0.2 - 0.3 \%$). Hence, this route was not considered for the synthesis of trifluoro glucose **1.37** on a hundred milligrams scale.

3.3 New strategy for the synthesis of 2,3,4-trifluoro-D-glucopyranose

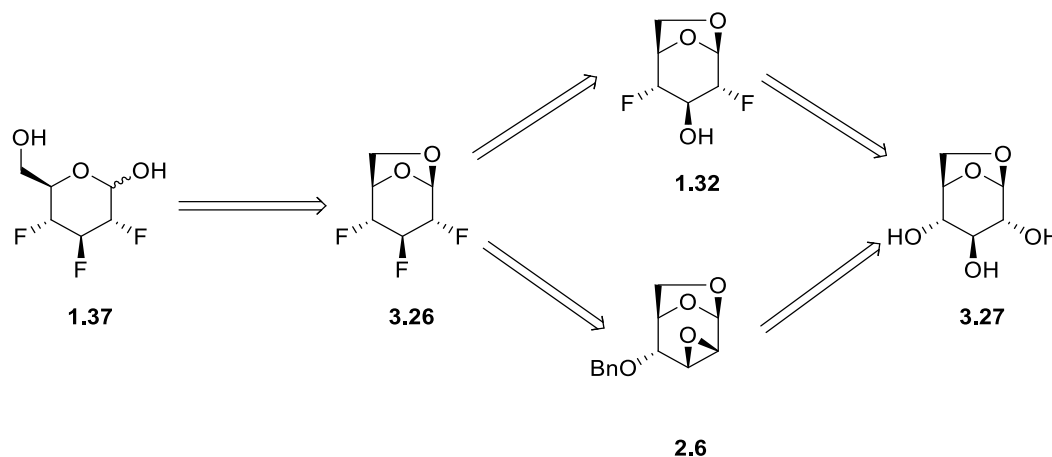
3.3.1 Retrosynthetic overview

Given the good results reported for the anomeric hydrolysis of the levoglucosan derivatives **2.1** to access 2,3-difluoro glucose **1.42** (Scheme 3.5),⁴³ we envisioned that trifluoro glucose **1.37** could be obtained in a similar fashion from trifluoro levoglucosan **3.26** (Scheme 3.6).



Scheme 3.5: Anomeric hydrolysis of 4-*O*-benzyl-2,3-difluoro levoglucosan **2.1**

As detailed below, synthesis of trifluoro levoglucosan **3.26** was envisaged *via* retentive deoxofluorination of 2,4-difluoro levoglucosan **1.32** which, following reported procedures,^{50,51,52} could be prepared from the commercial and cheap levoglucosan **3.27**.

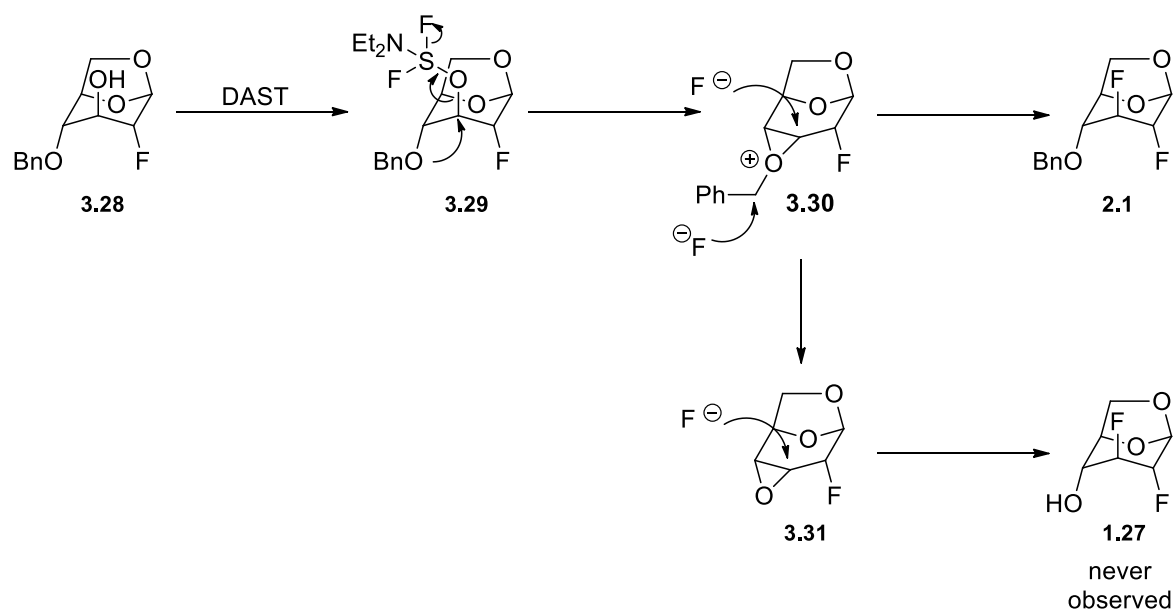


Scheme 3.6: Retrosynthetic approach of trifluoro glucose **1.37**

Alternatively, trifluoro levoglucosan **3.26** could be prepared following a synthesis reported by Sarda and co-workers starting from the Černý epoxide **2.6**,⁵³ a compound easily accessible from levoglucosan **3.27**.⁵²

3.3.2 Retentive deoxofluorination on levoglucosan derivatives

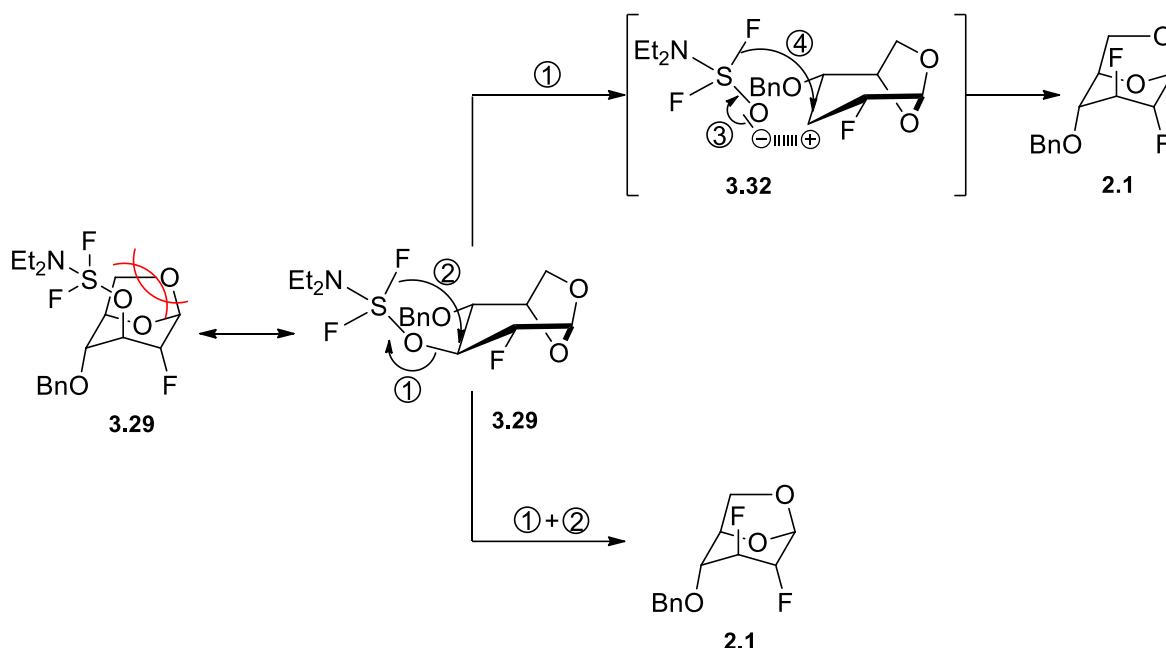
It is well assumed in the existing literature that the retentive deoxofluorination of the 2-fluoro levoglucosan derivatives **3.28** is induced by a participation from the neighbouring benzyl ether.^{43,54} As shown below (**Scheme 3.7**), such contribution would lead to the formation of oxiranium **3.30**, which then would be selectively opened at C3 to afford the desired 2,3-difluoro levoglucosan derivatives **2.1** (chairlike transition state *cf* **Scheme 2.4**). However, the highly reactive benzylic position of the oxiranium intermediate **3.30** could also undergo a fluoride attack to give the fluoro epoxide **3.31**. The latter could either be left unreacted or, most probably, be cleaved at C3 by a fluoride to give the 2,3-difluoro levoglucosan **1.27**. However, when performed in our group, the deoxofluorination of **3.30** always gave **2.1** as a single product and this in high yields (79-86%), thus questioning the occurrence of such mechanism.



Scheme 3.7: Mechanism initially proposed for the retentive deoxyfluorination of compound **3.28**

Instead, an alternative mechanism recently proposed by Horník and co-workers was considered (**Scheme 3.8**).⁵⁴ The latter suggests that due to important steric clashes between the 1,6-anhydro bridge and the bulky DAST adduct, intermediate **3.29** would be forced into a boat like conformation in which the antiperiplanar relationship between the benzyl ether and the DAST adduct no longer exists, thus preventing a potential anchimeric assistance. The stereoselective insertion of the C3 fluorine would instead proceed *via* a nucleophilic substitution with internal return (S_Ni) mechanism, existing in two slightly different versions. The first involving a concerted process (①+②), and the second the generation of a tight ion pair (①). In this second mechanism, the spontaneous departure of the DAST adduct would lead to intermediate **3.32**, on which two fragments oppositely charged hold tight together through important electrostatic interactions. The negatively charged

leaving group would then release a nucleophilic fluorine which would attack the carbocation from the same face from which the leaving group was expelled.



Scheme 3.8: Retentive deoxofluorination *via* S_Ni mechanism

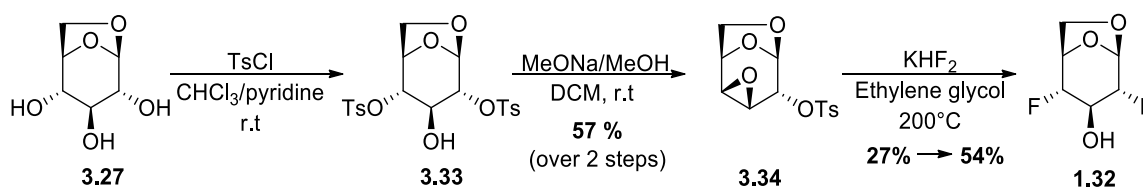
Ultimately, these observations convinced us that a retentive deoxofluorination on 2,4-difluoro levoglucosan **1.32** would be possible, and this despite the inability of the $-CF$ bonds flanking the hydroxyl to provide anchimeric assistance.

3.4 New synthesis of 2,3,4-trifluoro-D-glucopyranose

3.4.1 Synthesis of 2,3,4-trifluoro levoglucosan *via* C3 fluorination of 2,4-difluoro levoglucosan and levoallosan

3.4.1.1 Synthesis of 2,4-difluoro-levoglucosan

The synthesis of trifluoro glucose **1.37** proposed by our team started by the large scale synthesis of tosyl-epoxide **3.34** following a procedure reported by Rasmussen and co-workers (**Scheme 3.9**).⁵²



Scheme 3.9: Synthesis of 2,4-difluoro levoglucosan **1.32**

At first, treatment of levoglucosan **3.27** with tosyl-chloride in presence pyridine afforded the crude 2,4-ditosyl levoglucosan **3.33** which, without further purification, was subjected to basic conditions that yielded exclusively the tosyl epoxide **3.34**, obtained as a pure material after recrystallisation from cold solvents (overall yield: 57 %, m= 21 g).

Concerning the epoxidation step, the selectivity toward **3.34** was explained through the effects of hyperconjugation on both C2-OTs₂ and C4-OTs₄ bonds. As illustrated below (**Figure 3.2**), regarding a matter of bond polarisation, the electronic delocalisation from the C5-C6 bonding orbital ($\sigma_{\text{C5-C6}}$) to the C4-OTs₄ anti-bonding orbital ($\sigma^*_{\text{C4-OTs4}}$) is more efficient than the delocalisation from the $\sigma_{\text{C1-O}}$ to the $\sigma^*_{\text{C2-OTs2}}$. Ultimately, this results in the C4-OTs₄ bond being longer and weaker than the C2-OTs₂, and therefore more readily broken upon attack from the C3 alcoholate on intermediate **3.35**.

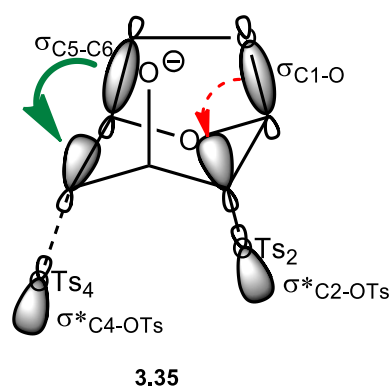


Figure 3.2: Impact of hyperconjugation on C4-OTs₄ and C2-OTs₂ bonds (lengths exaggerated)

As reported by Pacák and co-workers, treatment of tosyl epoxide **3.34** with potassium hydrogen difluoride (KHF₂) in refluxing ethylene glycol didn't produce any selective C4 fluorination, but instead afforded the 2,4-difluoro levoglucosan **1.32** in 27% yield.⁵⁰ Even if achieved in a much higher yield than Pacák and co-workers (5%), the di-fluorination step remained considerably low yielding and was therefore considered for further optimisation (**Table 3.1**). At first, the Pacák conditions were repeated on similar scales to assess the reproducibility of the results (**Entry 1 and 2**). Interestingly, similar yields were obtained with anhydrous and wet solvents.

Table 3.1: Difluorination of tosyl epoxide **3.34**

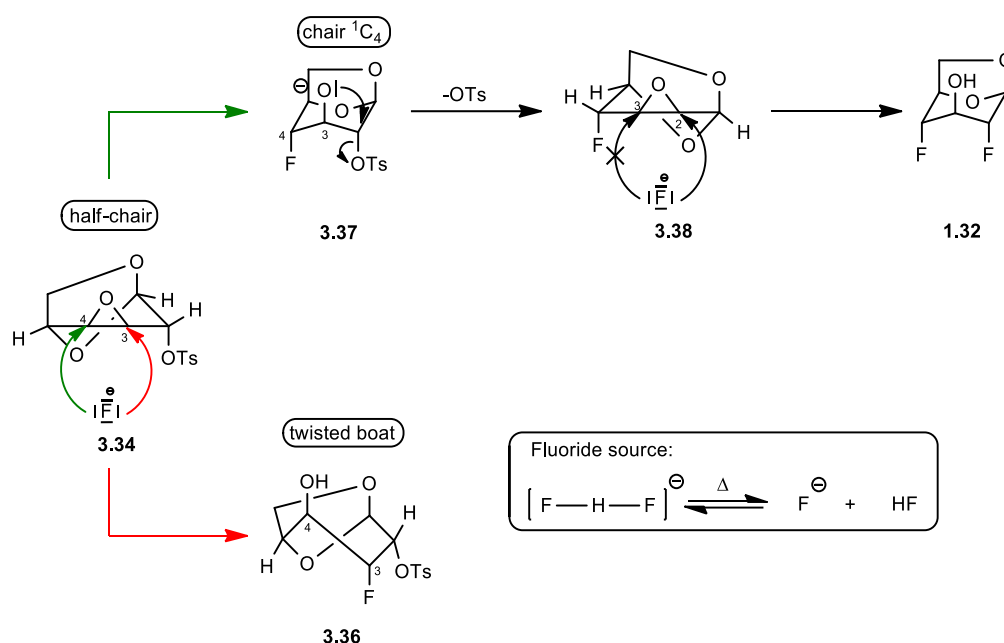
Entry	Conditions	m 3.34 (g)	KHF ₂ :KF (equiv.)	T (°C)	Time (min)	Yield (%)
1	Batch (wet)	0.1	16:0	200	90	27
2	Batch (dry)	0.2	16:0	200	90	24

3	Microwave	0.2	5:0	200	30	/
4	Microwave	0.2	5:0	150	5	/
5	Microwave	0.2	5:0	100	5	/
6	Batch	0.5	16:0	200	90	22
7	Batch	1.0	16:0	200	90	24
8	Batch	2.0	16:0	200	120	16
9	Batch (dry)	1.0	6:6	170	120	11
10	Batch (wet)	1.0	6:6	170	120	34
11	Batch (wet)	2.0	6:6	170	120	46
12	Batch (wet)	4.0	6:6	170	120	54

In view of the good results reported for the opening of the Černý epoxide using KHF_2 under microwave irradiation, similar conditions were attempted on tosyl epoxide **3.34** (**Entry 3 to 5**).⁵⁵ Being only poorly soluble in ethylene glycol and this even at high temperatures, KHF_2 was engaged in reduced excess to avoid the heterogeneous mixture observed with the previous conditions, potentially hazardous if handled under microwave irradiation. Presumably due to the steep temperature gradient resulting from the first temperature conditions investigated, only degradation products were observed by ^{19}F NMR (**Entry 3**). Despite the milder temperature conditions investigated next, conditions involving micro-wave irradiation led exclusively to complex mixtures of degradation products (**Entry 4 and 5**), and were hence no further investigated. Instead, Pacák conditions were upscaled to produce enough 2,4-difluoro levoglucosan **1.32** to investigate the next steps of the synthesis. Pleasingly, the reaction could be transposed to a gram scale with no apparent decreases in yield (**Entry 6 and 7**). However, a further increase in scale up to 2 g resulted in a slight decrease in yield accompanied by an increase in reaction time (**Entry 8**). Ultimately, a similar procedure using a mixture of KHF_2 and potassium fluoride (KF) as fluoride source was investigated.³⁴ When conducted under anhydrous conditions, this procedure led only to a reduced yield in 2,4-difluoro levoglucosan **1.32** of 11% (**Entry 9**), which increased up to 34% upon utilisation of wet solvent (**Entry 10**). On initial consideration, the presence of a polar protic solvent such as water, potential competing nucleophile, seems counter-intuitive to favouring the nucleophilic attack of fluoride. Furthermore, the presence of polar protic species were expected to help the solvation of the fluoride, and therefore hamper their nucleophilic character. However,

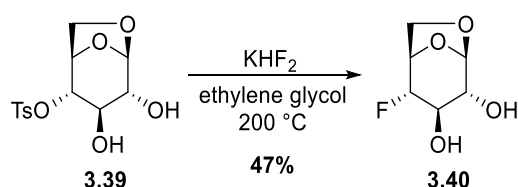
these negative effects could have been counterbalanced by the ability of water to solubilise both KF and KHF_2 salts, which potentially allowed to release a larger quantity of fluoride anion in the reaction mixture. Pleasingly, higher yields were obtained upon upscaling (**Entry 11** and **12**).

To explain the sequential insertion of two fluorine atoms, the following mechanism was proposed (**Scheme 3.10**).



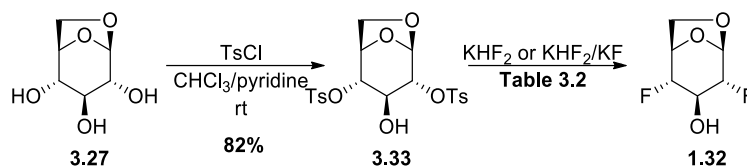
Scheme 3.10: Proposed mechanism for the 2,4-difluorination of tosyl epoxide **3.34**

Given the highly unstable twist boat conformation that would result from a C3 fluoride insertion on **3.34** (compound **3.36**), this reaction was never observed. Instead, the C4 fluoride attack is preferred, for which compound **3.37** presenting a stable 1C_4 conformation is obtained (*cf* half chair transition, Fürst-Plattner rule). The resulting C3 alcoholate then would displace the vicinal tosyl to afford the fluoro epoxide **3.38**, which would selectively be opened at C2 to give 2,4-difluoro levoglucosan **1.32** (Fürst-Plattner rule). A similar mechanism had already been advanced by Barford and co-workers to explain the formation of 4-fluoro levoglucosan **3.40** following treatment of its 4-tosylated counterpart **3.39** with KHF_2 (**Scheme 3.11**).⁵⁶



Scheme 3.11: Formation of 4-fluoro levoglucosan **3.40** *via* treatment of 4-tosyl levoglucosan **3.39** with KHF_2

Given the clean retention of configuration observed for this reaction, it was anticipated that similar conditions could afford 2,4-difluoro levoglucosan **1.32** starting from 2,4-ditosyl levoglucosan **3.33** (Scheme 3.12, Table 3.2). The latter was prepared from levoglucosan **3.27** as described for the synthesis of tosyl epoxide **3.34** (Scheme 3.9), and purified by column chromatography (82% yield).



Scheme 3.12: Synthesis of 2,4-difluoro levoglucosan **1.32** from 2,4-ditosyl levoglucosan **3.33**

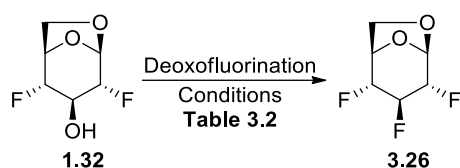
Pleasingly, 2,4-difluoro levoglucosan **1.32** could be observed by ^{19}F NMR on the crude mixture resulting from treatment of 2,4-ditosyl levoglucosan **3.33** with KHF_2 at 200 °C (Entry 1).⁵⁰ However, given the loss in molecular weight resulting from this transformation, as well as the small scale investigated, **1.32** could not be isolated. Then, difluorination was investigated in a slightly larger scale using the mixture $\text{KHF}_2\text{:KF}$ as source of fluoride (Entry 2). Conditions for which the desired **1.32** was obtained in a promising yield of 50%.³⁴ Subsequently, similar conditions were examined starting from about 6 g of di-tosyl levoglucosan **3.33**, and resulted in a slightly reduced yield of 35% (Entry 3). Despite being observed following upscaling of the reaction, such decrease in yield was not imputed to the poor mixing or heating transfer inherent to larger reaction environment, but instead to the slightly impure batch of di-tosyl levoglucosan **3.33** used in these conditions. Assumption ascertained in the next experiment where a yield of 56% in **1.32** was achieved starting from slightly more than 8 g of pure **3.33** (Entry 4).

Table 3.2: Difluorination of 2,4-ditosyl levoglucosan **3.33**

Entry	Conditions	$m_{3.33}$ (g)	$\text{KHF}_2\text{:KF}$ (equiv.)	T (°C)	Time (min)	Yield (%)
1	Batch (wet)	0.1	16:0	200	120	Traces
2	Batch (wet)	0.2	6:6	200	120	50
3	Batch (wet)	6.3	6:6	170	120	35
4	Batch (wet)	8.3	6:6	170	120	56

3.4.1.2 Attempted C3 fluorination *via* deoxofluorination of 2,4-difluoro levoglucosan

With 2,4-difluoro levoglucosan **1.32** in hand, deoxofluorination was then investigated (**Scheme 3.13**, **Table 3.3**).



Scheme 3.13: Deoxofluorination of 2,4-difluoro levoglucosan **1.32**

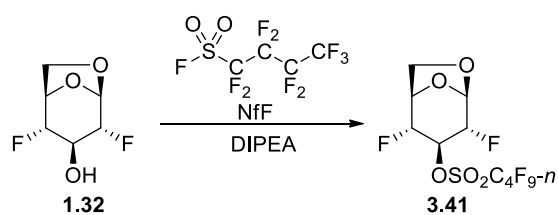
It is noteworthy that trifluoro levoglucosan **3.26** being a volatile compound, all the experiments presented in this section had to be performed in sealed tube reactors, and the reaction and extraction solvents carefully evaporated under controlled pressure (500 mmHg). At first, conditions similar to those reported by Sarda and co-workers for the deoxofluorination of levoglucosan derivatives were investigated (**Entry 1**).⁵³ After 3 days of reaction, TLC revealed the formation of a single product of high retention factor (*R_f*) which could have corresponded to trifluoro levoglucosan **3.26**. However, multiple spots were observed on the TLC run prior to purification by column chromatography, indicating that the product formed had been degraded upon workup. This potentially being due to the release of hydrogen fluoride (HF) occurring while quenching DAST with methanol. Hence, the reaction was instead quenched in a large volume of saturated bicarbonate solution, a method known to limit the release of HF. Unfortunately, this afforded similar results than with the methanol quenching. Then, deoxofluorination conditions involving neat DAST at room temperature were investigated (**Entry 2**). After 8h of reaction, a product of similar *R_f* as the one formed in the previous conditions could be observed by TLC. Instead of quenching the reaction and risking the degradation of the product formed, an aliquot of the reaction mixture was taken and its ¹⁹F NMR spectrum recorded, on which mainly starting **1.32** could be observed. The temperature was then increased to 50 °C for the next 14h before the ¹⁹F NMR spectrum of a second aliquot was taken which, as previously, indicated the absence of reaction.

Table 3.3: Deoxofluorination of 2,4-difluoro levoglucosan **1.32**

Entry	Deoxofluorinating reagent (equiv.)	Fluoride source (equiv.)	Solvent	T(°C)	Time (h)	Yield (%)
1	DAST (3.4)	/	DCM	r.t	72	/
2	DAST (3.6)	/	/	r.t → 50	24	/

3	DAST (2.5)	HF-pyr (cat)	DCM	50	24	/
4	DAST (3.6)	/	/	70	48	/
5	DAST (1.5)	/	DCE	100	0.33	/
6	NfF (3.0)	TBAT (0.8)	THF	r.t	16	/
7	NfF (3.0)	TBAT (0.8)	ACN	80	18	/

Next, a procedure involving diluted DAST in presence of catalytic quantities of hydrogen fluoride pyridine (HF-pyr) was examined (**Entry 3**), but produced similar results than the neat DAST conditions. Given that only signals corresponding to the starting could be observed on the NMR of the ongoing reactions (**Entry 2 and 3**), the main problem seemed to be that the C3 hydroxyl of **1.32** and DAST could not react in a first place. Considering this, it was decided to investigate conditions that would force the reaction, such as neat DAST with temperature as high as possible, here 70 °C to avoid any risks of DAST degradation and hence explosion (**Entry 4**).⁵⁷ After 2 days of reaction, NMR analysis of the reaction mixture indicated the *quasi*-complete conversion of **1.32** into a difluorinated product which could potentially be the adduct formed between DAST and **1.32** (not shown). Once again, no traces of signals corresponding to trifluoro levoglucosan **3.26** could be observed. Ultimately, deoxofluorination of **1.32** using DAST was investigated under micro-wave conditions, with no results (**Entry 5**). In absence of encouraging results with DAST, deoxofluorination of difluoro levoglucosan **1.32** was attempted using perfluoro-1-butanesulfonyl fluoride, commonly referred to as NfF, a reagent increasingly used within our group for deoxofluorinating primary and secondary alcohols under mild conditions.⁵⁸ At first, a procedure involving NfF and tetrabutylammonium triphenyldifluorosilicate (TBAT) as fluoride source was investigated, and resulted in the *quasi*-complete consumption of **1.32** after 16 hours of reaction (**Entry 6**).⁵⁹ After quenching and workup, NMR analysis of the reaction mixture revealed the presence of perfluorobutanesulfonate esters **3.41** as main product (**Scheme 3.14**).



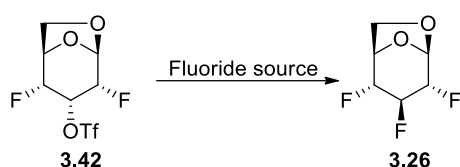
Scheme 3.14: Reaction between NfF and 2,4-difluoro levoglucosan **1.32** assisted by N,N-diisopropylethylamine (DIPEA)

These conditions being investigated on a reduced scale, isolation of **3.41** by column chromatography was deemed unworthy and hence not attempted. According to what had been observed by a member of our group, full conversion of the perfluorobutanesulfonate esters into the desired fluorinated product can usually be achieved by heating the reaction above 60 °C. However, similar results were achieved when these conditions were re-investigated with a temperature of 80 °C (**Entry 7**). These last conditions being run on larger scale, adduct **3.41** could be partially isolated before being treated with neat Et₃N-3HF at 120 °C to displace the -OSO₂C₄F₉-*n* group, conditions which surprisingly resulted in the total absence of reaction.

Concerning the deoxofluorination with DAST, the main issue seemed to be the absence of reaction between the activated form of DAST and the C3 hydroxyl from **1.32**, presumably due to the deactivation entailed by the C2 and C4 antiperiplanar fluorines, or the steric hindrance generated by the 1,6-anhydro bridge. A problem which surprisingly was not encountered when using NfF, much more voluminous than DAST. However, despite being easier to install, even harsh conditions could not ensure its displacement by a fluorine anion.

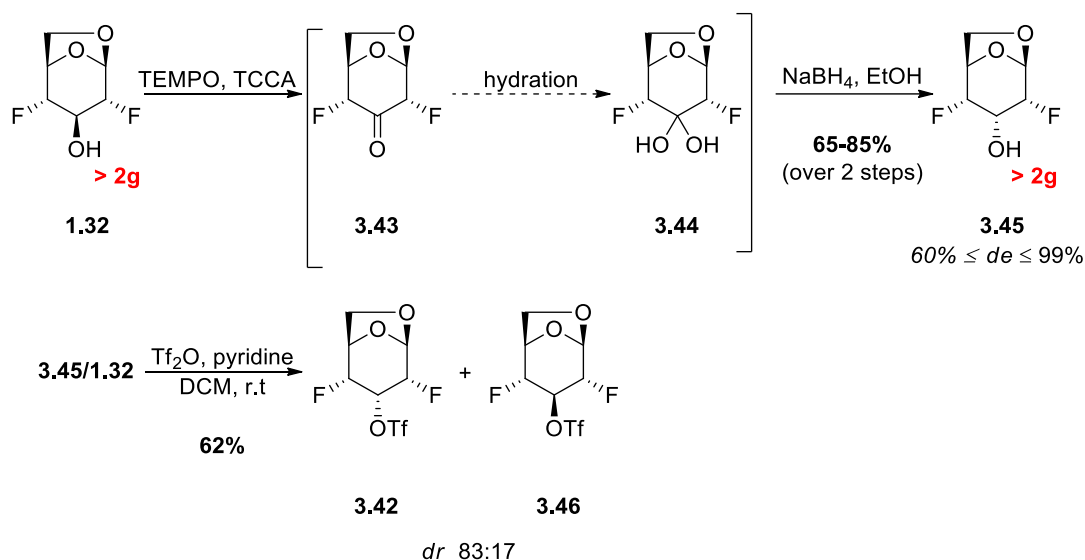
3.4.1.3 Attempted C3 fluorination *via* triflate displacement on a 2,4-difluoro levoallosan derivatives

In the absence of encouraging results concerning the deoxyfluorination of 2,4-difluoro levoglucosan **1.32**, synthesis of trifluoro levoglucosan **3.26** was envisioned *via* C3 triflate displacement on the 2,4-difluoro levoallosan derivatives **3.42** (**Scheme 3.15**).



Scheme 3.15: Triflate displacement from 2,4-difluoro-3-*O*-(trifluoromethanesulfonyl) levoallosan **3.42**

At first, the triflate derivatives of 2,4-difluoro levoallosan **3.42** was synthesised from 2,4-difluoro levoglucosan **1.32** (**Scheme 3.16**).



Scheme 3.16: Synthesis of 2,4-difluoro-3-*O*-(trifluoromethanesulfonyl) levoallosan **3.42**

In a first step, 2,4-difluoro levoglucosan **1.32** was oxidised following a standard TEMPO/TCCA procedure which afforded two difluorinated products showing similar ^{19}F NMR signals, which seemed to correspond to ketone **3.43** and its hydrate form **3.44**. When conducted in THF and in presence of a catalytic quantity of EtOH,²⁵ reduction of the ketone/hydrate mixture **3.43/3.44** using NaBH_4 afforded the equatorial alcohol **3.45** in a diastereomeric excess (*de*) comprised in between 60 and 90%. Then, replacement of THF by EtOH led to virtually complete selectivity toward **3.45** (*de* \approx 99%). This selectivity was attributed to the repulsive interaction generated by the two highly polarised $-\text{C}-\text{F}$ bonds, which presumably prevented the approach of any hydride from the equatorial face of the C3 ketone (**Figure 3.3**).²⁵

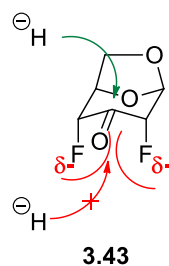
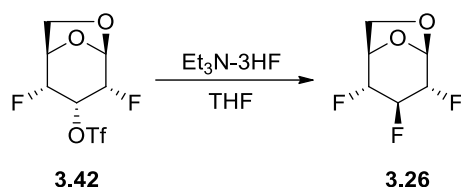


Figure 3.3: Electrostatic clashes between the $-\text{C}-\text{F}$ bonds in **3.43** and approaching hydrides

Pleasingly, this oxidation-reduction sequence could be performed on a 2+ g scale without suffering from significantly decreased yields. Due to their close *R_f* values, diastereoisomers **1.32** and **3.45** were kept as a mixture and converted into the corresponding triflate **3.42** and **3.46**, before being separated by careful chromatography.

To finish, displacement of the equatorial triflate on **3.42** was investigated with $\text{Et}_3\text{N}-3\text{HF}$ as fluoride source (**Scheme 3.17**).

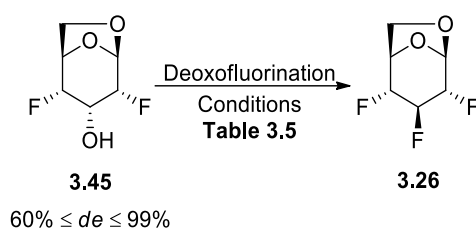


Scheme 3.17: Displacement of triflate from compound **3.42** with Et₃N-3HF as fluoride source

At first, mild conditions reported for the displacement of a triflate adjacent to a fluorine were attempted (50 °C, 0.03 mol.L⁻¹), but resulted in a total absence of reaction.⁶⁰ Therefore, slightly harsher conditions involving higher concentration and temperature were trialled (80 °C, 0.30 mol.L⁻¹), still with no results.⁶¹ Due to the lack of both encouraging results and time, our studies concerning the triflate displacement with fluoride were not pursued. However, several procedure from the literature were kept in mind for further investigations, this includes the microwave conditions reported by O'Hagan and co-workers⁶² involving neat Et₃N-3HF at 180°C and, also, the investigation of different fluoride sources.

3.4.1.4 Deoxofluorination of 2,4-difluoro levoallosan

At last, synthesis of trifluoro levoglucosan **3.26** was envisaged *via* deoxofluorination of 2,4-difluoro levoallosan **3.45** (**Scheme 3.18**), easily accessible from its levoglucosan counterpart **1.32** on multi-gram scale (*cf* **Scheme 3.16**). In absence of potential anchimeric assistance, and steric clashes on the adduct formed upon reaction between **3.45** and DAST or NfF (not shown), deoxofluorination of the equatorial C3 hydroxyl was anticipated to occur without retention of configuration.



Scheme 3.18: Deoxofluorination of 2,4-difluoro levoallosan **3.45**

Given the lack of reactivity of 2,4-difluoro levoglucosan **1.32** toward deoxofluorinating reagents (*cf* **3.4.1.2**), the latter was not separated from **3.45** prior to reaction. The yield in trifluoro levoglucosan **3.26** displayed later in this section were calculated based on the initial quantity of **3.45** only (**Table 3.4**). As mentioned previously, trifluoro levoglucosan **3.26** being a volatile compound, all the experiments presented in this section were performed in sealed tube reactors, and the reaction and extraction solvents carefully evaporated under controlled pressure.

Table 3.4: Deoxofluorination of 2,4-difluoro levoallosan **3.45**

Entry	Deoxofluorinating reagent (equiv.)	Fluoride source (equiv.)	Solvent	T(°C)	Time (h)	Yield in 3.26 (%)
1	DAST (3.0)	/	DCM	50	36	Traces
2	NfF (2.0)	Et ₃ N-3HF (1.9)	THF	25 → 90	72	50*
3	NfF(1.9)	Et ₃ N-3HF (1.9)	THF	90	96-192	43-69

*Yield estimated by ¹⁹F NMR

At first, deoxofluorination conditions reported by Sarda and co-workers were repeated with a temperature of 50 °C (**Entry 1**).⁵³ After 36 h, no traces of signal corresponding to 2,4-difluoro allosan **3.45** could be observed on the fluorine decoupled proton NMR (¹⁹F[¹H] NMR) of the reaction mixture. Also, minor signals presumably corresponding to the desired **3.26** could be distinguished (*cf* **Figure 3.4**). Given the volatility of **3.26** and the reduced scale on which these conditions were investigated (< 100 mg), isolation by column chromatography was not attempted. These conditions were then repeated on a larger scale, which enable isolation of a fraction containing **3.26** and a few fluorinated impurities (Yield ≈ 8%). Next, deoxofluorination of **3.45** was examined using NfF in combination Et₃N-HF, known to be one of the most reactive fluoride source for this reaction (**Entry 2**).^{63,58} After 4 h at r.t, full conversion of **3.45** into the NfF adduct was observed by ¹⁹F[¹H] NMR, but no signals corresponding to trifluoro levoglucosan **3.26**. Hence, reaction was heated up to 50 °C for the following 20 h, with no significant results. Further increase in temperature up to 80 °C resulted in the conversion of a slight portion of the NfF adduct into the desired **3.26** (after 24 h). Finally, a last increase in temperature up to 90 °C maintained over the last 24 h enable to transform more than 50% of the NfF adduct into **3.26**. Considering the numerous aliquots taken for NMR analysis and the small scale of the reaction, isolation of trifluoro levoglucosan **3.26** was not attempted. At last, similar conditions were repeated on 300 mg of **3.45** at a temperature of 90 °C (**Entry 3**). After 4 days of reaction, ¹⁹F[¹H] NMR analysis indicated full consumption of both **3.45** and its corresponding NfF adduct, as well as formation of trifluoro levoglucosan **3.26** as main product. Column chromatography then afforded the latter as a pure material in a promising yield of 69%, alongside with traces of NfF adduct. When investigated on a gram scale, full consumption of starting **3.45** could not be reached despite several addition of extra NfF and Et₃N (1 equiv. of both, twice). Hence, after 8 days of reaction, these conditions produced the desired **3.26** in a slightly decreased yield of 43% (≈ 600 mg) for a conversion of 75%. However, time prevented us to optimise this reaction on larger scale.

Owing to its particular geometry, the trifluorinated motif from **3.26** could easily be identified by ^{19}F [^1H] NMR. As detailed below, the ^{19}F [^1H] NMR spectra recorded on reaction mixtures containing **3.26** all exhibited a set of signals composed of two doublets and one triplet, all showing a magnitude of about 12.0 Hz (**Figure 3.4**). The rough equality between the two observable coupling constants clearly indicated a symmetrical trifluorinated motif corresponding to the trifluoro levoglucosan **3.26**, in which the central F_3 couple similarly with the antiperiplanar F_2 and F_4 ($^3J_{\text{F}_3-\text{F}_2} \approx ^3J_{\text{F}_3-\text{F}_4}$).

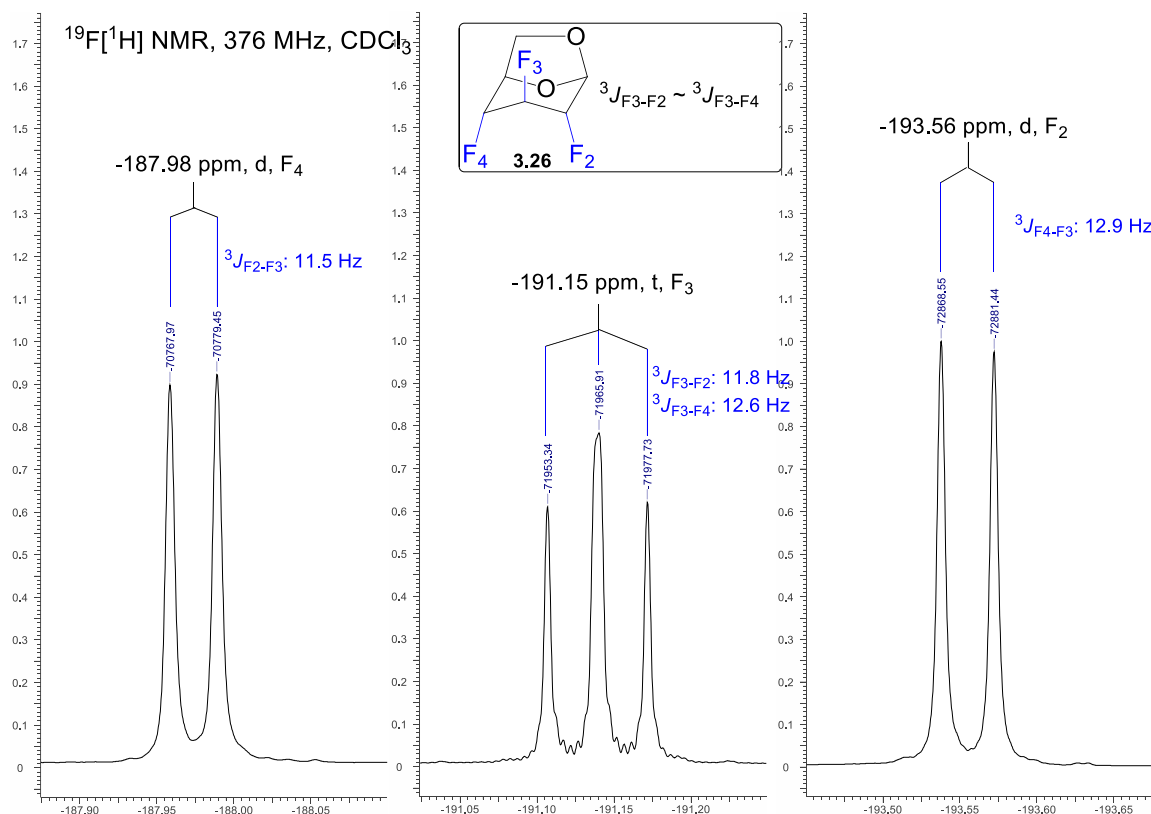


Figure 3.4: ^{19}F [^1H] NMR spectrum recorded for 2,3,4-trideoxy-2,3,4-trifluoro levoglucosan **3.26**

Once isolated, the structure of **3.26** was ascertained *via* an extensive NMR study, as well as by the crystal structure shown below, obtained after recrystallisation from a mixture hexane/DCM (**Figure 3.5**).

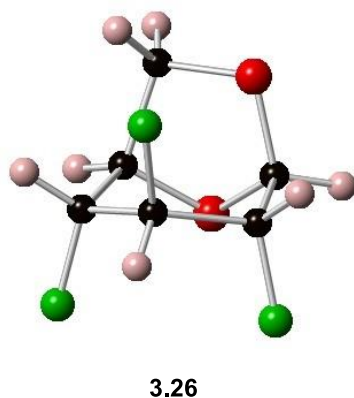
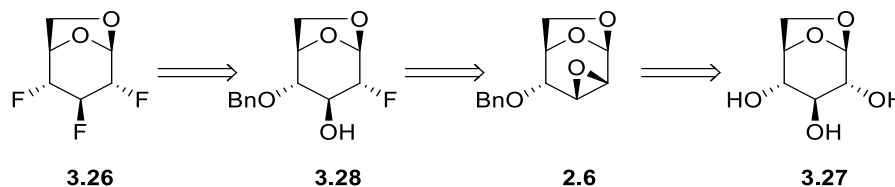


Figure 3.5: X-ray crystallographic analysis of 2,3,4-trifluoro-levoglucosan **3.26**

3.4.2 Synthesis of 2,3,4-trifluoro levoglucosan *via* the Sarda synthesis

As mentioned earlier in this chapter, synthesis of trifluoro levoglucosan **3.26** could be achieved by repeating a known synthesis reported by Sarda and co-workers (*cf* section 3.3.1).⁵³ This synthesis starts from 2-fluoro levoglucosan derivatives **3.28**, a compound synthesisable *via* regioselective fluorination of the Černý epoxide **2.6**,⁴³ accessible in 4 steps from levoglucosan **3.27** (Scheme 3.19).⁵²

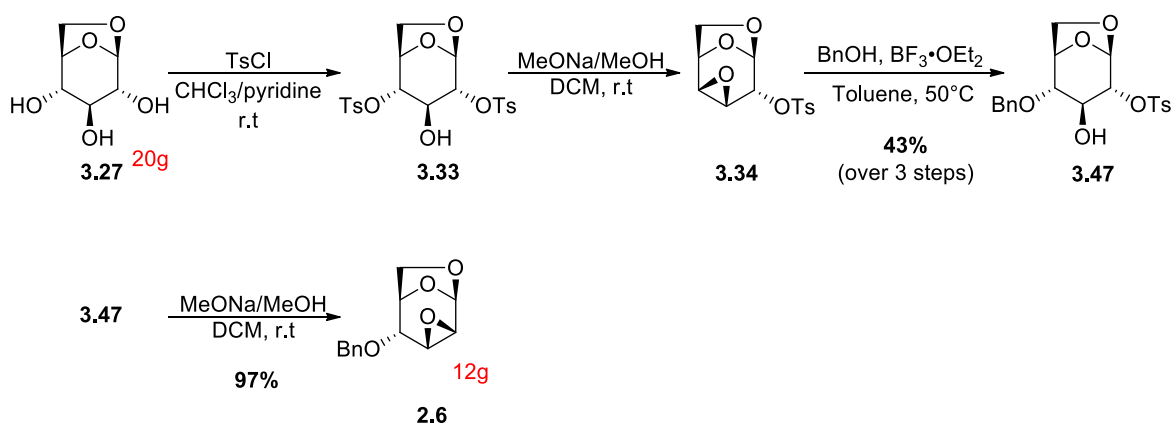


Scheme 3.19: Alternative retrosynthetic approach of trifluoro glucose **3.16**

With a total of 11 steps, this alternative route is considerably longer than those previously proposed, but was the most convenient as previously investigated in our group for the synthesis of 2,3-difluoro glucose **1.42**.⁴³ Also, considering that trifluoro glucose **1.37** was needed in a restricted timeframe regarding the transport rate measurement experiments, safe access to 2,3,4-trifluoro levoglucosan **3.26** to investigate the final anomeric hydrolysis was on top of our priorities.

3.4.2.1 Synthesis of the Černý epoxide

As detailed below (Scheme 3.20), the Černý epoxide **2.6** could be accessed by pursuing the procedure followed to synthesise the tosyl epoxide **3.34** described earlier in this thesis (*cf* Scheme 3.9).⁴³ However, as the latter had been entirely consumed, synthesis of the Černý epoxide **2.6** was started from levoglucosan **3.27** (Scheme 3.20).



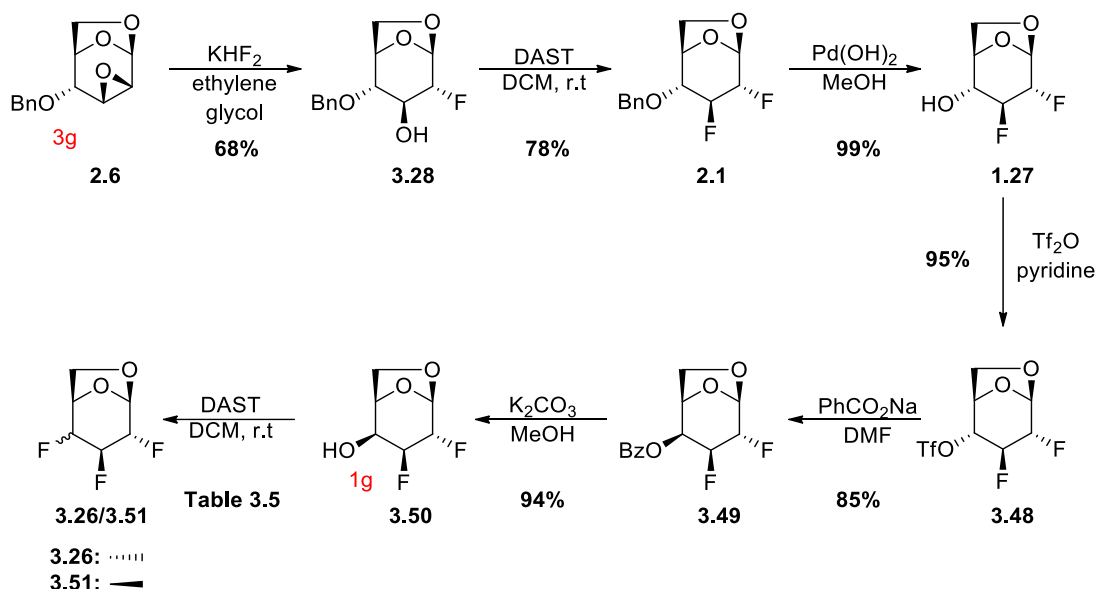
Scheme 3.20: Synthesis of the Černý epoxide **2.6** from levoglucosan **3.27**

After re-synthesis following the exact same procedure than previously, tosyl epoxide **3.34** was selectively opened at C4 with benzyl alcohol to give the levoglucosan derivative **3.47**, which could

be obtained as a pure material after the unreacted benzyl alcohol was washed away with diethyl ether. To finish, treatment with sodium methoxide followed by a standard aqueous workup led to pure Černý epoxide **2.6** in a *quasi*-quantitative yield.

3.4.2.2 Synthesis of 2,3,4-trifluoro levoglucosan

To start, treatment of the Černý epoxide **2.6** with KHF_2 in refluxing ethylene glycol exclusively gave the 2-fluoro levoglucosan derivatives **3.28** (Scheme 3.21). This reaction had previously been reported by our group on 500 mg with a yield of *circa* 70% which, pleasingly, was maintained upon upscaling to 3 g.⁴³ With the 2-fluoro levoglucosan derivative **3.28** in hand, synthesis of trifluoro levoglucosan **3.26** could be achieved by repeating a 6 steps sequence described by Sarda and co-workers.⁵³ Contrary to what was suggested in the procedure followed, deoxyfluorination of **3.28** using DAST was not conducted in refluxing toluene, but instead in DCM at room temperature. Even if investigated in reduced scale compared to Sarda and co-workers, these safe conditions afforded the 4-*O*-benzyl-2,3-difluoro levoglucosan **2.1** in an improved yield of 78%. Then, standard hydrogenolysis conditions using Pearlman's catalyst led to pure 2,3-difluoro levoglucosan **1.27** in a *quasi*-quantitative yield.



Scheme 3.21: Synthesis of the mixture trifluoro levogluco and galactosan **3.26/3.51** from the Černý epoxide **2.6**

In the next step, the C4 hydroxyl group of **1.27** was efficiently converted into the corresponding triflate **3.48** using triflic anhydride (Tf_2O) in presence of pyridine. To effect the desired C4 inversion, the triflate was displaced with a benzoate group, thus leading to the levogalactosan derivative **3.49**. Deprotection of the C4 hydroxyl using classic methanolysis conditions then afforded the 2,3-difluoro levogalactosan **3.50** in 94% yield.

Subsequent treatment with DAST in refluxing DCM resulted in the formation of a single product by thin layer chromatography (TLC), which by $^{19}\text{F}[^1\text{H}]$ NMR analysis appeared to be an inseparable mixture of two trifluorinated products in a 54:46 ratio (**Entry 1, Table 3.5**).

Table 3.5: Deoxyfluorination of 2,3-difluoro levoglactosan **3.50**

Entry	T(°C)	DAST addition time (min)	Yield (%)	Ratio (3.26/3.51)*
1	50	5	80	54:46
2	0 → r.t	10	83	69:31
3	0 → r.t	20	50	97:3

*Ratio estimated by ^{19}F NMR.

The major product exhibiting a set of signals corresponding to the trifluoro levoglucosan **3.26**, detailed previously in this chapter (*cf* **Figure 3.4**). And the minor showing as two doublets of different magnitudes and a doublet of doublets exhibiting both of them, suggesting a non-symmetrical trifluorinated motif corresponding to the trifluoro levoglactosan **3.51** (**Figure 3.6**).

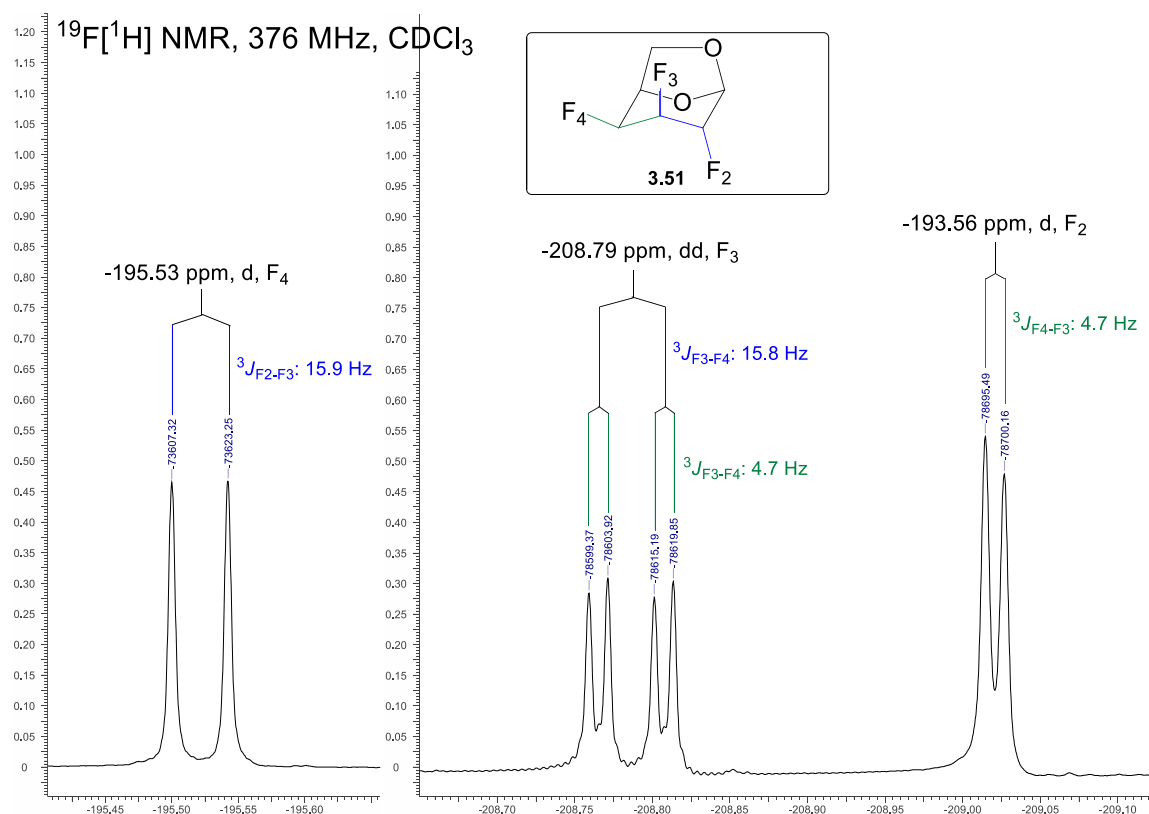
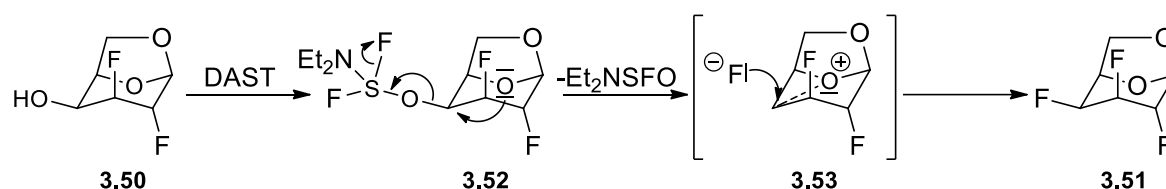


Figure 3.6: $^{19}\text{F}[^1\text{H}]$ NMR spectrum of the mixture **3.26/3.51**, details of trifluoro levoglactosan **3.51**

Then, the use of lower temperature as well as a longer DAST addition time resulted in a better selectivity toward the trifluoro levoglucosan **3.26** (**Entry 2 and 3**). However, an addition time

exceeding 10 min seemed to negatively affect the yield of the reaction (**Entry 3**). Considering the absence of differentiation by TLC and the volatility of **3.26** and **3.51**, separation was not attempted at that stage.

The retentive deoxofluorination of **3.50** was attributed to the participation of the pyranose ring oxygen in **3.52**, leading to the transient *epi*-oxonium intermediate **3.53** then rapidly attacked by a nucleophilic fluoride to give **3.51** (Scheme 3.22).

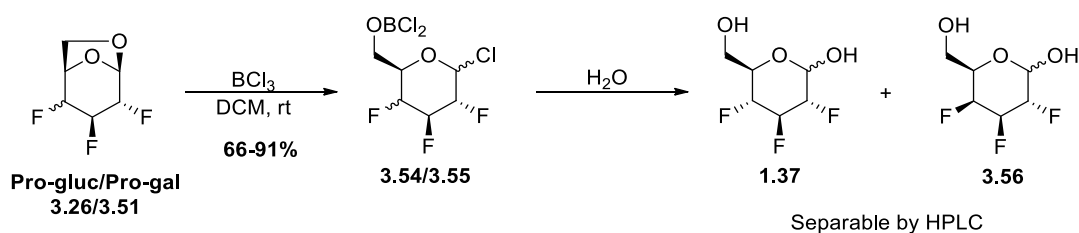


Scheme 3.22: Proposed mechanism for the retentive deoxyfluorination of **3.50**

A participation of the ring oxygen has recently been invoked by Karban and co-workers to rationalise a similar C4 retentive deoxofluorination on levoglucosan derivatives presenting a C2-C3 epoxide motif.⁴⁴ Contrary to certain examples found in Karban's paper, the ring contraction provoked by a C5 fluorine entry on the *epi*-oxonium intermediate was never observed (not shown).

3.4.3 Anomeric hydrolysis of the mixture 2,3,4-trifluoro levoglucos and -galactosan

To finish, cleavage of the 1,6-anhydro bridge was envisioned following a procedure developed by our group (Scheme 3.23).⁴³ At first, anomeric hydrolysis was investigated on the mixture of trifluoro levoglucos- and galactosan **3.26/3.51** following the procedure shown below. To start, treatment of **3.26/3.51** with boron trichloride would afford the mixture of corresponding anomeric chlorides **3.54/3.55** which, upon water addition to the reaction mixture, would be hydrolysed into the free trifluoro sugars **1.37** and **3.56**. However, instead of being recovered after complete evaporation of the reaction mixture, as for the 2,3-difluoro glucose, the trifluoro sugars were believed to be sufficiently hydrophobic to be extracted from the aqueous phase.

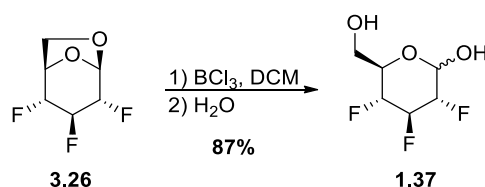


Scheme 3.23: Anomeric hydrolysis of 2,3,4-trifluoro levoglucosan **3.26** and galactosan **3.51**

When first attempted, these conditions gave the mixture of trifluoro glucose and galactose **1.37/3.56** only in low yields (24 and 45 %). Considering the spot to spot conversion observed in both cases, such poor yields seemed to indicate a loss of material during workup or purification. Similar reaction conditions were then re-investigated with a different workup procedure involving the complete evaporation of the reaction mixture, and this time afforded the trifluoro sugars **1.37** and **3.56** in high to excellent yields (66 to 91%). After a first purification by column chromatography yielding a complex mixture of **1.37** and **3.56**, several attempts using HPLC were necessary to ensure the *quasi*-complete separation of the two trifluoro sugars.

3.4.4 Anomeric hydrolysis of 2,3,4-trifluoro levoglucosan

Anomeric hydrolysis of the pure trifluoro levoglucosan **3.26** was performed on 150 mg scale, and afforded 2,3,4-trifluoro-D-glucopyraose **1.37** in 87% yield (**Scheme 3.24**).



Scheme 3.24: Anomeric hydrolysis of 2,3,4-trifluoro levoglucosan **3.26**

3.5 Structural analysis

3.5.1 Study of intramolecular H-bonds in 2,4-difluoro allosan

As mentioned earlier, our team has been interested in the study of $\text{OH}\cdots\text{F}$ intramolecular bonds in levoglucosan type structures (*cf* **chapter 2**).⁶⁶ Regarding this matter, our attention was drawn to the 2,4-difluoro allosan **3.45** presenting a geometry favourable to the formation of a bifurcated H-bond involving OH_3 as donor, and both F_2 and F_4 as acceptors. Hence, before being treated with triflic acid, a small fraction of the mixture **3.45/1.32** was kept aside and repeatedly subjected to HPLC separation until a sufficient quantity of **3.45** could be isolated and analysed by ^1H NMR (**Figure 3.7**).

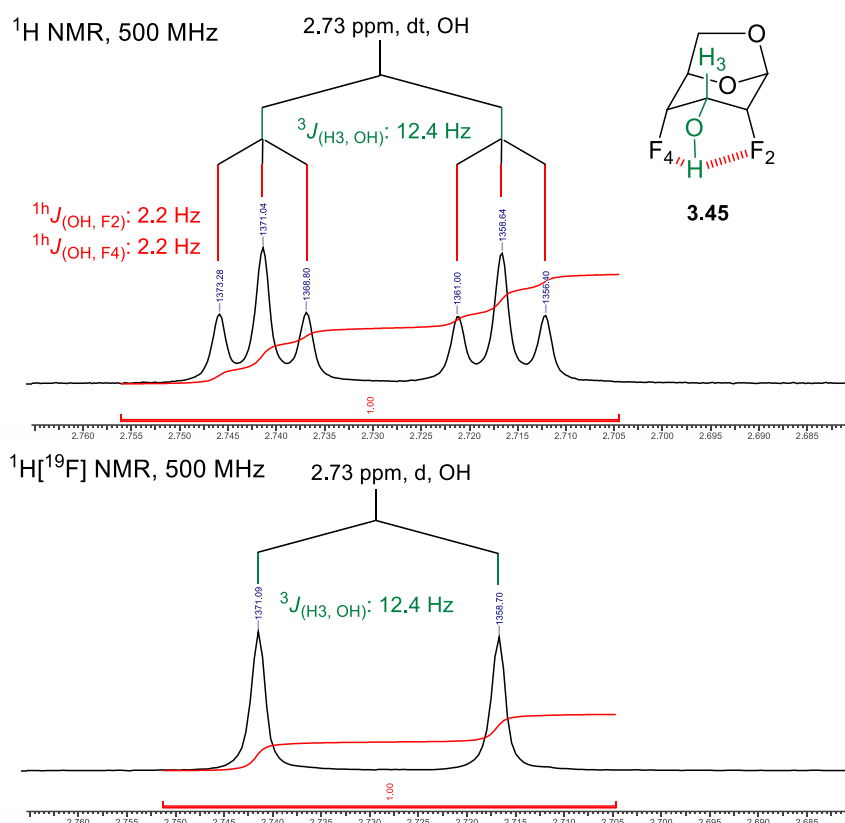


Figure 3.7: ^1H and $^1\text{H}[^{19}\text{F}]$ NMR spectra recorded for 2,4-difluoro allosan **3.45**

The presence of both $\text{OH}\cdots\text{F}_2$ and $\text{OH}\cdots\text{F}_4$ interactions was evidenced by the two through space $^1\text{H}/(\text{OH}, \text{F})$ couplings observed on the OH_3 signal, which disappeared upon fluorine decoupling. Interestingly, the exact same magnitude of 2.2 Hz measured for both $^1\text{H}/(\text{OH}, \text{F})$ coupling, as well as the $^3\text{J}(\text{H}_3\text{-OH})$ of 12.4 Hz, indicating a symmetrical bifurcated H-bond, suggested two H-bond of similar strengths. Hence, it seemed that the polarisation of the C1-O bond didn't substantially impede the electron transfer from the C1-O to C2-F bond (hyperconjugation), which ultimately would have resulted in F_2 being a worst H-bond acceptor than F_4 . As illustrated below, this would have resulted in a geometry where the C3-OH hydrogen points toward F_4 , for which a $^3\text{J}(\text{H}_3\text{-OH})$ below 12 Hz would have been observed (**Figure 3.8**).

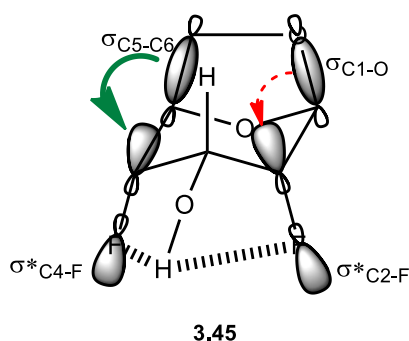


Figure 3.8: Effect of the bond polarisation of C5-C6 and C1-O on the H-accepting abilities of F_2 and F_4 in **3.45** (hyperconjugation)

It is noteworthy that the ^1H and $^1\text{H}[^{19}\text{F}]$ NMR spectra shown on the previous page (**Figure 3.7**) were recorded from a sample containing a non-negligible quantity of water and presenting a concentration in substrate largely above those recommended for the study of intramolecular H-bond, thus suggesting that intramolecular $\text{OH}\cdots\text{F}$ bonds were not as easy to disrupt as initially believed (see also 2-fluoro levoglucosan **1.26**, **Figure 2.1**).^{34,67} Recrystallisation of **3.45** from a mixture acetone/hexane afforded crystals suitable for X-ray diffraction analysis, which showed a structure similar to the one observed in solution. (**Figure 3.9**)

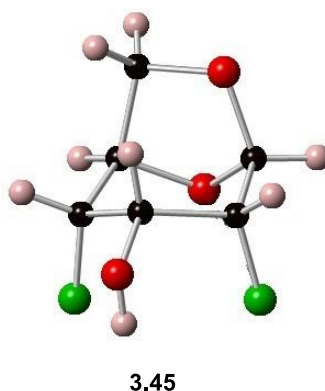


Figure 3.9: X-ray crystallographic analysis of 2,4-difluoro-allosan **3.45**

3.5.2 Crystal structure of fluoro levoglucosan derivatives

While repeating the Sarda synthesis, several intermediates that were obtained pure could be recrystallised and their structure analysed by X-ray diffraction. This afforded the crystal structures shown below which confirmed the NMR data obtained for these compounds (**Figure 3.10**).

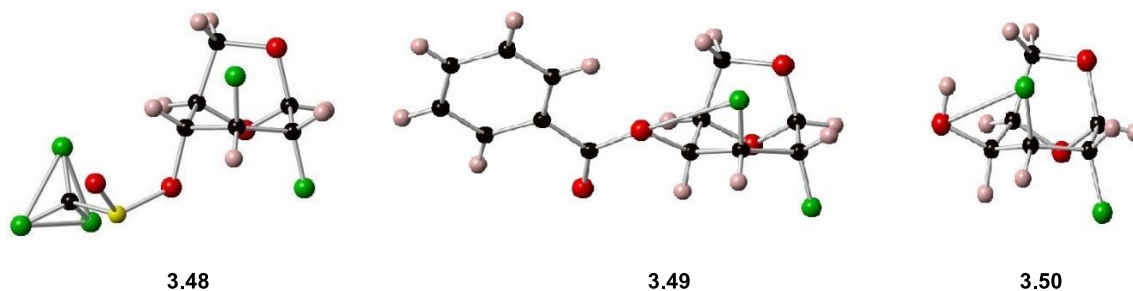


Figure 3.10: X-ray crystallographic analysis of the fluorinated derivatives of levoglucosan **3.48**, **3.49**, and **3.50**

3.5.3 Conformational and configurational analysis of 2,3,4-trifluoro-D-gluco- and galactopyranose

Recrystallisation of both trifluoro glucose **1.37** and galactose **3.56** from a mixture Et_2O /hexane afforded crystals suitable for X-ray diffraction analysis. As shown below (**Figure 3.11**), both compounds crystallised in their β -anomer form and adopted a $^4\text{C}_1$ conformation with minimal

distortion, thus evidencing that the introduction of a CHF-CHF-CHF motif does not drastically alter the shape of the natural carbohydrates.

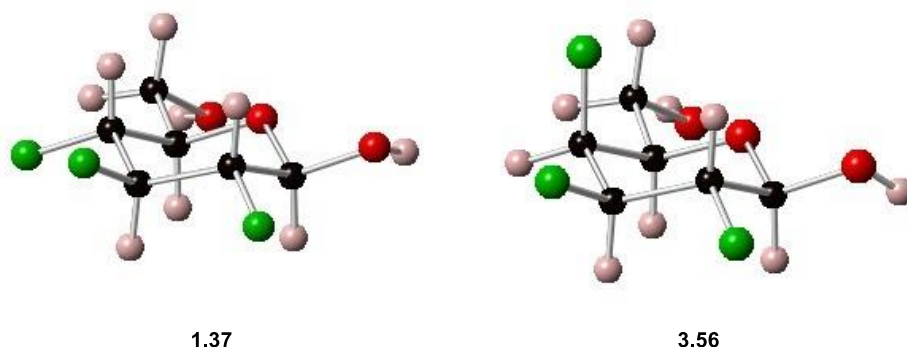


Figure 3.11: X-ray crystallographic analysis of trifluoro glucose **1.37** and galactose **3.56**

The structure of **1.37** could also be ascertained in solution by analysing the coupling constants displayed on the $^1\text{H}[^{19}\text{F}]$ NMR spectra. For instance, the gluco configuration could be deduced from the $^3J_{\text{H-H}}$ of *circa* 8.5 Hz displayed on the H₂, H₃ and H₄ signals of each anomers, which clearly evidenced the 1,2 diaxial relationship between C3-H₃ and both C2-H₂ and C4-H₄ bonds (**Figure 3.12**).

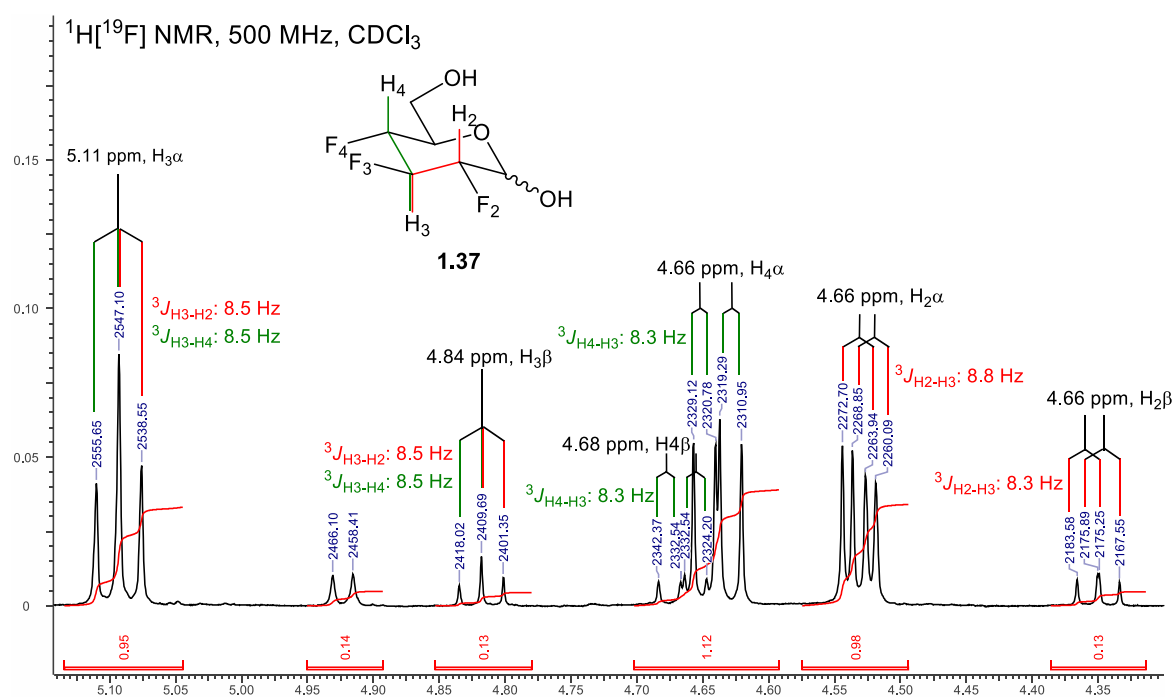


Figure 3.12: $^1\text{H}[^{19}\text{F}]$ NMR spectrum of trifluoro glucose **1.37** in CDCl_3

On the spectrum of **3.56**, shown below (**Figure 3.13**), coupling constants of *circa* 9.5 Hz could be observed on the H₂ and H₃ signals of both anomers. Like previously, such large $^3J_{\text{H-H}}$ values attested of the antiperiplanarity of C2-H₂ and C3-H₃. The axial orientation of C4-F₄, corresponding to a galacto configuration, was confirmed by the small $^3J_{\text{H-H}}$ values observed on each of the H₃ and H₄ signals (2.9 to 3.4 Hz), corresponding to an acute torsion angle between C₃-H₃ and C₄-H₄.

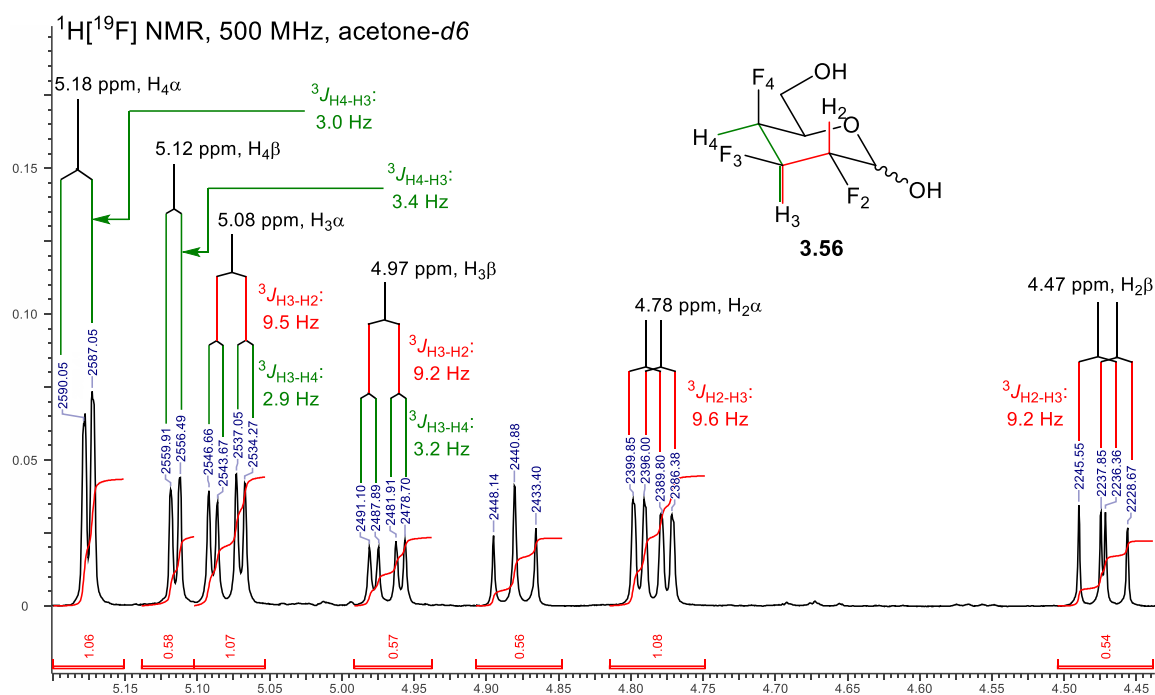


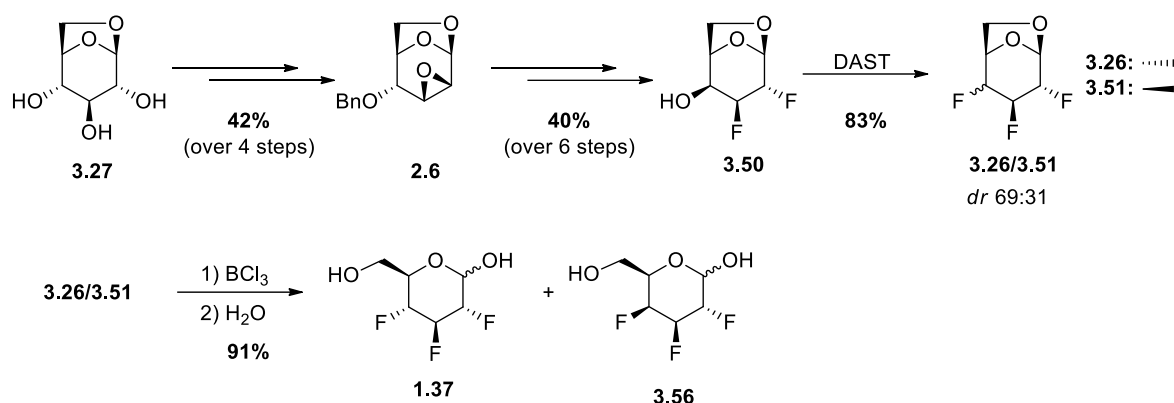
Figure 3.13: ¹H[¹⁹F] NMR spectrum of trifluoro glucose **3.56** in acetone-*d*₆

Interestingly, both H₄ showed as doublets, therefore indicating that they were unable to couple either with the equatorial H₃, or the axial H₅. Considering the harmony between the ³J_{H3-H4} and ³J_{H4-H3} values of a same anomer, the absence of coupling was believed to occur between H₄ and H₅. This was later verified by the non-presence on the H₅ signals of a small coupling constant of about 3.0 Hz, which should appear in case of coupling between C4-H₄ and C5-H₅ (not shown). Such absence of coupling was believed to result from a slight distortion of the ⁴C₁ conformation adopted by **3.56** in acetone-*d*₆, forcing C4-H₄ and C5-H₅ into a dihedral angle of approximately 90°.

3.6 Summary

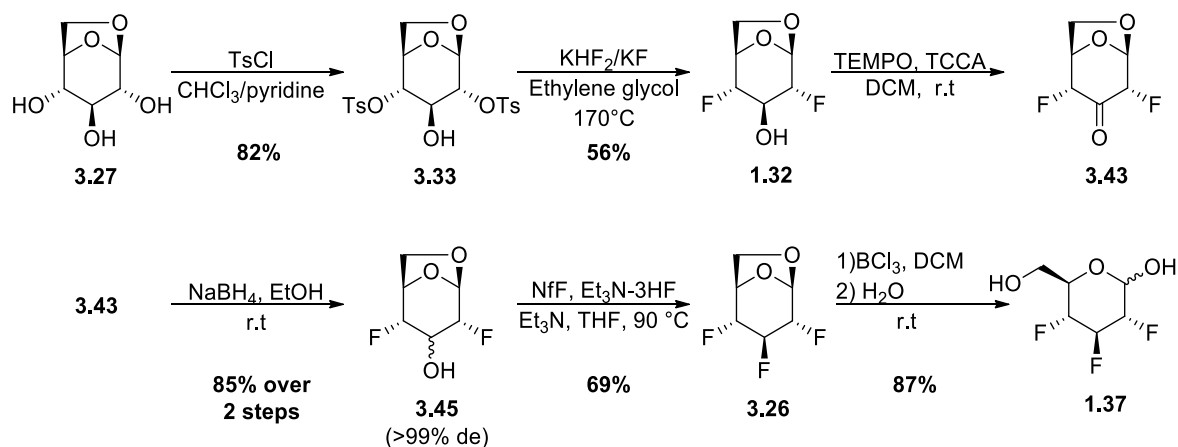
With 12 steps and an overall yield of 9%, our synthetic route based on the Sarda synthesis is considerably more efficient and slightly more straightforward than the synthesis of trifluoro glucose **1.37** already published (**Scheme 3.25**).^{41,49} Pleasingly, this new synthetic pathway gave access to more than 200 mg of trifluoro glucose **1.37**, a sufficient quantity to conduct the experiments necessary to determine its transport rate across RBC membrane, but also to undertake an in-depth NMR characterisation (see experimental section). Contrary to when performed by Sarda and co-workers, deoxyfluorination of 2,3-difluoro levogalactosan **3.50** didn't occur with a clean inversion of configuration, and thereby gave access to the trifluoro galactose **3.56**, a new fluorinated analogue of galactose at that time. Even if obtained in reduced quantities, as for now, we believed that an adjustment of the deoxyfluorination conditions of **3.50** could lead to reversed outcomes and thus afford the trifluoro galactosan **3.51** as main product. Finally, it is noteworthy that re-

investigation of the Sarda synthesis enabled us to complete the characterisation of the different intermediates leading to trifluoro levoglucosan **3.26** and **3.51** galactosan, for which only the ^{13}C NMR were disponible in the original paper.



Scheme 3.25: Synthesis of trifluoro glucose **1.37** *via* the Sarda procedure

By proceeding *via* deoxofluorination of 2,4-difluoro levoallosan **3.45**, synthesis of trifluoro glucose **1.37** could be achieved in only 6 steps with an overall yield of 24% (**Scheme 3.26**). Besides, all the steps could be performed on a multigram scale, apart from the C3 deoxofluorination which was performed starting from 300 mg of difluoro levoallosan **3.45** (43% yield on 1+ g scale). Due to a lack of time, anomeric hydrolysis of the pure trifluoro levoglucosan **3.26** could not be optimised on large scale, and afforded 2,3,4-trifluoro-D-glucopyraose **1.37** in 87% yield (150 mg scale). After further upscaling and optimisation of the two final steps, this short and convenient synthesis could be used to produce 2,3,4-trifluoro-D-glucopyraose **1.37** on gram to multi-gram scales.



Scheme 3.26: Synthesis of **1.37** *via* deoxofluorination of 2,4-difluoro levoallosan **3.45**

Chapter 4: Synthesis of 2,3-dideoxy-2,2,3,3-tetrafluoro-D-glucopyranose

4.1 Previous syntheses of 2,2,3,3-tetrafluoro-D-gluco- and galactopyranose

For the sake of simplicity, 2,3-dideoxy-2,2,3,3-tetrafluoro-D-gluco- **1.40** and galactopyranose **4.1** will be referred to as tetrafluoro glucose and galactose respectively (**Figure 4.1**).

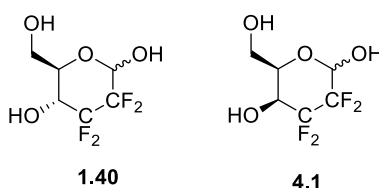
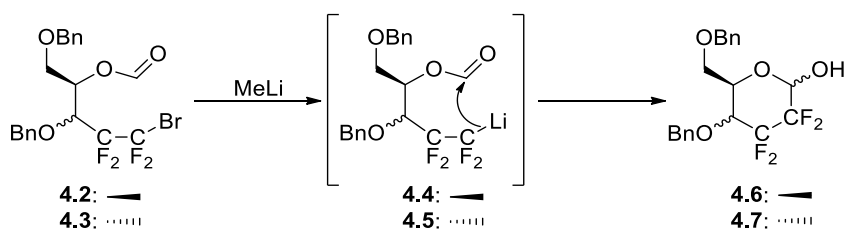


Figure 4.1: Tetrafluoro glucose **1.40** and galactose **4.1**

4.1.1 Enantioselective syntheses proposed by the Linclau group

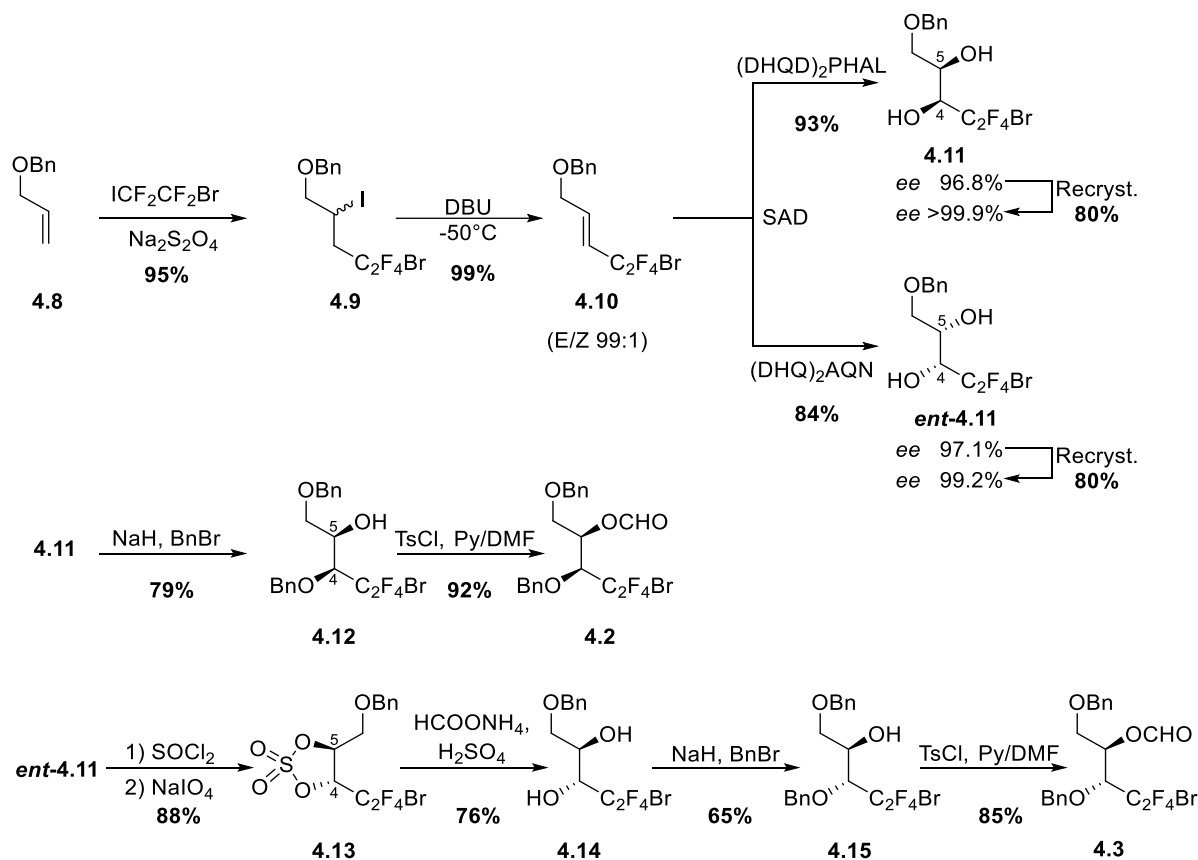
Based on a fluorinated building block approach, our group has designed a divergent synthesis giving access to both tetrafluoro glucose **1.40** and tetrafluoro galactose **4.1**.⁶⁸ As shown below (**Scheme 4.1**), the key step of this synthesis is the anionic cyclisation of intermediates **4.4** and **4.5**, respectively leading to the benzyl protected galactose **4.6** and glucose **4.7**. In both cases, the cyclisation is triggered upon lithium-bromine (Li-Br) exchange between methyllithium (MeLi) and the brominated species **4.2** and **4.3**. This anionic cyclisation process, developed within our group, has been extensively used over the past fifteen years to synthesise various tetrafluorinated pentoses and hexoses.^{69,70,22,71}



Scheme 4.1: Formation of benzyl protected tetrafluoro galactose **4.6** and glucose **4.7** through Li-Br mediated anionic cyclisation of precursors **4.2** and **4.3**

This synthesis of tetrafluoro galactose **4.1** and glucose **1.40**, initially published in 2008, has recently been re-edited within our group after thorough optimisation and upscaling work.⁷¹ As both

syntheses proceed through the exact same pathway, they are discussed together, and only the most recent version is detailed below. The synthesis starts with the preparation of the cyclization precursors **4.1** and **4.2** from the commercially available and cheap allyl benzyl ether **4.8** and 1-bromo-2-iodotetrafluoroethane (**Scheme 4.2**).

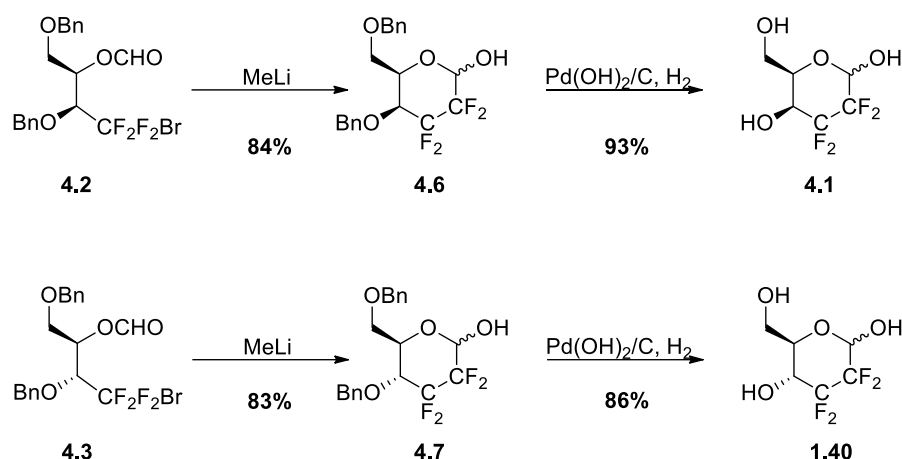


Note: Carbons are numbered according to their future position on the carbohydrate backbone

Scheme 4.2: Synthesis of precursors **4.2** and **4.3**

At first, allyl benzyl ether **4.8** and bromiodotetrafluoroethane were coupled through a radical process resulting in the β -iodotetrafluoroalkane **4.9** which, after treatment with 1,8-diazabicyclo[5.4.0]undec-7-ene (DBU) at low temperature, was almost exclusively converted into the (*E*)-alkene **4.10**.⁷² Then, Sharpless asymmetric dihydroxylation (SAD) gave access to both *syn*-diols **4.11** and **ent-4.11** in high enantiomeric excesses after recrystallization, hence avoiding the need of further purification *via* chiral HPLC or derivatisation.⁷³ Thanks to its increased acidity, the C4 hydroxyl of diol **4.11** could be selectively deprotonated and benzylated to afford **4.12**, then converted into galactose precursor **4.2** *via* Vilsmeier-Haack formylation of the C5 hydroxyl. For the tetrafluoroglucose synthesis, prior inversion of the C5 hydroxyl of **ent-4.11** was required. To this end, **ent-4.11** was converted into the cyclic sulphate **4.13** which, thanks to the repulsive interactions generated by the tetrafluoroalkylidene moiety, could be regioselectively opened at C5 with a formate anion (not shown). Despite the mild conditions investigated, hydrolysis of the residual C4 sulphate simultaneously cleaved the C5 formate ester, thus yielding the *anti*-diol **4.14**. The latter

was then converted into glucose precursor **4.3** following the same benzylation/formylation sequence as described for the preparation of galactose precursor **4.2**. As mentioned previously, treatment of **4.2** and **4.3** with MeLi triggered the anionic cyclisation process which afforded the di-*O*-benzyl protected tetrafluoro sugars **4.6** and **4.7** (Scheme 4.3). To finish, standard hydrogenolysis conditions allowed cleavage of both benzyl ether groups and led to the unprotected tetrafluoro galactose **4.1** and glucose **1.40**.

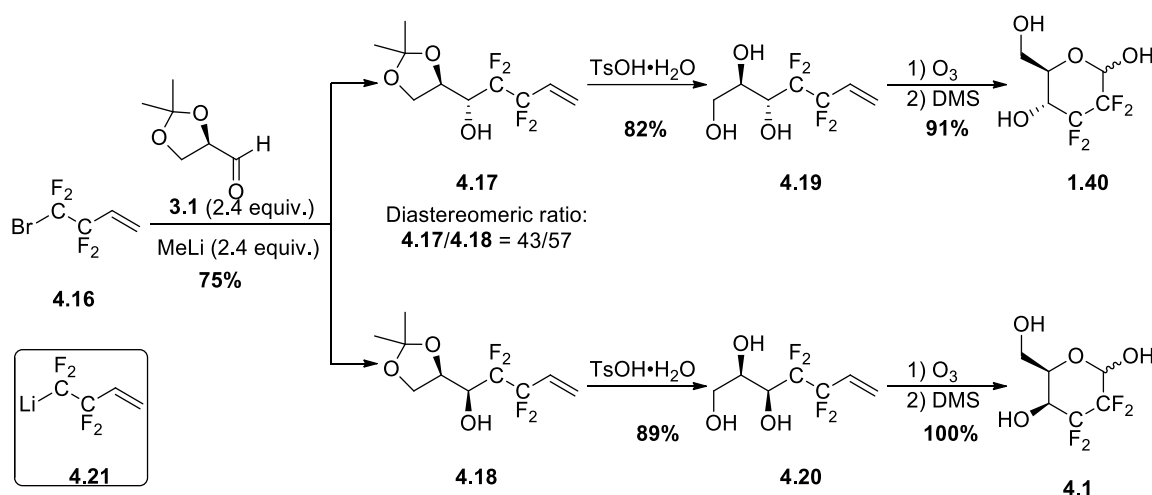


Scheme 4.3: Completion of the synthesis of tetrafluoro galactose **4.1** and glucose **1.40**

Remarkably, the seven synthetic steps leading to the enantiopure tetrafluoro galactose **4.1** could be achieved in high to excellent yields, thus affording the target compound in a satisfying overall yield of 38%. However, concerning the synthesis of tetrafluoro glucose **1.40**, the three additional steps required to invert the C4 configuration of **ent-4.11** strongly affected the overall efficiency of the synthesis. In fact, despite the high yields managed for most of the reactions, the tetrafluoro glucose **1.40** was obtained in an overall yield of only 16%. It is noteworthy that most of the steps were reported on gram to multi-gram scales, the preparation of (*E*)-alkene **4.10** being reported in a 20-plus gram scale. However, although being well optimised, this approach remained time consuming and slightly too complex to be conveniently upscaled.

4.1.2 Diastereoselective synthesis proposed by the Konno group

Inspired by Gassman and O'Reilly's work regarding the alkyllithium mediated coupling of perfluoroethyl iodide to carbonylated derivatives (Barbier type procedure, not shown),^{74, 75} Konno and co-workers developed in 2011 a highly efficient coupling method of commercial 4-bromo-3,3,4,4-tetrafluoro-but-1-ene **4.16** to various electrophiles (not shown).⁷⁶ Using this methodology, they then designed the syntheses of various 2,2,3,3-tetrafluorinated sugar derivatives, among which a new divergent synthesis leading to the tetrafluoro glucose **1.40** and galactose **4.1** (Scheme 4.4).⁷⁷



Scheme 4.4: Synthesis of tetrafluoro glucose **1.40** and galactose **4.1** proposed by Konno

Coupling of 4-bromo-3,3,4,4-tetrafluorobut-1-ene (bromo-tetrafluorobutene) **4.16** to D-glyceraldehyde acetonide **3.1** afforded a 43:57 mixture of coupling adducts **4.17** and **4.18**, which were separated by column chromatography.⁷⁵ Subsequently, acid hydrolysis of the acetonide protecting groups using *p*-toluenesulfonic acid monohydrate (TsOH·H₂O) yielded the corresponding triols **4.19** and **4.20**, which following ozonolysis spontaneously cyclised to afford the target sugars **1.40** and **4.1**. Despite only being described on small scale, this three step sequence constituted the most efficient route to tetrafluoro glucose **1.40** and galactose **4.1**, obtained in 24% and 38% overall yield respectively. Furthermore, given its shortness, this synthetic route appeared ideal for scaling-up were it not for the large excess of MeLi and aldehyde **3.1** required (2.4 equiv. each) to afford the coupling adduct mixture **4.17/4.18** in good yield. Key reasons for this excess include the competing addition of MeLi on the electrophilic aldehyde **3.1** (Barbier type conditions). Such high consumption in starting materials is particularly penalising considering that aldehyde **3.1** is fairly expensive to buy from common chemical suppliers and has instead to be prepared prior to coupling (*cf* section 4.3). However, despite the consequent wastage of reagents that would result from the coupling step, large scale optimisation of this route remained the most suitable option for the multi-gram preparation of tetrafluoro glucose **1.40**.

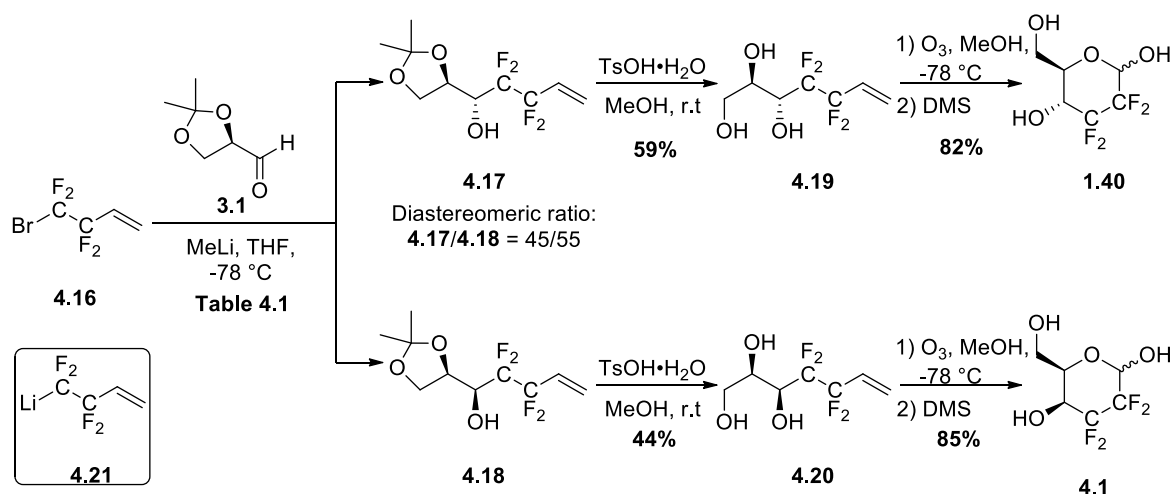
4.2 Objectives

Besides being required in sufficient quantities to determine its exchange rates across RBC membranes (± 150 mg), tetrafluoro glucose **1.40** is needed in large quantities to support a variety of projects currently ongoing within our group. While the current synthesis of tetrafluoro galactose **4.1** is satisfactory on large scale, this is not the case for the glucose derivatives **1.40**. Therefore, a straightforward and convenient multi-gram synthesis of this sugar is still required.

First, our attempts to upscale Konno's synthesis are described, followed by a number of modifications introduced to increase the proportion of the tetrafluoroglucose isomer **1.40** and facilitate the diastereomer separations on large scale.

4.3 The upscaling of the Konno synthesis

Prior to coupling with bromo-tetrafluorobutene **4.16**, aldehyde **3.1** had to be prepared on large scale through oxidative cleavage of 1,2:5,6-diisopropylidene-D-mannitol (not shown).⁷⁸ Inconveniently, the freshly prepared **3.1** underwent vigorous polymerisation only a few hours after its purification by distillation, regardless of the storage conditions. Contrary to what was stated in the procedure followed,⁷⁸ cracking of the resulting polymer by re-distillation under reduced pressure didn't allow good recovery of aldehyde **3.1** (< 50%). Therefore, to avoid the synthesis of a fresh batch of **3.1** before each coupling reaction, the latter was stored as a stock solution in dry tetrahydrofuran (THF) at -40 °C. Pleasingly, no polymerised material was now observed in the stock solution, even after several days of storage. This problem being solved, our efforts were directed toward the large-scale optimisation of the alkyllithium mediated coupling (**Scheme 4.5**, **Table 4.1**).



Scheme 4.5: Investigation of Konno's synthesis on large scale

When repeated following Konno's conditions, coupling between bromo-tetrafluorobutene **4.16** and aldehyde **3.1** afforded the coupling adduct mixture **4.17/4.18** in an unexpected low yield of 7% (**Entry 1**). This was most certainly due to the poor mixing resulting from the progressive solidification underwent by the reaction medium at -78 °C. Given its propensity to solidify under low temperatures and its relatively high concentration in the reaction medium, aldehyde **3.1** was deemed responsible for causing the solidification. Hence, to prevent such phenomenon, Konno's conditions were re-investigated using a medium half concentrated than in the original procedure (**Entry 2**). Although small aggregates of solidified material were still observed, these conditions yielded a reaction medium as a solution which, as expected, led to an improved yield in coupling

adducts **4.17/4.18** (27%). Further dilution of the reaction medium completely prevented the build-up of solidified material and resulted in an additional increase in yield up to 45% (**Entry 3**). Unfortunately, given the tight deadline in which tetrafluoro glucose **1.40** was required for the transport rate studies, these optimised conditions could not be investigated on larger scales. Instead, the mixture of coupling adducts **4.17/4.18** produced over these first series of experiments were combined and the synthesis continued (**Scheme 4.5**).

Table 4.1: Intermolecular coupling between aldehyde **3.1** and **4.16**

Entry	Bromide 4.16 (equiv.)	Aldehyde 3.1 (equiv.)	MeLi (equiv.)	[3.1] (mol.L ⁻¹)	Yield ¹ (%)	Reaction mixture state at -78 °C
Konno's conditions	1.0	2.4	2.4	0.8	75	/
1	1.0	2.4	2.4	0.8	7	Solid
2	1.0	2.4	2.4	0.4	27	Heterogeneous
3	1.0	2.4	2.4	0.3	45	Liquid

¹ Cumulated yield (**4.17** + **4.18**)

When attempted with the solvent system reported by Konno and co-workers, separation of the coupling adducts **4.17** and **4.18** by column chromatography gave only poor results. Indeed, complete separation could be achieved only after several HPLC runs with an optimised solvent system. Furthermore, for reasons not understood, acetonide hydrolysis never went to completion, and this even with stoichiometric quantities of TsOH·H₂O. Despite these problems, ozonolysis of both triols **4.19** and **4.20** efficiently afforded the sugars **1.40** and **4.1** which, after a final column chromatography to ensure complete purity, were isolated in sufficient quantities for the NMR transport studies (± 150 mg).

On a general note, it appeared that the high yields achieved by Konno and co-worker could not be reproduced, even on small scale. This was especially flagrant for the coupling step which, due to the incompatibility of aldehyde **3.1** with the reaction conditions, gave the coupling adduct mixture **4.17/4.18** in yields far below those expected (**Entry 1**). Even though the solidification phenomenon could be avoided upon dilution of the reaction medium, the yield of the desired adducts **4.17/4.18** remained moderate (**Entry 2** and **3**). Such lack of efficiency was attributed to the negative impact of high dilution factors on either or both the Li-Br exchange and the nucleophilic addition of tetrafluorobutenyle lithium **4.21** on aldehyde **3.1**, both being bimolecular processes. Hence, to enable the investigation of the coupling on more concentrated media, the use of a new aldehyde

substrate, less inclined to solidify under low temperature, was considered. In addition, it was aimed to achieve a diastereomer ratio more skewed towards the gluco-precursor.

4.4 Modifications of the Konno synthesis

4.4.1 Ley's aldehyde as substitute to D-glyceraldehyde acetonide

4.4.1.1 Synthesis of Ley's aldehyde

Despite being a useful chiral building-block, D-glyceraldehyde acetonide **3.1** appears to be a capricious substrate due to its propensity to rapidly polymerise, racemise, or form hydrates.^{78,79,80} Hence, other protected derivatives of D-glyceraldehyde such as dispiroketal **4.22**, 2-O-benzyl **4.23**, and butane-2,3-diacetal (BDA) **4.24**, have been investigated as potential substitutes (**Figure 4.2**).^{81,82,83,84} Despite being configurationally stable, both **4.22** and **4.23** have proved sensitive to both hydration and polymerisation when stored for extended periods of time. Only the BDA protected glyceraldehyde **4.24**, commonly referred to as the Ley aldehyde or Ley's aldehyde, has been found left unaltered after several months of storage under low temperatures (<-40 °C).

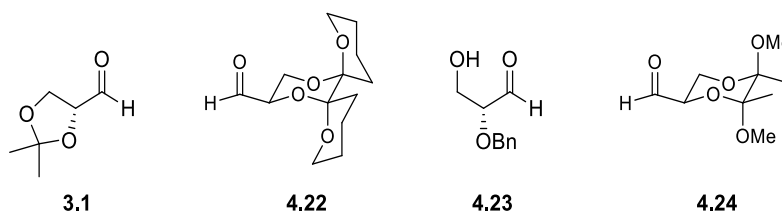
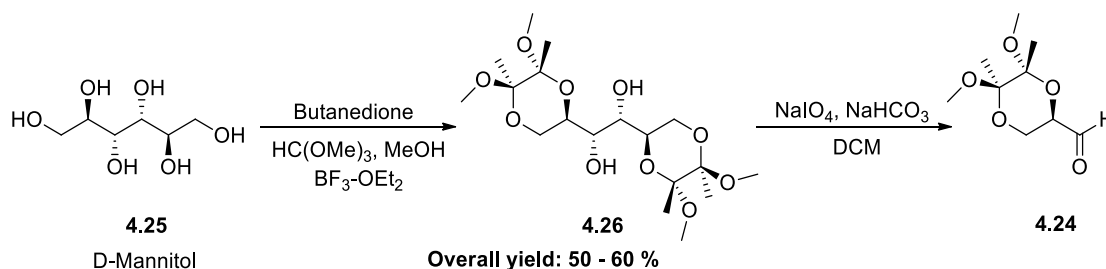


Figure 4.2: Potential substitute of D-glyceraldehyde acetonide **3.1** as chiral building block

Similarly to aldehyde **3.1**, Ley's aldehyde **4.24** can be prepared in a two step sequence starting from D-mannitol **4.25** (**Scheme 4.6**).⁸⁴



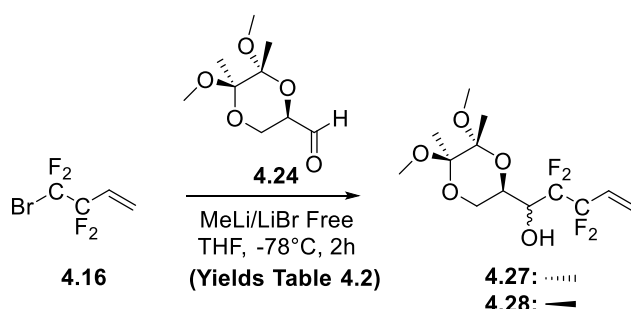
Scheme 4.6: Synthesis of Ley's aldehyde **4.24** from D-mannitol **4.25**

At first, the terminal 1,2 diol groups of D-mannitol **4.25** are selectively protected as their butane-2,3-diacetals to give compound **4.26**, then cleaved using sodium periodate in dichloromethane. Being straightforward, inexpensive, and consisting of two robust synthetic steps, this synthesis has proved ideal for large scale optimisations.^{85,86} Besides, a single purification by distillation after the

oxidative cleavage step is sufficient to obtain pure aldehyde **4.24**. Possible aldehyde epimerisation can be easily checked as this leads to a diastereomer instead of an enantiomer. When repeated in our group, this quick and simple synthesis afforded the enantiopure aldehyde **4.24** in yields comparable to those reported in the literature (50 to 60% over two steps).^{85,86} More than three months after synthesis, the different batches of aldehyde **4.24** stored in the freezer showed no signs of degradation by NMR (racemisation, polymerisation, hydrate formation).

4.4.1.2 Coupling between bromo-tetrafluorobutene and Ley's aldehyde

At first, coupling between bromo-tetrafluorobutene **4.16** and Ley's aldehyde **4.24** were investigated following Konno's conditions (Scheme 4.7, Table 4.2).



Scheme 4.7: Coupling reaction between bromide **4.16** and aldehyde **4.24** in batch conditions

On a similar scale as the Konno paper, coupling between **4.16** and **4.24** afforded the coupling adduct mixture **4.27/4.28** in a moderate yield of 44% (Entry 1). However, it seems important to highlight that the same conditions investigated with aldehyde **3.1** afforded the corresponding coupling mixture **4.17/4.18** in only 9% yield. Pleasingly, no traces of solidified material could be observed in the reaction mixture despite the high concentration of aldehyde **4.24** in the medium (0.8 mol.L⁻¹).

Table 4.2: Intermolecular coupling between aldehyde **4.24** and **4.16**

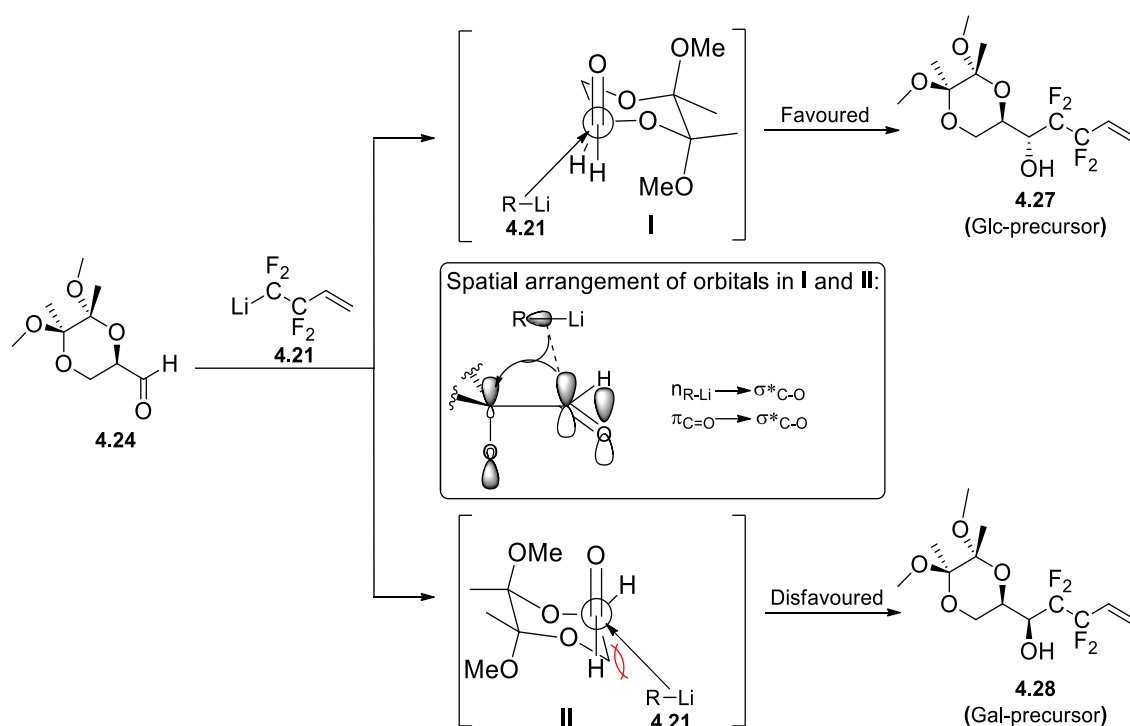
Entry	Bromide 4.16 (g / equiv.)	Aldehyde 4.24 (g / equiv.)	MeLi (mL / equiv.)	[4.24] (mol.L ⁻¹)	Yield ¹ (%)	Mixture state at -78 °C
1	0.8 / 1.0	2.2 / 2.4	6.1 / 2.4	0.8	44	Homogeneous liquid
2	4.2 / 1.0	5.1 / 1.2	30 / 2.4	0.8	37	Homogeneous liquid

¹Cumulated yield (**4.27** + **4.28**)

Upon upscaling, coupling was attempted following a modified version of the Konno procedure involving halved quantities of the electrophile partner (Entry 2), conditions previously investigated within our group for the coupling of bromo-tetrafluorobutene **4.16** with a sulfinylimine derivatives of D-glyceraldehyde (not shown).⁸⁷ Despite resulting in a slightly decreased yield of 37%, these

modified conditions enabled to maximise the conversion of the valuable aldehyde **4.24** into the desired coupling adducts **4.27** and **4.28**. Indeed, only 5 g of aldehyde **4.24** was required to produce around 2.2 g of the mixture **4.27/4.28** while, assuming that a 44% yield could have been reproduced on such scale, Konno's conditions would have produced only about 2.6 g of **4.27/4.28** from more than 10 g of aldehyde **4.24**.

Interestingly, replacement of D-glyceraldehyde acetone **3.1** by the Ley aldehyde **4.24** induced a marked diastereoselectivity in favour of the *anti*-coupling adduct **4.27**, which is the precursor of tetrafluoro glucose **1.40** (*dr* **4.27/4.28** > 80:20 by ^{19}F NMR). Such diastereomeric bias can be explained as follows (Scheme 4.8).



Scheme 4.8: Polar Felkin-Anh model applied to aldehyde **4.24**

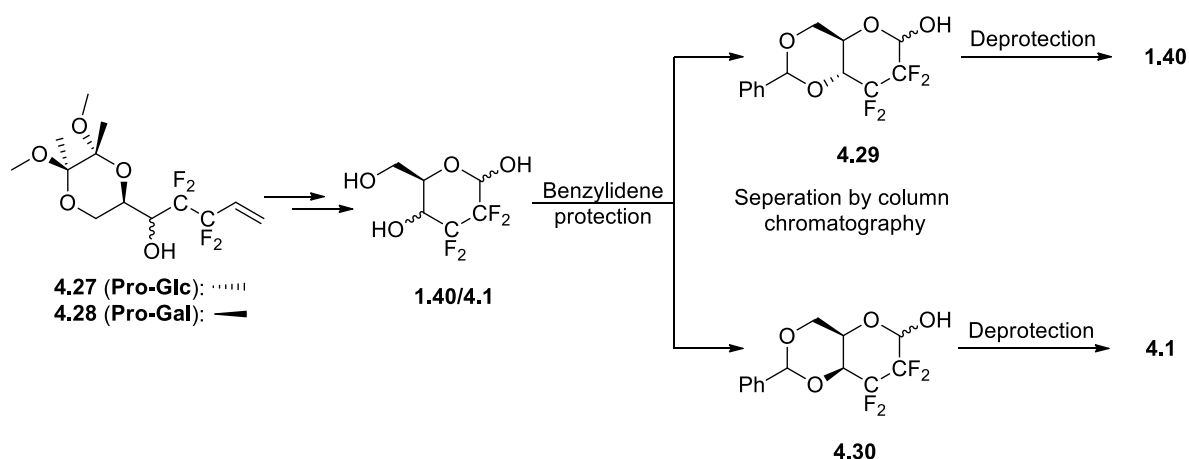
In accordance with a polar felkin-ahn model, aldehyde **4.24** would preferably adopt the conformations **I** and **II** where the optimal alignment between the π system orbitals ($\pi_{\text{C=O}}$) and the σ^* orbital of the adjacent C-O bond ($\sigma^*_{\text{C-O}}$) allows a stabilising hyperconjugative delocalisation of electrons ($\pi_{\text{C=O}} \rightarrow \sigma^*_{\text{C-O}}$). In addition, the electrons transferred by the incoming lithiated **4.21** into the $\pi^*_{\text{C=O}}$ can be directly delocalised into the $\sigma^*_{\text{C-O}}$, thus enabling stabilisation of the forming bond.^{88,89} By considering the Bürgi-Dunitz trajectories corresponding to the less hindered faces of **I** and **II**, it could be observed that the attack of **4.21** on conformer **II**, leading to the *syn*-adduct **4.28**, was disfavoured due to a steric clash generated by the adjacent $-\text{CH}_2$ substituent.^{90,91} Such steric repulsions appeared to be considerably reduced in the case of conformer **I**, for which the approach

of **4.21** occurs alongside of a hydrogen atom, thereby explaining the diastereoselective bias in favour of the *anti*-adduct **4.27**.

Surprisingly, no examples of organolithium additions on aldehyde **4.24** with which to compare our results could be found in the literature. Apart from a few examples of addition of organozinc in the presence of chiral auxiliaries,^{92,93} the selectivity resulting from the addition of organometallic reagents on **4.24** seems to have never been described. It is only briefly stated in an early paper published by Ley and co-workers that the addition of Grignard reagents has been studied and showed a selectivity similar to the one observed with the dispiroketal aldehyde **4.22**,⁸⁴ a substrate showing a marked selectivity toward the *anti*-addition product, regardless of the organometallic reagent investigated.^{81,82} Unfortunately, no further traces of such a study could be found in the literature.

4.4.2 Improved separation of the diastereoisomers

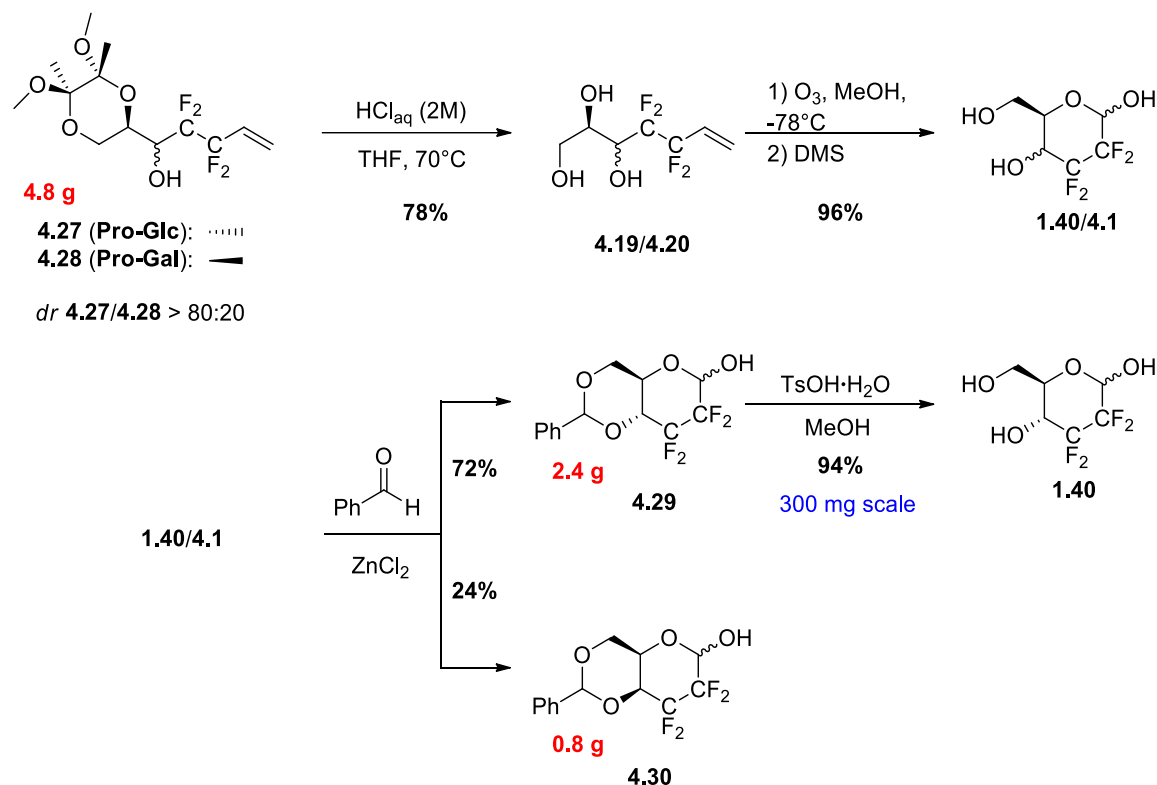
While replacement of D-glyceraldehyde acetonide **3.1** by the Ley aldehyde **4.24** induced a marked diastereoselectivity in favour of the desired *anti*-coupling adduct **4.27**, complete separation of the latter from the *syn*-coupling adduct **4.28** appeared as tedious as the resolution of the coupling adducts mixture **4.17/4.18**, obtained in Konno's original synthesis. Hence, a new strategy was investigated whereby the tetrafluorosugars **1.40** and **4.1** were synthesised as a mixture before being derivatised as their 4,6-*O*-benzylidene protected counterparts **4.29** and **4.30**, and separated by column chromatography (Scheme 4.9).



Scheme 4.9: Alternative synthesis of the tetrafluorosugars **1.40** and **4.1**

Based on what had been observed with similar substrates, the dramatic structural differences induced by the installation of a benzylidene protecting group on **1.40** and **4.1** was expected to considerably facilitate the separation by column chromatography. Synthesis of pure

tetrafluorosugars **1.40** and **4.1** following this alternative pathway was carried out as described below (Scheme 4.10).

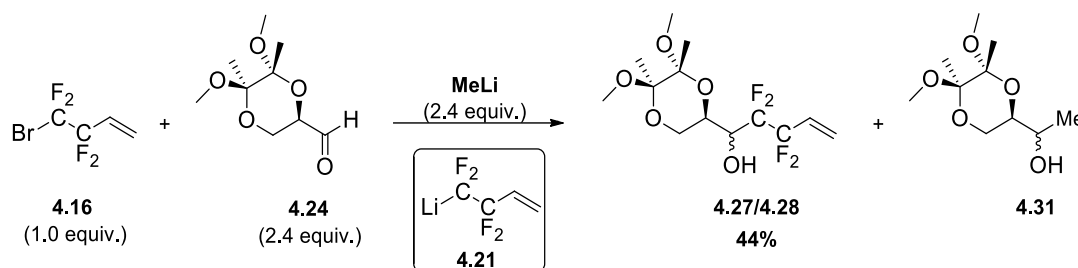


Scheme 4.10: Large scale synthesis of the 4,6-*O*-benzylidene-protected tetrafluoroglucose **4.29** followed by its deprotection on small scale

Once isolated, coupling adducts mixture **4.27/4.28** was treated with dilute aqueous hydrochloric acid in refluxing THF, providing the corresponding triol mixture **4.19/4.20** in a high yield. Subsequent ozonolysis gave the unprotected tetrafluorosugars **1.40/4.1** as a crude mixture which was quickly filtered over a pad of silica before being engaged in the next step. Benzylidene acetal formation using benzaldehyde as solvent then efficiently afforded the 4,6-protected sugars **4.29** and **4.30** which, pleasingly, could be completely isolated after a single separation by column chromatography. As detailed above, this three-step sequence could easily be conducted on multigram scale and afforded more than two grams of the 4,6-*O*-benzylidene tetrafluoroglucose **4.29**. As the latter was used in various ongoing projects at that time, only a small portion of 300 mg was subjected to classic hydrolysis conditions ($\text{TsOH} \cdot \text{H}_2\text{O}$ in MeOH), which afforded the 2,3-dideoxy-2,2,3,3-tetrafluoro-D-glucopyranose **1.40** in a high yield of 94%.

4.5 Summary

Besides being stable over long periods of time, aldehyde **4.24** could be coupled to 4-bromo-tetrafluorobutene **4.16** following Konno's conditions without causing complete solidification of the reaction mixture. However, despite the absence of experimental difficulties, we could not reproduce the high yields achieved by Konno using this substrate. Indeed, even on a small scale, the coupling adducts mixture **4.27/4.28** was obtained in only 44% yield while alcohol **4.31** resulting from the addition of MeLi on aldehyde **4.24** was formed in large quantities (non-quantified).



Scheme 4.11: Coupling reaction between bromo-tetrafluorobutene **4.16** and aldehyde **4.24** following a Barbier type procedure

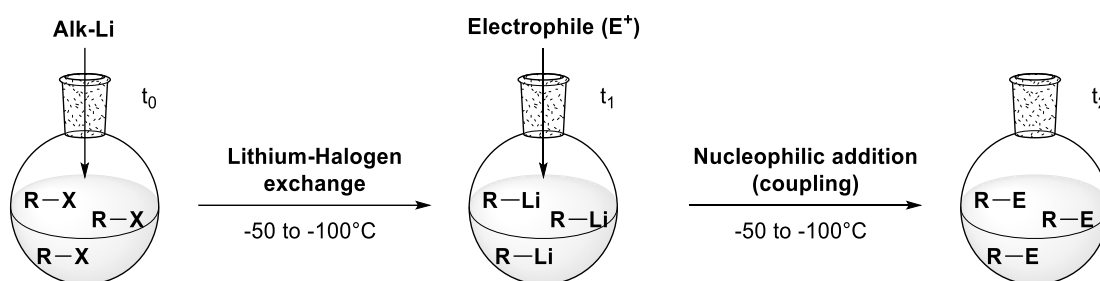
As envisioned, the 4,6-benzylidene protected tetrafluoro glucose **4.29** and galactose **4.30** could be smoothly separated by column chromatography before being deprotected under acidic conditions. Despite lengthening the synthesis, this late stage separation proved less time and solvent consuming than the repeated HPLC runs that would have been necessary to the complete resolution of the adduct mixture **4.27/4.28**, especially on large quantities. Furthermore, installation and removal of the benzylidene acetals both proved high yielding and hence didn't significantly affect the overall efficiency of this synthesis. Indeed, owing to the marked diastereoselectivity of the coupling reaction toward the *syn*-adduct **4.27** (*dr* **4.27/4.28** > 80:20), this synthesis afforded tetrafluoro glucose **1.40** in an overall yield of 22%, comparable to the one reported by Konno and co-workers (24%), and this on a multigram scale. Hence, if further optimisation of the low yielding coupling step could be achieved, this alternative route would constitute the most convenient option for the large-scale synthesis of tetrafluoro glucose **1.40**.

Concerning the coupling step, the main problem remained that the Li-Br exchange process yielding tetrafluorobutenyl lithium **4.21** was competing with the reaction between MeLi and aldehyde **4.24**. In other words, aldehyde **4.24** was believed too reactive to be present in the reaction mixture during the Li-Br exchange. Therefore, the decision was made to investigate an alternative procedure involving the generation of tetrafluorobutenyl lithium **4.21** in the absence of an electrophile using flow chemistry.

Chapter 5: Introduction to alkyllithium mediated coupling under micro-flow conditions

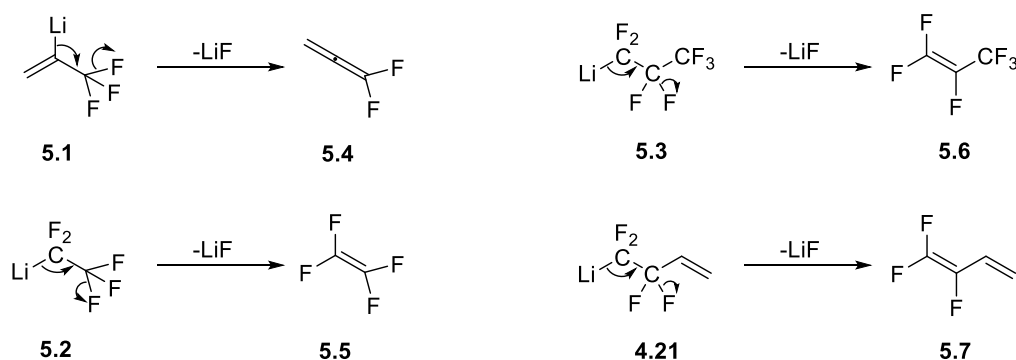
5.1 Alkyllithium mediated coupling under batch conditions: scope and limitations

Due to the high reactivity of alkyllithium reagents towards electrophile substrates, reductive couplings are usually conducted according to a one pot sequential procedure allowing the lithiated intermediate **R-Li** to be generated in absence of electrophile **E⁺** (**Scheme 5.1**).



Scheme 5.1: Generation of lithiated intermediates **R-Li** in absence of electrophiles **E⁺**

Owing to certain constraints inherent to batch reactors, this sequential procedure is particularly lengthy and hence ill adapted to the handling of short lived lithiated intermediates such as the β -fluoro lithiated species, prone to fast lithium-fluoride elimination (**Scheme 5.2**).⁹⁴ Instead, a Barbier type procedure enabling trapping of these highly unstable lithiated intermediates upon formation is generally preferred.^{74,75,76,76,77,95,96,97,98}



Scheme 5.2: Examples of unstable β -fluoro lithiated species

The main issue concerning the sequential method described above lies in the utilisation of batch reactors, which because of their small surface to volume ratio, struggle to dissipate the heat

generated by the Li-Hal exchange and the nucleophilic addition (slow cooling). Hence, to maintain the cryogenic conditions crucial to prevent highly unstable lithiated species from extremely rapid degradation, both alkyllithium reagents and electrophile substrates ought to be added in a controlled manner (dropwise addition), thus leading to procedure times largely exceeding the life-time of certain unstable lithiated intermediates, even under cryogenic temperatures.

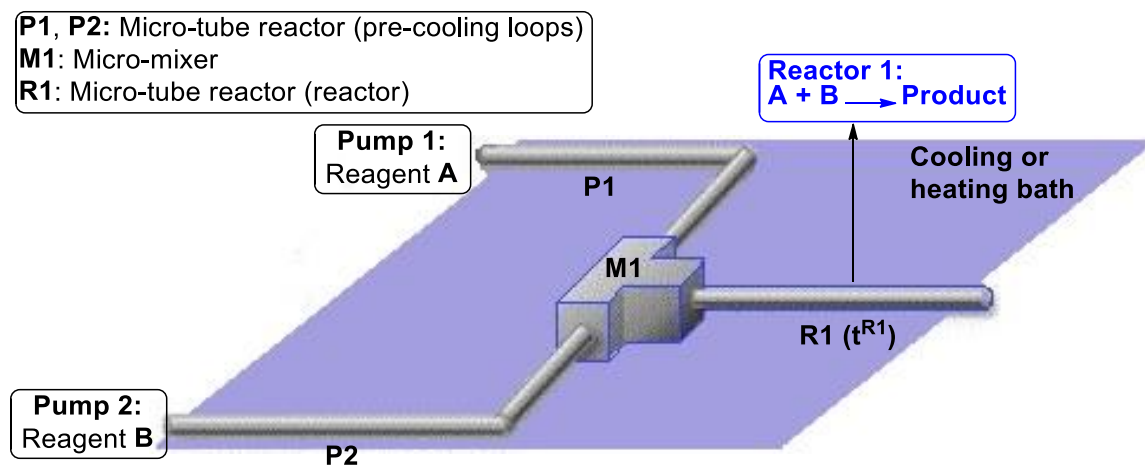
As explained in the following sections, the sequential procedure can be performed with very reduced time-scales when transposed onto micro-flow conditions, and is hence suitable for coupling involving highly unstable β -fluoro lithiated species.^{99,100,101,102}

5.2 Alkylolithium mediated coupling under micro-flow conditions:

Background

5.2.1 Description of micro-flow reactors

As their name suggests, micro-flow reactors consist of miniaturised versions of continuous flow reactors used in industry to synthesise organic compounds on kilogram- to tonne-scale. At its simplest (**Scheme 5.3**), a micro-flow setup is constituted of a single reactor (**Reactor 1**) in which a single chemical process is conducted. Apart from the pumps used to feed the reagent solutions, such system is constituted of four distinct elements.



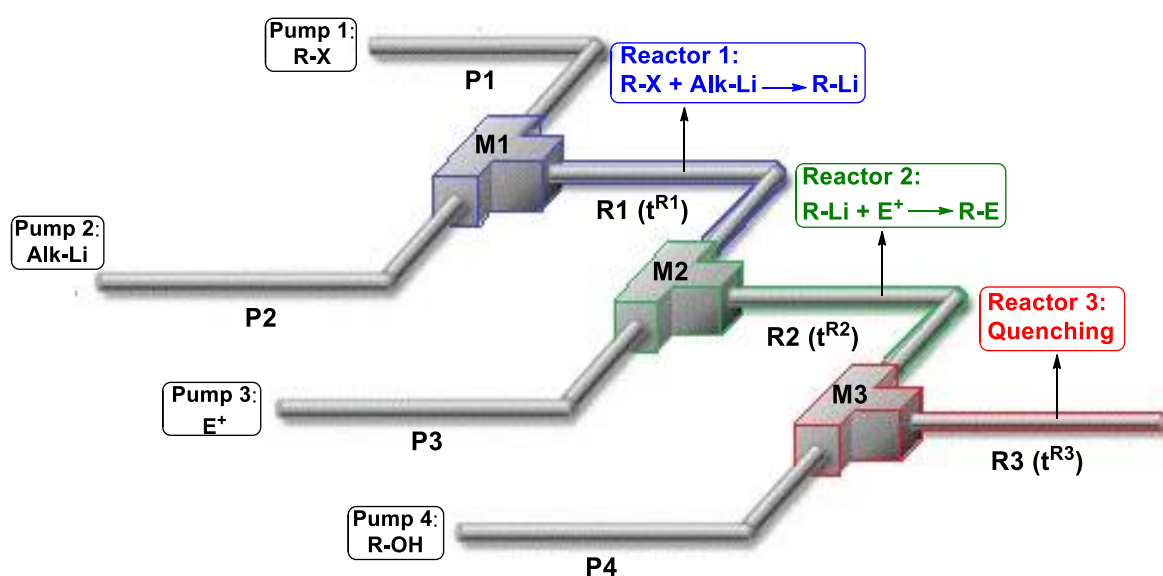
Scheme 5.3: Single reactor micro-flow setup

To start, a pair of micro-tube reactors called pre-cooling loops (**P1** and **P2**) through which the reagent solutions are brought to the desired temperature prior to reaction (*i.e.* cooling or heating bath temperature). Then, a micro-mixer (**M1**), where the reaction is triggered upon blending of the reactive substances. And finally, a micro-tube reactor (**R1**) through which the reaction is pursued for a certain duration, called residence time (t^{R1}), determined by both the inner volume of the

micro-tube reactor and the flowrate. As detailed later in this chapter, the inner volumes of micro-mixers being considerably reduced compared to those of micro-tube reactors, these are generally neglected while calculating the residence times. Hence, the residence time t^{R1} associated to **Reactor 1** will depend only on the inner volume of **R1** and the flowrates imposed in **P1** and **P2**.

5.2.2 Multi-reactor setup and alkyllithium mediated couplings

When transposed into micro-flow conditions, alkyllithium mediated couplings are usually performed using a multi-reactor setup allowing the lithiated intermediate **R-Li** to be generated and reacted in two separate reactors, thus limiting the risks of side reactions between alkyllithium reagents and electrophiles (**Scheme 5.4**). Besides, owing to their narrow inner volumes, micro-reactors enable **R-Li** intermediates to be quickly generated and transferred from **Reactor 1** to **Reactor 2** where they are reacted, thereby minimising the risks of degradation. Although not indicated on the scheme below, the entire setup is usually immersed in a cooling bath.



Scheme 5.4: Multi-reactor micro-flow setup

For each coupling investigated using this method, the main challenge lies in finding temperatures and residence times (t^{R1}) allowing efficient formation of the **R-Li** intermediate, while at the same time preventing its degradation. Hence, in order to determine or at least approach these optimal conditions, each coupling reaction studied ought first to be investigated using various t^{R1} and temperature conditions. Fortunately, micro-flow reactors are powerful optimisation tools enabling rapid and convenient screening of temperature and residence time conditions. Contrary to batch reactions, flow processes can quickly be stopped and restarted by switching off or on the pumps feeding the system. Hence, during a same run, a flow setup can be “paused” as many times as desired to modify the t^{R1} and/or the temperature. If sufficient volumes of reagent solutions are

available, several tens of t^{R1} and temperature conditions can be screened in a single run. Finally, given that micro-tube reactors are easily interchangeable and the flowrates smoothly adjustable *via* the pumps, t^{R1} ranging from several minutes down to split seconds can be covered.

5.2.3 Micro-flow reactor: properties and benefits

5.2.3.1 Micro-tube reactors

With dimensions ranging from 0.5 to 2 millimetres in inner diameter, and from a few centimetres to meters in length, micro-tube reactors exhibit inner volumes significantly smaller than those of batch vessels. By virtue of such narrowed reaction environments, chemical processes conducted under micro-flow conditions generally reach completion in a time-span ranging from several seconds down to the split second. Hence, even highly unstable **R-Li** intermediates such as those displayed in **Scheme 5.2** can be efficiently generated and reacted within time-scales fitting their lifetimes.^{99,101,103} Being handcrafted from HPLC stainless steel lines, micro-tube reactor can be designed with the exact desired inner volumes. A great scalability which, together with the accurate flowrate control granted by the pumps, enables a precise residence time control to the milli-second. As illustrated later in this chapter, such high-resolution time control is of pivotal importance for screening residence times t^{R1} below the second time-scale, as it is often the case with highly unstable lithiated intermediates (*cf* section 5.3.2).^{104,105}



Figure 5.1: Micro-tube reactor ($\approx 100 \text{ cm} < L < 200 \text{ cm}$) used as pre-cooling loop (left), stainless steel micro-tube reactor (L highly variable) used as reactor (right)

5.2.3.2 Micro-mixers

Because of their complex inner structures, micro mixers cannot be manufactured without specific know-how and equipment, and thus must be ordered from specialised companies. Similarly to micro-tube reactors, micro-mixers are generally made of stainless steel and can be designed in different forms depending on the performances desired (**Figure 5.2**). With an inner diameter inferior to 1 mm, generally 250 or 500 micrometres (μm), and a total channel length of approximately 1 cm, these micro-mixing units confer an exceptionally fast and efficient mixing,

described as *quasi*-instantaneous, crucial given the extremely short reaction time investigated under micro-flow conditions.^{104,105}

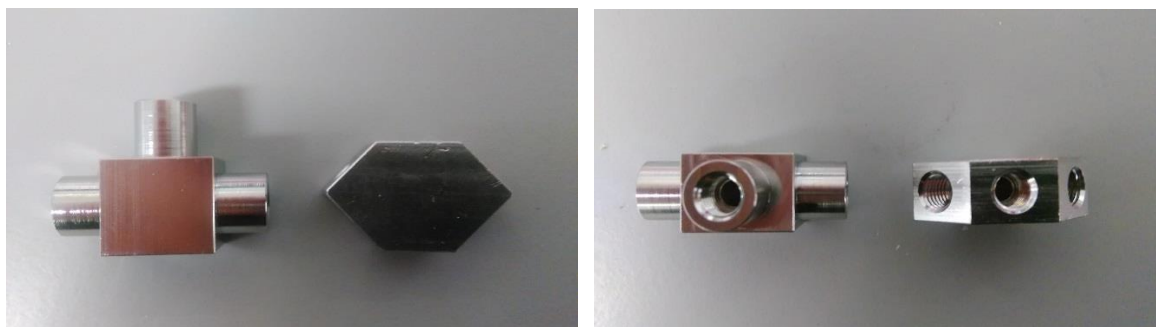


Figure 5.2: T-shaped and hexagonal micro-mixers, front view (left) and top view (right)

Thanks to their large surface to volume ratio, both micro-tube reactors and micro-mixers ensure a highly efficient heat transfer which translates into a precise temperature control. This, along with the high-resolution residence time control, is of critical importance to investigate the stability of short lived **R-Li** intermediates in **R1**.¹⁰⁶

To summarize, micro-flow technology enables the study and control of extremely fast chemical processes, usually involving highly unstable intermediates, by means of high resolution time and temperature controls. This domain of flow chemistry has recently been coined by Pr. Yoshida as “flash chemistry”, term for which he gave the following definition: “Flash chemistry is defined as a field of chemical synthesis where extremely fast reactions are conducted in a highly controlled manner to produce desired compounds with high selectivity.”¹⁰⁴

5.2.3.3 Optimisation of batch processes

Besides enabling convenient handling of short lived **R-Li** intermediates, micro-reactors have proved a powerful tool for optimising certain alkyllithium mediated couplings described in batch reactors. Indeed, by virtue of the highly efficient mixing and temperature control conferred by micro-spaces, transposition of coupling processes from batch to micro-flow conditions has on multiple occasions resulted in optimised yields and performances.^{107,108,100,109,110,111,112} In addition, owing to the short reaction times and the efficient heat transfer enabled by micro-reactors, exothermic reactions can be performed at temperatures much higher than those required under batch conditions. This is notably the case for certain couplings involving unstable lithiated intermediates for which good to excellent yields were achieved at 0 or 25 °C, temperatures at which most of the lithiated intermediates almost entirely degrade prior to coupling when handled in batch reactors.^{108, 100, 109, 110, 111,}

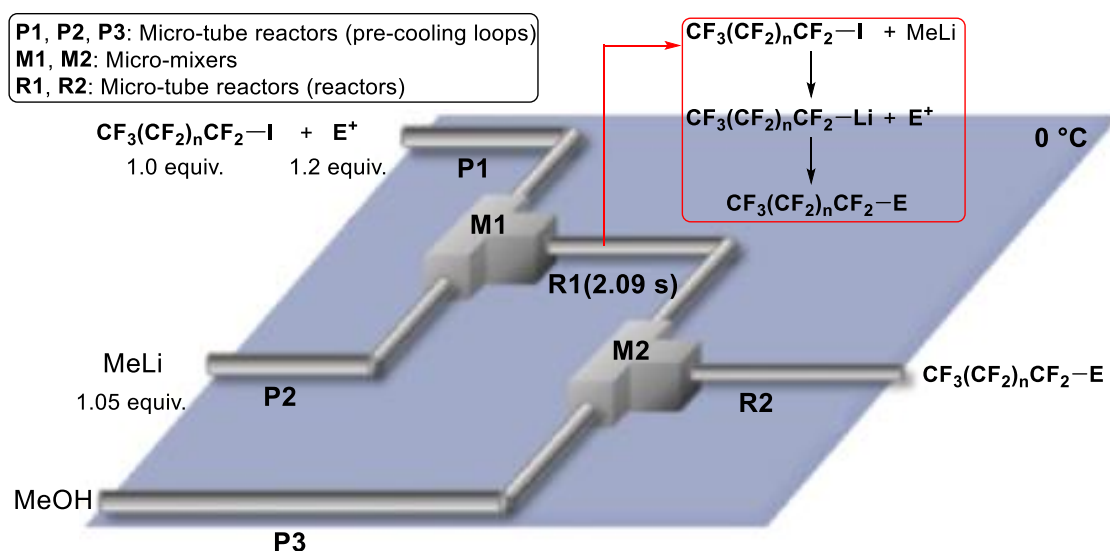
Although the production capacity of a micro reactor at any one time is considerably small, certain micro-flow processes have proved able to generate several grams of compound in a few tens of minutes, a throughput unreachable under batch conditions where gram to multi-gram scale processes usually take at least several hours to reach completion.^{103,113, 114,115, 116} In addition, due to the possibilities of thermal runaways or accumulations of dangerous intermediates (explosive, toxic), certain large-scale reactions remain unsafe when conducted in batch reactors. Two hazardous situations that are prevented while operating under micro-flow conditions, thanks to the reduced inner volumes and the efficient heat transfer provided by the reactors.

5.3 Perfluoroalkylation under micro-flow conditions

In 2011, a highly efficient alkyllithium mediated coupling of perfluoroalkyl iodides to electrophiles was developed under micro-flow conditions.¹⁰² This new methodology envisioned by Pr. Yoshida encompasses the generation of perfluoroalkyllithium both in presence and absence of electrophile.

5.3.1 Generation of perfluoroalkyllithium in the presence of electrophiles

At first, coupling between perfluoroalkyl iodides $\text{CF}_3(\text{CF}_2)_n\text{CF}_2\text{-I}$ and electrophiles E^+ were investigated using a flow system in which the perfluoroalkyllithium intermediate $\text{CF}_3(\text{CF}_2)_n\text{CF}_2\text{-Li}$ was generated in the presence of electrophiles (**Scheme 5.5**).

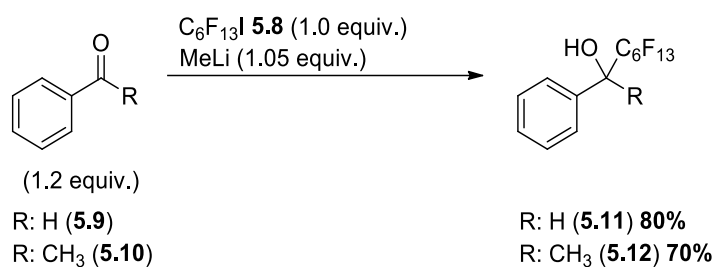


Scheme 5.5: Couplings of perfluoroalkyl iodides $\text{CF}_3(\text{CF}_2)_n\text{CF}_2\text{-I}$ to electrophiles E^+ under micro-flow conditions, formation of perfluoroalkyllithium $\text{CF}_3(\text{CF}_2)_n\text{CF}_2\text{-Li}$ in presence of electrophile

In this configuration, MeLi, electrophiles, and perfluoroalkyl iodides are simultaneously blended in micro-mixer **M1** and the resulting medium let to react throughout micro-tube reactor **R1**, before

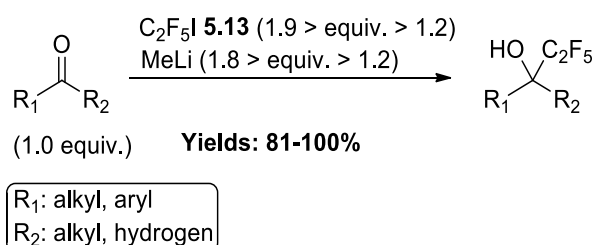
being quenched *via* addition of methanol in **M2**. This method can thus be described as a micro-flow version of the Barbier procedure.

When investigated using this setup, coupling between perfluorohexyliodide **5.8** and both benzaldehyde **5.9** and benzophenone **5.10** afforded the corresponding fluorohydrins **5.11** to **5.12** in high yields (**Scheme 5.6**). Comparable results were achieved when perfluorohexyliodide **5.8** was coupled with isocyanates derivatives (not shown).



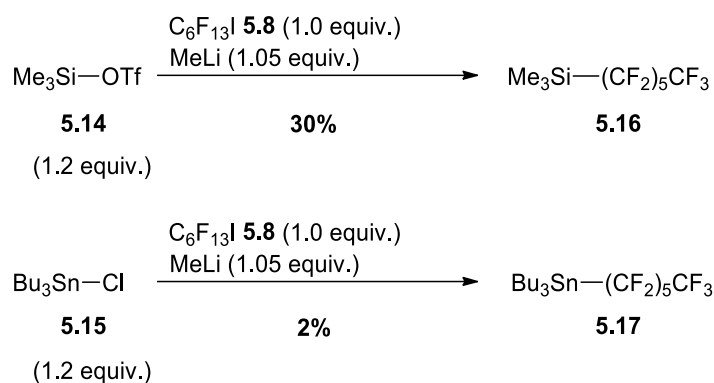
Scheme 5.6: Coupling of perfluorohexyliodide **5.8** to carbonylated derivatives using micro-flow reactor, generation of perfluoroalkyl lithium in presence of electrophile

It is noteworthy that contrary to similar couplings conducted by Gassman and co-workers in batch reactors (**Scheme 5.7**), only reduced excesses of perfluoroalkyl halides and MeLi were required to afford high yields, indicating that the lithium-iodide (Li-I) exchange was more efficient under micro-flow conditions than in batch ^{74,75}



Scheme 5.7: Coupling of perfluoroethyl iodide **5.13** to carbonylated derivatives using the Barbier procedure in batch reactor

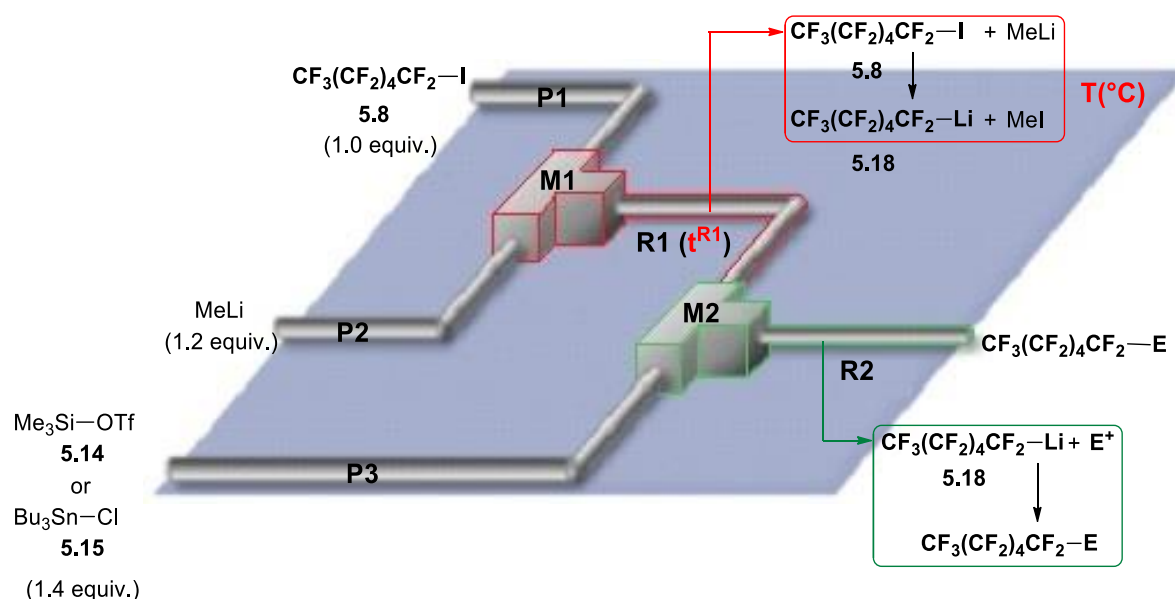
Owing to the efficient heat transfer provided by the setup, these good results could be achieved above cryogenic conditions, here at 0°C, a temperature at which only mediocre yields are usually achieved under batch conditions due to the rapid decomposition of perfluoroalkyllithium species. However, despite its considerable benefits, this method appeared ill-adapted to the handling of highly reactive electrophiles. In fact, couplings involving trimethylsilyl triflate **5.14** and tributyltin chloride **5.15** both gave the desired coupling adducts **5.16** and **5.17** in low yields (**Scheme 5.8**), this was attributed by Yoshida and co-workers to the rapid addition of MeLi on both **5.14** and **5.15** at the detriment of the Li-I exchange.



Scheme 5.8: Coupling of perfluorohexyliodide **5.8** with highly reactive electrophiles using micro-flow reactor, generation of perfluoroalkyl lithium in presence of electrophile

5.3.2 Generation of perfluoroalkyllithium in the absence of electrophiles

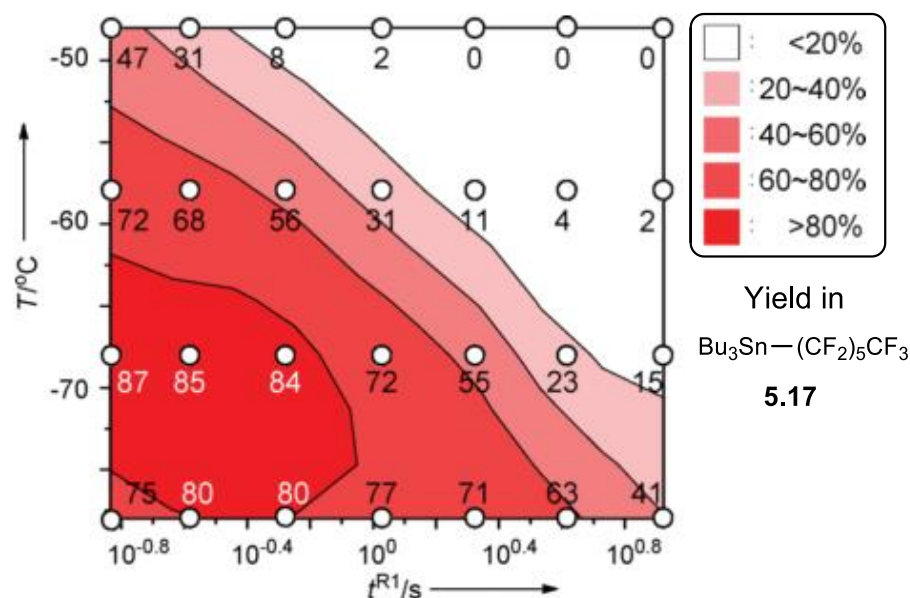
To prevent the MeLi addition to trimethylsilyl triflate **5.14** or tributyltin chloride **5.15**, Yoshida and co-workers decided to re-investigate these reactions using a micro-flow setup in which perfluorohexyl iodide **5.8** can be generated in absence of electrophiles (**Scheme 5.9**). Even though not indicated on the scheme below, **R2** is connected to a third micro-mixer in which the reaction mixture is quenched through the addition of methanol, as with the previous system.



Scheme 5.9: Couplings of perfluorohexyliodide **5.8** to electrophiles E^+ under micro-flow conditions, formation of perfluorohexyl lithium **5.18** in absence of electrophile

At first, coupling between tributyltin chloride **5.15** and perfluorohexyliodide **5.8** was investigated using various temperatures and residence time in **R1** (t^{R1}) to determine the optimal conditions for handling perfluorohexyl lithium **5.18**. Owing to the precise temperature and residence time controls granted by the setup, the high-resolution temperature-residence time profile displayed

below could be plotted (**Graphic 5.1**). As indicated on the latter, excellent yields in adduct **5.17** could be achieved with cryogenic temperatures, $T < -60\text{ }^{\circ}\text{C}$, and extremely short residence times, $t^{\text{R1}} \leq 0.40\text{ s}$. Due to the low stability of perfluorohexyl lithium **5.18**, any conditions involving temperatures or t^{R1} above these values invariably resulted in sensibly decreased yields.



Graphic 5.1: Impact of $T(^{\circ}\text{C})$ and t^{R1} on the yield in compound **5.17**¹⁰²

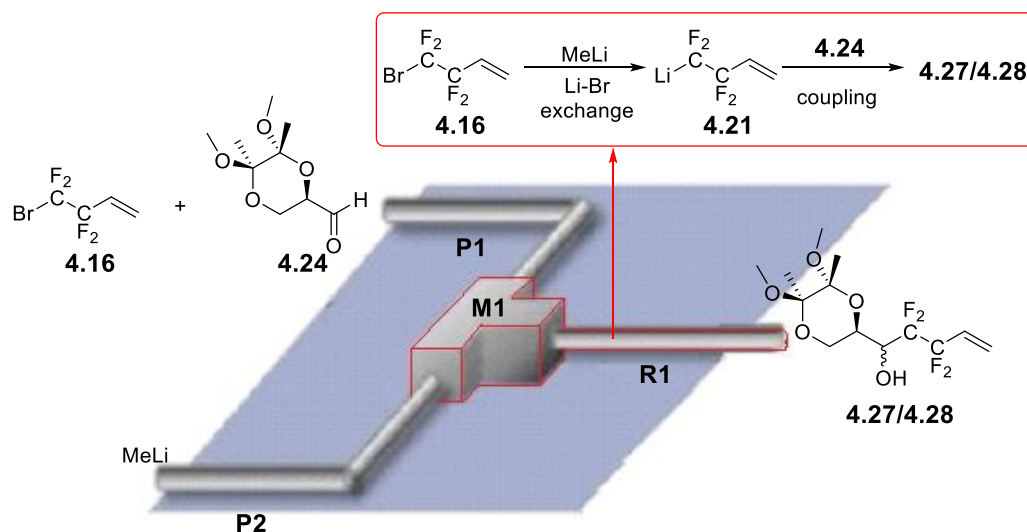
Ultimately, the temperature-residence time profile allowed the determination of the optimal conditions for coupling tributyltin chloride **5.15** and perfluorohexyl iodide **5.8**, $T = -70\text{ }^{\circ}\text{C}$ and $t^{\text{R1}} = 0.16\text{ s}$, for which adduct **5.17** was obtained in a 87 % yield. Using these optimized conditions, coupling between trimethylsilyl triflate **5.14** and **5.8**, previously achieved in a mediocre yield of 30%, was re-investigated and this time afforded the desired coupling adduct **5.16** in 82% yield.

In view of the outstanding results reported by Yoshida and co-workers, it was decided to investigate the coupling reaction between bromo-tetrafluorobutene **4.16** and aldehyde **4.24** using similar setups. Considering the lack of expertise of our group regarding flow chemistry, the decision was made to contact Pr. Yoshida to get advice on the feasibility of such a project. In response to our request, Pr. Yoshida generously proposed to share his expertise in flash flow chemistry by allowing me to carry out a short placement in his group, after which the technology and knowledges were transferred back to Southampton.

Chapter 6: Coupling between bromo-tetrafluorobutene and Ley's aldehyde under micro-flow conditions

6.1 Formation of the lithiated intermediate in the presence of Ley's aldehyde

At first, tetrafluorobutenyle lithium **4.21** was generated in presence of aldehyde **4.24** using a single reactor micro-flow system (Scheme 6.1).

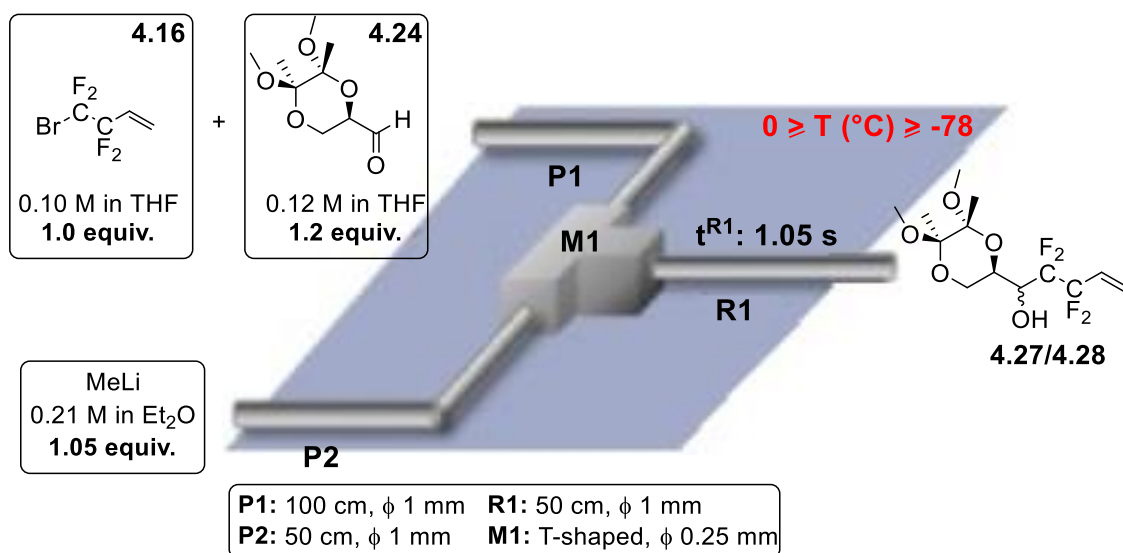


Scheme 6.1: Couplings of bromo-tetrafluorobutene **4.16** to Ley's aldehyde **4.24** under micro-flow conditions with formation of tetrafluorobutenyle lithium **4.21** in presence of aldehyde

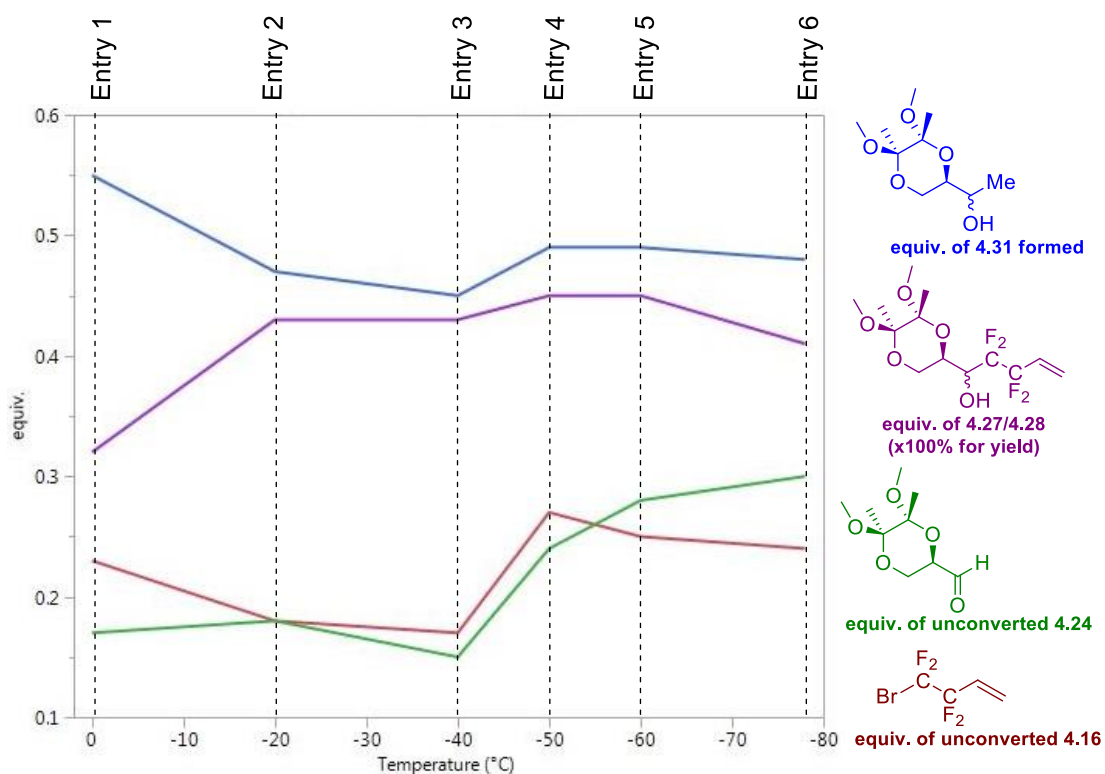
With this system, the reaction mixture was quenched at the outlet of the setup while being collected in a flask containing a saturated solution of ammonium chloride. Then, the different solutes present in the quenched mixture were quantified using gas chromatography (GC) analysis with an internal standard.

6.1.1 Investigation of Yoshida's coupling conditions

In a first series, the conditions reported by Yoshida and co-workers for the generation of perfluoroalkyllithium in presence of electrophiles were investigated with temperatures ranging from 0 to -78 °C (Scheme 6.2, Graphic 6.1).



Scheme 6.2: Investigation of Yoshida's conditions, formation of tetrafluorobutenyle lithium **4.21** in presence of aldehyde

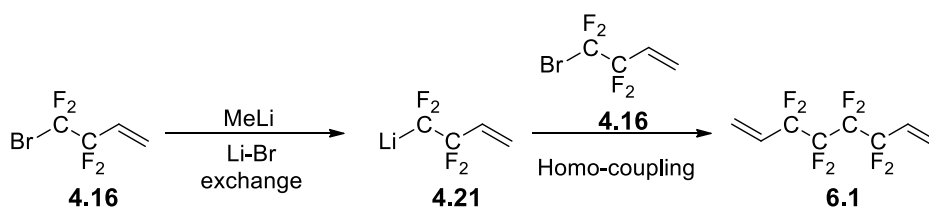


Graphic 6.1: Data collected while investigating conditions presented in **Scheme 6.2**

When examined at 0 °C (**Entry 1**), these conditions afforded the mixture of coupling adducts **4.27/4.28** in a moderate yield of about 30%, while producing more than 0.5 equiv. of alcohol **4.31**, resulting from the MeLi addition on aldehyde **4.24**. Small quantities of unreacted aldehyde **4.24** and bromo-tetrafluorobutene (bromide) **4.16** could be observed in the reaction mixture (≈ 0.2 equiv.). A first decrease in temperature down to -20 °C resulted in a slightly increased yield in adducts **4.27/4.28** ($\approx 40\%$), alongside with an inversely proportional reduction of alcohol **4.31** formed (**Entry 2**), thus suggesting that lower temperature favours the Li-Br exchange over the

competing addition of MeLi on aldehyde **4.24**. Similar results were obtained with a temperature of $-40\text{ }^{\circ}\text{C}$ (**Entry 3**). A further decrease in temperature down to $-50\text{ }^{\circ}\text{C}$ then led to slight increase in both yield in adducts **4.27/4.28** and quantity of alcohol **4.31** formed, accompanied by marked increase in both unconverted aldehyde **4.24** and bromide **4.16** (**Entry 4**). Comparable results were achieved as the temperature was decreased to -60 and then $-78\text{ }^{\circ}\text{C}$ (**Entry 5 and 6**). Overall, these conditions afforded the coupling adducts mixture **4.27/4.28** only in moderate yields ($\approx 40\%$). As indicated by the quantities of alcohol **4.31** formed, this was due to competing MeLi addition onto aldehyde **4.24**. Indeed, for each of the conditions probed, about half of the MeLi used was added to aldehyde **4.24** instead of reacting with bromide **4.16**, hence explaining the incomplete consumption of the latter. Similar to the batch conditions, the coupling reaction proceeded with a marked diastereoselectivity towards the *anti*-coupling adduct **4.27** (*dr* **4.27/4.28** $> 80:20$ by ^{19}F NMR).

Given that around half of the MeLi was reacted to give alcohol **4.31** (≈ 0.5 equiv.), the consumption of around 0.8 equiv. of bromide **4.16** could not solely be imputed to the Li-Br exchange. Hence, it was postulated that a certain portion of bromide **4.16** was consumed by a Wurtz-type coupling with tetrafluorobutenyl lithium **4.21**, yielding the octafluorinated-1,7-diene **6.1** (**Scheme 6.3**).



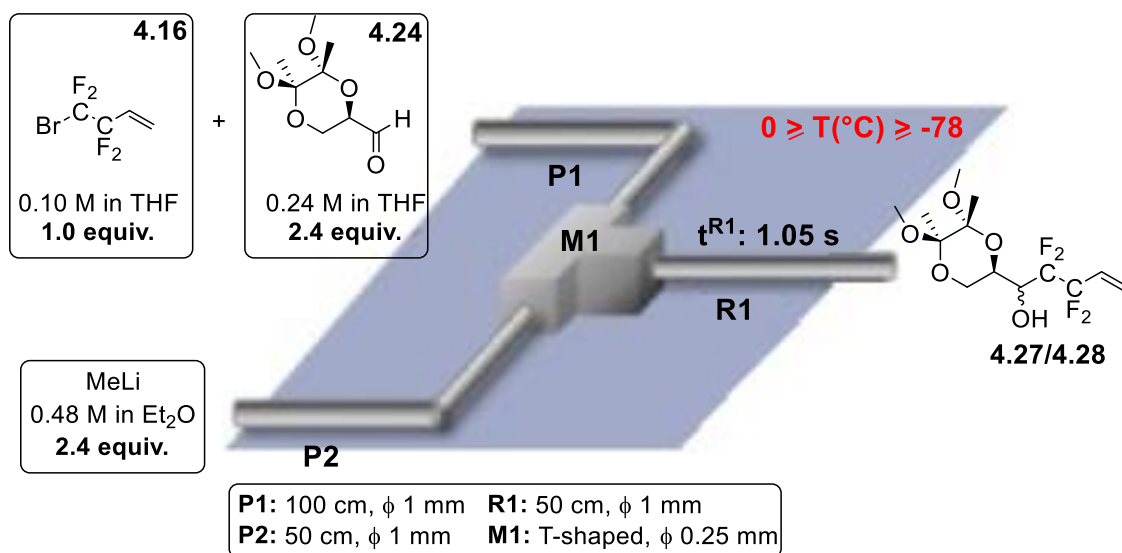
Scheme 6.3: Wurtz-type coupling between tetrafluoro bromide **4.16** and lithiated **4.21**

However, no signals which could have corresponded to **6.1** could be observed on the gas chromatograms. It was however strongly believed that this product was formed but couldn't be discriminated from THF, used as solvent for the reaction, as both were expected to be poorly retained by the apolar stationary phase used for analysis (GC). Besides, given the high boiling point of the adducts **4.27/4.28**, a steep temperature increase was necessary to avoid lengthy GC analysis, hence favouring the coelution of **6.1** with THF despite their different boiling points.

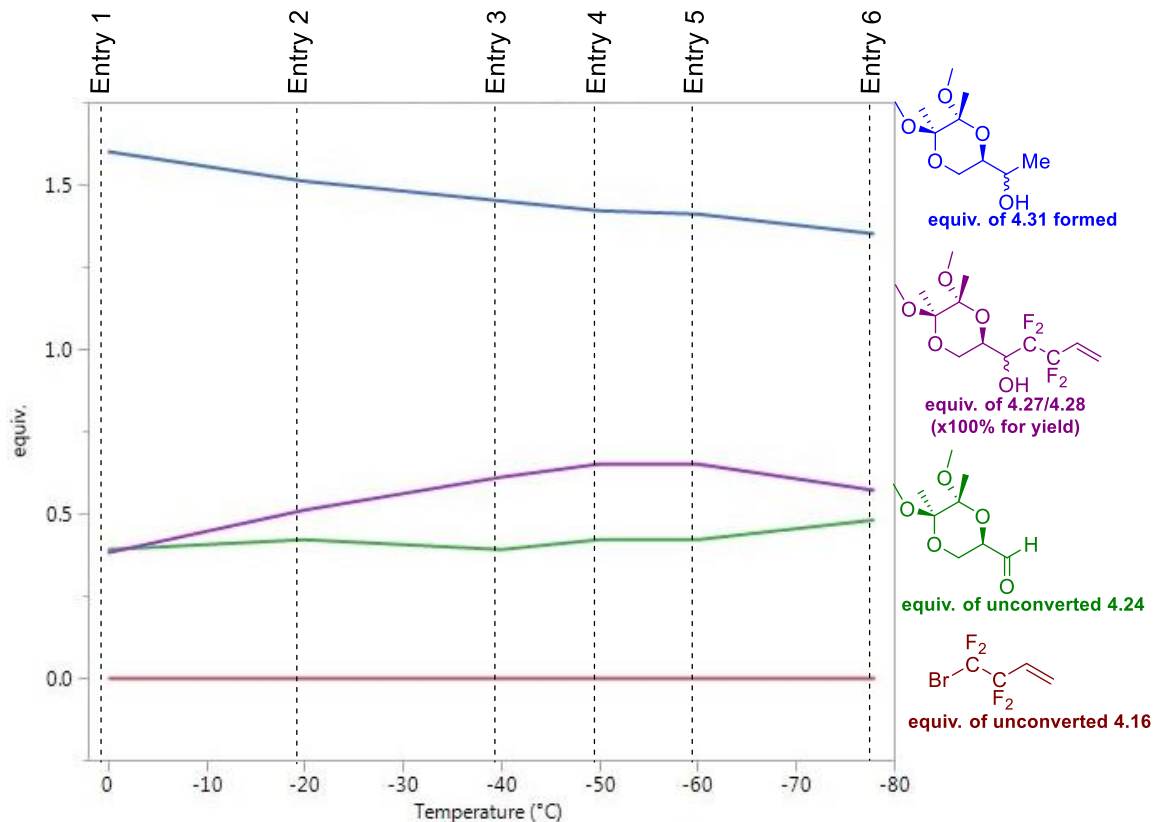
As previously observed by Yoshida and co-workers, the effectiveness of this method remains entirely dependent on the reactivity of the electrophile substrate investigated.¹⁰² However, even though the yields in coupling adducts **4.27/4.28** remained moderate (at best $\approx 45\%$), these conditions did not require large excess of both aldehyde **4.24** and MeLi as used in the Konno conditions, and hence would be suitable for upscaling. As a reminder, the same reaction conducted on large scale in batch reactor gave the coupling adducts **4.27/4.28** only in 37% yield with 1.2 equiv. of aldehyde **4.24** and 2.4 equiv. of MeLi (*cf* section **4.4.1.2**).

6.1.2 Investigation of Konno's coupling conditions

In a second series, the coupling conditions described by Konno and co-workers were transposed onto micro-flow conditions and investigated with temperatures ranging from 0 to -78 °C (**Scheme 6.4, Graphic 6.2**).



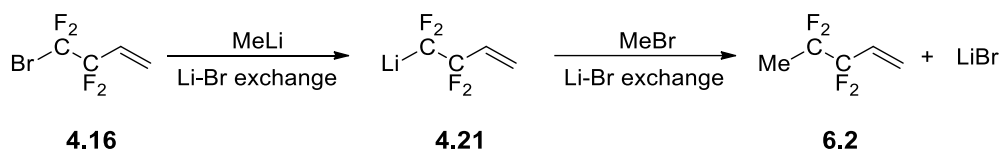
Scheme 6.4: Investigation of Konno's conditions, formation of tetrafluorobutenyl lithium **4.21** in presence of aldehyde



Graphic 6.2: Data collected while investigating conditions presented in **Scheme 6.4**

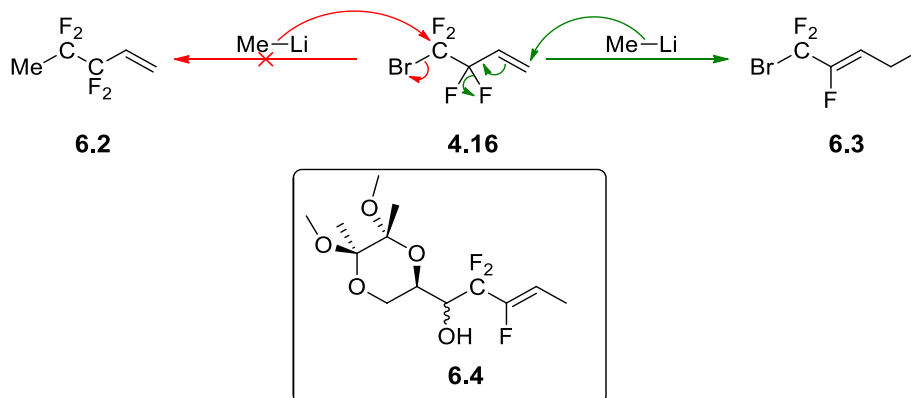
As indicated on the graph previous page, the yield in coupling adducts mixture **4.27/4.28** steadily increased from 40 to 60% approximately as the temperature was decreased from 0 to -60°C (**Entry 1** \rightarrow **5**). At the same time, the quantity of alcohol **4.31** formed gradually decreased from 1.6 down to 1.5 equiv., once again indicating that low temperatures favour Li-Br exchange over MeLi addition. To finish, a further drop of temperature from -60°C to -78°C resulted in a slightly decreased yield in adducts **4.27/4.28** (**Entry 5** \rightarrow **6**). With bromide **4.16** being entirely consumed at -78°C , it was presumed that the temperature was too low to ensure complete addition of tetrafluorobutenyle lithium **4.21** on aldehyde **4.24** within the t^{R1} investigated.

For all the conditions investigated, the incomplete conversion of the consumed bromide **4.16** into adducts **4.27/4.28** suggested that besides reacting with aldehyde **4.24**, lithiated **4.21** was also engaged in a Wurtz-type coupling with bromide **4.16** (*cf* **Scheme 6.3**). Alternatively, lithiated **4.21** could have reacted with the bromomethane (MeBr) formed upon Li-Br exchange between bromide **4.16** and MeLi, thus yielding tetrafluoropentene **6.2** (**Scheme 6.5**).



Scheme 6.5: Li-Br exchange between tetrafluorobutenyl lithium **4.21** and bromomethane

Also, the large excess of MeLi engaged could have promoted its nucleophilic addition onto bromide **4.16**. Given that direct substitution ($\text{S}_{\text{N}}2$ mechanism) of the bromide is impossible due to the electrostatic repulsions generated by the $\text{CF}_2\text{-CF}_2$ fragment, the MeLi addition was expected to occur on the activated alkene to give the trifluoropentene derivatives **6.3** ($\text{S}_{\text{N}}2'$ mechanism, **Scheme 6.6**). Such a process is known to be facilitated under higher temperatures, and hence could have explained the increase in yield as the temperature was decreased from 0 to -60°C (**Entry 1** \rightarrow **5**). However, this side reaction remained highly unlikely as the resulting **6.3** could have been lithiated as well, and coupled to aldehyde **4.24** to give the adduct **6.4**, which was never observed.



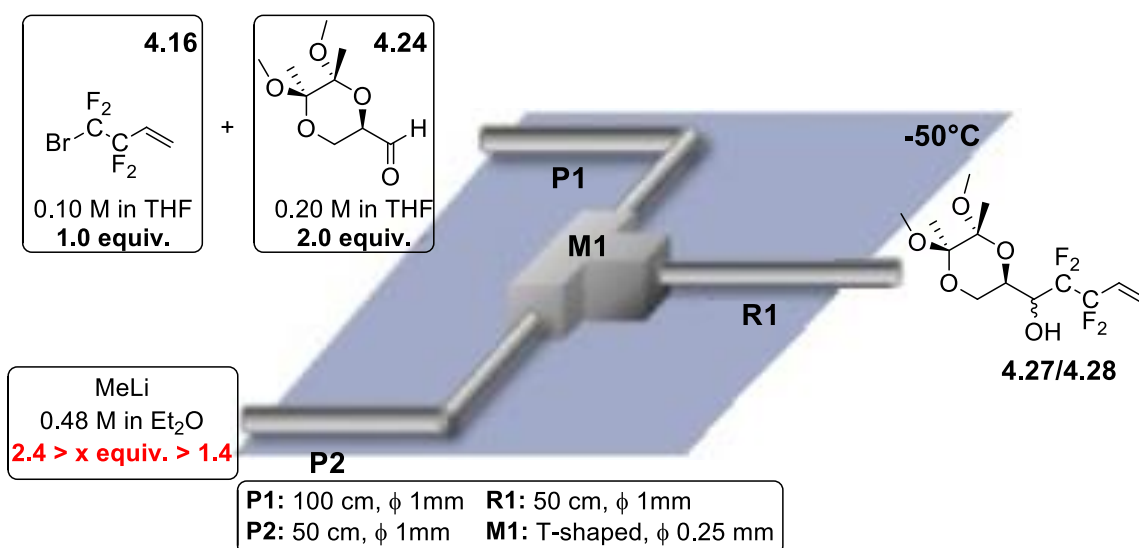
Scheme 6.6: MeLi addition on tetrafluorobutene bromide **4.16**.

Besides, neither tetrafluoropentene **6.2** resulting from reaction between tetrafluorobutenyle lithium **4.21** and MeBr (**Scheme 6.5**), nor the MeLi addition product **6.3** (**Scheme 6.6**), could be observed by GC analysis.

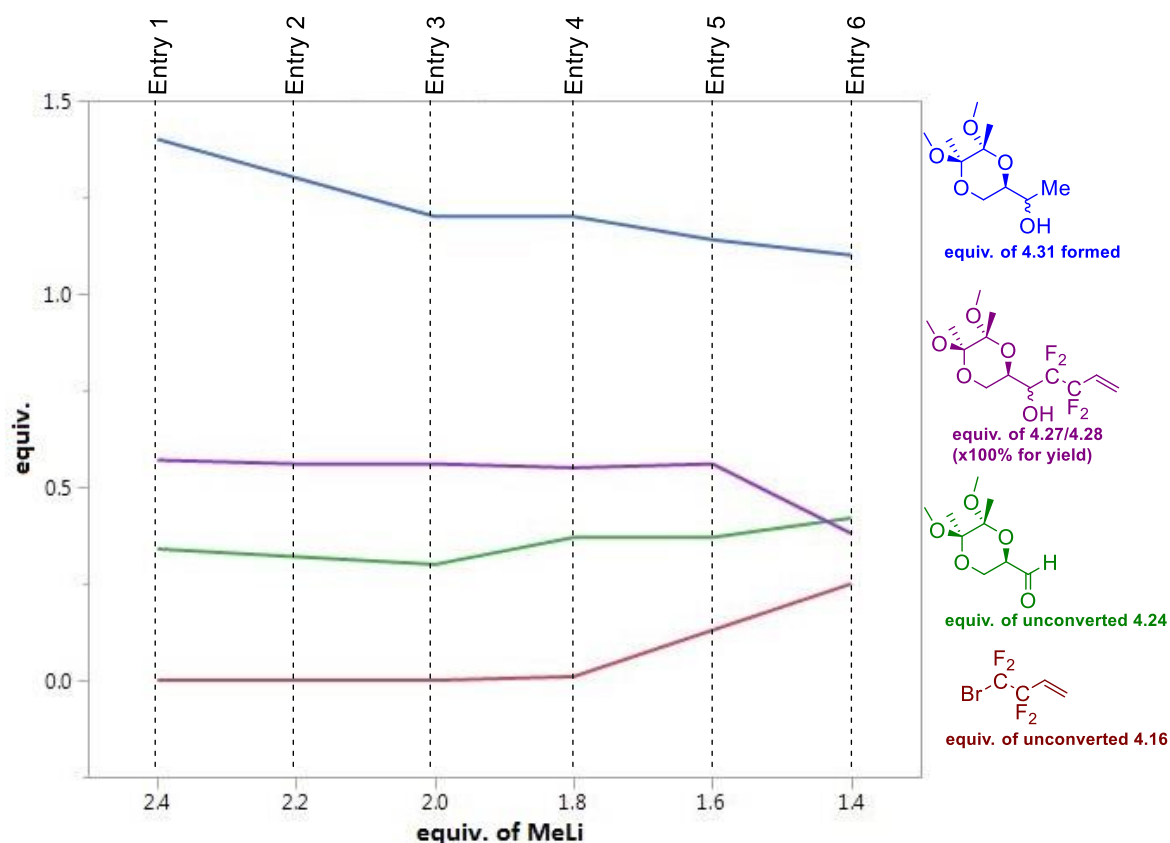
Despite achieving yields comparable to those reported by Konno and co-workers, the required large excess in MeLi and aldehyde **4.24** made this process still challenging for large scale reactions. Unsurprisingly, the utilisation of MeLi and aldehyde **4.24** on large quantities resulted in the formation of significant amounts of alcohol **4.31**. Indeed, regardless of the temperature investigated, about 1.5 equiv. of the aldehyde **4.24** and MeLi that were used were converted into alcohol **4.31**. Given the total absence of unreacted bromide **4.16**, it was assumed that there was an excess of MeLi, unnecessary to the full consumption of bromide **4.16**, that caused the formation of alcohol **4.31** in such large quantities.

6.1.3 Investigation of conditions involving a reduced excess of MeLi

With this third series, we wished to determine the minimal quantity of MeLi necessary to ensure the full conversion of bromide **4.16** (**Scheme 6.7, Graphic 6.3**). Hence, the quantity of MeLi, initially set at 2.4 equiv. as in Konno's conditions, was steadily diminished through an appropriate decrease of flowrate in **P2**. All the experiments were performed at -50 °C, the temperature at which the best results were achieved in the previous series (*cf* section **6.1.2**). In order to reduce the consumption of the valuable aldehyde **4.24**, the stoichiometry of the latter was reduced to 2.0 equiv. in all experiments.



Scheme 6.7: Investigation of adapted conditions involving reduced excesses of MeLi, formation of tetrafluorobutenyle lithium **4.21** in presence of aldehyde



Graphic 6.3: Data collected while investigating conditions presented in **Scheme 6.7**

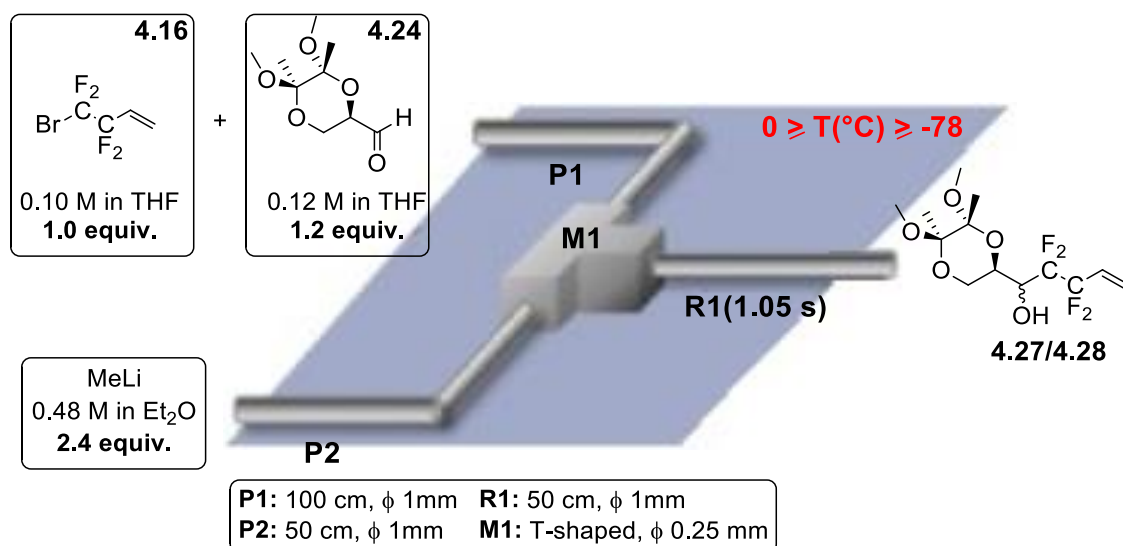
When 2.4 equiv. of MeLi was used, full consumption of bromide **4.16** took place and yielded the coupling adducts mixture **4.27/4.28** in a 55% yield (**Entry 1**). When compared to the 65% of yield achieved with 2.4 equiv of aldehyde **4.24** (cf **Entry 4** section 6.1.2), this indicated that the stoichiometry used by Konno and co-workers ought to be carefully respected to achieve optimum yields. Apart from a slight decrease in the quantity of alcohol **4.31** formed (0.1 equiv.), similar results were obtained when the quantity of MeLi was decreased from 2.4 down to 1.8 equiv., hence evidencing that a part of the MeLi used in Konno's conditions was superfluous (**Entry 1** → **5**). Then, following a further decrease in MeLi down to 1.6 equiv., small amounts of unreacted bromide **4.16** ($\approx 10\%$) started to appear in the crude mixture (**Entry 4** → **5**). Interestingly, the yield in coupling adducts **4.27/4.28** wasn't substantially impacted by the incomplete consumption of bromide **4.16**. To finish, a last decrease down to 1.4 equivalents of MeLi resulted in a further increased amount of unreacted bromide **4.16** (25%), an incomplete Li-Br exchange which this time caused the yield in coupling adducts **4.27/4.28** to drop down to $\approx 35\%$ (**Entry 5** → **6**). In view of these last results, investigation of conditions involving further decreased quantities of MeLi were aborted.

Disappointedly, the reduced quantities of MeLi barely managed to restrain the formation of alcohol **4.31**. In fact, the proportion of aldehyde **4.24** converted into **4.31** was never found below 1.2 equiv. Most remarkably, the quantity of alcohol **4.31** formed declined of only 0.2 equiv. as the quantity of MeLi engaged was dropped down from 2.4 to 1.4 equiv., thus clearly indicating the strong reactivity

of aldehyde **4.24** toward MeLi. As in the previous series, the low yields in adducts **4.27/4.28** achieved while bromide **4.16** was entirely or *quasi*-entirely consumed seemed to indicate that tetrafluorobutenyle lithium **4.21** either reacted with MeBr instead of aldehyde **4.24** (*cf* **Scheme 6.5**), or with bromide **4.16** (Wurtz-type coupling, *cf* **Scheme 6.3**). Even if as anticipated a certain portion of MeLi used in Konno's conditions was dispensable, it seemed that large excess of reagents were still required to achieve optimum yields (≥ 1.6 equiv.). The competition between MeLi addition to aldehyde **4.24** with the Li-Br exchange which, as observed in the previous series, remained prominent under flow conditions. Despite being slightly less-reagent consuming than the Konno procedure, these conditions remained too wasteful to be considered for large scale operations.

6.1.4 Investigation of adapted conditions involving reduced excesses of Ley's aldehyde

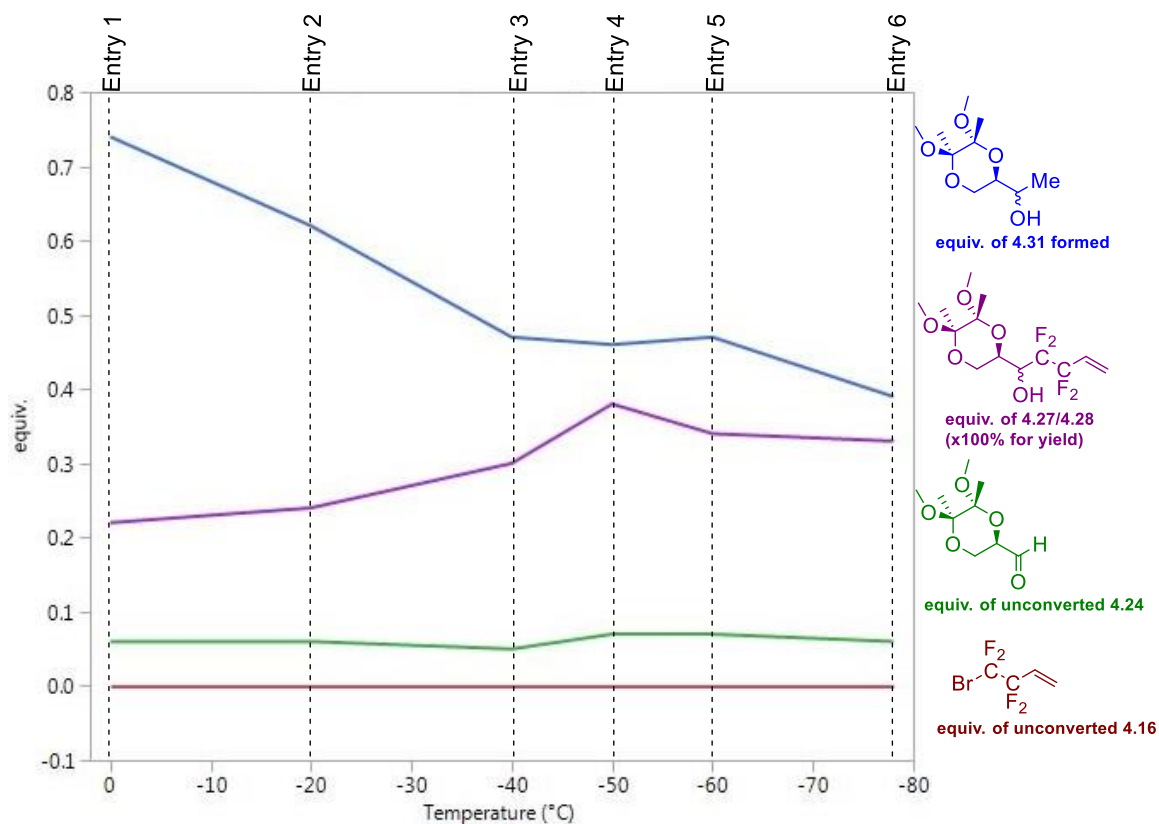
Finally, a modified version of the Konno procedure involving a reduced excess of aldehyde **4.24** was examined with temperatures ranging from 0 to -78 °C (**Scheme 6.8, Graphic 6.4**).



Scheme 6.8: Investigation of adapted conditions involving a reduced excesses of aldehyde **4.24**, formation of tetrafluorobutenyle lithium **4.21** in presence of aldehyde

When investigated at 0 °C (**Entry 1**), these conditions gave the mixture of coupling adducts **4.27/4.28** in only about 20% yield, while at the same time producing more than 0.7 equiv. of alcohol **4.31**. As in the second series (*cf* section **6.1.2**), the yield in coupling adducts mixture **4.27/4.28** steadily increased as the temperature was decreased from 0 to -50°C (20% → ≈ 40%, **Entry 1** → **4**). At the same time, the quantity of alcohol **4.31** formed gradually decreased from 0.7 down to 0.5 equiv., once again indicating that low temperatures favour Li-Br exchange over MeLi addition. Similar results were achieved as the temperature was decreased to -60 and then -78 °C (**Entry 5**

and 6). Regardless of the temperature examined, small quantities of leftover aldehyde **4.24** were observed in the reaction mixture (< 0.1 equiv.), while bromide **4.16** was entirely consumed.



Graphic 6.4: Data collected while investigating conditions presented in **Scheme 6.8**

When investigated in batch reactor, these conditions afforded yields comparable to those reported with the Konno procedure (*cf* section **4.4.1.2**). However, this appeared not to be the case under micro-flow conditions where they resulted in yields of $\pm 30\%$, half of those achieved with the micro-flow version of the Konno procedure. Like in the previous series, addition of MeLi to aldehyde **4.24** was presumed to remain the favoured pathway. Also, the difference between the quantity of bromide **4.16** consumed and the yield achieved once more indicated side reactions involving either or both **4.16** and its lithiated counterpart **4.21**. Being less efficient than Yoshida's conditions investigated in the very first series (*cf* section **6.1.1**), and this while using a larger excess of MeLi, these conditions were not considered for large scale investigations.

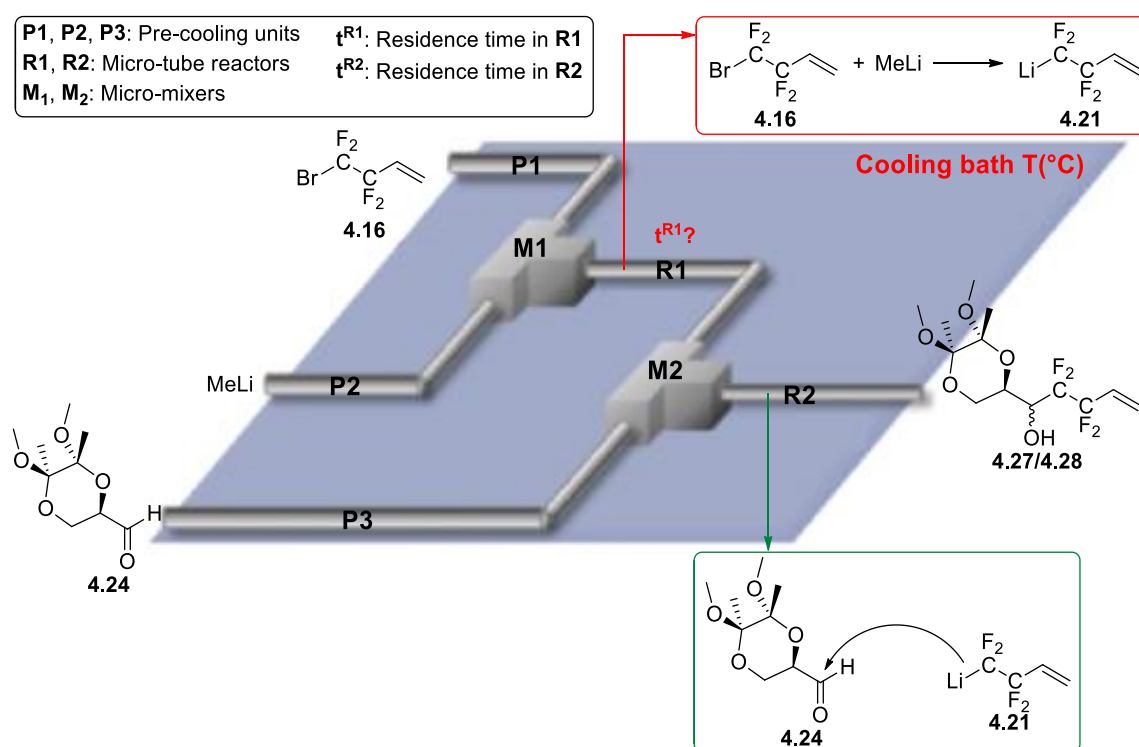
6.1.5 Conclusions

When investigated using a single reactor micro-flow setup, coupling between aldehyde **4.24** and tetrafluorobutene bromide **4.16** afforded the desired adducts mixture **4.27/4.28** in yields substantially higher than those achieved with batch reactors ($\approx 65\%$), but only when significant excess of both MeLi and aldehyde **4.24** were engaged. The utilisation of such quantities of starting

materials was necessary to ensure the full consumption of bromide **4.16** as reaction of MeLi with aldehyde **4.24** occurred with competitive rate, a problem already encountered by Yoshida and co-workers with highly reactive electrophiles.¹⁰² Considering this, it seemed clear that the only way to achieve high yields in adducts **4.27/4.28** while keeping the excess in aldehyde **4.2** and MeLi relatively low was to generate tetrafluorobutenyl lithium **4.21** in absence of electrophile.

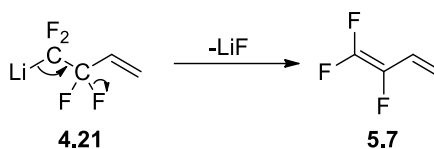
6.2 Formation of the lithiated intermediate in the absence of Ley's aldehyde

Coupling between aldehyde **4.24** and tetrafluorobutene bromide **4.16** was then investigated using a multi-reactor micro-flow system allowing the tetrafluorobutenyl lithium **4.21** to be generated in absence of aldehyde (**Scheme 6.9**). By compartmenting the chemical processes, this method should minimise the risk of side reactions between MeLi and the highly reactive aldehyde **4.24**, and hence circumvent the need of large excesses of these two reagents.



Scheme 6.9: Couplings of tetrafluorobutene bromide **4.16** of Ley's aldehyde **4.24** under micro-flow conditions with formation of tetrafluorobutenyl lithium **4.21** in absence of aldehyde

Since the LiF elimination from lithiated **4.21** results in a conjugated system, such process was anticipated to be very quick (**Scheme 6.10**). Hence, very short residence times in **R1** (**t_{R1}**) and cryogenic temperatures were envisioned as necessary to avoid significant degradation of the highly unstable lithiated **4.21** prior reaction with aldehyde **4.24**.

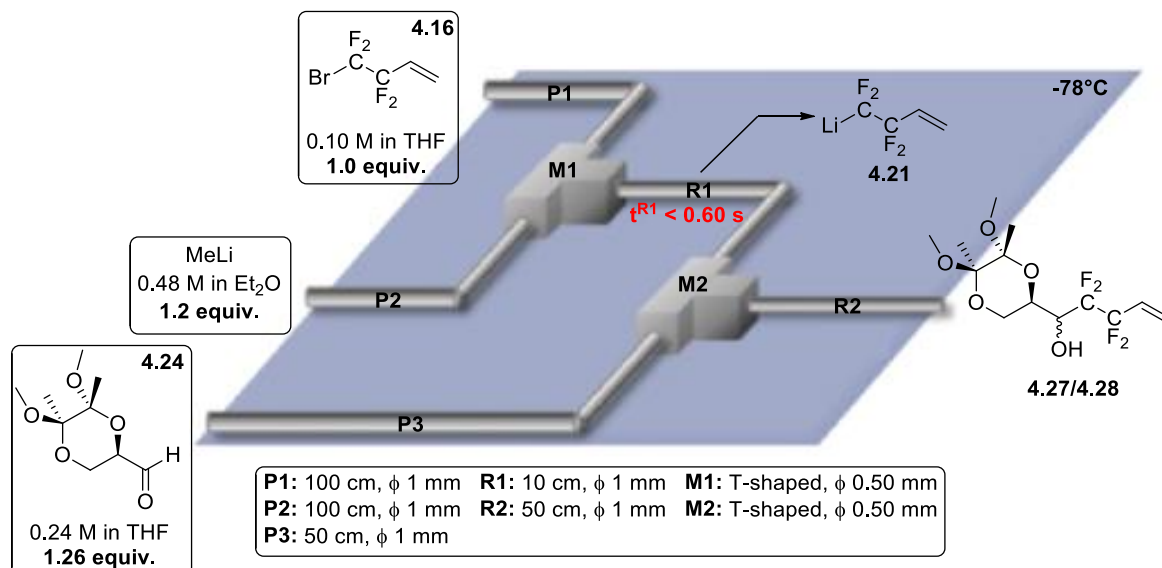


Scheme 6.10: LiF elimination from tetrafluorobutenyle lithium **4.21**

Like for the previous system, the reaction mixture was quenched at the outlet of the setup while being collected in a flask containing a saturated solution of ammonium chloride. Then, the different solutes present in the quenched mixture were quantified using GC analysis combined with an internal standard method.

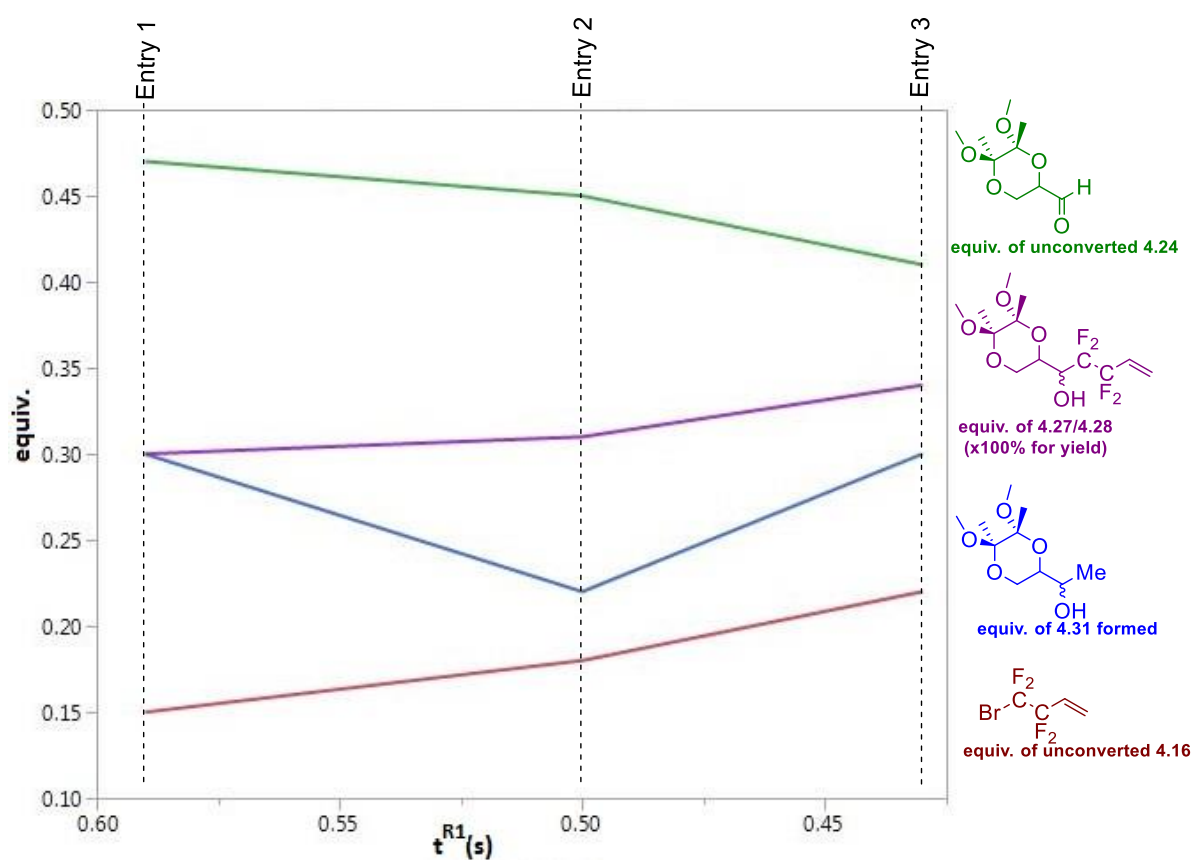
6.2.1 Investigation of Yoshida's coupling conditions

In a first series (**Scheme 6.11**, **Graphic 6.5**), the conditions reported by Yoshida and co-workers for the generation of perfluoroalkyl lithium in the absence of electrophiles were investigated with t^{R1} shorter than 0.6 s, and a temperature of -78°C , parameters with which yields above 80% were achieved for the perfluoroalkylation of tributyltin chloride **5.15** (*cf* section 5.3.2).¹⁰² In this series, the reduction of t^{R1} was achieved through an appropriate increase of flowrate in **P1** and **P2**, with the other parameters kept constant.



Scheme 6.11: Investigation of Yoshida's conditions, formation of tetrafluorobutenyle lithium **4.21** in absence of aldehyde

As detailed on the graph below, a residence time t^{R1} of 0.58 s afforded the mixture of coupling adducts **4.27/4.28** in a mediocre yield of 30%, alongside with 0.3 equiv. of alcohol **4.31** (**Entry 1**). At the same time, about 0.5 equiv. of unreacted aldehyde **4.24** as well as small quantities of unreacted bromide **4.16** (≈ 0.15 equiv.) were observed in the reaction mixture. Then, a first shortening in t^{R1} down to 0.50 s resulted in an infinitesimal increase in both the yield in adducts **4.27/4.28** and the quantity of unreacted bromide **4.16** (**Entry 2**). For unclear reasons, this first decrease in t^{R1} also led to a decreased quantity of alcohol **4.31** (≈ 0.2 equiv.) while the quantity of unreacted aldehyde **4.24** remained roughly the same. As in the previous experiment, a further shortening of t^{R1} down to 0.42 s produced a small increase in yield in adducts **4.27/4.28** and quantity of unreacted bromide **4.16**, with the former reaching about 32%, and the latter 0.2 equiv. (**Entry 3**).



Graphic 6.5: Data collected while investigating conditions presented in **Scheme 6.11**

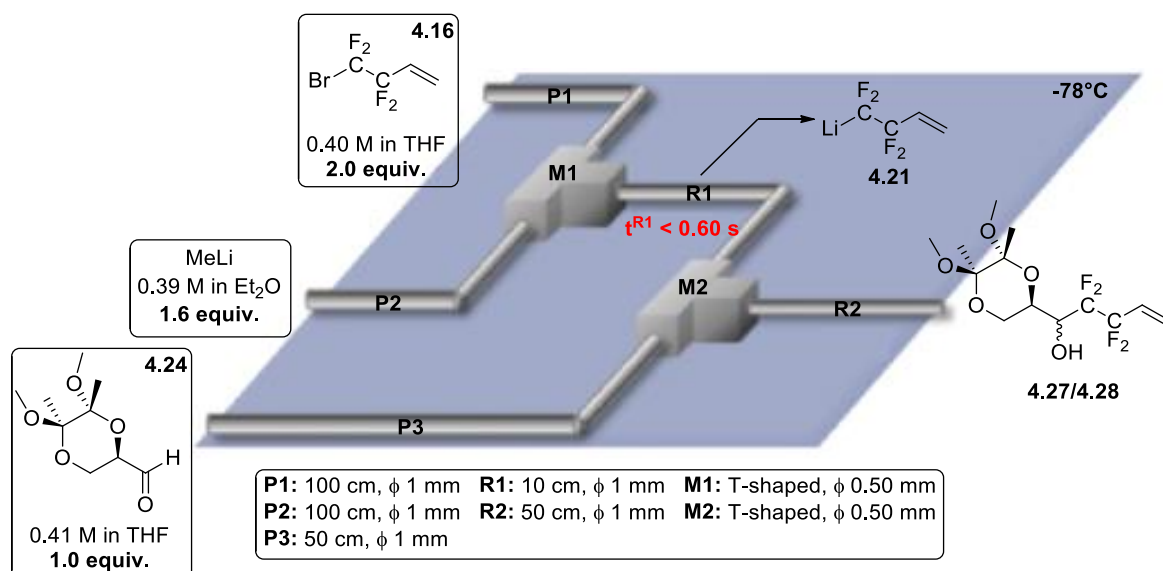
To explain such low yields in adducts **4.27/4.28**, it was advanced that tetrafluorobutenyl lithium **5.7** was mainly degraded prior to coupling (**Scheme 6.10**). Indeed, intermediate **4.21** being more unstable than “classic” perfluoroalkyllithiums for which these conditions were designed,¹⁰² it seemed probable that t^{R1} shorter would be necessary to achieve high yields. Alternatively, these poor yields in adducts **4.27/4.28** could have been caused by a slow mixing in **M1**, promoting the Wurtz-type coupling between bromide **4.16** and its lithiated counterpart **4.21** (**Scheme 6.3**),¹⁰³ as well as the reaction of the latter with MeBr (**Scheme 6.5**). This last hypothesis being supported by

the incomplete consumption of bromide **4.16**. Unfortunately, in the absence of adequate detection and quantification methods for octafluorinated-1,7-diene **6.1** and tetrafluoropentene **6.2**, it couldn't be determined to which extent these side reactions, and by deduction the LiF elimination from **4.21**, prevented the formation of the adducts **4.27/4.28**.

These conditions were thus investigated using a micro-mixer **M1** of smaller diameter which, providing a significantly faster mixing, was expected to limit the Wurtz-type coupling.¹⁰³ Unfortunately, the last available 0.25 mm micro-mixer was damaged during this series and could not be repaired. Given the waiting time of several months necessary to receive new micro-mixers from the only company manufacturing such pieces, these investigations were put aside.

6.2.2 Investigation of conditions promoting the formation of tetrafluorobutene lithium on large quantities

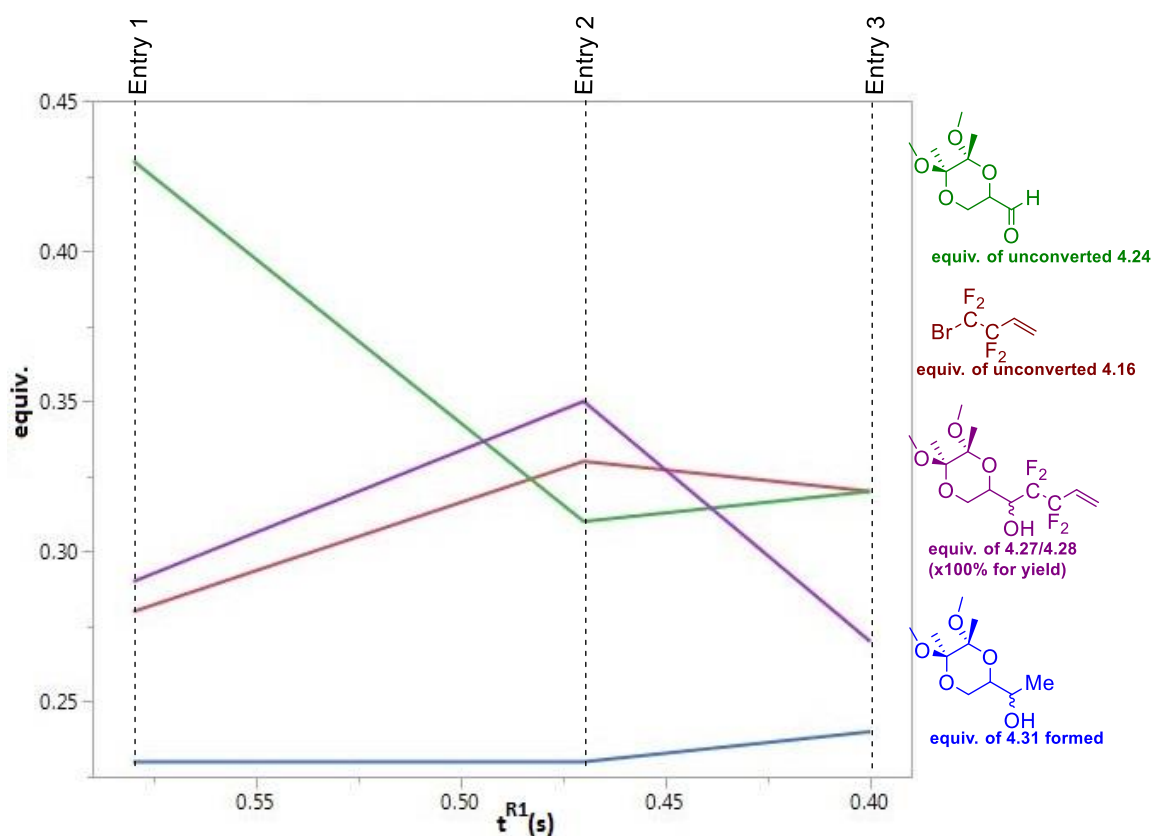
Due to the flowrate limitation imposed by the syringe pumps used and the impossibility to reduce the length of **R1** below 5 cm, the t^{R1} used so far were among the shortest reachable with our setup. Given that reduction of t^{R1} had almost no impact on the outcomes of the coupling in the previous series, and that complete consumption of bromide **4.16** was not achieved, it seemed unlikely that conditions involving shorter t^{R1} could have afforded significantly higher yields in adducts **4.27/4.28**, and for this reason were not examined. To promote the formation of the desired adducts, a strategy aiming at promoting the formation of tetrafluorobutenyle lithium **4.21** on large quantities was instead envisaged. Indeed, even assuming that the conditions investigated earlier could efficiently prevent the degradation of the lithiated intermediate **4.21** in **R1**, the low quantities of bromide **4.16** consumed (≈ 0.8 equiv.) were deemed insufficient to ensure high yields in adducts **4.27/4.28**, this especially since bromide **4.16** was potentially engaged in two side reactions. In absence of adapted micro-mixing pieces which could have promoted the Li-Br exchange through ultra-fast mixing (**M1** of 0.25 mm i.d), it was believed that formation of tetrafluorobutenyle lithium **4.21** could be promoted *via* the utilisation of both tetrafluorobutene bromide **4.16** and MeLi on large quantities (**Scheme 6.12**, **Graphic 6.6**). In order to preserve t^{R1} similar to those investigated in the previous series, the easiest solution to increase the quantities of MeLi and bromide **4.16** engaged consisted in increasing their concentrations in the reaction medium, while keeping the same flowrates settings and reactor dimensions as previously.



Scheme 6.12: Investigation of conditions involving large excesses of MeLi and tetrafluorobutene bromide **4.16**, formation of tetrafluorobutenyl lithium **4.21** in absence of aldehyde

As detailed above, MeLi was injected in substoichiometric quantities compared to bromide **4.16** to ensure its complete consumption in **R1**, and hence prevent the formation of the undesired alcohol **4.31**. Considering the significant quantities of unreacted aldehyde **4.24** resulting from the conditions attempted earlier (≈ 0.4 equiv.), it was this time decided to use this compound as limiting reagent. Ideally, these adjusted reagent quantities were anticipated to ensure the total consumption of aldehyde **4.24** while at the same time avoiding the formation of alcohol **4.31**. Furthermore, these conditions were of benefit from a reagent economy point of view given that the reagents used in excess were commercial and cheap (bromide **4.16** and MeLi).

As shown above, a t^{R1} of 0.58 s afforded the mixture of coupling adducts **4.27/4.28** in a low yield of 30%, and about 0.2 equiv. of alcohol **4.31** (**Entry 1**). Only 0.3 equiv. of unreacted bromide **4.16** were observed in the reaction mixture alongside with more than 0.4 equiv. of aldehyde **4.24**. A first shortening in t^{R1} down to 0.47s led to a slightly increased yield in adducts **4.27/4.28** (35%), meanwhile the quantity of unreacted aldehyde **4.24** dropped of 0.15 equiv. (**Entry 2**). For this second experiment, the quantity of alcohol **4.31** formed remained the same while the quantity of unreacted bromide **4.16** underwent a slight increase (0.33 equiv.). To finish, a further shortening in t^{R1} down to 0.40 s led to a 10% drop in yield in adducts **4.27/4.28**, the other reagent quantities remained roughly similar as those obtained in the previous experiment. (**Entry 3**).



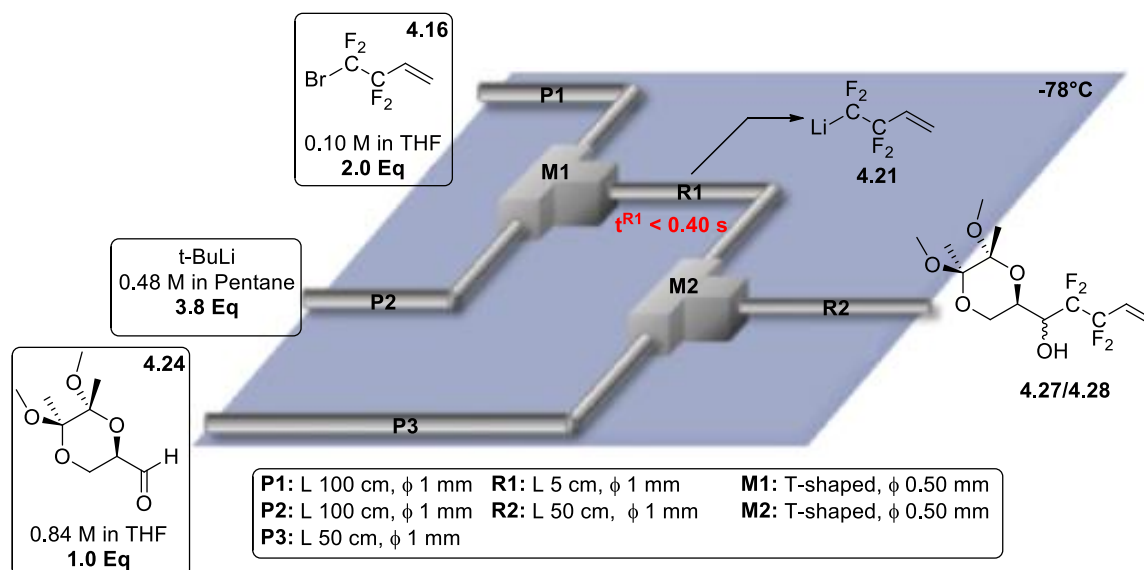
Graphic 6.6: Data collected while investigating conditions presented in **Scheme 6.12**

As indicated by the small leftover of bromide **4.16** and the reduced quantity of alcohol **4.31** resulting from each of these conditions, it appears that the 1.6 equiv. of MeLi engaged principally reacted with bromide **4.16**. The mediocre yields in adducts **4.27/4.28** achieved while large quantities of bromide **4.16** were consumed (≈ 1.7 equiv.) seemed to suggest that the highly concentrated medium in **R1** largely promoted the Wurtz-type coupling and the reaction between the lithiated intermediate **4.21** and MeBr (**Scheme 6.3** and **6.5**). Once again, the formation of alcohol **4.31** indicated an incomplete reaction between MeLi and bromide **4.16** in **R1**, which could be due to a slow mixing in **M1**.

In retrospect, it seems evident that due to both the highly concentrated medium and the presence of bromide **4.16** in excesses, but also to the non-optimal mixing in **M1** (0.50 mm i.d), side reactions involving the lithiated **4.21** were particularly favoured under these conditions.

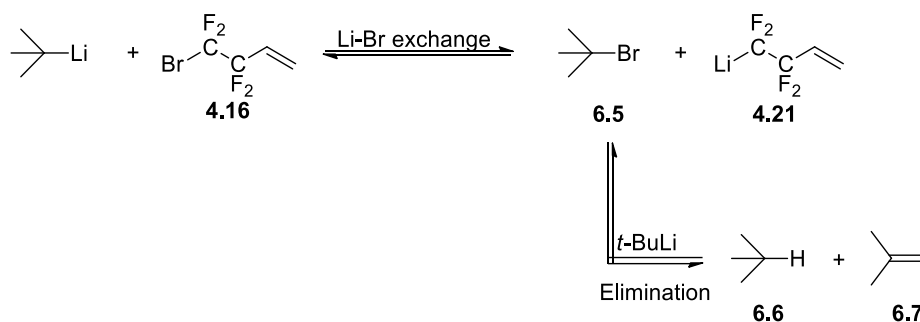
6.2.3 Investigation of conditions involving a different alkyllithium reagent

In a last series, coupling of tetrafluorobutene bromide **4.16** to aldehyde **4.24** was investigated using the highly reactive *tert*-butyllithium (*t*-BuLi) as alkyllithium reagent (**Scheme 6.13**, **Graphic 6.7**).



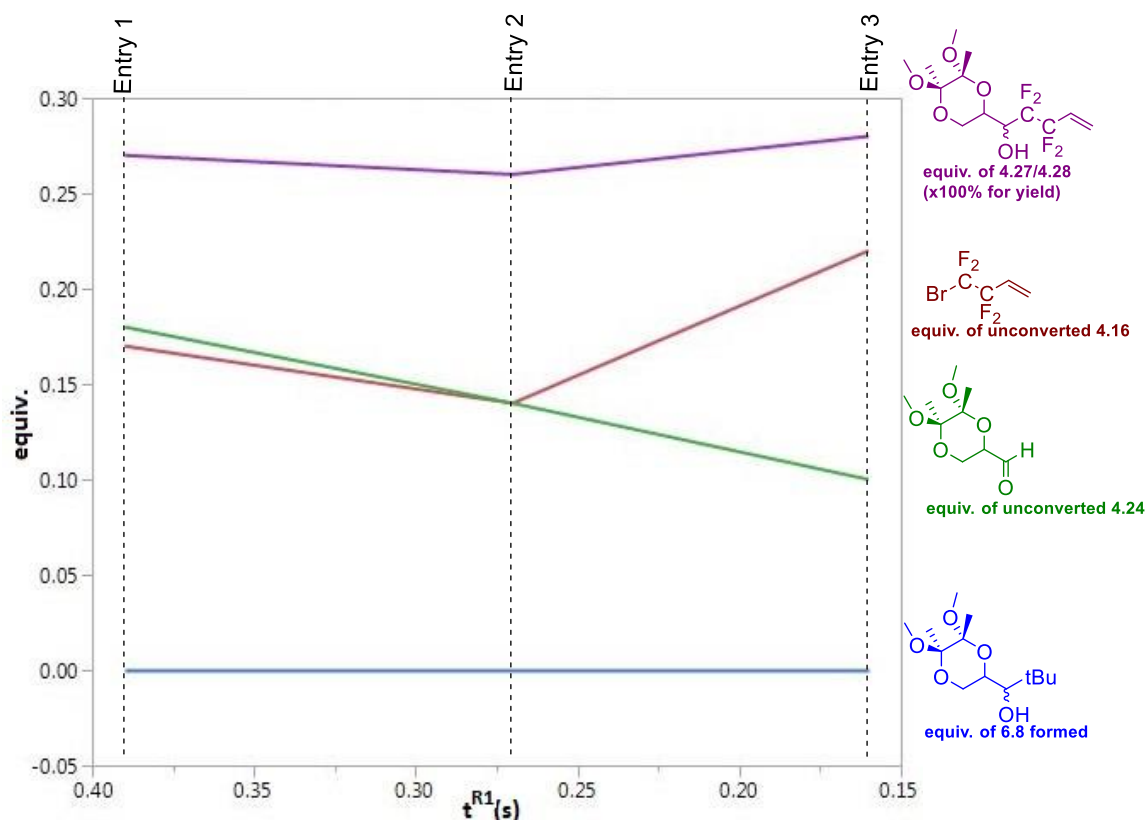
Scheme 6.13: Investigation of conditions involving *t*-BuLi as alkyllithium reagent, formation of tetrafluorobutenyle lithium **4.21** in absence of aldehyde

Owing to its highly basic character, *t*-BuLi was expected to react with the *tert*-butyl bromide **6.5** resulting from the Li-Br exchange, leading to the formation of *tert*-butyl alkane **6.6** and isobutyridene **6.7** (**Scheme 6.14**).



Scheme 6.14: Side reaction between *t*-BuLi and *t*-BuBr **7.5**

Considering this, 3.8 equiv. of *t*-BuLi instead of the 1.9 equiv. initially envisioned were engaged to maximise the conversion of the 2.0 equiv. of bromide **4.16** into lithiated **4.21**. Like in the previous series, aldehyde **4.24** was engaged as limiting reagent to hopefully ensure its full conversion into the desired adducts. To minimise the risks of LiF elimination from tetrafluorobutenyle lithium **4.21** prior to coupling (**Scheme 6.10**), t^{R1} were kept as low as possible by reducing the dimensions of **R1** to a minimum and pushing the flowrates to a maximum.

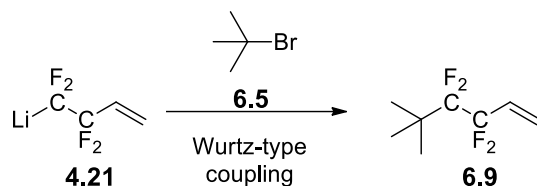


Graphic 6.7: Data collected while investigating conditions presented in **Scheme 6.13**

When investigated with a t^{R1} of 0.40 s, these conditions afforded the mixture of coupling adducts in a disappointing yield of around 30% (**Entry 1**). Pleasingly, no traces of *t*-BuLi addition product could be observed on the reaction mixture. Curiously, only 0.2 equiv. of unreacted aldehyde **4.24** were observed in the reaction mixture, meaning that about 0.5 equiv. of aldehyde were converted into a product which could not be detected by GC analysis. Similar results were achieved as t^{R1} was shortened down to 0.27 s, then to 0.15 s (**Entry 2** and **3**), apart from a slight increase in unconverted bromide **4.16** (**Entry 3**).

Disappointedly, each of these conditions afforded adducts **4.27/4.28** in yields around 30%, similar to those achieved in the previous series (*cf* section **6.2.2**). The absence of signal on the GC charts which could have corresponded to the *t*-BuLi addition product **6.8** seemed to indicate either that *t*-BuLi was fully consumed into **R1**, or simply not nucleophilic enough to react with aldehyde **4.24**. Given the large quantities of bromide **4.16** consumed (≈ 1.8 equiv.), such low yields seemed once more to indicate either the *quasi*-complete degradation of lithiated **4.21** in **R1** (**Scheme 7.10**), or its reaction with bromide **4.16** (Wurtz-type coupling **Scheme 6.3**). However, given the extremely short t^{R1} investigated in this series, it seemed unlikely that LiF elimination could have caused the degradation of such large quantities of lithiated **4.21**. Similarly, owing to the low concentrations of bromide **4.16** and hence lithiated **4.21** in the reaction medium (**R1**), coupling between these two

species was anticipated to be disfavoured in these conditions. Hence, it was suggested that *tert*-butyl bromide **6.5**, formed in significant quantities following the Li-Br exchange (≈ 1.9 equiv.), could have largely reacted with tetrafluorobutenyle lithium **4.21** to give the adduct **6.9** (Scheme 6.15).



Scheme 6.15: Wurtz-type coupling between *tert*-butyl bromide **6.5** and tetrafluorobutenyle lithium **4.21**

Unfortunately, in absence of adequate methods for the detection and quantification of the octafluorinated-1,7-diene **6.1** and adduct **6.9**, it couldn't be determined with certainty why the coupling adducts **4.27/4.28** were obtained in such low yields.

6.2.4 Conclusion

Despite our efforts to optimise several parameters, the desired adducts **4.27/4.28** were never obtained in yields above 40% when tetrafluorobutenyle lithium **4.21** was generated in absence of aldehyde **4.24**. Considering the *quasi*-complete consumption of tetrafluorobutene bromide **4.16** resulting from each of the conditions investigated, it seemed that either or both bromide **4.16** and lithiated **4.21** had undergone undesired side reactions while still in **R1** (wurtz-type coupling, bromine displacement), or alternatively that most of the lithiated intermediate **4.21** had been degraded following rapid LiF elimination. However, with the difficulties to detect and quantify the products resulting from these side reactions, it couldn't be determined which of these processes restricted the formation of the adducts **4.27/4.28**, and to which extent (Figure 6.1).

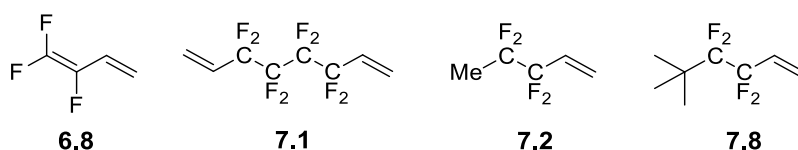


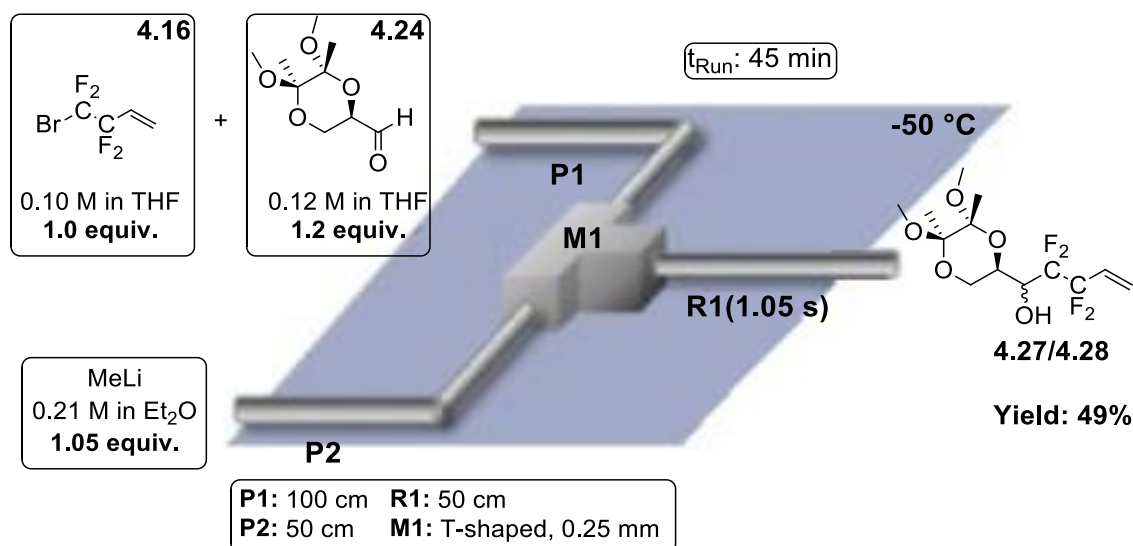
Figure 6.1: Potential side products formed in **R1**

Lacking this key information, the data collected during each series could not be clearly exploited and rationalised, hence making unclear which parameter needed to be optimised. As a result, our optimisation study could not be organised on a logical manner and a precious time was lost groping amongst conditions found on the literature. Indeed, even though only few results are presented in this chapter, numerous other conditions were examined but their results not included as being uninformative or non-contributive to our reasoning.

In the absence of encouraging results, as well as time to develop a new GC method which could have given access to the desired information, further investigations were deemed unworthy and hence aborted. Given the poor results obtained, none of the conditions involving the formation of tetrafluorobutenyle lithium **4.21** in absence of aldehyde **4.24** were considered for upscaling.

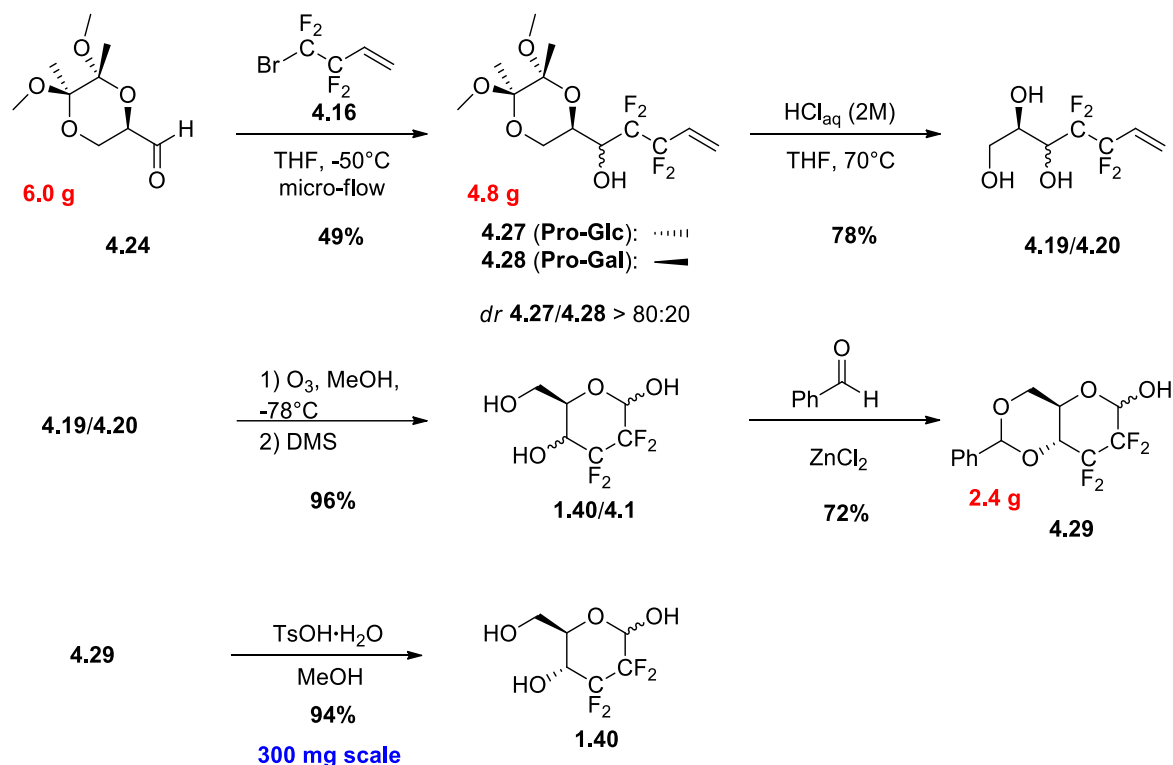
6.3 Large scale synthesis of 4,6-*O*-benzylidene-2,2,3,3-tetrafluoro-D-glucose and galactose

Affording the desired adducts **4.27/4.28** in yields around 60% after transposition onto micro-flow conditions, Konno's coupling conditions appeared at first sight to be the most suitable for the large-scale synthesis of 4,6-benzylidene tetrafluoro glucose **4.29** and galactose **4.30** (*cf* section 6.1.2). However, given the large excesses of MeLi and aldehyde **4.24** involved (2.4 equiv. each), these conditions were deemed too reagent-consuming to be worthwhile on large scales. This especially considering that most of the MeLi and aldehyde **4.24** engaged were converted into the undesired alcohol **4.31** (≈ 1.5 equiv.). Instead, coupling conditions reported by Yoshida and co-workers for the perfluoroalkylation under micro-flow conditions were preferred,¹⁰² for which yields of about 40% could be achieved with only 1.05 equiv. of MeLi and 1.2 equiv. of aldehyde **4.24** (*cf* section 6.1.1). Starting from 6 g of aldehyde **4.24**, these conditions produced about 5 g of the coupling adducts mixture **4.27/4.28** on a cumulative period of only 45 min (49% yield, **Scheme 6.17**). Despite being more efficient ($\approx 65\%$ yield), Konno's conditions would have required 9 g of aldehyde **4.24** (or 50% more) to produce the same amount of adducts **4.27/4.28**.



Scheme 6.17: Investigation of Yoshida's coupling conditions on large scale, formation of tetrafluorobutenyle lithium **4.21** in presence of aldehyde

Using the micro-flow technology developed by Yoshida, a convenient and efficient synthesis of 2,3-dideoxy-2,2,3,3-tetrafluoro-D-glucopyranose **1.40** could be achieved (25% overall yield, **Scheme 6.18**, cf section 4.4.2).



Scheme 6.18: Large scale synthesis of the 4,6-*O*-benzylidene-tetrafluoroglucose **4.29** using micro-flow technology, followed by its deprotection on reduced scale

Given the numerous examples of large scale and high yielding benzylidene cleavage found throughout the literature, we are confident that hydrolysis of **4.29** can easily be transposed on large scales, and ultimately that this modified version of the Konno synthesis constitutes the most convenient option for the multigram-scale preparation tetrafluoro glucose **1.40**. Besides, even though not investigated due to the lack of time, further upscaling of this short synthesis is believed to be easily achievable and hence could produce several grams of both 4,6-*O*-benzylidene-tetrafluoroglucose **4.29** and galactose **4.30**. Indeed, the coupling steps performed under micro-flow conditions could be upscaled at will simply by increasing the time during which the flow system is run, and this without sacrificing its efficiency. In addition, the other steps constituting this synthesis are widely described in the literature and known to be tolerant to large scale conditions.

Chapter 7: Experimental

7.1 General conditions

Chemical reagents were obtained from commercial sources and used without further purification, unless stated otherwise. All air/moisture sensitive reactions were carried out under inert atmosphere (Ar) in flame-dried glassware. Anhydrous THF, Et₂O, DCM, Et₃N, MeOH, ethylene glycol, pentane and DMF were purchased in sealed containers and used without further purification. Reactions were monitored by TLC (MERCK Kieselgel 60 F254, aluminium sheet), visualised under UV light (254 nm), and by staining with KMnO₄ (10% aq). Column chromatography was performed on silica gel (MERCK Geduran 60 Å, particle size 40-63 µm). All reported solvent mixtures are volume measures. Preparative HPLC was carried out using Biorad Bio-Sil D 90-10 columns (250 × 10 at 10 mL.min⁻¹ and 1250 × 22 mm at 20 mL min⁻¹).

¹H NMR, ¹³C NMR and ¹⁹F NMR spectra were recorded in CDCl₃, acetone-*d*₆, CD₃OD or D₂O solutions using Bruker, AV400 (400, 101 and 376 MHz respectively) and AV500 (500, 126 and 471 MHz respectively) spectrometers. ¹H and ¹³C chemical shifts (δ) are quoted in ppm relative to residual solvent peaks as appropriate. ¹⁹F spectra were externally referenced to CFCl₃. The coupling constants (*J*) were recorded in Hertz (Hz). The proton NMR signals were designated as follows: s (singlet), d (doublet), t (triplet), q (quartet), quin (quintet), m (multiplet), or a combination of the above. The coupling constants have not been averaged.

Fourier-transform infrared (FT-IR) spectra are reported in wavenumbers (cm⁻¹) and were collected on a PerkinElmer Spectrum one FT6IR fitted with an ATR accessory using neat samples (solids and liquids). The abbreviations s (strong), m (medium), w (weak) and br (followed by either s, m or w to indicate the strength of a broad peak) are used when reporting spectra.

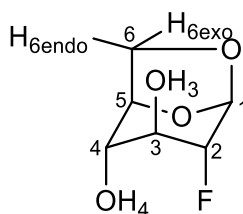
Electrospray mass spectra were obtained from a Waters 2700 sample manager ESI, and recorded in *m/z* (abundance percentage). HRMS was obtained from a Bruker APEX III FTICR-MS. Samples were run in HPLC methanol or MeCN.

Optical rotations were collected on an Optical Activity POLAAR 2001 at 589 nm with samples in MeOH, H₂O, CHCl₃, or their deuterated equivalents.

GC analyses were performed on a SHIMADZU GC-2014 gas chromatograph equipped with a flame ionization detector using a fused silica capillary column (column, HP-5; 0.32 mm x 30 m). Analytical standard grade heptane purchased from Sigma-Aldrich was used as internal standard for the quantification of the solutes.

7.2 Study of intramolecular hydrogen bonding in levoglucosan derivatives

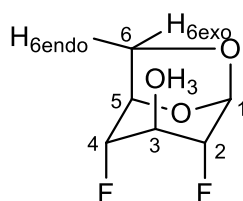
7.2.1 Characterisation data of 1,6-Anhydro-2-deoxy-2-fluoro- β -D-glucopyranoside (1.26)



1.26

Mp 118-120 °C (hexane/acetone), lit. 129-130 °C (ether/acetone).¹¹⁷ **[α]_D** -79.2 (c 1.20, MeOH, 21 °C), lit -75 (c 1.20, MeOH, 20 °C).¹¹⁸ **IR** (neat) 3287 (m, br.), 2970 (w), 2934 (w), 2910 (w), 1044 (s), 1011 (s) cm^{-1} . **^1H NMR** (500 MHz, CDCl_3) δ 5.60 (1H, br. q, J 1.8 Hz, H_1), 4.63 (1H, m, from which could be extracted J 5.4 Hz, H_5), 4.34 (1H, br. dq, J 45.2, 1.7 Hz, H_2), 4.21 (1H, dd, J 7.6, 0.9 Hz, $\text{H}_{6\text{endo}}$), 4.02 (1H, ddquin, J 15.7, 6.5, 1.8 Hz, H_3), 3.83 (1H, m, from which could be extracted J 7.3, 5.8, 1.2 Hz, $\text{H}_{6\text{exo}}$), 3.66 (1H, br. dq, J 10.9, 1.7 Hz, H_4), 2.60 (1H, dd, J 11.0, 1.4 Hz, OH_4), 2.16 (1H, dd, J 6.4, 0.6 Hz, OH_3) ppm. **$^1\text{H}[^{19}\text{F}]$ NMR** (500 MHz, CDCl_3) δ 5.58 (1H, br. t, J 1.6 Hz, H_1), 4.62 (1H, m, from which could be extracted J 5.3 Hz, H_5), 4.32 (1H, q, J 1.5 Hz, H_2), 4.19 (1H, dd, J 7.7, 0.9 Hz, $\text{H}_{6\text{endo}}$), 4.00 (1H, dqin, J 6.4, 1.9 Hz, H_3), 3.81 (1H, dd, J 7.7, 5.6 Hz, $\text{H}_{6\text{exo}}$), 3.65 (1H, br. dq, J 10.9, 1.9 Hz, H_4), 2.58 (1H, d, J 10.9 Hz, OH_4), 2.15 (1H, d, J 6.4 Hz, OH_3) ppm. **^{13}C NMR** (101 MHz, acetone- d_6) δ 99.3 (1C, d, J 30.1 Hz, C_1), 90.2 (1C, d, J 179.0 Hz, C_2), 76.9 (1C, s, C_5), 71.9 (1C, d, J 26.4 Hz, C_3), 71.6 (1C, d, J 5.1 Hz, C_4), 65.3 (1C, s, C_6) ppm. **^{19}F NMR** (471 MHz, CDCl_3) δ -187.5 (1F, br. ddd, J 45.2, 15.7, 1.3 Hz) ppm. **$^{19}\text{F}[^1\text{H}]$ NMR** (471 MHz, CDCl_3) δ -187.5 (1F, s) ppm. NMR data match those previously reported.¹¹⁸ **MS** (ESI-) (m/z) 209.8 [$\text{M}+\text{HCO}_2$] $^-$.

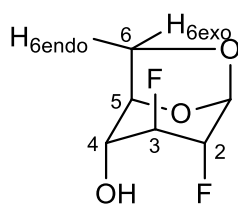
7.2.2 Characterisation data of 1,6-anhydro-2,4-dideoxy-2,4-difluoro- β -D-glucopyranoside (1.32)



1.32

Rf 0.38 (petroleum ether/acetone 70:30). **Mp** 96-98 °C (chloroform/acetone), lit 99-100 °C (no solvent given).¹¹⁷ **[α]_D** -63.0 (c 0.82, water, 21 °C), lit -62 (c 0.82, water 20 °C).¹¹⁷ **IR** (neat) 3454 (w, br.), 2961 (w), 1038 (s), 1016 (s) cm⁻¹. **¹H NMR** (500 MHz, CDCl₃) δ 5.61 (1H, br. dt, *J* 3.8, 1.4 Hz, H₁), 4.78 (1H, br. ddq, *J* 12.9, 5.7, 1.3 Hz, H₅), 4.45 (1H, m, from which could be extracted *J* 46.4 Hz, H₄), 4.30 (1H, br. dquin, *J* 46.4, 1.3 Hz, H₂), 4.11 (1H, m, from which could be extracted *J* 18.0, 6.1 Hz, H₃), 4.04 (1H, dt, *J* 7.8, 0.9 Hz, H_{6endo}), 3.80 (1H, m, from which could be extracted *J* 7.8, 5.4, 4.3, 1.1, 0.4 Hz, H_{6exo}), 2.30 (1H, br. d, *J* 6.1 Hz, OH₃) ppm. **¹³C NMR** (101 MHz, CDCl₃) δ 99.3 (1C, d, *J* 28.6 Hz, C₁), 89.9 (1C, dd, *J* 181.9, 5.1 Hz, C₄), 88.0 (1C, dd, *J* 184.1, 4.4 Hz, C₂), 74.3 (1C, d, *J* 22.7 Hz, C₅), 69.5 (1C, dd, *J* 29.3, 27.9 Hz, C₃), 64.7 (1C, d, *J* 9.5 Hz, C₆) ppm. **¹⁹F NMR** (471 MHz, CDCl₃) δ -183.3 (1F, m, from which could be extracted *J* 46.3, 17.3, 12.8, 4.1, 0.9 Hz, F₄), -188.4 (1F, ddd, *J* 46.5, 18.4, 3.9 Hz, F₂) ppm. **¹⁹F[¹H] NMR** (471 MHz, CDCl₃) δ -183.3 (1F, s, F₄), -188.4 (1F, s, F₂) ppm. ¹H and ¹³C NMR had not yet been described in CDCl₃. Product could not be ionised.

7.2.3 1,6-Anhydro-2,3-dideoxy-2,3-difluoro-β-D-glucopyranoside (**1.27**)

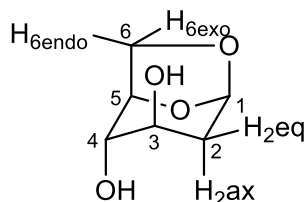


1.27

To a solution of 4-*O*-benzylated levoglucosan **2.1** (2.22 g, 8.66 mmol, 1 equiv) in ethyl acetate (1.1 mL) was added Pd(OH)₂/C (20%, 300 mg, 0.43 mmol, 0.05 equiv) and the resulting solution degassed with H₂. Stirring under H₂ atmosphere was continued at rt for 12h before the mixture was filtered over a pad of Celite® and concentrated under vacuum. Purification by column chromatography (petroleum ether/acetone 60:40) afforded 1.43 g (8.59 mmol, 99%) of 2,3-difluoro levoglucosan **1.27** as a white solid. **Rf** 0.16 (petroleum ether/ethyl acetate 80:20). **Mp** 92-94 °C (chloroform). **[α]_D** -61.6 (c 0.70, CHCl₃, 22 °C), lit -59 (c 0.7, CHCl₃).⁵³ **IR** (neat) 3286 (w, br.), 2970 (w), 2917 (w), 1041 (s), 1028 (s), 1014 (s) cm⁻¹. **¹H NMR** (500 MHz, CDCl₃) δ 5.58 (1H, br. q, *J* 1.8 Hz, H₁), 4.70 (1H, ddquin, *J* 43.2, 12.3, 1.7 Hz, H₃), 4.66 - 4.61 (1H, m, H₅), 4.43 (1H, ddqd, *J* 44.1, 12.4, 1.6, 0.6 Hz, H₂), 4.08 (1H, br dt, *J* 7.8, 1.2 Hz, H_{6endo}), 3.86 (1H, br. ddt, *J* 7.8, 5.8, 1.8 Hz, H_{6exo}), 3.78 (1H, br. ddq, *J* 13.0, 11.3, 1.6 Hz, H₄), 2.58 (1H, dt, *J* 11.4, 0.8 Hz, OH₄) ppm. **¹H[¹⁹F] NMR** (500 MHz, CDCl₃) δ 5.59 (1H, br. t, *J* 1.7 Hz, H₁), 4.72 (1H, quin, *J* 1.7 Hz, H₃), 4.65 (1H, m, from which could be extracted *J* 5.8 Hz, H₅), 4.45 (1H, m, from which could be extracted *J* 1.6 Hz, H₂), 4.10 (1H, ddd, *J* 7.7, 1.1, 0.4 Hz, H_{6endo}), 3.87 (1H, dd, *J* 7.7, 5.8 Hz, H_{6exo}), 3.80 (1H, br. dq, *J* 11.3, 1.5 Hz, H₄), 2.60 (1H, d, *J* 11.3 Hz, OH₄) ppm. **¹³C NMR** (101 MHz, CDCl₃) δ 98.6 (1C, d, *J* 27.1 Hz, C₁), 88.2 (1C, dd, *J* 181.2, 30.1 Hz, C₃), 84.3 (1C,

dd, J 180.1, 28.2 Hz, C₂), 75.7 (1C, s, C₅), 67.7 (1C, dd, J 27.5, 1.8 Hz, C₄), 64.8 (1C, d, J 4.4 Hz, C₆) ppm. ¹⁹F NMR (471 MHz, CDCl₃) δ -187.4 (1F, m, J 43.2, 14.3, 12.3 Hz, F₃), -193.7 (1F, m, J 44.1, 15.0, 12.3 Hz, F₂) ppm. ¹⁹F[¹H] NMR (471 MHz, CDCl₃) δ -187.4 (1F, d, J 14.3 Hz, F₃), -193.7 (1F, d, J 15.0 Hz, F₂) ppm. ¹H and ¹³C NMR had not yet been described in CDCl₃. MS (CI) (m/z) 167.0 [M+H]⁺.

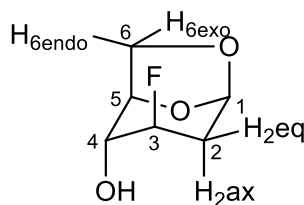
7.2.4 1,6-Anhydro-2-deoxy- β -D-arabino-hexopyranoside (1.28)



1.28

Following a similar procedure as described in 7.2.3 using MeOH as solvent, the 4-*O*-benzylated levoglucosan derivatives **2.2** (153 mg, 0.65 mmol) was converted into compound **1.28** (83 mg, 0.58 mmol, 89%), obtained as a dense colourless gel. *R*_f 0.12 (petroleum ether/acetone 60:40). [α]_D -120.3 (c 1.10, water, 21 °C), lit -119 (c 1.10, water, 20 °C).¹¹⁹ IR (neat) 3369 (m, br.), 2960 (w), 2899 (w), 1124 (s), 1042 (s) cm⁻¹. ¹H NMR (500 MHz, CDCl₃) δ 5.65 (1H, br. d, J 1.4 Hz, H₁), 4.56 (1H, m, from which could be extracted J 5.4 Hz, H₅), 4.36 (1H, ddd, J 7.6, 0.8, 0.2 Hz, H_{6endo}), 3.91 - 3.85 (1H, m, from which could be extracted J 7.4, 5.2, 1.6 Hz, H₃), 3.80 (1H, dd, J 7.6, 5.4 Hz, H_{6exo}), 3.76 (1H, br. dq, J 9.5, 1.6 Hz, H₄), 2.57 (1H, d, J 7.5 Hz, OH₃), 2.31 (1H, d, J 9.5 Hz, OH₄), 2.18 (1H, ddd, J 15.3, 5.2, 1.5 Hz, H_{2ax}), 1.86 (1H, m, from which could be extracted J 15.3, 2.0, 1.2 Hz, H_{2eq}) ppm. ¹³C NMR (101 MHz, acetone-*d*₆) δ 100.1 (1C, s, C₁), 76.2 (1C, s, C₅), 72.1 (1C, s, C₄), 68.3 (1C, s, C₃), 64.4 (1C, s, C₆), 35.4 (1C, s, C₂) ppm. No NMR data had been reported in CDCl₃. HRMS (ESI⁺) for C₆H₁₀NaO₄ [M+Na]⁺ calcd. 169.0477, found. 169.0471.

7.2.5 1,6-Anhydro-2,3-dideoxy-3-fluoro- β -D-arabino-hexopyranoside (1.29)



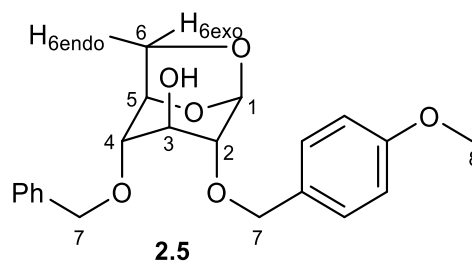
1.29

The 4-*O*-benzylated levoglucosan derivative **2.3** (102 mg, 0.43 mmol) was dissolved in MeOH (1 mL) and pumped at a flow rate of 1.0 mL.min⁻¹ through a 20% Pd(OH)₂ cartridge installed in the H-Cube[®] flow hydrogenation reactor. The solution of starting material was passed through the system a

single time under 50 bar of H₂ at rt before being flushed out with MeOH (10 mL). Evaporation of the solvent under vacuum afforded 64 mg (0.43 mmol, 100%) of pure **1.29** as a translucent oil. **Rf** 0.26 (petroleum ether/acetone 70:30). $[\alpha]_D -101.6$ (c 0.25, CHCl₃, 19 °C). **IR** (neat) 3391 (w, br.), 2964 (w, br.), 1028 (s) cm⁻¹. **¹H NMR** (500 MHz, CDCl₃) δ 5.57 (1H, br. d, *J* 1.1 Hz, H₁), 4.67 (1H, m, from which could be extracted *J* 46.7 Hz, H₃), 4.55 (1H, m, from which could be extracted *J* 6.0 Hz, H₅), 4.22 (1H, dt, *J* 7.6, 1.1 Hz, H_{6endo}), 3.84 (1H, br. ddd, *J* 7.6, 6.0, 4.0 Hz, H_{6exo}), 3.81 (1H, m, from which could be extracted *J* 10.0, 2.0, 0.9 Hz, H₄), 2.38 (1H, d, *J* 9.9 Hz, OH₄), 2.10 (1H, dddd, *J* 38.5, 15.8, 4.6, 1.9 Hz, H_{2ax}), 2.04 (1H, m, from which could be extracted *J* 23.3, 15.8 Hz, H_{2eq}) ppm. **¹H[¹⁹F] NMR** (500 MHz, CDCl₃) δ 5.57 (1H, br. d, *J* 1.3 Hz, H₁), 4.67 (1H, ddt, *J* 4.7, 3.3, 1.5 Hz, H₃), 4.55 (1H, m, from which could be extracted *J* 6.0 Hz, H₅), 4.22 (1H, dd, *J* 7.6, 1.2 Hz, H_{6endo}), 3.84 (1H, dd, *J* 7.5, 6.0 Hz, H_{6exo}), 3.82 (1H, m, from which could be extracted *J* 10.0 Hz, H₄), 2.38 (1H, d, *J* 10.0 Hz, OH₄), 2.10 (1H, ddd, *J* 15.8, 4.5, 1.9 Hz, H_{2ax}), 2.04 (1H, m, from which could be extracted *J* 15.8, 1.5 Hz, H_{2eq}) ppm. **¹³C NMR** (101 MHz, CDCl₃) δ 99.8 (1C, s, C₁), 88.1 (1C, d, *J* 177.1 Hz, C₃), 75.4 (1C, s, C₅), 68.6 (1C, d, *J* 26.4 Hz, C₄), 64.3 (1C, d, *J* 5.9 Hz, C₆), 33.3 (1C, d, *J* 20.5 Hz, C₂) ppm. **¹⁹F NMR** (471 MHz, CDCl₃) δ -177.3 (1F, m, from which could be extracted *J* 46.7, 38.5, 23.3, 10.8, 4.0 Hz) ppm. **¹⁹F[¹H] NMR** (471 MHz, CDCl₃) δ -177.3 (1F, s) ppm. **MS** (EI) (*m/z*) 148.1 [M]⁺.

7.2.6 Attempted synthesis of 2-deoxy-2,2-difluoro levoglucosan (1.30)

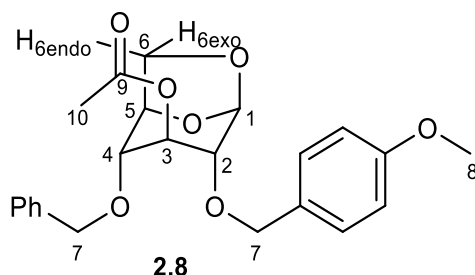
7.2.6.1 1,6-Anhydro-4-*O*-benzyl-2-*O*-(*p*-methoxybenzyl)- β -D-glucopyranoside (**2.5**)



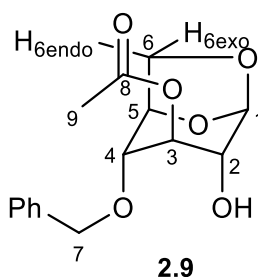
To a 1 M solution of sodium 4-methoxybenzylate in 4-methoxybenzyl alcohol (73.2 mL, 73.2 mmol, 5.6 equiv) was added portion wise the Černý epoxide **2.6** (3.08 g, 13.1 mmol, 1 equiv). The resulting mixture was stirred at 80 °C for 4 h before being neutralised with Dowex 50 H⁺ and filtered on Büchner. Purification by column chromatography (petroleum ether/acetone 90:10 to 80:20) afforded 4.52 g (12.1 mmol, 92%) of compound **2.5** as a white solid. **Rf** 0.12 (petroleum ether/acetone 80:20). **Mp** 90-92 °C (hexane/DCM). $[\alpha]_D -27.7$ (c 0.70, CHCl₃, 24 °C). **IR** (neat) 3422 (w, br.), 2991 (w), 2966 (w), 2900 (w), 2864 (w), 1613 (m), 1514 (s), 1251 (s), 1083 (s) cm⁻¹. **¹H NMR** (500 MHz, CDCl₃) δ 7.45 - 7.28 (7H, m, H_{Ar}), 6.93 - 6.85 (2H, m, H_{Ar}), 5.42 (1H, br. s, H₁), 4.71 (1H, d, *J* 21.1 Hz, H₇), 4.69 (1H, d, *J* 21.1 Hz, H₇), 4.63 (2H, s, H₇), 4.57 (1H, br. dd, *J* 5.3, 1.0 Hz, H₅), 3.85 (1H, br. t, *J* 3.9 Hz, H₃), 3.81 (1H, dd, *J* 7.5, 0.6 Hz, H_{6endo}), 3.81 (3H, s, H₈), 3.66 (1H, dd, *J* 7.5, 5.0 Hz,

H_{6exo}), 3.34 (1H, m, from which could be extracted J 4.2, 0.6 Hz, H₄), 3.25 (1H, br. d, J 4.1 Hz, H₂) ppm. **¹³C NMR** (101 MHz, CDCl₃) δ 159.4 (1C, s, C_{Ar}), 137.9 (1C, s, C_{Ar}), 129.8 (1C, s, C_{Ar}), 129.6 (2C, s, C_{Ar}), 128.5 (2C, s, C_{Ar}), 127.9 (1C, s, C_{Ar}), 127.9 (2C, s, C_{Ar}), 113.9 (2C, s, C_{Ar}), 101.4 (1C, s, C₁), 79.7 (1C, s, C₄), 79.1 (1C, s, C₂), 75.3 (1C, s, C₅), 71.8 (2C, s, C₇), 70.6 (1C, s, C₃), 66.6 (1C, s, C₆), 55.3 (1C, s, C₈) ppm. **MS** (ESI+) (m/z) 395.2 [M+Na]⁺, 411.2 [M+K]⁺. **HRMS** (ESI+) for C₂₁H₂₄NaO₆ [M+Na]⁺ Calcd. 395.1471, Found. 395.1464.

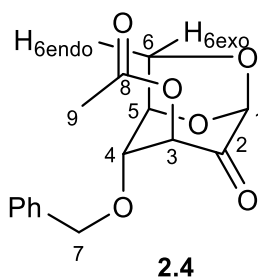
7.2.6.2 3-*O*-Acetyl-1,6-anhydro-4-*O*-benzyl-2-*O*-(*p*-methoxybenzyl)- β -D-glucopyranoside (2.8)



To a solution of compound **2.5** (1.00 g, 2.69 mmol, 1 equiv) in anhydrous pyridine (2.5 mL) at 0 °C was added acetic anhydride (0.7 mL, 7.46 mmol, 2.8 equiv). The resulting mixture was stirred at rt for 3 h before being concentrated under vacuum. Purification by column chromatography (petroleum ether/acetone 80:20) afforded 1.12 g (2.69 mmol, 100%) of compound **2.8** as a slightly orange oil. **Rf** 0.25 (petroleum ether/acetone 80:20). **[α]_D** -48.3 (c 0.70, CHCl₃, 24 °C). **IR** (neat) 2959 (w), 2900 (w), 2837 (w), 1734 (s), 1513 (s), 1227 (s), 1095 (s, br.), 1025 (s, br.) cm⁻¹. **¹H NMR** (400 MHz, CDCl₃) δ 7.75 - 7.28 (7H, m, H_{Ar}), 6.90 - 6.82 (2H, m, H_{Ar}), 5.37 (1H, br. s, H₁), 5.07 - 5.02 (1H, m, H₃), 4.80 (1H, d, J 12.5 Hz, H₇), 4.74 (1H, d, J 12.0 Hz, H₇), 4.70 (1H, d, J 12.5 Hz, H₇), 4.64 - 4.55 (1H, m, H₅), 4.59 (1H, d, J 12.2 Hz, H₇), 3.88 (1H, br. d, J 7.3 Hz, H_{6endo}), 3.80 (3H, s, H₈), 3.70 (1H, dd, J 7.3, 5.9 Hz, H_{6exo}), 3.26 (1H, br. d, J 1.0 Hz, H₄), 3.22 (1H, br. d, J 1.0 Hz, H₂), 2.06 (3H, s, H₁₀) ppm. **¹³C NMR** (101 MHz, CDCl₃) δ 169.7 (1C, s, C₉), 159.4 (1C, s, C_{Ar}), 137.8 (1C, s, C_{Ar}), 129.9 (1C, s, C_{Ar}), 129.7 (2C, s, C_{Ar}), 128.5 (2C, s, C_{Ar}), 127.9 (2C, s, C_{Ar}), 127.8 (1C, s, C_{Ar}), 113.8 (2C, s, C_{Ar}), 100.5 (1C, s, C₁), 74.9 (1C, s, C₄), 74.3 (1C, s, C₅), 73.7 (1C, s, C₂), 71.2 (1C, s, C₇), 71.1 (1C, s, C₇), 68.8 (1C, s, C₃), 65.0 (1C, s, C₆), 55.3 (1C, s, C₈), 21.2 (1C, s, C₁₀) ppm. **MS** (ESI+) (m/z) 437.2 [M+Na]⁺, 851.4 [2M+Na]⁺. **HRMS** (ESI+) for C₂₃H₂₆NaO₇ [M+Na]⁺ Calcd. 437.1516, Found. 437.1578.

7.2.6.3 3-*O*-Acetyl-1,6-anhydro-4-*O*-benzyl- β -D-glucopyranoside (**2.9**)

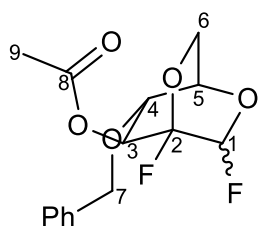
To a solution of compound **2.8** (989 mg, 2.39 mmol, 1 equiv) in DCM (58 mL) was added water (1 mL) and DDQ (759 mg, 3.34 mmol, 1.4 equiv). The resulting mixture was stirred at rt for 12 h before being dilute with DCM (70 mL), quenched with sat. aq. NaHCO₃ (40 mL), and washed with brine (2x80 mL). After drying over MgSO₄, solvent was removed under vacuum and the resulting syrup chromatographed (petroleum ether/acetone 90:10 to 80:20) to afford pure **2.9** (532 mg, 1.81 mmol, 75%) as a pale yellow solid. **Rf** 0.44 (petroleum ether/acetone 70:30). **Mp** 80-82 °C (hexane/DCM). **[α]_D** -6.7 (c 0.80, CHCl₃, 24 °C). **IR** (neat) 3532 (w, br.), 2959 (w), 2900 (w), 1738 (s), 1227 (s, br.), 1044 (s) cm⁻¹. **¹H NMR** (400 MHz, CDCl₃) δ 7.46 - 7.29 (5H, m, H_{Ar}), 5.46 (1H, br. s, H₁), 5.01 (1H, br. t, *J* 1.5 Hz, H₃), 4.83 (1H, d, *J* 12.0 Hz, H₇), 4.70 (1H, d, *J* 12.2 Hz, H₇), 4.57 (1H, br. d, *J* 5.6 Hz, H₅), 3.97 (1H, d, *J* 7.3 Hz, H_{6endo}), 3.78 (1H, dd, *J* 7.5, 5.7 Hz, H_{6exo}), 3.53 (1H, br. dd, *J* 11.9, 1.3 Hz, H₂), 3.33 (1H, br. d, *J* 1.2 Hz, H₄), 2.68 (1H, d, *J* 12.2 Hz, OH₂), 2.10 (3H, s, H₉) ppm. **¹³C NMR** (101 MHz, CDCl₃) δ 169.9 (1C, s, C₈), 137.3 (1C, s, C_{Ar}), 128.6 (2C, s, C_{Ar}), 128.1 (1C, s, C_{Ar}), 128.0 (2C, s, C_{Ar}), 101.3 (1C, s, C₁), 74.5 (1C, s, C₅), 74.3 (1C, s, C₄), 71.3 (1C, s, C₇), 70.5 (1C, s, C₃), 68.1 (1C, s, C₂), 65.2 (1C, s, C₆), 21.1 (1C, s, C₉) ppm. **MS** (ESI+) (*m/z*) 295.1 [M+H]⁺, 317.1 [M+Na]⁺, 611.2 [2M+Na]⁺. **HRMS** (ESI+) for C₁₅H₁₈NaO₆ [M+Na]⁺ Calcd. 317.1001, Found. 317.0989.

7.2.6.4 3-*O*-Acetyl-1,6-anhydro-4-*O*-benzyl- β -D-arabino-hexopyranos-2-uloside (**2.4**)

To a solution of compound **2.9** (106 mg, 0.36 mmol, 1 equiv) in anhydrous DCM (6.4 mL) at 0 °C was added TCCA (168 mg, 0.72 mmol, 2 equiv) and TEMPO (2.2 mg, 0.014 mmol, 0.04 equiv). The resulting mixture was stirred at rt for 1 h before being filtered through a pad of Celite®. Filtrate was then washed with brine (2x20 mL), dried over MgSO₄, and concentrated under vacuum to afford 95 mg of crude ketone **2.4**. ¹H NMR analysis indicated >90% purity and the material was accordingly

used for the next reaction without further purification. **Rf** 0.42 (petroleum ether/acetone 70:30). **¹H NMR** (400 MHz, CDCl₃) δ 7.45 - 7.30 (5H, m, H_{Ar}), 5.45 (1H, d, *J* 5.1 Hz, H₃), 5.30 (1H, s, H₁), 4.83 (1H, dd, *J* 5.7, 1.8 Hz, H₅), 4.70 (1H, d, *J* 12.2 Hz, H₇), 4.66 (1H, d, *J* 12.2 Hz, H₇), 3.91 (1H, dd, *J* 7.8, 6.1 Hz, H_{6exo}), 3.87 (1H, dd, *J* 7.8, 2.0 Hz, H_{6endo}), 3.68 (1H, d, *J* 5.1 Hz, H₄), 2.16 (3 H, s, H₉) ppm.

7.2.6.5 3-O-Acetyl-2,6-anhydro-4-O-benzyl-2-fluoro-D-mannopyranosyl fluorides (2.10/2.11)



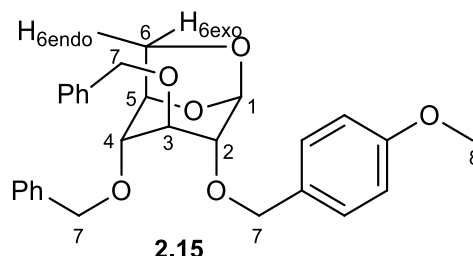
2.11(α)/2.11(β)
85:15

To a solution of crude **2.4** (91 mg, 0.31 mmol, 1 equiv) in anhydrous DCM (1.2 mL) at 0 °C was added DAST (0.12 mL, 0.98 mmol, 3.1 equiv) dropwise. The resulting mixture was stirred overnight at rt before being dilute with DCM (20 mL) and quenched with sat. aq. NaHCO₃ (8 mL) at 0 °C. The layers were separated and the organic phase washed with brine (2x20 mL), dried over MgSO₄, and concentrated under vacuum. Purification by column chromatography (pentane/acetone 90:10 to 80:20) afforded 64 mg (0.20 mmol, 65%) of an inseparable mixture of **2.11(α)/2.12(β)** (ratio 85:15) as a white solid. **Rf** 0.44 (pentane/acetone 80:20). [**α**]_D -18.9 (c 0.50, CHCl₃, 24 °C). **IR** (neat) 2977 (w), 2912 (w), 1751 (s), 1164 (s), 977 (s) cm⁻¹. **¹H NMR** (500 MHz, CDCl₃) δ 7.43 - 7.28 (10H, m, H_{Arα+β}), 5.73 (1H, br. dd, *J* 64.5, 1.1 Hz, H_{1α}), 5.68 (1H, dd, *J* 66.5, 5.6 Hz, H_{1β}), 5.63 (1H, ddt, *J* 3.3, 2.2, 1.2 Hz, H_{3β}), 5.31 (1H, br. ddd, *J* 2.7, 1.1, 0.5 Hz, H_{3α}), 4.83 (1H, d, *J* 12.5 Hz, H_{7β}), 4.66 (1H, d, *J* 12.4 Hz, H_{7β}), 4.64 (1H, d, *J* 12.1 Hz, H_{7α}), 4.58 (1H, d, *J* 12.1 Hz, H_{7α}), 4.45 (1H, br. dd, *J* 10.5, 1.6 Hz, H_{6α}), 4.27 - 4.23 (1H, m, H_{5β}), 4.23 - 4.18 (1H, m, H_{5α}), 4.20 (1H, m, from which could be extracted *J* 3.7, 1.0 Hz, H_{6β}), 4.07 (1H, m, from which could be extracted *J* 10.5 Hz, H_{6α}), 3.99 (1H, dd, *J* 9.8, 5.2 Hz, H_{6β}), 3.87 (1H, m, from which could be extracted *J* 2.4, 1.3 Hz, H_{4α}), 3.59 (1H, m, from which could be extracted *J* 5.1, 2.3 Hz, H_{4β}), 2.18 (1H, s, H_{9β}), 2.17 (3 H, s, H_{9α}) ppm. **¹³C NMR** (101 MHz, ¹³C δ 169.4 (1C, s, C_{8α}), 136.6 (1C, s, C_{Arα}), 128.7 (2C, s, C_{Arα}), 128.3 (1C, s, C_{Arα}), 127.9 (2C, s, C_{Arα}), 104.9 (1C, dd, *J* 239.1, 26.4 Hz, C_{2α}), 104.6 (1C, dd, *J* 229.6, 21.3 Hz, C_{1α}), 80.0 (1C, t, *J* 5.1 Hz, C_{4α}), 73.6 (1C, dd, *J* 17.6, 5.1 Hz, C_{3α}), 71.2 (1C, s, C_{7α}), 70.3 (1C, t, *J* 2.2 Hz, C_{5α}), 66.2 (1C, d, *J* 5.1 Hz, C_{6α}), 20.7 (1C, s, C_{9α}) ppm. ¹³C signals corresponding to the β anomer too weak to be interpreted. **¹⁹F NMR** (471 MHz, CDCl₃) δ -131.0 (1F, m, from which could be extracted *J* 66.7, 11.3, 5.2 Hz, F_{1β}), -136.8 (1F, dd, *J* 64.5, 16.1 Hz, F_{1α}), -146.9 (1F, m, F_{2β}), -148.3 (1F, br. dt, *J* 16.1, 1.8 Hz, F_{2α}) ppm. **¹⁹F[¹H] NMR** (376 MHz, CDCl₃) δ -131.2 (1F, d, *J* 10.4 Hz, F_{1β}), -137.0 (1F, d, *J* 15.6 Hz, F_{1α}), -147.1 (1F, d, *J* 12.1 Hz, F_{2β}), -148.6 (1F,

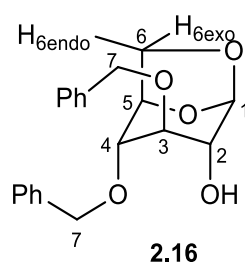
d, J 15.6 Hz, $F_{2\alpha}$) ppm. **MS** (ESI+) (m/z) 337.2 $[M+Na]^+$, 353.1 $[M+K]^+$, 651.4 $[2M+Na]^+$. **HRMS** (ESI+) for $C_{15}H_{16}F_2NaO_5$ $[M+Na]^+$ Calcd. 337.0863, Found. 337.0856.

7.2.7 Synthesis of 2-O-methoxy levoglucosan

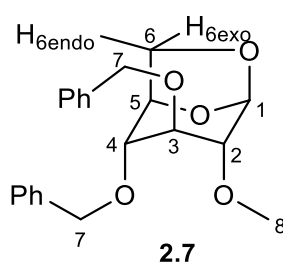
7.2.7.1 1,6-Anhydro-3,4-di-O-benzyl-2-O-(*p*-methoxybenzyl)- β -D-glucopyranoside (**2.15**)



To a solution of compound **2.5** (1.00 g, 2.69 mmol, 1 equiv) in dry DMF (79 mL) was added sodium hydride in mineral oil (60%, 268 mg, 6.70 mmol, 2.5 equiv). After 30 minutes at rt, the resulting solution was cooled at 0 °C and BnBr added (0.8 mL, 6.69 mmol, 2.5 equiv). The resulting mixture was stirred overnight at rt before being dilute with Et₂O (50 mL), quenched with water (50 mL) at 0 °C, and the resulting aqueous layer extracted with Et₂O (3x100 mL). The combined organic layers were dried over MgSO₄ and concentrated under vacuum. Purification by column chromatography (petroleum ether/acetone 90:10 to 80:20) afforded 1.24 g (2.69 mmol, 100%) of compound **2.14** as a translucent oil. **Rf** 0.29 (petroleum ether/acetone 80:20). $[\alpha]_D -33.4$ (c 0.60, CHCl₃, 24 °C). **IR** (neat) 2896 (w, br.), 1512 (m), 1246 (m), 1070 (s, br.), 1026 (s, br.) cm⁻¹. **¹H NMR** (400 MHz, CDCl₃) δ 7.41 - 7.28 (8H, m, H_{Ar}), 7.27 - 7.22 (4H, m, H_{Ar}), 6.90 - 6.83 (2H, m, H_{Ar}), 5.43 (1H, br. s, H₁), 4.63 (1H, d, J 12.5 Hz, H₇), 4.62 - 4.58 (1H, m, H₅), 4.57 (1H, d, J 12.5 Hz, H₇), 4.53 (1H, d, J 12.2 Hz, H₇), 4.48 (1H, d, J 12.2 Hz, H₇), 4.47 (1H, d, J 12.2 Hz, H₇), 4.41 (1H, d, J 12.0 Hz, H₇), 3.91 (1H, br. dd, J 7.2, 0.9 Hz, H_{6endo}), 3.81 (3H, s, H₈), 3.68 (1H, br. dd, J 7.1, 5.9 Hz, H_{6exo}), 3.61 - 3.53 (1H, m, H₃), 3.37 - 3.33 (2H, m, H₂ and H₄) ppm. **¹³C NMR** (101 MHz, CDCl₃) δ 138.0 (1C, s, C_{Ar}), 137.9 (1C, s, C_{Ar}), 130.0 (1C, s, C_{Ar}), 129.6 (2C, s, C_{Ar}), 128.5 (2C, s, C_{Ar}), 128.4 (2C, s, C_{Ar}), 127.9 (3C, s, C_{Ar}), 127.8 (1C, s, C_{Ar}), 127.8 (1C, s, C_{Ar}), 127.7 (2C, s, C_{Ar}), 113.8 (2C, s, C_{Ar}), 100.7 (1C, s, C₁), 76.2 (1C, s, C₄), 75.9 (1C, s, C₂), 74.4 (1C, s, C₅), 72.0 (1C, s, C₇), 71.5 (2C, s, C₇), 71.2 (1C, s, C₃), 65.5 (1C, s, C₆), 55.3 (1C, s, C₈) ppm. **MS** (ESI+) (m/z) 485.3 $[M+Na]^+$, 501.3 $[M+K]^+$, 947.8 $[2M+Na]^+$. **HRMS** (ESI+) for $C_{28}H_{30}NaO_6$ $[M+Na]^+$ Calcd. 485.1940, Found. 485.1962.

7.2.7.2 1,6-Anhydro-3,4-di-*O*-benzyl- β -D-glucopyranoside (**2.16**)

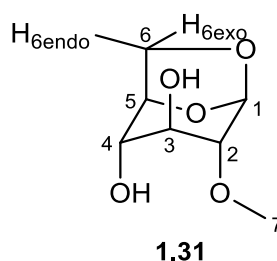
Following the same procedure as described in **7.2.6.3**, compound **2.15** (1.24 g, 2.68 mmol) was converted into the 3,4-di-*O*-benzylated levoglucosan **2.16** (794 mg, 2.32 mmol, 87%), obtained as a translucent oil. **Rf** 0.17 (petroleum ether/acetone 90:10 to 80:20). $[\alpha]_D -39.8$ (c 0.70, CHCl₃, 24 °C). **IR** (neat) 3452 (w, br.), 2955 (w), 2897 (w), 1454 (w), 1071 (s), 1052 (s) cm⁻¹. **¹H NMR** (500 MHz, CDCl₃) δ 7.40 - 7.28 (10H, m, H_{Ar}), 5.47 (1H, br. t, *J* 1.6 Hz, H₁), 4.65 (1H, d, *J* 12.0 Hz, H₇), 4.62 - 4.58 (1H, m, H₅), 4.58 (1H, d, *J* 12.1 Hz, H₇), 4.53 (1H, d, *J* 12.7 Hz, H₇), 4.50 (1H, d, *J* 12.3 Hz, H₇), 4.18 (1H, dd, *J* 7.2, 1.0 Hz, H_{6endo}), 3.76 (1H, dd, *J* 7.2, 5.9 Hz, H_{6exo}), 3.67 (1H, dt, *J* 3.3, 1.7 Hz, H₃), 3.65 (1H, br. s, H₂), 3.41 - 3.38 (1H, m, H₄), 2.69 - 2.50 (1H, br. s, OH₂) ppm. **¹³C NMR** (101 MHz, CDCl₃) δ 137.7 (1C, s, C_{Ar}), 137.3 (1C, s, C_{Ar}), 128.6 (2C, s, C_{Ar}), 128.5 (2C, s, C_{Ar}), 128.1 (1C, s, C_{Ar}), 127.9 (1C, s, C_{Ar}), 127.8 (2C, s, C_{Ar}), 127.7 (2C, s, C_{Ar}), 101.7 (1C, s, C₁), 76.6 (1C, s, C₃), 75.2 (1C, s, C₄), 74.0 (1C, s, C₅), 72.1 (1C, s, C₇), 71.1 (1C, s, C₇), 67.6 (1C, s, C₂), 65.0 (1C, s, C₆) ppm. NMR data match those previously reported.¹²⁰ **MS** (ESI+) (*m/z*) 365.3 [M+Na]⁺, 707.5 [2M+Na]⁺. **HRMS** (ESI+) for C₂₀H₂₂NaO₅ [M+Na]⁺ Calcd. 365.1365, Found. 365.1367.

7.2.7.3 1,6-Anhydro-3,4-di-*O*-benzyl-2-*O*-methyl- β -D-glucopyranoside (**2.7**)

To a solution of compound **2.16** (645 mg, 1.88 mmol, 1 equiv) in dry DMF (12.3 mL) was added sodium hydride in mineral oil (60%, 183 mg, 4.57 mmol, 2.4 equiv). After 30 minutes at rt, the resulting solution was cooled at 0 °C and MeI added (0.48 mL, 7.71 mmol, 4.1 equiv). The reaction mixture was then allowed to reach rt and the stirring continued for 12 h. After quenching with methanol (1.2 mL), the solution was concentrated to a syrup before being dissolved in DCM (25 mL). The resulting organic layer was then washed with water (2x25 mL), dried over MgSO₄, and the solvent removed under vacuum. Purification by column chromatography (petroleum ether/acetone 90:10 to 70:30) afforded 591 mg (1.66 mmol, 88%) of compound **2.7** as a translucent oil. **Rf** 0.55

(petroleum ether/acetone 70:30). $[\alpha]_D^{25}$ -19.0 (c 1.00, CHCl_3 , 22 °C). **IR** (neat) 3030 (w), 2894 (w), 1454 (m), 1090 (s), 1027 (s) cm^{-1} . **^1H NMR** (500 MHz, CDCl_3) δ 7.28 - 7.42 (10H, m, H_{Ar}), 5.50 (1H, br. s, H_1), 4.63 (1H, d, J 12.6 Hz, H_7), 4.59 - 4.57 (1H, m, H_5), 4.58 (1H, d, J 12.6 Hz, H_7), 4.57 (1H, d, J 12.1 Hz, H_7), 4.54 (1H, d, J 12.1 Hz, H_7), 3.93 (1H, dd, J 7.2, 1.0 Hz, $\text{H}_{6\text{endo}}$), 3.70 (1H, dd, J 7.1, 5.8 Hz, $\text{H}_{6\text{exo}}$), 3.58 (1H, tt, J 2.3, 1.2 Hz, H_3), 3.39 (3H, s, H_8), 3.34-3.37 (1H, m, H_4), 3.18 - 3.16 (1H, m, H_2) ppm. **^{13}C NMR** (101 MHz, CDCl_3) δ 137.9 (1C, s, C_{Ar}), 137.9 (1C, s, C_{Ar}), 128.5 (2C, s, C_{Ar}), 128.5 (2C, s, C_{Ar}), 127.9 - 127.8 (4C, m, C_{Ar}), 127.7 (2C, s, C_{Ar}), 100.1 (1C, s, C_1), 79.1 (1C, s, C_2), 76.5 (1C, s, C_4), 75.7 (1C, s, C_3), 74.4 (1C, s, C_5), 72.0 (1C, s, C_7), 71.2 (1C, s, C_7), 65.4 (1C, s, C_6), 57.8 (1C, s, C_8) ppm. **MS** (ESI+) (m/z) 357.3 $[\text{M}+\text{H}]^+$, 379.3 $[\text{M}+\text{Na}]^+$, 735.6 $[2\text{M}+\text{Na}]^+$. **HRMS** (ESI+) for $\text{C}_{21}\text{H}_{24}\text{NaO}_5$ $[\text{M}+\text{Na}]^+$ calcd. 379.1521, found. 379.1520; for $\text{C}_{42}\text{H}_{48}\text{NaO}_{10}$ $[2\text{M}+\text{Na}]^+$ calcd. 735.3145, found. 735.3143.

7.2.7.4 1,6-Anhydro-2-O-methyl- β -D-glucopyranoside (**1.31**)



Following a similar procedure as described in **7.2.3** using methanol as solvent, compound **2.7** (481 mg, 1.35 mmol) was converted into the 2-O-methyl levoglucosan derivatives **1.31** (83 mg, 0.58 mmol, 89%), obtained as a white solid. **Rf** 0.11 (petroleum ether/acetone 60:40). **Mp** 88-90 °C (petroleum ether/acetone), lit 92-94°C (hexane/acetone).¹²¹ $[\alpha]_D^{25}$ -73.4 (c 1.45, Acetone, 21°C), lit -75 (c 1.20, MeOH, 20 °C).¹²¹ **IR** (neat) 3461 (w, br.), 3403 (w, br.), 2982 (w), 2909 (w), 1103 (s), 1042 (s), 1005 (s) cm^{-1} . **^1H NMR** (500 MHz, CDCl_3) δ 5.58 (1H, br. t, J 1.8 Hz, H_1), 4.59 (1H, m, from which could be extracted J 5.3 Hz, H_5), 4.22 (1H, br. dd, J 7.6, 0.3 Hz, $\text{H}_{6\text{endo}}$), 3.90 (1H, dquin, J 7.7, 1.9 Hz, H_3), 3.80 (1H, dd, J 7.6, 5.3 Hz, $\text{H}_{6\text{exo}}$), 3.65 (1H, br. dq, J 11.6, 1.9 Hz, H_4), 3.51 (3H, s, H_7), 3.20 (1H, br. q, J 1.7 Hz, H_2), 2.88 (1H, d, J 11.6 Hz, OH_4), 2.40 (1H, d, J 7.7 Hz, OH_3) ppm. **^{13}C NMR** (101 MHz, CDCl_3) δ 100.3 (1C, s, C_1), 79.1 (1C, s, C_2), 76.8 (1C, s, C_5), 70.9 (1C, s, C_4), 69.9 (1C, s, C_3), 65.4 (1C, s, C_6), 58.0 (1C, s, C_7) ppm. **MS** (ESI+) (m/z) 177.2 $[\text{M}+\text{H}]^+$, 199.1 $[\text{M}+\text{Na}]^+$. **HRMS** (ESI+) for $\text{C}_7\text{H}_{12}\text{NaO}_5$ $[\text{M}+\text{Na}]^+$ calcd. 199.0582, found. 199.0577; for $\text{C}_{14}\text{H}_{24}\text{NaO}_{10}$ $[2\text{M}+\text{Na}]^+$ calcd. 375.1267, found. 375.1257.

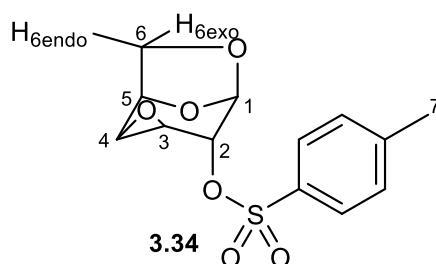
7.2.8 Experimental procedure for sample preparation

Molecular sieves 3Å (2 g, beads 4-8 mesh) were activated by heating at 160 °C under reduced pressure (0.15 mmHg) for 16 hours. After cooling, the activated molecular sieves (3 spatulas) were placed under argon atmosphere and then added to a dry solution of levoglucosan in CDCl₃ (7-19 mM). The resulting solution was left standing for 40 minutes under argon and then 0.6 mL of the supernatant solution was added to the NMR tube which was previously flame-dried under reduced pressure and placed under argon. The NMR tube was closed with a valve and immediately submitted for data acquisition.

7.3 Synthesis of 2,3,4-trideoxy,2,3,4-trifluoro-D-glucopyranose

7.3.1 Synthesis of trifluoro levoglucosan *via* deoxofluorination of 2,4-dideoxy-2,4-difluoro levoglucosan

7.3.1.1 1,6:3,4-Dianhydro-2-*O*-*p*-tolylsulfonyl-β-D-galactopyranoside (**3.34**)

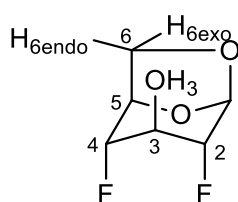


To a solution of levoglucosan **3.27** (19.8 g, 122 mmol, 1 equiv) in dry pyridine (100 mL) at 0 °C was added a solution of *p*-toluenesulfonyl chloride (46.7 g, 245 mmol, 2 equiv) in a mixture of dry pyridine (93 mL) and chloroform (130 mL) dropwise. The reaction mixture was then allowed to reach rt overnight. After 15 h, the reaction mixture was quenched with water (70 mL) and diluted with DCM (270 mL). The organic phase was washed with 10% aq. H₂SO₄ (5x150 mL), dried over MgSO₄ and concentrated to give the 2,4-di-*O*-tosyl levoglucosan **3.33** (52.66 g) as a white foam, reacted in the next step without further purification.

To a solution of crude **3.33** in dry DCM (180 mL) at 0 °C was added sodium methoxide (25 wt. % in MeOH, 34 mL, 149 mmol, 1.3 equiv). The resulting mixture was allowed to reach rt and then stirred for 1 h. The reaction mixture was diluted with DCM (120 mL) and the organic phase washed with water (3x180 mL), dried over MgSO₄ and concentrated. Recrystallisation of the white solid obtained from a cold hexane/DCM afforded 20.7 g (89.0 mmol, 57% over two steps) of pure **3.34** as translucent crystals. **Rf** 0.43 (petroleum ether/acetone 70:30). **Mp** 136-138 °C (hexane/DCM), lit

149 °C (CHCl₃/EtOH).¹²² [α]_D -41.5 (c 0.99, CHCl₃, 22 °C), lit -41 (c 1.35, CHCl₃, 25 °C).¹²² IR (neat) 2966 (w), 1359 (m), 1172 (s), 1006 (s) cm⁻¹. ¹H NMR (400 MHz, CDCl₃) δ 7.89 - 7.81 (2H, m, from which could be extracted *J* 8.3 Hz, H_{Ar}), 7.42 - 7.35 (2H, m, *J* 7.8 Hz, H_{Ar}), 5.18 (1H, br. s, H₁), 4.85 (1H, t, *J* 4.9 Hz, H₅), 4.40 (1H, s, H₂), 3.95 (1H, d, *J* 6.6 Hz, H_{6endo}), 3.62 (1H, t, *J* 4.3 Hz, H₄), 3.51 (1H, dd, *J* 6.6, 4.9 Hz, H_{6exo}), 3.15 (1H, dd, *J* 3.9, 1.5 Hz, H₃), 2.47 (3H, s, H₇) ppm. ¹³C NMR (101 MHz, CDCl₃) δ 145.7 (1C, s, C_{Ar}), 132.8 (1C, s, C_{Ar}), 130.2 (2C, s, C_{Ar}), 128.0 (2C, s, C_{Ar}), 98.1 (1C, s, C₁), 71.8 (1C, s, C₂), 71.6 (1C, s, C₅), 64.8 (1C, s, C₆), 52.8 (1C, s, C₄), 47.6 (1C, s, C₃), 21.7 (1C, s, C₇) ppm. NMR data match those previously reported.¹²³ MS (ESI+) (m/z) 299.2 [M+H]⁺, 321.2 [M+Na]⁺.

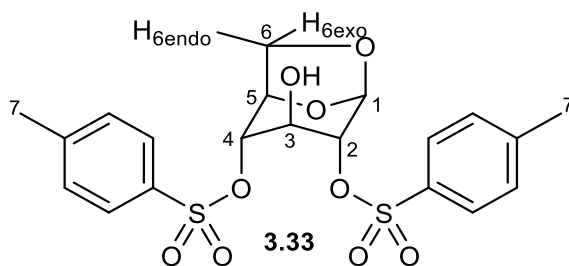
7.3.1.2 1,6-Anhydro-2,4-dideoxy-2,4-difluoro- β -D-glucopyranoside (**1.32**) synthesised from tosyl epoxide **3.34**



1.32

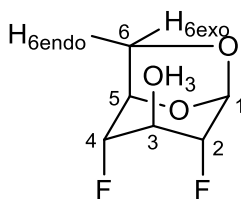
To a solution of tosyl epoxide **3.34** (4.04 g, 13.5 mmol, 1 equiv) in ethylene glycol (34 mL) were added potassium hydrogen fluoride (6.34 g, 81.2 mmol, 6 equiv) and potassium fluoride (4.72 g, 81.4 mmol, 6 equiv). The resulting mixture was stirred for 2 h in a setup let open to the air at 170 °C before being allowed to cool down and loaded onto a silica gel column (CHCl₃/acetone 70:30), which afforded 1.26 g (7.61 mmol, 56%) of pure 2,4-difluoro levoglucosan **1.32** as slightly orange crystals. See **7.2.2** for characterisation data.

7.3.1.3 1,6-Anhydro-2,4-di-*O*-*p*-tolylsulfonyl- β -D-glucopyranoside (**3.33**)



Following the same procedure as described in **7.3.1.1**, levoglucosan **3.27** (4.99 g, 30.8 mmol) was converted into 2,4-di-*O*-tosyl levoglucosan **3.33** (11.9 g, 25.3 mmol, 82%), obtained pure as a white solid after column chromatography (DCM/ethyl acetate 60:40). **R_f** 0.64 (DCM/ethyl acetate 60:40). **Mp** 110-112 °C (hexane/DCM), lit 118 °C (no solvent given).¹²² **[α]_D** -45.0 (c 1.00, CHCl₃, 22 °C), lit -44 (c 0.99, CHCl₃, no T °C given).¹²² **IR** (neat) 3537 (m), 2982 (w, br.), 2909 (w, br.), 1357 (m), 1172 (s), 1012 (s) cm⁻¹. **¹H NMR** (400 MHz, CDCl₃) δ 7.81 (4H, m, from which could be extracted *J* 8.3, 5.9 Hz, H_{Ar}), 7.44 - 7.30 (4H, m, H_{Ar}), 5.34 (1H, s, H₁), 4.65 (1H, br. d, *J* 4.9 Hz, H₅), 4.35 (1H, dd, *J* 3.9, 1.5 Hz, H₄), 4.19 (1H, br. d, *J* 3.4 Hz, H₂), 3.99 (1H, d, *J* 8.1 Hz, H_{6endo}), 3.96 - 3.89 (1H, m, H₃), 3.68 (1H, dd, *J* 8.1, 5.4 Hz, H_{6exo}), 2.60 (1H, d, *J* 5.4 Hz, OH₃), 2.47 (3H, s, H₇), 2.46 (3H, s, H₇) ppm. **¹³C NMR** (101 MHz, CDCl₃) δ 145.5 (1C, s, C_{Ar}), 145.5 (1C, s, C_{Ar}), 133.1 (1C, s, C_{Ar}), 132.8 (1C, s, C_{Ar}), 130.1 (2C, s, C_{Ar}), 130.0 (2C, s, C_{Ar}), 128.0 (2C, s, C_{Ar}), 127.9 (2C, s, C_{Ar}), 100.0 (1C, s, C₁), 79.2 (1C, s, C₄), 78.0 (1C, s, C₂), 74.9 (1C, s, C₅), 69.7 (1C, s, C₃), 66.3 (1C, s, C₆), 21.7 (2C, s, C₇) ppm. NMR data match those previously reported.¹²³ **MS** (ESI+) (*m/z*) 471.3 [M+H]⁺, 493.4 [M+Na]⁺. **HRMS** (ESI+) for C₂₀H₂₂NaO₉S₂ [M+Na]⁺ Calcd. 493.0603, Found. 493.0608.

7.3.1.4 1,6-Anhydro-2,4-dideoxy-2,4-difluoro- β -D-glucopyranoside (**1.32**) synthesised from 2,4-di-*O*-tosyl levoglucosan **3.33**

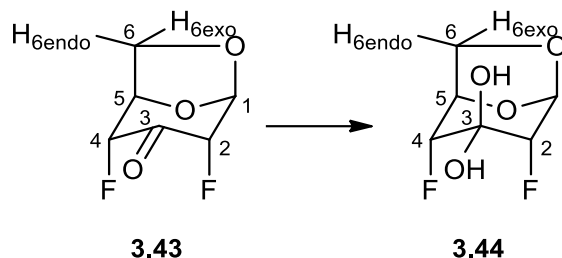


1.32

Following the same procedure as described in **7.3.1.2**, 2,4-di-*O*-tosyl levoglucosan **3.33** (8.36 g, 17.8 mmol) was converted into 2,4-difluoro levoglucosan **1.32** (1.51 g, 9.09 mmol, 55%), obtained pure as a white solid after column chromatography (DCM/ethyl acetate 60:40). See **7.2.2** for characterisation data.

7.3.2 Synthesis of trifluoro levoglucosan *via* triflate displacement on 2,4-dideoxy-2,4-difluoro 3-*O*-(trifluoromethanesulfonyl) levoallosan

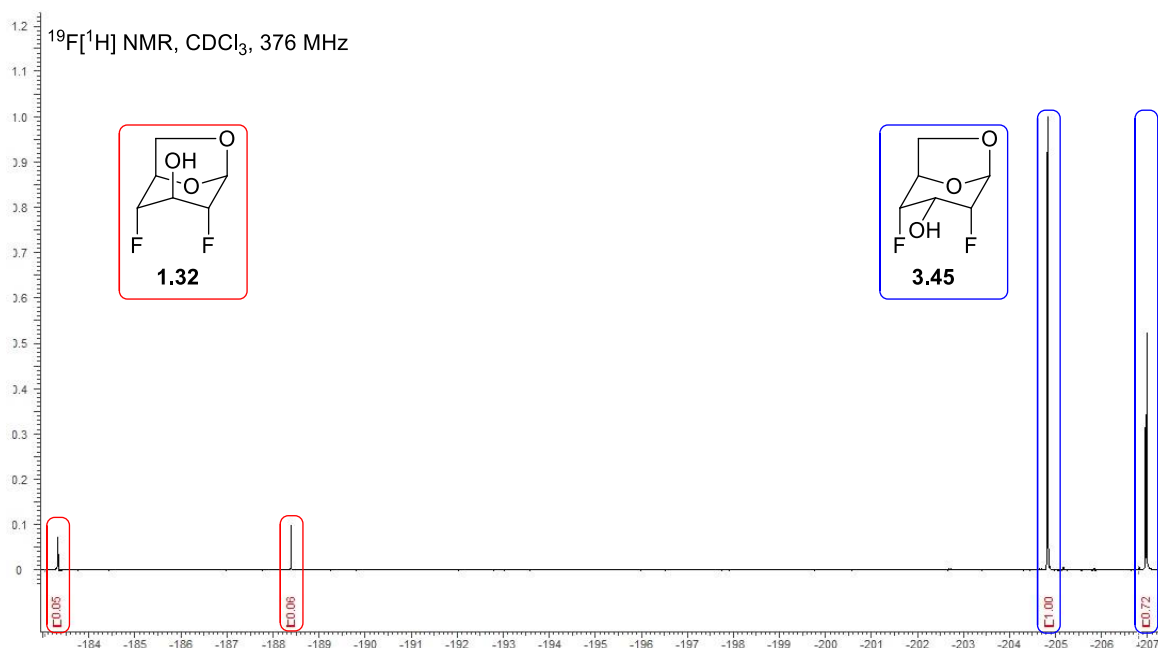
7.3.2.1 Oxidation of 2,4-difluoro levoglucosan (**1.32**)



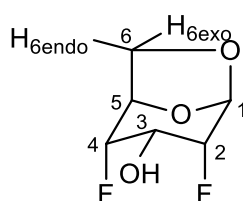
To a solution of 2,4-difluoro levoglucosan **1.32** (2.12 g, 12.7 mmol, 1 equiv) in anhydrous DCM (210 mL) at 0 °C was added TCCA (5.91 g, 25.4 mmol, 2 equiv) and TEMPO (105 mg, 0.67 mmol, 0.05 equiv). The resulting mixture was stirred at rt for 2 h before being filtered through a pad of Celite®, dried over MgSO₄, and concentrated under vacuum. Filtration over a pad of silica (DCM/acetone 90:10 to 60:40) afforded 2.24 g of an inseparable mixture of two difluorinated products, assumed to be 1,6-anhydro-2,4-dideoxy-2,4-difluoro-β-D-arabino-hexopyranos-3-uloside **3.43** and its hydrate form **3.44**. **Rf** 0.52 (petroleum ether/acetone 80:20). **MS** (ESI-) (m/z) 227.6 [**3.43'**+HCO₂]⁻.

7.3.2.2 Reduction of the mixture **3.43/3.44**

To a solution of mixture **3.43/3.44** (2.24 g, ≈ 12.8 mmol, 1 equiv) in anhydrous Et₂O (100 mL) was added NaBH₄ (979 mg, 26.2 mmol, ≈ 2.1 equiv) followed by EtOH (12 drops). The resulting solution was stirred at rt for 16 h before being cooled down to 0 °C and quenched with water (40 mL). The layers were separated and the aqueous phase was extracted with ethyl acetate (3x80 mL). Organic phases were combined, dried over MgSO₄, and concentrated under vacuum. Filtration over a pad of silica (DCM/acetone 70:30) afforded 1.47 g (8.84 mmol, 72%) of an inseparable mixture of diastereoisomers **3.45/1.32** (*dr* 94:6). Analytical sample of pure **3.45** was obtained by HPLC (DCM/ethyl acetate 70:30).



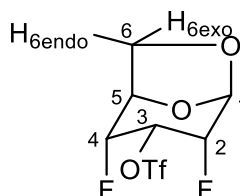
Major isomer: 1,6-Anhydro-2,4-dideoxy-2,4-difluoro- β -D-allopyranoside (3.45).



Rf 0.70 (DCM/acetone 70:30). **Mp** 108-110 °C (Hexane/DCM), lit 113-115 °C (ethyl acetate).¹²⁴ $[\alpha]_D$ -69.0 (c 1.06, MeOH, 24 °C), lit -85 (c 0.6, CHCl_3 , 23-25 °C).¹²⁴ **IR** (neat) 3265 (m, br.), 2989 (w), 2915 (w), 1339 (m), 1033 (s) cm^{-1} . **^1H NMR** (500 MHz, CDCl_3) δ 5.67 (1H, br. t, J 2.1 Hz, H_1), 4.90 - 4.83 (1H, m, H_5), 4.68 (1H, m, from which could be extracted J 48.5 Hz, H_4), 4.57 (1H, m, from which could be extracted J 49.8 Hz, H_2), 3.92 - 3.75 (1H, m, $\text{H}_{6\text{exo}}$), 3.84 (1H, m, from which could be extracted J 26.4, 12.4, 4.2 Hz, H_3), 3.72 (1H, br. dt, J 8.4, 1.1 Hz, $\text{H}_{6\text{endo}}$), 2.73 (1H, dt, J 12.4, 2.3 Hz, OH_3) ppm. **^1H ^{19}F NMR** (500 MHz, CDCl_3) δ 5.67 (1H, d, J 2.6 Hz, H_1), 4.87 (1H, m, from which could be extracted J 5.6, 2.8 Hz, H_5), 4.68 (1H, br. t, J 3.4 Hz, H_4), 4.57 (1H, m, from which could be extracted J 4.1, 2.8, 1.1 Hz, H_2), 3.84 (1H, m, from which could be extracted J 12.1, 4.1 Hz, H_3), 3.83 (1H, m, from which could be extracted J 8.6, 5.6 Hz, $\text{H}_{6\text{exo}}$), 3.72 (1H, dd, J 8.4, 1.0 Hz, $\text{H}_{6\text{endo}}$), 2.73 (1H, d, J 12.4 Hz, OH_3) ppm. **^{13}C NMR** (101 MHz, CDCl_3) δ 98.5 (1C, d, J 24.2 Hz, C_1), 88.0 (1C, d, J 184.9 Hz, C_2), 86.5 (1C, d, J 184.9 Hz, C_4), 73.6 (1C, d, J 19.1 Hz, C_5), 63.7 (1C, d, J 6.6 Hz, C_6), 62.8 (1C, t, J 18.3 Hz, C_3) ppm. **^{19}F NMR** (471 MHz, CDCl_3) δ -204.8 (1F, m, from which could be extracted J 48.4, 27.4, 6.7 Hz, F_4), -207.0 (1F, br. dddt, J 49.9, 25.6, 8.9, 2.3 Hz, F_2) ppm. **^{19}F ^1H NMR** (471 MHz, CDCl_3) δ -204.8 (1F, d, J 9.3 Hz, F_4), -207.0 (1F, d, J 9.3 Hz, F_2) ppm. Product could not be ionised.

Minor isomer: 1,6-Anhydro-2,4-dideoxy-2,4-difluoro- β -D-glucopyranoside (1.32). See 7.2.2 for characterisation data.

7.3.2.3 1,6-Anhydro-2,4-dideoxy-2,4-difluoro-3-O-(trifluoromethanesulfonyl)- β -D-allopyranoside (3.42)

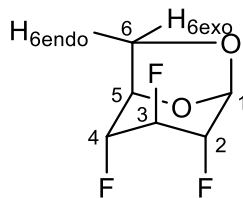


3.42

To a solution of mixture **3.45/1.32** (205 mg, 1.23 mmol, 1 equiv) in dry DCM (3.2 mL) at 0 °C was added pyridine (0.12 mL, 1.48 mmol, 1.2 equiv). Stirring was continued at 0 °C for 10 minutes before Tf₂O (0.21 mL, 1.26 mmol, 1 equiv) was added. The resulting mixture was allowed to warm to rt and stirred for an additional hour before being filtered through a pad of silica. Solvent was removed under vacuum and the resulting orange oil purified by column chromatography (hexane/DCM 80:20 to 60:40) which afforded 218 mg (0.73 mmol, 51%) of compound **3.42** as a white solid. **R_f** 0.24 (pentane/DCM 50:50). **Mp** 108-110 °C (Pentane/DCM). [α]_D -50.2 (c 0.52, CHCl₃, 22 °C). **¹H NMR** (500 MHz, CDCl₃) δ 5.71 (1H, br. t, *J* 2.2 Hz, H₁), 4.95 - 4.91 (1H, m, H₅), 4.90 (1H, tt, *J* 24.3, 3.9 Hz, H₃), 4.87 (1H, m, from which could be extracted *J* 50.9 Hz, H₄), 4.75 (1H, m, from which could be extracted *J* 50.3 Hz, H₂), 3.88 (1H, m, from which could be extracted *J* 8.6, 5.1, 2.2 Hz, H_{6exo}), 3.80 (1H, br. dt, *J* 8.9, 1.0 Hz, H_{6endo}) ppm. **¹H[¹⁹F] NMR** (500 MHz, CDCl₃) δ 5.71 (1H, d, *J* 2.8 Hz, H₁), 4.94 (1H, br. dd, *J* 4.8, 2.7 Hz, H₅), 4.90 (1H, t, *J* 3.8 Hz, H₃), 4.88 - 4.84 (1H, m, H₄), 4.76 (1H, m, from which could be extracted *J* 3.9, 2.6, 1.4 Hz, H₂), 3.88 (1H, dd, *J* 8.8, 5.6 Hz, H_{6exo}), 3.80 (1H, dd, *J* 8.8, 0.9 Hz, H_{6endo}) ppm. **¹³C NMR** (101 MHz, CDCl₃) δ 118.3 (1C, q, *J* 319.1 Hz, -CF₃), 98.4 (1C, d, *J* 23.5 Hz, C₁), 85.6 (1C, d, *J* 195.1 Hz, C₄), 84.3 (1C, d, *J* 197.3 Hz, C₂), 75.7 (1C, t, *J* 16.9 Hz, C₃), 73.9 (1C, d, *J* 19.1 Hz, C₅), 63.7 (1C, d, *J* 5.9 Hz, C₆) ppm. **¹⁹F NMR** (376 MHz, CDCl₃) δ -75.04 (3F, s, -CF₃), -202.1 - -202.5 (1F, m), -204.2 (1F, ddd, *J* 50.3, 24.3, 10.4 Hz) ppm. **¹⁹F[¹H] NMR** (376 MHz, CDCl₃) δ -75.0 (1F, s, -CF₃), -202.3 (1F, d, *J* 10.4 Hz), -204.2 (1F, d, *J* 10.4 Hz) ppm. Product could not be ionised.

7.3.3 Synthesis of trifluoro levoglucosan *via* deoxofluorination of 2,4-dideoxy-2,4-difluoro levoallosan

7.3.3.1 1,6-Anhydro-2,3,4-trideoxy-2,3,4-trifluoro- β -D-glucopyranoside (**3.26**)

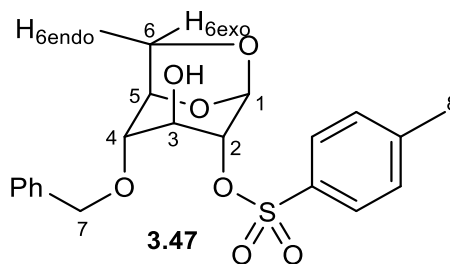


3.26

To a solution of 2,4-difluoro levoallosan **3.45** (335 mg, 2.02 mmol, 1 equiv) in anhydrous THF (5.7 mL) in a sealed tube reactor was added triethylamine (1.62 mL, 11.6 mmol, 5.8 equiv), triethylamine trihydrofluoride (0.63 mL, 3.86 mmol, 1.9 equiv), and NfF (0.65 mL, 3.92 mmol, 1.9 equiv). The resulting mixture was stirred at 90 °C for 4 days before being quenched with sat. aq. NaHCO₃ (17 mL). The layers were separated and the aqueous phase was diluted with water (20 mL) to dissolve the large amount of salts formed over quenching, and extracted with DCM (3x50 mL). Organic phases were combined, dried over MgSO₄, and concentrated under vacuum. Purification by column chromatography (pentane/DCM 90:10 to 50:50) afforded 234 mg (1.39 mmol, 69%) of trifluoro levoglucosan **3.26** as a white solid. **R_f** 0.64 (pentane/ethyl acetate 80:20). **Mp** 66-68 °C (hexane/DCM). **[α]_D** -53.8 (c 1.30, CHCl₃, 24 °C), lit -56.0 (c 1.32, CHCl₃, 22 °C).⁵³ **¹H NMR** (400 MHz, CDCl₃) δ 5.62 (1H, br. s, H₁), 4.85 - 4.78 (1H, m, H₅), 4.83 (1H, dtquin, *J* 42.5, 15.2, 1.7 Hz, H₃), 4.57 (1H, ddd, *J* 44.7, 14.9, 1.2 Hz, H₄), 4.43 (1H, ddd, *J* 45.5, 15.2, 1.2 Hz, H₂), 3.97 (1H, dd, *J* 8.1, 1.0 Hz, H_{6endo}), 3.90 - 3.78 (1H, m, H_{6exo}) ppm. **¹³C NMR** (101 MHz, CDCl₃) δ 98.6 (1C, dd, *J* 28.6, 2.2 Hz, C₁), 87.2 (1C, dt, *J* 178.3, 33.7 Hz, C₃), 86.4 (1C, ddd, *J* 182.7, 31.5, 4.4 Hz, C₄), 84.5 (1C, ddd, *J* 182.7, 27.9, 3.7 Hz, C₂), 73.5 (1C, dd, *J* 21.6, 1.8 Hz, C₅), 64.1 (1C, dd, *J* 9.2, 2.6 Hz, C₆) ppm. **¹⁹F NMR** (376 MHz, CDCl₃) δ ppm -188.0 (1F, ddtd, *J* 44.8, 15.7, 10.9, 4.3 Hz, F₄), -191.1 (1F, dquin, *J* 42.4, 14.1 Hz, F₃), -193.6 (1F, m, from which could be extracted *J* 45.1, 15.6, 12.1, 3.5 Hz, F₂) ppm. **¹⁹F[¹H] NMR** (376 MHz, CDCl₃) δ ppm -188.0 (1F, d, *J* 12.1 Hz, F₄), -191.1 (1F, t, *J* 12.1 Hz, F₃), -193.6 (1F, d, *J* 12.1 Hz, F₂) ppm. Product could not be ionised.

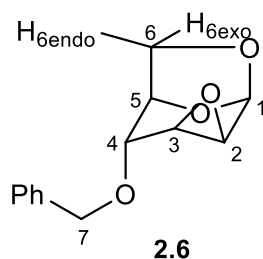
7.3.4 Synthesis of trifluoro levoglucosan *via* the Sarda synthesis

7.3.4.1 1,6-Anhydro-4-*O*-benzyl-2-*O*-*p*-tolylsulfonyl- β -D-glucopyranoside (**3.47**)

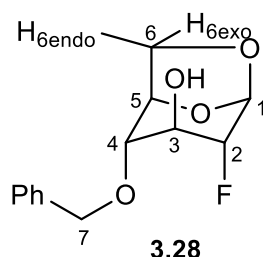


Following the same procedure as described in **7.3.1.1**, levoglucosan **3.27** (20.0 g, 123 mmol) was converted into crude tosyl epoxide **3.34** (26.5 g, \approx 89.0 mmol,) which was converted into compound **3.47** as described below.

To a solution of crude tosyl epoxide **3.34** (26.5 g, \approx 89.0 mmol, 1 equiv) in dry toluene (150 mL) was added benzyl alcohol (28 mL, 270 mmol, 3 equiv) followed by $\text{BF}_3 \cdot \text{OEt}_2$ (2.3 mL, 18.1 mmol, 0.2 equiv). The resulting mixture was stirred overnight at 50 °C before being cooled down to rt and washed with sat. aq. NaHCO_3 (2x150 mL), and water (2x150 mL). The organic layer was then dried over MgSO_4 and the solvent removed under vacuum to afford crude **3.47** as a sticky white solid. Repeated washing of the crude product with diethyl ether followed by filtration enabled to remove the leftover of unreacted benzyl alcohol and afforded 21.5 g (52.9 mmol, 43% over 3 steps) of pure **3.47** as a white solid. **Rf** 0.33 (petroleum ether/acetone 60:40). **Mp** 122-124 °C (Hex/Acetone), lit 124-125 °C (no solvent given).¹²⁵ $[\alpha]_D$ -20.6 (c 2.09, CHCl_3 , 20°C), lit -19 (c 2.09, CHCl_3 , 22°C).¹²⁵ **IR** (neat) 3503 (w), 2970 (w), 1597 (w), 1212 (m), 1007 (s) cm^{-1} . **^1H NMR** (500 MHz, CDCl_3) δ 7.86 - 7.81 (2H, m, from which could be extracted J 8.3 Hz, H_{Ar}), 7.41 - 7.28 (7H, m, H_{Ar}), 5.34 (1H, br. s, H_1), 4.70 (1H, d, J 12.2 Hz, H_7), 4.62 (1H, d, J 12.1 Hz, H_7), 4.58 (1H, br. dd, J 5.3, 0.9 Hz, H_5), 4.22 (1H, br. d, J 3.7 Hz, H_2), 3.98 (1H, dtt, J 5.2, 4.0, 1.0 Hz, H_3), 3.85 (1H, br. d, J 7.5 Hz, $\text{H}_{6\text{endo}}$), 3.64 (1H, dd, J 7.5, 5.3 Hz, $\text{H}_{6\text{exo}}$), 3.34 (1H, br. dd, J 4.0, 1.3 Hz, H_4), 2.46 (3H, s, H_8), 2.39 (1H, d, J 5.2 Hz, OH_3) ppm. **^{13}C NMR** (101 MHz, CDCl_3) δ 145.3 (1C, s, C_{Ar}), 137.5 (1C, s, C_{Ar}), 133.1 (1C, s, C_{Ar}), 130.0 (2C, s, C_{Ar}), 128.6 (2C, s, C_{Ar}), 128.0 (3C, s, C_{Ar}), 127.9 (2C, s, C_{Ar}), 99.9 (1C, s, C_1), 79.2 (1C, s, C_2), 78.5 (1C, s, C_4), 75.2 (1C, s, C_5), 71.8 (1C, s, C_8), 70.2 (1C, s, C_3), 66.5 (1C, s, C_6), 21.7 (1C, s, C_7) ppm. NMR data match those previously reported.¹²⁵ **MS** (ESI+) (m/z) 429.3 $[\text{M}+\text{Na}]^+$, 445.3 $[\text{M}+\text{K}]^+$, 835.5 $[2\text{M}+\text{Na}]^+$.

7.3.4.2 1,6:2,3-Dianhydro-4-*O*-benzyl- β -D-mannopyranoside (**2.6**)

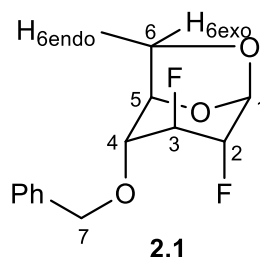
To a solution of compound **3.47** (21.5 g, 52.8 mmol, 1 equiv) in dry DCM (110 mL) at 0 °C was added sodium methoxide (25 wt. % in MeOH, 16 mL, 69.9 mmol, 1.3 equiv). The resulting reaction mixture was allowed to reach rt and stirred for an additional 90 min before being diluted with DCM (100 mL) and washed with water (3x150 mL). The organic layer was then dried over MgSO₄ and the solvent removed under vacuum to afford 12.0 g (51.2 mmol, 97%) of pure **2.6** as a dense clear oil which solidified upon standing. **Rf** 0.57 (petroleum ether/acetone 70:30). **Mp** 60-62 °C (DCM), lit 61-63 °C (petroleum ether/Et₂O).¹²⁶ **[α]_D** -26.6 (c 0.95, CHCl₃, 20 °C), lit -27 (c 0.95, CHCl₃, 20 °C).¹²⁶ **IR** (neat) 3015 (w), 2971 (w), 2900 (w), 2869 (w), 1103 (s), 978 (s) cm⁻¹. **¹H NMR** (500 MHz, CDCl₃) δ 7.43 - 7.30 (5H, m, H_{Ar}), 5.72 (1H, br. dd, *J* 3.2, 0.6 Hz, H₁), 4.75 (2H, s, H₇), 4.52 (1H, m, from which could be extracted *J* 6.5 Hz, H₅), 3.72 (1H, m, from which could be extracted *J* 7.0, 6.3, 0.3 Hz, H_{6exo}), 3.68 (1H, br. ddd, *J* 7.7, 2.1, 0.5 Hz, H_{6endo}), 3.67 (1H, m, H₄), 3.46 (1H, ddd, *J* 3.8, 3.1, 0.8 Hz, H₂), 3.20 (1H, br. ddd, *J* 3.8, 1.6, 0.7 Hz, H₃) ppm. **¹³C NMR** (101 MHz, CDCl₃) δ 137.3 (1C, s, C_{Ar}), 128.7 (2C, s, C_{Ar}), 128.2 (1C, s, C_{Ar}), 127.9 (2C, s, C_{Ar}), 97.6 (1C, s, C₁), 73.8 (1C, s, C₄), 72.2 (1C, s, C₇), 71.6 (1C, s, C₅), 65.8 (1C, s, C₆), 54.4 (1C, s, C₂), 47.8 (1C, s, C₃) ppm. NMR data match those previously reported.¹²⁷ **MS** (CI) (*m/z*) 252.1 [M+NH₄]⁺.

7.3.4.3 1,6-Anhydro-4-*O*-benzyl-2-deoxy-2-fluoro- β -D-glucopyranoside (**3.28**)

To a solution of epoxide **2.6** (3.00 g, 12.8 mmol, 1 equiv) in anhydrous ethylene glycol (52 mL) was added potassium hydrogen fluoride (13.0 g, 166 mmol, 13 equiv). The resulting mixture was stirred for 2 h at 200 °C before being cooled down to rt and poured into a 5% aq. K₂CO₃ soln. (30 mL). The obtained slurry was extracted with chloroform (5x120 mL) and the combined organic layers dried over MgSO₄ before solvent removal under reduced pressure. Purification by column chromatography (DCM/ethyl acetate 90:10 to 80:20) afforded 2.23 g (8.77 mmol, 68%) of pure **3.28**.

as a white solid. **Rf** 0.27 (CHCl₃/acetone 95:05). **Mp** 62-64 °C (Hexane/DCM), lit 129-130 °C (no solvent given).⁵⁰ **[α]_D** -46.0 (c 1.00, CHCl₃, 22 °C), lit -72 (c 0.80, water, 20 °C).⁵⁰ **IR** (neat) 3436 (w, br.), 3035 (w), 2997 (w), 2976 (w), 2915 (w), 1011 (s) cm⁻¹. **¹H NMR** (400 MHz, CDCl₃) δ 7.42 - 7.29 (5H, m, H_{Ar}), 5.55 (1H, br. d, *J* 5.4 Hz, H₁), 4.73 (1H, d, *J* 12.3 Hz, H₇), 4.68 (1H, d, *J* 12.3 Hz, H₇), 4.62 (1H, br. dd, *J* 5.4, 1.0 Hz, H₅), 4.27 (1H, br. dd, *J* 47.2, 3.2 Hz, H₂), 4.00 (1H, m, from which could be extracted *J* 19.7 Hz, H₃), 3.88 (1H, br. dd, *J* 7.4, 0.7 Hz, H_{6endo}), 3.69 (1H, br. dd, *J* 7.2, 5.5 Hz, H_{6exo}), 3.35 (1H, br. d, *J* 3.6 Hz, H₄), 2.28 (1H, d, *J* 5.4 Hz, OH₃) ppm. **¹³C NMR** (101 MHz, CDCl₃) δ 137.5 (1C, s, C_{Ar}), 128.6 (2C, s, C_{Ar}), 128.1 (1C, s, C_{Ar}), 127.9 (2C, s, C_{Ar}), 99.6 (1C, d, *J* 30.1 Hz, C₁), 89.8 (1C, d, *J* 183.4 Hz, C₂), 78.2 (1C, d, *J* 6.6 Hz, C₄), 75.1 (1C, s, C₅), 71.8 (1C, s, C₇), 70.1 (1C, d, *J* 25.7 Hz, C₃), 66.3 (1C, s, C₆) ppm. **¹⁹F NMR** (376 MHz, CDCl₃) δ -187.8 (1F, ddd, *J* 46.8, 19.5, 5.2 Hz, F₂) ppm. **¹⁹F[¹H] NMR** (376 MHz, CDCl₃) δ -187.8 (1F, s, F₂) ppm. NMR data match those previously reported.⁴³ **MS** (ESI+) (m/z) 277.2 [M+Na]⁺. **HRMS** (ESI+) for C₁₃H₁₅FO₄ [M+Na]⁺ calcd. 277.0852, found. 277.0847.

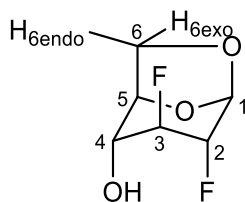
7.3.4.4 1,6-Anhydro-4-*O*-benzyl-2,3-dideoxy-2,3-difluoro-β-D-glucopyranoside (**2.1**)



To a solution of compound **3.28** (2.84 g, 11.1 mmol, 1 equiv) in dry DCM (53 mL) at 0 °C was added DAST (6.1 mL, 49.8 mmol, 4.5 equiv) dropwise. The resulting mixture was stirred at rt under argon for 19 h. Reaction mixture was quenched by adding MeOH (6.5 mL) carefully at 0 °C. The solvent was evaporated and the sample dried under high vacuum to give a brown oil as crude mixture. Purification by column chromatography (pentane/DCM 70:30 to 40:60) afforded 2.22 g (8.67 mmol, 78%) of pure **2.1** as a yellowish oil. **Rf** (petroleum ether/acetone 70:30). **[α]_D** -34.9 (c 2.85, CHCl₃, 20 °C), lit -36 (c 2.85, CHCl₃, 22 °C).⁵³ **IR** (neat) 2963 (w, br.), 2906 (w, br.), 1096 (m), 1014 (s) cm⁻¹. **¹H NMR** (400 MHz, CDCl₃) δ 7.45 - 7.29 (5H, m, H_{Ar}), 5.58 (1H, br. d, *J* 2.9 Hz, H₁), 4.78 (1H, d, *J* 12.2 Hz, H₇), 4.76 (1H, ddquin, *J* 44.3, 15.9, 1.8 Hz, H₃), 4.68 (1H, d, *J* 12.2 Hz, H₇), 4.66 (1H, m, H₅), 4.42 (1H, br. dd, *J* 45.7, 15.6 Hz, H₂), 3.87 (1H, br. d, *J* 7.6 Hz, H_{6endo}), 3.76 (1H, m, from which could be extracted *J* 7.2, 6.0 Hz, H_{6exo}), 3.49 (1H, br. d, *J* 16.9 Hz, H₄) ppm. **¹³C NMR** (101 MHz, CDCl₃) δ 137.0 (1C, s, C_{Ar}), 128.7 (2C, s, C_{Ar}), 128.2 (1C, s, C_{Ar}), 127.9 (2C, s, C_{Ar}), 98.7 (1C, dd, *J* 29.3, 2.2 Hz, C₁), 88.5 (1C, dd, *J* 179.7, 30.8 Hz, C₃), 85.9 (1C, dd, *J* 182.7, 27.1 Hz, C₂), 74.8 (1C, dd, *J* 26.0, 4.8 Hz, C₄), 74.3 (1C, d, *J* 2.9 Hz, C₅), 71.7 (1C, s, C₇), 65.5 (1C, d, *J* 2.9 Hz, C₆) ppm. **¹⁹F NMR** (376 MHz, CDCl₃) δ -187.2 (1F, m, from which could be extracted *J* 45.1, 15.0, 12.8 Hz, F₃), -192.4 (1F, m, from which could be extracted *J* 45.1, 15.8, 12.8, 3.5 Hz, F₂) ppm. **¹⁹F[¹H] NMR** (376 MHz, CDCl₃) δ -187.2 (1F, d, *J* 12.1

Hz, F₃), -192.4 (1F, d, *J* 12.1 Hz, F₂) ppm. NMR data match those previously reported.⁴³ **MS** (EI) (*m/z*) 256.1 [M]⁺.

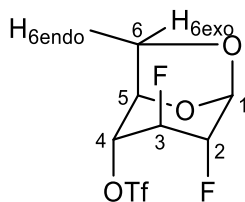
7.3.4.5 1,6-Anhydro-2,3-dideoxy-2,3-difluoro-β-D-glucopyranoside (**1.27**)



1.27

Following the same procedure as described in **7.2.3** using MeOH as solvent, compound **2.1** (2.22 g, 8.66 mmol) was converted into the 2,3-difluoro levoglucosan **1.27** (1.43 g, 8.59 mmol, 99%), obtained as a white solid. **Rf** 0.11 (petroleum ether/acetone 60:40). **¹H NMR** (400 MHz, CDCl₃) δ 5.57 (1H, br. d, *J* 1.7 Hz, H₁), 4.70 (1H, ddquin, *J* 43.0, 12.5, 1.7 Hz, H₃), 4.63 (1H, m, H₅), 4.43 (1H, br. ddd, *J* 44.3, 12.5, 1.5 Hz, H₂), 4.08 (1H, br. d, *J* 7.6 Hz, H_{6endo}), 3.85 (1H, m, from which could be extracted *J* 7.6, 6.1 Hz, H_{6exo}), 3.78 (1H, br. t, *J* 12.5 Hz, H₄), 2.65 (1H, d, *J* 11.2 Hz, OH₄) ppm. **¹⁹F NMR** (376 MHz, CDCl₃) δ -187.6 (1F, dq, *J* 42.9, 13.4 Hz), -193.9 (1F, dt, *J* 44.6, 13.2 Hz) ppm. **¹⁹F[¹H] NMR** (376 MHz, CDCl₃) δ -187.6 (1F, d, *J* 15.6 Hz), -193.9 (1F, d, *J* 13.9 Hz) ppm. See **7.2.2** for the full characterisation data.

7.3.4.6 1,6-Anhydro-2,3-dideoxy-2,3-difluoro-4-O-(trifluoromethanesulfonyl)-β-D-glucopyranoside (**3.48**)

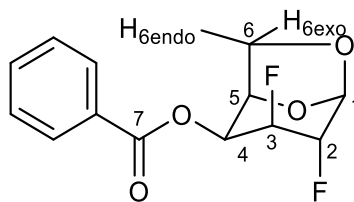


3.48

To a solution of 2,3-difluoro levoglucosan **1.27** (1.43 g, 8.59 mmol, 1 equiv) in dry DCM (22 mL) at 0 °C was added dry pyridine (0.74 mL, 9.15 mmol, 1.1 equiv), followed by triflic anhydride (1.42 mL, 8.56 mmol, 1 equiv). The resulting mixture was stirred for 3 h at rt before being filtered through a pad of silica and the solvent removed under vacuum to afford 2.44 g (8.20 mmol, 95%) of pure **3.48** as a white solid. **Rf** 0.56 (petroleum ether/ ethyl acetate 80:20). **Mp** 56-58 °C (CHCl₃). **[α]_D** -67.3 (c 1.00, CHCl₃, 22 °C). **IR** (neat) 1414 (s), 1202 (s), 1139 (s), 945 (s, br.) cm⁻¹. **¹H NMR** (400 MHz, CDCl₃) δ 5.65 (1H, br. d, *J* 2.0 Hz, H₁), 4.86 (1H, ddquin, *J* 43.6, 14.7, 1.7 Hz, H₃), 4.85 (1H, m, H₄), 4.83 (1H, m, H₅), 4.47 (1H, br. dd, *J* 45.2, 14.4 Hz, H₂), 4.06 (1H, d, *J* 8.3 Hz, H_{6endo}), 3.90 (1H, br. dd, *J* 7.9, 6.2

Hz, H_{6exo}) ppm. **¹³C NMR** (101 MHz, CDCl₃) δ 118.4 (1C, q, *J* 319.6 Hz, CF₃), 98.8 (1C, dd, *J* 28.6, 2.2 Hz, C₁), 87.2 (1C, dd, *J* 183.4, 33.7 Hz, C₃), 84.2 (1C, dd, *J* 184.9, 27.1 Hz, C₂), 80.3 (1C, dd, *J* 31.5, 5.1 Hz, C₄), 73.8 (1C, s, C₅), 65.1 (1C, d, *J* 2.9 Hz, C₆) ppm. **¹⁹F NMR** (376 MHz, CDCl₃) δ -74.8 (3F, s, CF₃), -188.6 (1F, dq, *J* 43.3, 14.4 Hz, F₃), -193.8 (1F, dtd, *J* 45.1, 13.9, 3.5 Hz, F₂) ppm. **¹⁹F[¹H] NMR** (376 MHz, CDCl₃) δ -74.7 (3F, s, CF₃), -188.4 (1F, d, *J* 13.9 Hz, F₃), -193.6 (1F, d, *J* 13.9 Hz, F₂) ppm. **MS** (CI) (*m/z*) 299.1 [M+H]⁺. **HRMS** (CI) for C₇H₈F₅O₅ [M+H]⁺ calcd. 299.0013, found. 298.9985.

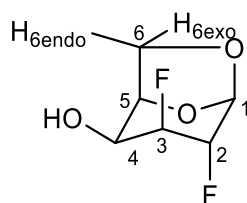
7.3.4.7 1,6-Anhydro-4-*O*-benzoyl-2,3-dideoxy-2,3-difluoro-β-D-galactopyranoside (**3.49**)



3.49

To a solution of compound **3.48** (2.51 g, 8.43 mmol, 1 equiv) in dry DMF (41 mL) was added sodium benzoate (6.13 g, 42.5 mmol, 5 equiv). The resulting mixture was stirred for 16 h at 80 °C before being quenched with water (38 mL) and extracted with ethyl acetate (3x110 mL). The combined organic layer were dried over MgSO₄ and the solvent removed under vacuum. Purification by column chromatography (pentane/ethyl acetate 90:10 to 80:20) afforded 1.94 g (7.17 mmol, 85%) of pure **3.49** as a white solid. **Rf** 0.48 (pentane/ethyl acetate 90:10). **Mp** 82-84 °C (hexane/DCM), lit 89-90 °C (no solvent given).⁵³ [α]_D -32.4 (c 1.72, CHCl₃, 22 °C), lit -31 (c 1.72, CHCl₃, 22 °C).⁵³ **IR** (neat) 2951 (w), 1729 (s), 1249 (s), 1030 (s) cm⁻¹. **¹H NMR** (400 MHz, CDCl₃) δ 8.12 - 8.02 (2H, m, H_{Ar}), 7.67 - 7.58 (1H, m, H_{Ar}), 7.54 - 7.44 (2H, m, H_{Ar}), 5.61 (1H, br. d, *J* 1.2 Hz, H₁), 5.38 (1H, br. dt, *J* 26.2, 4.4 Hz, H₄), 5.14 (1H, dddq, *J* 47.0, 9.3, 4.6, 1.7 Hz, H₃), 4.72 (1H, m, H₅), 4.67 (1H, br. ddt, *J* 44.1, 11.2, 1.7 Hz, H₂), 4.41 (1H, d, *J* 7.6 Hz, H_{6endo}), 3.83 (1H, br. t, *J* 6.4 Hz, H_{6exo}) ppm. **¹³C NMR** (101 MHz, CDCl₃) δ 165.1 (1C, s, C₇), 133.8 (1C, s, C_{Ar}), 129.9 (2C, s, C_{Ar}), 128.9 (1C, s, C_{Ar}), 128.6 (2C, s, C_{Ar}), 98.5 (1C, d, *J* 25.7 Hz, C₁), 86.2 (1C, dd, *J* 182.7, 27.1 Hz, C₂), 85.2 (1C, dd, *J* 184.9, 33.0 Hz, C₃), 71.8 (1C, s, C₅), 66.1 (1C, d, *J* 16.1 Hz, C₄), 64.6 (1C, d, *J* 3.7 Hz, C₆) ppm. **¹⁹F NMR** (376 MHz, CDCl₃) δ -194.9 (1F, ddd, *J* 43.8, 15.2, 8.7 Hz), -205.9 (1F, m, from which could be extracted *J* 46.8, 26.0, 15.6, 10.4 Hz) ppm. **¹⁹F[¹H] NMR** (376 MHz, CDCl₃) δ -194.9 (1F, d, *J* 15.6 Hz), -205.9 (1F, d, *J* 15.0 Hz) ppm. **MS** (ESI⁺) (*m/z*) 271.1 [M+H]⁺. **HRMS** (ESI⁺) for C₁₃H₁₃F₂O₄ [M+H]⁺ Calcd. 271.0782, Found. 271.0779.

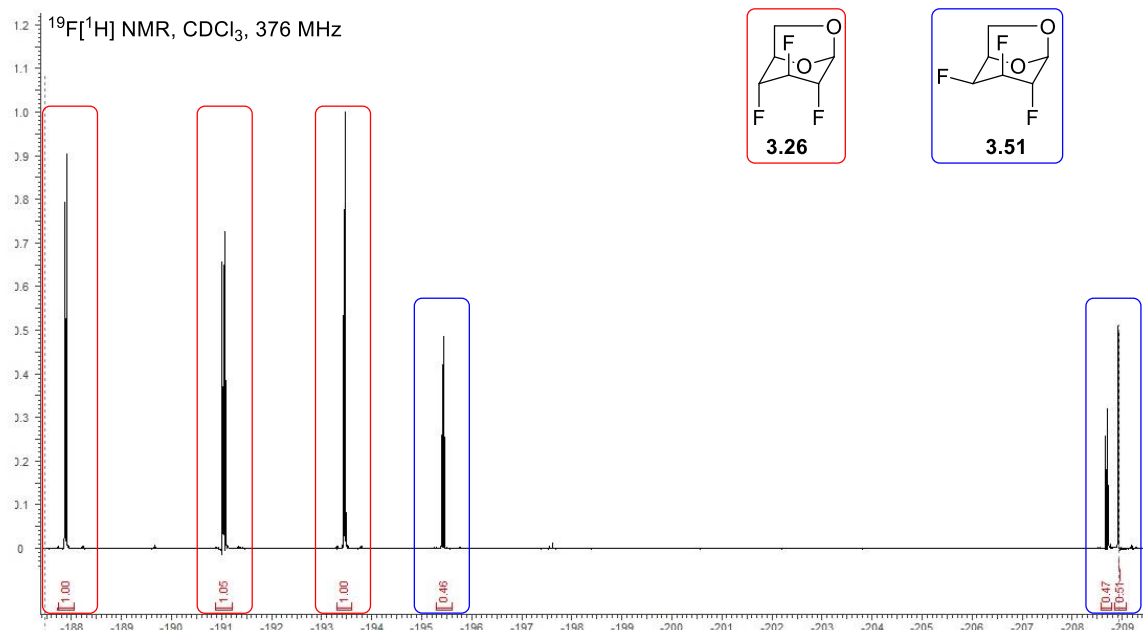
7.3.4.8 1,6-Anhydro-2,3-dideoxy-2,3-difluoro- β -D-galactopyranoside (**3.50**)

**3.50**

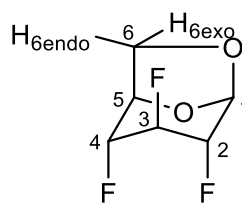
To a solution of compound **3.49** (1.89 g, 6.99 mmol, 1 equiv) in dry MeOH (12 mL) was added K_2CO_3 (136 mg, 0.98 mmol, 0.14 equiv). The resulting mixture was stirred at rt for 1.5 h before being concentrated under vacuum. Purification by column chromatography (pentane/Et₂O 80:20 to 50:50) afforded 1.09 g (6.57 mmol, 94%) of pure 2,4-difluoro levogalactosan **3.50** as a white solid. **Rf** 0.37 (pentane/Et₂O 50:50). **Mp** 125-127 °C (Hex/Et₂O), lit 117-119 °C (no solvent given).⁵³ **[α]_D** -40.1 (c 1.05, CHCl₃, 22 °C), lit -39 (c 1.05, CHCl₃, 22 °C).⁵³ **IR** (neat) 3537 (w), 2909 (w), 1598 (w), 1357 (m), 1172 (s) cm⁻¹. **¹H NMR** (400 MHz, CDCl₃) δ 5.52 (1H, br. d, *J* 1.5 Hz, H₁), 4.89 (1H, dddq, *J* 47.2, 9.3, 4.6, 1.5 Hz, H₃), 4.63 (1H, br. ddt, *J* 44.3, 11.3, 1.7 Hz, H₂), 4.53 (1H, br. t, *J* 4.8 Hz, H₅), 4.15 (1H, d, *J* 8.1 Hz, H_{6endo}), 4.14 (1H, br. ddt, *J* 26.4, 9.3, 4.4 Hz, H₄), 3.74 (1H, m, from which could be extracted *J* 6.8 Hz, H_{6exo}), 2.34 (1H, dd, *J* 9.4, 4.3 Hz, OH₄) ppm. **¹³C NMR** (101 MHz, CDCl₃) δ 98.0 (1C, d, *J* 25.7 Hz, C₁), 87.3 (1C, dd, *J* 177.5, 33.0 Hz, C₃), 86.0 (1C, dd, *J* 181.9, 27.9 Hz, C₂), 73.9 (1C, s, C₅), 64.7 (1C, d, *J* 18.3 Hz, C₄), 63.5 (1C, d, *J* 3.7 Hz, C₆) ppm. **¹⁹F NMR** (376 MHz, CDCl₃) δ -195.2 (1F, m, from which could be extracted *J* 43.3, 13.9, 10.4 Hz), -208.6 (1F, m, from which could be extracted *J* 46.8, 26.0, 14.0, 10.4, 3.5 Hz) ppm. **¹⁹F[¹H] NMR** (376 MHz, CDCl₃) δ -195.2 (1F, d, *J* 13.9 Hz), -208.6 (1F, d, *J* 13.9 Hz) ppm. **MS** (CI) (*m/z*) 166.1 [M]⁺⁺.

7.3.4.9 Deoxofluorination of 1,6-Anhydro-2,3-dideoxy-2,3-difluoro- β -D-galactopyranoside (**3.50**)

To a solution of 2,4-difluoro levogalactosan **3.50** (100 mg, 0.60 mmol, 1 equiv) in dry DCM (2.3 mL) at 0 °C was added DAST (0.24 mL, 1.96 mmol, 3.3 equiv) dropwise. The resulting mixture was stirred at rt under argon for 24 h until TLC indicated completion of the reaction. Reaction mixture was quenched by adding sat. aq. NaHCO₃ (5 mL) carefully at 0 °C and the resulting aqueous layer extracted with DCM (3x10 mL). The combined organic layers were combined, dried over MgSO₄, filtered, and the solvent slowly evaporated under controlled reduced pressure (600 mBar). Purification by column chromatography (pentane/DCM 80:20 to 50:60) afforded 92 mg (0.50 mmol, 83%) of an inseparable mixture of diastereoisomers **3.26/3.51** (*dr* 69:31).



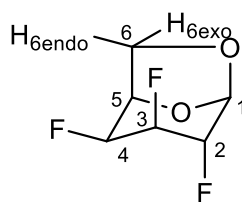
Major isomer: 1,6-anhydro-2,3,4-trideoxy-2,3,4-trifluoro- β -D-glucopyranoside (3.26)



3.26

See **7.3.3.1** for the full characterisation data.

Minor isomer: 1,6-anhydro-2,3,4-trideoxy-2,3,4-trifluoro- β -D-galactopyranoside (3.51)



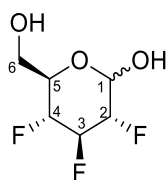
3.51

^{19}F NMR (376 MHz, CDCl_3) δ -195.5 (1F, ddd, J 44.6, 16.0, 8.7 Hz), -208.8 (1F, m, J 46.8, 24.3, 15.6, 12.2, 5.2 Hz), -209.0 (1F, br. d, J 43.4 Hz) ppm. **^{19}F NMR** (376 MHz, CDCl_3) δ -195.5 (1F, d, J 15.6 Hz), -208.8 (1F, dd, J 15.6, 5.2 Hz), -209.0 (1F, d, J 5.2 Hz) ppm.

7.4 Anomeric hydrolysis of the mixture 2,3,4-trideoxy-2,3,4-trifluoro levoglucosan and -galactosan

To a solution of the mixture **3.26/3.51** (89 mg, 0.53 mmol, 1 equiv) in DCM (3.6 mL) at 0 °C was added BCl_3 (1 M in DCM, 2.2 mL, 2.2 mmol, 4.2 equiv) dropwise. The resulting mixture was stirred at rt for 2 h before being quenched with water (5 mL). DCM was then removed under reduced pressure and the resulting aqueous phase was stirred for an additional 1 h at rt. The remaining water was evaporated to give a brown dense oil then purified by column chromatography (pentane/acetone 90:10 to 60:40), which afforded 90 mg (0.48 mmol, 91%) of a complex mixture of **1.37** and **3.56**. *Quasi* complete separation of the two diastereoisomers could be achieved *via* repeated HPLC separations (pentane/acetone 70:30).

Major isomer (83% yield): 2,3,4-trideoxy-2,3,4-trifluoro-D-glucopyranose (**1.37**)



1.37

Rf 0.12 (pentane/ethyl acetate 60:40). **Mp** 98–100 °C (CHCl_3 /Acetone), lit 103–105 °C (CHCl_3).⁴¹ $[\alpha]_D^{25} +28.0$ for α/β 0.30:1.00 (c 0.99, CD_3OD , 21 °C), lit +40.1 for α/β 1:0.98 (c 1.15, THF-*d*8, 22 °C).⁴¹ **IR** (neat) 3367 (m, br.), 3111 (m, br.), 2961 (m), 1032 (s), 995 (s) cm^{-1} .

^1H and ^{19}F NMR in CDCl_3 :

^1H NMR (500 MHz, CDCl_3) δ 5.49 (1H, br. q, J 3.0 Hz, $\text{H}_{1\alpha}$), 5.09 (1H, m, from which could be extracted J 55.0, 16.6, 14.0, 8.4, 7.9 Hz, $\text{H}_{3\alpha}$), 4.92 (1H, br. dd, J 7.6, 3.0 Hz, $\text{H}_{1\beta}$), 4.82 (1H, m, from which could be extracted J 53.1, 16.5, 15.9, 8.3 Hz, $\text{H}_{3\beta}$), 4.66 (1H, m, from which could be extracted J 50.4 Hz, $\text{H}_{4\beta}$), 4.64 (1H, dddd J 50.9, 15.1, 9.9, 8.3 Hz, $\text{H}_{4\alpha}$), 4.53 (1H, dddd, J 49.8, 12.9, 8.9, 3.9 Hz, $\text{H}_{2\alpha}$), 4.35 (1H, m, from which could be extracted J 50.9, 14.5, 8.1, 7.6 Hz, $\text{H}_{2\beta}$), 4.13 (1H, m, from which could be extracted J 9.8, 4.4, 2.5 Hz, $\text{H}_{5\alpha}$), 4.03 – 3.73 (4H, m, $\text{H}_{6\alpha+\beta}$), 3.60 (1H, m, from which could be extracted J 9.9, 6.5, 4.9, 2.2 Hz, $\text{H}_{5\beta}$), 3.34 (1H, br. s, $\text{OH}_{1\alpha}$), 1.84 (1H, br. s, $\text{OH}_{6\alpha}$) ppm. **$^1\text{H}[^{19}\text{F}]$ NMR** (500 MHz, CDCl_3) δ 5.51 (1H, br. d, J 3.6 Hz, $\text{H}_{1\alpha}$), 5.11 (1H, t, J 8.5 Hz, $\text{H}_{3\alpha}$), 4.94 (1H, d, J 7.7 Hz, $\text{H}_{1\beta}$), 4.84 (1H, t, J 8.3 Hz, $\text{H}_{3\beta}$), 4.68 (1H, dd, J 9.8, 8.3 Hz, $\text{H}_{4\beta}$), 4.66 (1H, dd, J 9.3, 8.3 Hz, $\text{H}_{4\alpha}$), 4.55 (1H, dd, J 8.8, 3.8 Hz, $\text{H}_{2\alpha}$), 4.37 (1H, dd, J 8.3, 7.7 Hz, $\text{H}_{2\beta}$), 4.14 (1H, ddd, J 9.9, 4.2, 2.4 Hz, $\text{H}_{5\alpha}$), 4.05 – 3.76 (4H, m, $\text{H}_{6\alpha+\beta}$), 3.62 (1H, ddd, J 9.8, 4.7, 2.4 Hz, $\text{H}_{5\beta}$), 3.36 (1H, br. s, $\text{OH}_{1\alpha}$), 1.86 (1H, br. s, $\text{OH}_{6\alpha}$) ppm. **^{19}F NMR** (471 MHz, CDCl_3) δ -195.3 (1F, m, from which could be extracted J 53.2, 13.6 Hz, $\text{F}_{3\beta}$), -199.4 (1F, m, from which could be extracted J 50.9, 14.4 Hz, $\text{F}_{2\alpha}$ or $\text{F}_{4\alpha}$), -200.0 (1F, dddt, J 50.9, 15.9, 13.0, 2.9 Hz, $\text{F}_{2\beta}$ or $\text{F}_{4\beta}$), -200.8 (1F, m, from which could be extracted J 50.7, 14.5 Hz, $\text{F}_{2\beta}$ or

$F_{4\beta}$), -201.2 (1F, m, from which could be extracted J 54.9, 13.5 Hz, $F_{3\alpha}$), -201.5 (1F, dtd, J 49.9, 13.6, 2.0 Hz, $F_{2\alpha}$ or $F_{4\alpha}$) ppm. **$^{19}\text{F}[^1\text{H}]$ NMR** (471 MHz, CDCl_3) δ -195.3 (1F, t, J 12.9 Hz, $F_{3\beta}$), -199.4 (1F, dd, J 12.9, 2.1 Hz, $F_{2\alpha}$ or $F_{4\alpha}$), -200.0 (1F, dd, J 13.6, 2.9 Hz, $F_{2\beta}$ or $F_{4\beta}$), -200.8 (1F, dd, J 12.5, 2.5 Hz, $F_{2\beta}$ or $F_{4\beta}$), -201.1 (1F, t, J 12.9 Hz, $F_{2\alpha}$ or $F_{4\alpha}$), -201.5 (1F, dd, J 12.9, 2.1 Hz, $F_{2\alpha}$ or $F_{4\alpha}$) ppm.

^1H and ^{19}F NMR in acetone- d_6 :

^1H NMR (500 MHz, acetone- d_6) δ 6.52 (1H, br. d, J 6.3 Hz, $\text{OH}_{1\beta}$), 6.35 (1H, br. d, J 4.6 Hz, $\text{OH}_{1\alpha}$), 5.44 (1H, quin, J 3.5 Hz, $\text{H}_{1\alpha}$), 5.01 (1H, m, from which could be extracted J 56.0, 17.1, 13.7, 8.7, 8.3 Hz, $\text{H}_{3\alpha}$), 4.99 - 4.94 (1H, m, $\text{H}_{1\beta}$), 4.98 (1H, dddt, J 54.6, 16.8, 15.9, 8.3, Hz, $\text{H}_{3\beta}$), 4.68 (1H, br. dddd, J 51.4, 16.4, 9.8, 8.2 Hz, $\text{H}_{4\alpha}$), 4.68 (1H, dddd, J 51.3, 14.8, 9.6, 8.3 Hz, $\text{H}_{4\beta}$), 4.57 (1H, dddd, J 50.8, 13.1, 9.0, 3.8 Hz, $\text{H}_{2\alpha}$), 4.28 (1H, ddt, J 51.6, 15.1, 8.2 Hz, $\text{H}_{2\beta}$), 4.05 - 3.97 (2H, m, $\text{H}_{5\alpha}$ and $\text{OH}_{6\beta}$), 3.90 (1H, br. t, J 6.6 Hz, $\text{OH}_{6\alpha}$), 3.87 - 3.63 (5H, m, $\text{H}_{6\alpha+\beta}$ and $\text{H}_{5\beta}$) ppm. **$^1\text{H}[^{19}\text{F}]$ NMR** (500 MHz, acetone- d_6) δ 6.52 (1H, br. d, J 6.4 Hz, $\text{OH}_{1\beta}$), 6.35 (1H, br. d, J 4.5 Hz, $\text{OH}_{1\alpha}$), 5.44 (1H, t, J 4.1 Hz, $\text{H}_{1\alpha}$), 5.01 (1H, t, J 8.5 Hz, $\text{H}_{3\alpha}$), 4.98 (1H, t, J 8.3 Hz, $\text{H}_{3\beta}$), 4.96 (1H, dd, J 8.3, 6.4 Hz, $\text{H}_{1\beta}$), 4.68 (1H, m, from which could be extracted J 9.6, 8.3 Hz, $\text{H}_{4\alpha}$), 4.68 (1H, dd, J 9.5, 8.4 Hz, $\text{H}_{4\beta}$), 4.56 (1H, dd, J 9.0, 3.8 Hz, $\text{H}_{2\alpha}$), 4.28 (1H, dd, J 8.4, 7.8 Hz, $\text{H}_{2\beta}$), 4.06 - 3.97 (1H, m, $\text{OH}_{6\beta}$), 4.02 (1H, m, from which could be extracted J 9.8, 3.8, 2.1, 0.5 Hz, $\text{H}_{5\alpha}$), 3.89 (1H, br. t, J 6.0 Hz, $\text{OH}_{6\alpha}$), 3.86 - 3.64 (5H, m, $\text{H}_{6\alpha+\beta}$ and $\text{H}_{5\beta}$) ppm. **^{19}F NMR** (471 MHz, acetone- d_6) δ -196.1 (1F, dquin, J 54.6, 13.9 Hz, $F_{3\beta}$), -199.9 (1F, m, from which could be extracted J 51.4, 14.7 Hz, $F_{2\alpha}$ or $F_{4\alpha}$), -200.5 (1F, dddt, J 51.6, 15.9, 13.1, 2.9 Hz, $F_{2\beta}$ or $F_{4\beta}$), -201.5 - -201.8 (2F, m, $F_{3\alpha}$ and $F_{2\beta}$ or $F_{4\beta}$), -202.0 (1F, dtd, J 50.2, 13.0, 2.0 Hz, $F_{2\alpha}$ or $F_{4\alpha}$) ppm. **$^{19}\text{F}[^1\text{H}]$ NMR** (471 MHz, acetone- d_6) δ -196.1 (1F, t, J 12.9 Hz, $F_{3\beta}$), -199.9 (1F, dd, J 12.9, 2.1 Hz, $F_{2\alpha}$ or $F_{4\alpha}$), -200.5 (1F, dd, J 12.9, 2.9 Hz, $F_{2\beta}$ or $F_{4\beta}$), -201.7 (1F, t, J 12.9 Hz, $F_{3\alpha}$), -201.7 (1F, dd, J 12.1, 2.9 Hz, $F_{2\beta}$ or $F_{4\beta}$), -202.0 (1F, dd, J 12.9, 2.1 Hz, $F_{2\alpha}$ or $F_{4\alpha}$) ppm.

^1H and ^{19}F NMR in CD_3OD :

^1H NMR (500 MHz, CD_3OD) δ 5.35 (1H, q, J 3.5 Hz, $\text{H}_{1\alpha}$), 4.98 (1H, dddt, J 56.0, 17.0, 13.8, 8.6 Hz, $\text{H}_{3\alpha}$), 4.90 (1H, m, from which could be extracted J 54.3, 16.8, 15.9, 8.4 Hz, $\text{H}_{3\beta}$), 4.84 (1H, dd, J 7.7, 2.8 Hz, $\text{H}_{1\beta}$), 4.60 (1H, dddd, J 51.3, 17.8, 10.0, 8.2 Hz, $\text{H}_{4\alpha}$), 4.60 (1H, dddd, J 51.1, 15.9, 9.9, 8.1 Hz, $\text{H}_{4\beta}$), 4.51 (1H, dddd, J 50.4, 13.2, 8.9, 3.8, 0.4 Hz, $\text{H}_{2\alpha}$), 4.23 (1H, ddt, J 51.5, 15.1, 8.3 Hz, $\text{H}_{2\beta}$), 4.01 (1H, m, from which could be extracted J 9.7, 7.1, 4.1, 0.6 Hz, $\text{H}_{5\alpha}$), 3.86 (1H, dq, J 12.4, 2.0 Hz, $\text{H}_{6\beta}$), 3.80 (1H, dq, J 12.4, 2.0 Hz, $\text{H}_{6\alpha}$), 3.75 (1H, ddd, J 12.4, 4.1, 1.8 Hz, $\text{H}_{6\alpha}$), 3.72 (1H, ddd, J 12.4, 4.7, 2.0 Hz, $\text{H}_{6\beta}$), 3.61 (1H, m, from which could be extracted J 9.8, 4.5, 2.1 Hz, $\text{H}_{5\beta}$) ppm. **$^1\text{H}[^{19}\text{F}]$ NMR** (500 MHz, CD_3OD) δ 5.35 (1H, d, J 3.8 Hz, $\text{H}_{1\alpha}$), 4.98 (1H, br. t, J 8.4 Hz, $\text{H}_{3\alpha}$), 4.90 (1H, t, J 8.4 Hz, $\text{H}_{3\beta}$), 4.84 (1H, d, J 7.7 Hz, $\text{H}_{1\beta}$), 4.61 (1H, dd, J 9.8, 8.3 Hz, $\text{H}_{4\beta}$), 4.60 (1H, dd, J 9.9, 8.2 Hz, $\text{H}_{4\alpha}$), 4.51 (1H, dd, J 9.0, 3.8 Hz, $\text{H}_{2\alpha}$), 4.23 (1H, t, J 8.1 Hz, $\text{H}_{2\beta}$), 4.01 (1H, br. ddd, J 9.8, 4.1, 2.3 Hz, $\text{H}_{5\alpha}$), 3.86 (1H, dd, J 12.4, 2.1 Hz, $\text{H}_{6\beta}$), 3.81 (1H, dd, J 12.4, 2.1 Hz, $\text{H}_{6\alpha}$), 3.75 (1H, dd, J 12.4, 4.1 Hz, $\text{H}_{6\alpha}$), 3.72 (1H, m, J 12.4, 4.7 Hz, $\text{H}_{6\beta}$), 3.61 (1H, ddd, J 9.8, 4.7, 2.1 Hz, $\text{H}_{5\beta}$) ppm. **^{19}F NMR** (471 MHz, CD_3OD) δ -

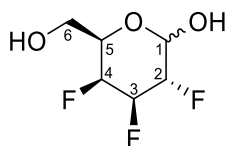
197.1 (1F, m, from which could be extracted J 54.4, 13.6, 1.4 Hz, $F_{3\beta}$), -200.9 (1F, m, from which could be extracted J 51.5, 14.3 Hz, $F_{2\alpha}$ or $F_{4\alpha}$), -201.7 (1F, dddt, J 51.5, 15.7, 12.9, 2.9 Hz, $F_{2\beta}$ or $F_{4\beta}$), -202.6 (2F, m, $F_{3\alpha}$ and $F_{2\beta}$ or $F_{4\beta}$), -203.1 (1F, dtd, J 50.0, 13.6, 2.1 Hz, $F_{2\alpha}$ or $F_{4\alpha}$) ppm. **$^{19}\text{F}[^1\text{H}]$ NMR** (471 MHz, CD_3OD) δ -197.1 (1F, t, J 12.9 Hz, $F_{3\beta}$), -200.9 (1F, dd, J 12.2, 2.1 Hz, $F_{2\alpha}$ or $F_{4\alpha}$), -201.7 (1F, dd, J 12.9, 2.9 Hz, $F_{2\beta}$ or $F_{4\beta}$), -202.6 (1F, dd, J 12.2, 2.9 Hz, $F_{2\beta}$ or $F_{4\beta}$), -202.7 (1F, t, J 12.9 Hz, $F_{3\alpha}$), -203.1 (1F, dd, J 12.9, 2.1 Hz, $F_{2\alpha}$ or $F_{4\alpha}$) ppm.

^{13}C NMR in acetone- d_6 :

^{13}C NMR (101 MHz, acetone- d_6) δ 93.7 (1C, ddd, J 22.7, 10.3, 1.5 Hz, $\text{C}_{1\beta}$), 92.7 (1C, dt, J 185.6, 19.8 Hz, $\text{C}_{3\beta}$), 91.2 (1C, ddd, J 187.8, 17.6, 8.1 Hz, $\text{C}_{2\beta}$), 91.1 (1C, ddd, J 185.6, 20.5, 19.8 Hz, $\text{C}_{3\alpha}$), 90.0 (1C, dd, J 21.3, 10.3 Hz, $\text{C}_{1\alpha}$), 88.0 (1C, ddd, J 189.3, 14.7, 8.1 Hz, $\text{C}_{2\alpha}$), 86.9 (1C, ddd, J 184.1, 17.6, 8.1 Hz, $\text{C}_{4\beta}$), 86.9 (1C, ddd, J 182.7, 18.3, 7.3 Hz, $\text{C}_{4\alpha}$), 72.6 (1C, dd, J 23.5, 5.9 Hz, $\text{C}_{5\beta}$), 68.6 (1C, dd, J 23.5, 5.9 Hz, $\text{C}_{5\alpha}$), 60.0 (1C, s, $\text{C}_{6\beta}$), 59.9 (1C, s, $\text{C}_{6\alpha}$) ppm.

HRMS (ESI-) for $\text{C}_6\text{H}_8\text{F}_3\text{O}_3$ $[\text{M}-\text{H}]^-$ Calcd. 185.0426, Found. 185.0435.

Minor isomer (8% yield): 2,3,4-trideoxy-2,3,4-trifluoro-D-galactopyranose (3.56)



3.56

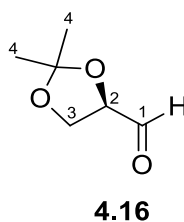
Rf 0.12 (pentane/ethyl acetate 60:40). **Mp** 114-116 °C (CHCl_3 /acetone). $[\alpha]_D^{+25}$ +62.4 for α/β 1.00:0.64 (c 0.21, CD_3OD , 21 °C). **IR** (neat) 3362 (w, br.), 3134 (w, br.), 2961 (w), 1159 (m), 1059 (s) cm^{-1} . **^1H NMR** (500 MHz, acetone- d_6) δ 6.46 (1H, br. d, J 7.2 Hz, $\text{OH}_{1\beta}$), 6.28 (1H, br. d, J 4.5 Hz, $\text{OH}_{1\alpha}$), 5.47 (1H, q, J 4.4 Hz, $\text{H}_{1\alpha}$), 5.18 (1H, m, from which could be extracted J 51.4, 7.6, 3.7, 3.0, 0.7 Hz, $\text{H}_{4\alpha}$), 5.13 - 4.87 (3H, m, $\text{H}_{3\alpha+\beta}$, $\text{H}_{1\beta}$), 5.11 (1H, dddd, J 51.2, 6.7, 3.7, 3.0 Hz, $\text{H}_{4\beta}$), 4.78 (1H, m, from which could be extracted J 51.2, 11.5, 9.6, 3.9, 0.8 Hz, $\text{H}_{2\alpha}$), 4.47 (1H, dddd, J 52.6, 13.2, 9.1, 7.7, 1.2 Hz, $\text{H}_{2\beta}$), 4.20 (1H, dd, J 6.0, 5.2 Hz, $\text{OH}_{6\beta}$), 4.16 (1H, m, from which could be extracted J 29.7, 6.8 Hz, $\text{H}_{5\alpha}$), 4.11 (1H, dd, J 6.5, 5.1 Hz, $\text{OH}_{6\alpha}$), 3.78 (1H, m, from which could be extracted J 27.0, 7.5, 5.4, 1.8 Hz, $\text{H}_{5\beta}$), 3.73 - 3.61 (4H, m, $\text{H}_{6\alpha+\beta}$) ppm. **$^1\text{H}[^{19}\text{F}]$ NMR** (500 MHz, acetone- d_6) δ 6.46 (1H, d, J 7.1 Hz, $\text{OH}_{1\beta}$), 6.28 (1H, br. dd, J 4.5, 0.6 Hz, $\text{OH}_{1\alpha}$), 5.47 (1H, t, J 4.2 Hz, $\text{H}_{1\alpha}$), 5.18 (1H, br. d, J 3.0 Hz, $\text{H}_{4\alpha}$), 5.12 (1H, br. d, J 3.4 Hz, $\text{H}_{4\beta}$), 5.08 (1H, dd, J 9.5, 2.9 Hz, $\text{H}_{3\alpha}$), 4.97 (1H, dd, J 9.2, 3.2 Hz, $\text{H}_{3\beta}$), 4.88 (1H, t, J 7.4 Hz, $\text{H}_{1\beta}$), 4.78 (1H, br. dd, J 9.6, 3.8 Hz, $\text{H}_{2\alpha}$), 4.47 (1H, dd, J 9.2, 7.7 Hz, $\text{H}_{2\beta}$), 4.19 (1H, br. dd, J 6.1, 5.4 Hz, $\text{OH}_{6\beta}$), 4.16 (1H, br. t, J 6.9 Hz, $\text{H}_{5\alpha}$), 4.10 (1H, dd, J 6.4, 5.1 Hz, $\text{OH}_{6\alpha}$), 3.78 (1H, dd, J 7.7, 6.0 Hz, $\text{H}_{5\beta}$), 3.75 - 3.61 (4H, m, $\text{H}_{6\alpha+\beta}$) ppm. **^{13}C NMR** (101 MHz, acetone- d_6) δ 94.1 (1C, dd, J 22.7, 10.3 Hz, $\text{C}_{1\beta}$), 90.9 (1C, dd, J 184.9, 18.3 Hz, $\text{C}_{2\beta}$), 90.5 (1C, dd, J 20.5, 9.5 Hz, $\text{C}_{1\alpha}$), 89.8

(1C, ddd, J 188.5, 19.1, 17.6 Hz, $C_{3\beta}$), 87.9 (1C, ddd, J 181.2, 16.1, 8.8 Hz, $C_{4\alpha}$), 87.4 (1C, ddd, J 187.8, 19.1, 17.6 Hz, $C_{3\alpha}$), 87.1 (1C, ddd, J 181.9, 16.1, 8.8 Hz, $C_{4\beta}$), 87.0 (1C, ddd, J 187.8, 17.6, 2.2 Hz, $C_{2\alpha}$), 72.6 (1C, dd, J 17.6, 5.1 Hz, $C_{5\beta}$), 68.7 (1C, ddd, J 19.1, 3.7, 1.5 Hz, $C_{5\alpha}$), 59.3 – 59.0 (2C, m, $C_{6\alpha+\beta}$) ppm. ^{19}F NMR (471 MHz, acetone- d_6) δ -202.7 (1F, dqd, J 47.7, 14.1, 6.4 Hz, $F_{3\beta}$), -207.7 (1F, dtt, J 52.2, 13.8, 3.6 Hz, $F_{2\beta}$ or $F_{4\beta}$), -208.0 (1F, m, from which could be extracted J 48.6 Hz, $F_{3\alpha}$), -208.7 (1F, dddd, J 51.5, 13.6, 12.2, 3.6 Hz, $F_{2\alpha}$ or $F_{4\alpha}$), -219.7 (1F, m, from which could be extracted J 51.0, 26.5, 15.7 Hz, $F_{2\beta}$ or $F_{4\beta}$), -222.5 (1F, m, from which could be extracted J 52.2, 28.6, 15.1 Hz, $F_{2\alpha}$ or $F_{4\alpha}$) ppm. $^{19}\text{F}[^1\text{H}]$ NMR (471 MHz, acetone- d_6) δ -202.7 (1F, dd, J 15.0, 13.6 Hz, $F_{3\beta}$), -207.7 (1F, d, J 14.3 Hz, $F_{2\beta}$ or $F_{4\beta}$), -208.0 (1F, dd, J 15.0, 13.6 Hz, $F_{3\alpha}$), -208.7 (1F, d, J 13.6 Hz, $F_{2\alpha}$ or $F_{4\alpha}$), -219.7 (1F, d, J 15.0 Hz, $F_{2\beta}$ or $F_{4\beta}$), -222.5 (1F, d, J 15.0 Hz, $F_{2\alpha}$ or $F_{4\alpha}$) ppm. MS (ESI-) (m/z) 231.7 [$\text{M}+\text{HCO}_2$] $^-$.

7.5 Synthesis of 2,3-dideoxy-2,2,3,3-tetrafluoro-D-glucopyranose

7.5.1 The upscaling of Konno's synthesis

7.5.1.1 (2R)-2,3-O-isopropylidene-D-glyceraldehyde (4.16)



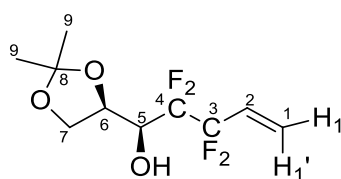
To a solution of D-mannitol (18.1 g, 69.0 mmol, 1 equiv) in DCM (180 mL) was added sat. aq. NaHCO_3 (7.2 mL) followed by NaIO_4 (29.4 g, 138 mmol, 2 equiv) added portionwise over 2-3 minutes. The resulting mixture was stirred for 2 h while the temperature was maintained under 30 °C. MgSO_4 (9.07 g) was then added and the stirring continued for 20 minutes. The reaction mixture was filtered and the resulting cake was rinsed with DCM (50 mL), the filtrate was then concentrated under vacuum. Purification by distillation (27 °C at 6.4 mbar) gave pure **4.16** (10.6 g, 81.1 mmol, 59%) as a translucent oil. ^1H NMR (400 MHz, CDCl_3) δ ppm 9.72 (1H, br. t, J 1.3 Hz, H_1), 4.43 - 4.34 (1H, m, H_2), 4.17 (1H, br. td, J 8.4, 0.9 Hz, H_3), 4.10 (1H, ddd, J 8.8, 4.6, 1.0 Hz, H_3), 1.49 (3H, s, H_4), 1.42 (3H, s, H_4). NMR data match those previously reported.⁷⁸

7.5.1.2 Alkyl lithium mediated coupling between 4-bromo-3,3,4,4-tetrafluoro-but-1-ene (4.16) and D-glyceraldehyde acetonide (3.1)

To a solution of 4-bromo-3,3,4,4-tetrafluoro-but-1-ene **4.16** (1.05 g, 13.5 mmol, 1 equiv) and D-glyceraldehyde acetonide **3.1** (4.22 g, 32.5 mmol, 2.4 equiv) in THF (54 mL) at -78 °C was added

MeLi (1.6 M in Et₂O, 20.3 mL, 32.5 mmol, 2.4 equiv). The resulting mixture was stirred at -78°C for 2 h before being quenched with sat. aq. NH₄Cl (10 mL) and the resulting aqueous layer extracted with ethyl acetate (3x25 mL). Organic layers were combined, dried over MgSO₄, and the solvent removed under reduced pressure. Purification by column chromatography (hexane/ethyl acetate 80:20) afforded 233 mg (0.90 mmol, 7%) of a complex mixture of diastereoisomers **4.17/4.18** (ratio 45:55), entirely resolved after repeated HPLC separations (pentane/Et₂O 80:20).

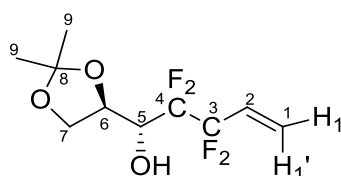
Major isomer (4% yield): (1S)-2,2,3,3-Tetrafluoro-1-[(4R)-2,2-dimethyl-1,3-dioxoran-4-yl]-4-penten-1-ol (4.18)



4.18

R_f 0.38 (hexane/ethyl acetate 80:20). [α]_D +13.0 (c 1.30, CHCl₃, 21 °C), lit +13.7 (c 1.2, CHCl₃, 25 °C).⁷⁷ IR (neat) 3430 (w, br.), 2936 (w), 1374 (m), 1098 (s, br.), 1063 (s, br.) cm⁻¹. ¹H NMR (400 MHz, CDCl₃) δ 6.05 (1H, br. ddt, *J* 17.4, 12.0, 11.6 Hz, H₂), 5.90 (1H, m, from which could be extracted *J* 16.9 Hz, H_{1'}), 5.71 (1H, d, *J* 11.0 Hz, H₁), 4.50-4.37 (2H, m, H₆ and H₅), 4.16-4.01 (2H, m, H₇), 2.44 (1H, br. s, OH), 1.46 (3H, s, H₉), 1.40 (3H, s, H₉) ppm. ¹³C NMR (101 MHz, CDCl₃) δ 126.7 (1C, t, *J* 24.2 Hz, C₂), 123.9 (1C, t, *J* 9.5 Hz, C₁), 118.9 - 114.7 (1C, m, CF₂), 116.6 - 112.2 (1C, m, CF₂), 109.0 (1C, s, C₈), 73.9 (1C, br. d, *J* 2.2 Hz, C₆), 68.7 (1C, dd, *J* 27.1, 22.0 Hz, C₅), 63.9 (1C, dd, *J* 4.8, 1.8 Hz, C₇), 26.2 (1C, s, C₉), 25.3 (1C, s, C₉) ppm. ¹⁹F NMR (376 MHz, CDCl₃) δ -113.8 (1F, dd, *J* 263.6, 12.1 Hz), -115.1 (1F, m, from which could be extracted *J* 263.6, 12.1 Hz), -122.0 (1F, br. d, *J* 275.7 Hz), -126.0 (1F, dd, *J* 277.4, 19.1 Hz) ppm. ¹⁹F[¹H] NMR (376 MHz, CDCl₃) δ -113.8 (1F, d, *J* 265.3 Hz), -115.1 (1F, br. dt, *J* 263.6, 3.5 Hz), -122.0 (1F, br. dd, *J* 275.7, 3.5 Hz), -126.0 (1F, dd, *J* 277.4, 3.5 Hz) ppm. NMR data match those previously reported.⁷⁷ MS (ESI-) (*m/z*) 303.6 [M+HCO₂]⁻.

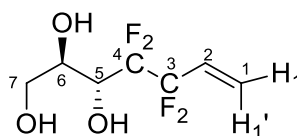
Minor isomer (3% yield): (1R)-2,2,3,3-Tetrafluoro-1-[(4R)-2,2-dimethyl-1,3-dioxoran-4-yl]-4-penten-1-ol (4.17)



4.17

R_f 0.42 (hexane/ethyl acetate 80:20). **[α]_D** -5.2 (c 1.20, CHCl₃, 21 °C), lit -8.5 (c 1.2, CHCl₃, 25 °C).⁷⁷ **IR** (neat) 3461 (w, br.), 2990 (w), 1374 (m), 1095 (s, br.), 1066 (s) cm⁻¹. **¹H NMR** (400 MHz, CDCl₃) δ 6.07 (1H, br. ddt, *J* 17.4, 11.8, 11.6 Hz, H₂), 5.89 (1H, br. dt, *J* 17.4, 2.2 Hz, H_{1'}), 5.69 (1H, d, *J* 11.0 Hz, H₁), 4.46 (1H, m, from which could be extracted *J* 10.3, 6.6 Hz, H₆), 4.16 (1H, dd, *J* 8.6, 6.6 Hz, H₇), 3.97 (1H, ddt, *J* 19.9, 8.1, 4.0 Hz, H₅), 3.89 (1H, t, *J* 7.7 Hz, H₇), 2.83 (1H, d, *J* 8.3 Hz, OH), 1.47 (3H, s, H₉), 1.42 (3H, s, H₉) ppm. **¹³C NMR** (101 MHz, CDCl₃) δ 127.1 (1C, t, *J* 24.2 Hz, C₂), 123.5 (1C, t, *J* 9.9 Hz, C₁), 116.7 (1C, m, *J* 254.6, 58.7, 34.5, 30.8 Hz, CF₂), 114.1 (1C, m, *J* 248.7, 44.0, 34.5, 30.8 Hz, CF₂), 110.3 (1C, s, C₈), 72.4 (1C, br. t, *J* 1.5 Hz, C₆), 68.7 (1C, dd, *J* 29.0, 23.1 Hz, C₅), 66.7 (1C, d, *J* 3.7 Hz, C₇), 26.3 (1C, s, C₉), 25.3 (1C, s, C₉) ppm. **¹⁹F NMR** (376 MHz, CDCl₃) δ -113.8 (1F, dd, *J* 263.6, 12.1 Hz), -115.6 (1F, ddd, *J* 263.6, 13.9, 5.2 Hz), -121.9 (1F, br. dt, *J* 274.8, 4.8 Hz), -128.2 (1F, dd, *J* 275.7, 19.1 Hz) ppm. **¹⁹F[¹H] NMR** (376 MHz, CDCl₃) δ -113.8 (1F, d, *J* 263.6 Hz), -115.6 (1F, dd, *J* 263.6, 5.2 Hz), -121.9 (1F, dd, *J* 275.7, 5.2 Hz), -128.2 (1F, d, *J* 274.0 Hz) ppm. NMR data match those previously reported.⁷⁷ **MS** (ESI-) (*m/z*) 303.7 [M+HCO₂]⁻, 1077.8 [4M+HCO₂]⁻.

7.5.1.3 (2R,3R)-4,4,5,5-tetrafluoro-6-hepten-1,2,3-triol (**4.19**)

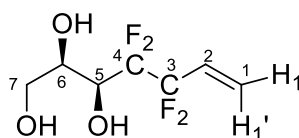


4.19

To a solution of coupling adduct **4.17** (418 mg, 1.62 mmol, 1 equiv) in MeOH (14 mL) at 0 °C was added *p*-toluenesulfonic monohydrate (31 mg, 0.16 mmol, 0.1 equiv). The resulting mixture was stirred at rt for 6 h before being quenched with sat. aq. NaHCO₃ (4 mL) and extracted with ethyl acetate (3x25 mL). Organic layers were combined, dried over MgSO₄, and the solvent removed under reduced pressure. Purification by column chromatography (petroleum ether/acetone 70:30) afforded 208 mg (0.95 mmol, 59%) of pure triol **4.19** as a white solid, the unreacted starting material **4.17** was recovered. **R_f** 0.14 (petroleum ether/acetone 70:30). **Mp** 40-42 °C (hexane/acetone), lit 38-39 °C (no solvent given).⁷⁷ **[α]_D** -19.2 (c 1.20, MeOH, 21 °C), lit -17.5 (c 1.2, MeOH, 25 °C).⁷⁷ **IR** (neat) 3352 (w, br.), 2898 (w), 1522 (m), 1240 (s), 1036 (s) cm⁻¹. **¹H NMR** (400 MHz, CDCl₃) δ 6.07 (1H, br. ddt, *J* 17.4, 12.2, 11.7 Hz, H₂), 5.90 (1H, br. dt, *J* 17.4, 2.2 Hz, H_{1'}), 5.71 (1H, d, *J* 11.0 Hz, H₁), 4.23 (1H, m, from which could be extracted *J* 11.0, 4.9 Hz, H₆), 4.07 (1H, br. dt, *J* 19.8, 7.0 Hz, H₅), 3.84-3.72 (2H, m, H₇), 3.18-3.02 (1H, m, OH), 2.55 (1H, br. s, OH), 2.00 (1H, br. s, OH) ppm. **¹⁹F NMR** (376 MHz, CDCl₃) δ -113.7 (1F, dd, *J* 263.6, 12.1 Hz), -115.2 (1F, br. ddd, *J* 263.6, 12.1, 5.2 Hz), -121.30 (1F, br. dt, *J* 274.0, 5.2 Hz), -127.9 (1F, dd, *J* 274.8, 19.9 Hz) ppm. **¹⁹F[¹H] NMR** (376 MHz,

CDCl_3) δ ppm -113.8 (1F, d, J 263.6 Hz), -115.6 (1F, dd, J 263.6, 5.2 Hz), -121.9 (1F, dd, J 275.7, 5.2 Hz), -128.2 (1F, d, J 274.0 Hz). NMR data match those previously reported.⁷⁷

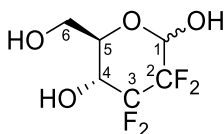
7.5.1.4 (2R,3S)-4,4,5,5-tetrafluoro-6-hepten-1,2,3-triol (**4.20**)



4.20

Following the same procedure as described in **7.5.1.3**, coupling adduct **4.18** (602 mg, 2.33 mmol) was converted into triol **4.20** (230 mg, 1.02 mmol, 44%), obtained pure as a white solid after column chromatography (petroleum ether/acetone 70:30). R_f 0.14 (petroleum ether/acetone 70:30). **Mp** 55-56 °C (hexane/acetone), lit 62-63 °C (no solvent given).⁷⁷ $[\alpha]_D +6.3$ (c 1.10, MeOH, 21 °C), lit +8.1 (c 1.1, MeOH, 25 °C).⁷⁷ **IR** (neat) 3321, (w, br.), 2926 (w, br.), 2902 (w), 1375 (w), 1190 (s), 1021 (s) cm^{-1} . **^1H NMR** (400 MHz, CDCl_3) δ 6.06 (1H, br. ddt, J 17.5, 11.6, 11.5 Hz, H_2), 5.91 (1H, m, from which could be extracted J 17.4 Hz, H_1), 5.73 (1H, d, J 11.0 Hz, H_1), 4.47-4.31 (1H, m, H_6), 4.12-3.87 (3H, m, H_5 and H_7 and H_7), 3.13 (1H, br. d, J 6.1 Hz, OH), 2.84 (1H, br. s, OH), 2.09 (1H, br. s, OH) ppm. **^{19}F NMR** (376 MHz, CDCl_3) δ -113.9 (1F, dd, J 263.6, 10.4 Hz), -115.1 (1F, m, from which could be extracted J 263.6 Hz), -122.9 (1F, br. d, J 275.7 Hz), -126.3 (1F, dd, J 275.7, 17.3 Hz) ppm. **$^{19}\text{F}\{^1\text{H}\}$ NMR** (376 MHz, CDCl_3) δ -113.9 (1F, d, J 263.6 Hz), -115.1 (1F, br. dt, J 263.6, 5.2 Hz), -122.9 (1F, d, J 274.0 Hz), -126.3 (1F, dd, J 275.7, 3.5 Hz) ppm. NMR data match those previously reported.⁷⁷

7.5.1.5 2,3-dideoxy-2,2,3,3-tetrafluoro-D-glucopyranose (**1.40**)

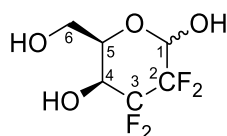


1.40

A mixture of ozone and oxygen was gently bubbled through a stirred solution of triol **4.19** (207 mg, 0.95 mmol) in MeOH (20 mL) at -78 °C until the solution became pale blue (approx. 0.5 h). The excess ozone was purged from the solution by bubbling oxygen through for 5 min. Dimethyl sulfide (2 mL) was added, and the reaction mixture was allowed to warm to room temperature over 30 min. The resulting mixture was concentrated under vacuum. Purification of the residue by column chromatography (petroleum ether/acetone 60:40) gave 170 mg (0.77 mmol, 81%) of tetrafluorinated glucose **1.40** as a dense gel. R_f 0.24 (petroleum ether/acetone 60:40). $[\alpha]_D$: +53.7

for α/β 1.00:0.70 (c 0.90, CD₃OD, 24 °C), lit +30.32 (c 0.94, MeOH, 23 °C).⁶⁸ **IR** (neat) 3497 (m, br.), 3370 (m, br.), 3210 (m, br.), 1207 (m), 1076 (s), 1013 (s) cm⁻¹. **¹H NMR** (400 MHz, D₂O) δ 5.42 (1H, br. dt, *J* 8.1, 2.6 Hz, H_{1 α}), 5.15 (1H, br. d, *J* 15.4 Hz, H_{1 β}), 4.14 - 3.99 (3H, m), 3.95 - 3.75 (4H, m), 3.71 (1H, ddd, *J* 10.0, 4.9, 2.0 Hz, H_{5 β}) ppm. **¹³C NMR** (101 MHz, D₂O) δ 119.2 - 108.0 (4C, m, CF₂), 90.7 (1C, dd, *J* 37.4, 27.4 Hz, C_{1 α}), 90.6 (1C, dd, *J* 26.4, 19.0 Hz, C_{1 β}), 73.8 (1C, br. t, *J* 2.9 Hz, C₅), 69.7 (1C, br. t, *J* 2.9 Hz, C₅), 66.2 (1C, t, *J* 19.1 Hz, C₄), 65.9 (1C, t, *J* 19.1 Hz, C₄), 59.7 (1C, s, C₆), 59.5 (1C, s, C₆) ppm. **¹⁹F NMR** (376 MHz, D₂O) δ -121.2 (1F, m, from which could be extracted *J* 268.8 Hz, F _{α}), -129.9 (2F, m, F _{α}), -132.4 (2F, td, *J* 12.1, 3.5 Hz, F _{β}), -134.4 (1F, dt, *J* 269.2, 13.7 Hz, F _{α}), -136.8 (1F, dt, *J* 258.4, 12.1 Hz, F _{β}), -139.8 (1F, ddq, *J* 258.4, 15.6, 3.5 Hz, F _{β}) ppm. **¹⁹F[¹H] NMR** (376 MHz, D₂O) δ -121.2 (1F, dt, *J* 269.2, 5.0 Hz, F _{α}), -129.9 (2F, dd, *J* 12.1, 5.2 Hz, F _{α}), -132.4 (2F, dd, *J* 12.1, 3.5 Hz, F _{β}), -134.4 (1F, dt, *J* 270.5, 13.9 Hz, F _{α}), -136.8 (1F, dt, *J* 258.4, 13.9 Hz, F _{β}), -139.8 (1F, br. dt, *J* 258.4, 5.2 Hz, F _{β}) ppm. NMR data match those previously reported.⁶⁸ **MS** (ESI-) (m/z) 219.6 (M-H)⁻.

7.5.1.6 2,3-dideoxy-2,2,3,3-tetrafluoro-D-galactopyranose (**4.1**)



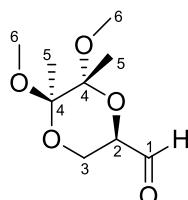
4.1

Following the same procedure as described in **7.5.1.5**, triol **4.20** (261 mg, 1.20 mmol) was converted into tetrafluoro galactose **4.1** (224 mg, 1.02 mmol, 85%), obtained pure as a dense gel after column chromatography (petroleum ether/acetone 60:40). **R_f** 0.24 (petroleum ether/acetone 60:40). **[α]_D** +35.2 for α/β 0.88:1.00 (c 0.90, CD₃OD, 21 °C), lit +31.22 (c 1.06, MeOH, 26 °C).⁶⁸ **IR** (neat) 3330 (m, br.), 1109 (s), 1044 (s, br.), 1003 (s) cm⁻¹. **¹H NMR** (400 MHz, D₂O) δ 5.37 (1H, dd, *J* 9.2, 6.2 Hz, H_{1 α}), 5.06 (1H, dt, *J* 13.6, 3.2 Hz, H_{1 β}), 4.36 (1H, br. t, *J* 5.5 Hz, H_{5 α}), 4.25 - 4.13 (2H, m, H_{4 α + β}), 3.97 - 3.88 (1H, m, H_{5 β}), 3.77 - 3.70 (4H, m, H_{6 α + β}) ppm. **¹³C NMR** (101 MHz, acetone-*d*₆) δ 114.3 (1C, dddd, *J* 269.2, 243.6, 24.9, 21.3 Hz, CF₂), 113.0 (1C, dddd, *J* 265.3, 248.7, 27.1, 20.5 Hz, CF₂), 111.8 (1C, tdd, *J* 260.4, 29.3, 21.3 Hz, CF₂), 110.9 (1C, dddd, *J* 267.0, 248.7, 28.6, 22.0 Hz, CF₂), 92.1 (1C, ddd, *J* 25.7, 22.0, 4.4 Hz, C₁), 91.6 (1C, ddd, *J* 37.4, 25.7, 2.2 Hz, C₁), 74.3 (1C, d, *J* 5.9 Hz, C₅), 69.5-68.4 (2C, m, C₄), 69.1 (1C, d, *J* 5.1 Hz, C₅), 60.0 (1C, d, *J* 2.2 Hz, C₆), 59.9 (1C, d, *J* 2.2 Hz, C₆) ppm. **¹⁹F NMR** (376 MHz, D₂O) δ -118.9 (1F, ddt, *J* 272.2, 17.3, 8.7 Hz, F _{α}), -119.6 (1F, ddt, *J* 270.5, 15.6, 8.7 Hz, F _{α}), -120.9 (1F, m, from which could be extracted *J* 270.5 Hz, F _{β}), -130.3 (1F, m, from which could be extracted *J* 270.5 Hz, F _{α}), -132.6 (1F, dtd, *J* 271.4, 13.9, 5.2 Hz, F _{α}), -134.1 (1F, dddd, *J* 272.2, 15.6, 10.4, 5.2 Hz, F _{β}), -136.7 (1F, dtd, *J* 263.6, 10.7, 5.2 Hz, F _{β}), -137.7 (1F, dtd, *J* 260.1, 15.4, 5.2 Hz, F _{β}) ppm. **¹⁹F[¹H] NMR** (376 MHz, D₂O) δ -118.9 (1F, ddd, *J* 270.5, 17.3, 8.7 Hz, F _{α}), -119.6 (1F, ddd, *J* 270.5, 15.6, 8.7 Hz, F _{α}), -120.9 (1F, ddd, *J* 270.5, 10.4, 5.2 Hz, F _{β}), -130.3 (1F, m, from which could

be extracted J 270.5 Hz, F_α), -132.6 (1F, ddd, J 270.9, 16.0, 11.3 Hz, F_α), -134.1 (1F, m, from which could be extracted J 270.5 Hz, F_β), -136.7 (1F, dt, J 261.8, 11.0 Hz, F_β), -137.7 (1F, ddd, J 260.1, 17.3, 5.2 Hz, F_β) ppm. NMR data match those previously reported.⁶⁸ **MS** (ESI-) (m/z) 219.3 (M-H)⁻.

7.5.2 Modifications of the Konno synthesis

7.5.2.1 (2R,5R,6R)-5,6-dimethoxy-5,6-dimethyl-1,4-dioxane-2-carbaldehyde (**4.24**)



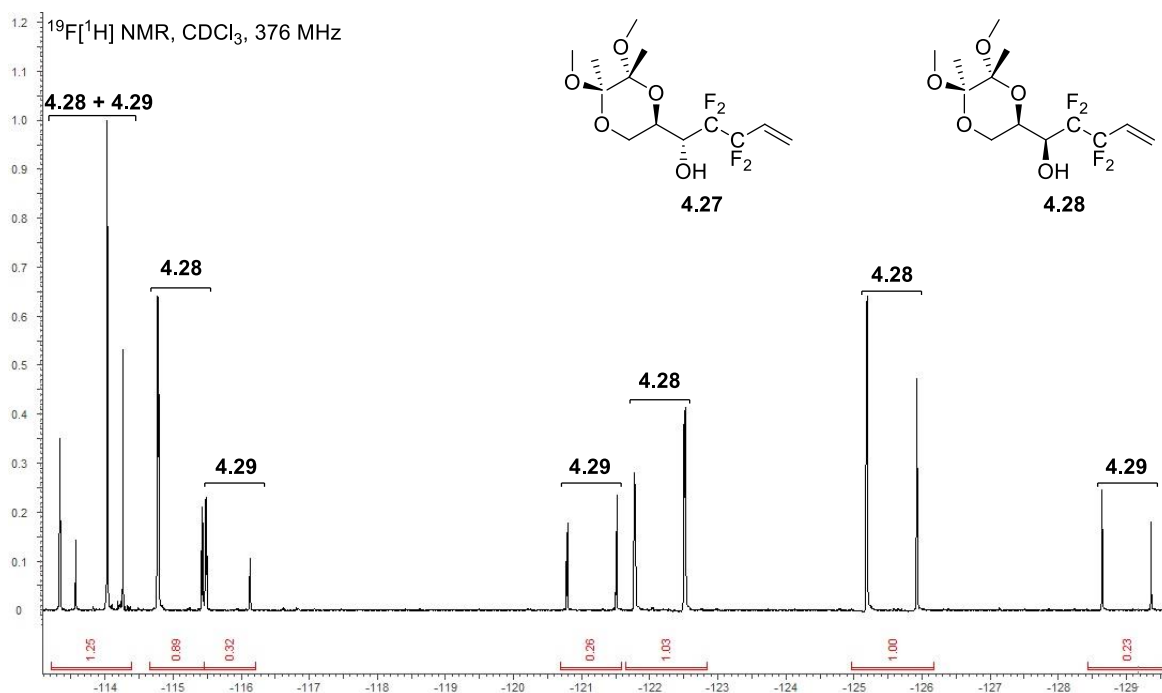
4.24

To a solution of D-mannitol **4.25** (15.5 g, 85.0 mmol, 1 equiv) in dry metanol (75 mL) were added anhydrous trimethyl orthoformate (37.5 mL, 343 mmol, 4 equiv), butane-2,3-dione (15.8 mL, 180 mmol, 2.1 equiv), and boron trifluoride tetrahydrofuran complex (2.5 mL, 22.7 mmol, 0.3 equiv). The resulting mixture was stirred for 4 h at rt before triethylamine (2.5 mL) was added and the solvent removed under vacuum. The residue obtained was dissolved in DCM (300 mL) and washed with aqueous NaCl (75 mL water, 75 mL brine). The organic phase was then dried over $MgSO_4$, and the solvent removed under vacuum to afford crude *syn*-diol **4.26**.

To a solution of crude diol **4.26** in DCM (200 mL) and sat. aq. $NaHCO_3$ (30 mL) was added $NaIO_4$ (25.1 g, 117 mmol, 1.4 equiv) portionwise. The resulting mixture was stirred overnight at rt before $MgSO_4$ (63 g) was added. Stirring was continued for a further 20 minutes and the reaction mixture was filtered over Celite®. The resultant filtrate was stirred with sodium thiosulfate (12 g) for 30 minutes then filtered and the solvent removed under vacuum. Purification by distillation of the residue obtained (60 °C at 0.9 mbar) gave pure **4.24** (11.8 g, 57.9 mmol, 59%) as a translucent oil. **Bp** 60 °C at 0.9 mmHg. $[\alpha]_D^{25}$ -101.5 (c 0.80, $CHCl_3$, 22 °C), lit -101.3 (c 0.80, $CHCl_3$, 25 °C).¹²⁸ **IR** (neat) 2950 (w, br.), 2834 (w), 1733 (m), 1372 (m), 1114 (s, br.), 1033 (s) cm^{-1} . **1H NMR** (400 MHz, $CDCl_3$) δ 9.66 (1H, s, H_1), 4.35 (1H, dd, J 10.0, 5.1 Hz, H_2), 3.77 - 3.65 (2H, m, H_3), 3.33 (3H, s, H_6), 3.27 (3H, s, H_6), 1.39 (3H, s, H_7), 1.31 (3H, s, H_7) ppm. **^{13}C NMR** (101 MHz, $CDCl_3$) δ 200.3 (1C, s, C_1), 99.8 (1C, s, C_4), 98.3 (1C, s, C_4), 72.4 (1C, s, C_2), 58.3 (1C, s, C_3), 48.4 (1C, s, C_6), 48.2 (1C, s, C_6), 17.6 (1C, s, C_5), 17.5 (1C, s, C_5) ppm.

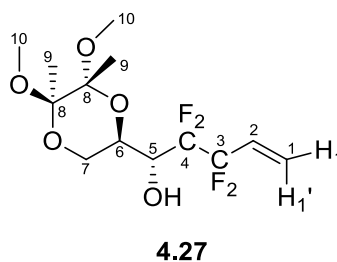
7.5.2.2 Akyllithium mediated coupling between 4-bromo-3,3,4,4-tetrafluoro-but-1-ene (4.16) and Ley's aldehyde (4.24)

To a solution of 4-bromo-3,3,4,4-tetrafluoro-but-1-ene **4.16** (4.18 g, 20.2 mmol, 1 equiv) and Ley's aldehyde **4.24** (5.09 g, 24.9 mmol, 1.2 equiv) in THF (164 mL) at -78 °C was added MeLi (1.6 M in Et₂O, 30 mL, 48.0 mmol, 2.4 equiv). The resulting mixture was stirred at -78 °C for 2 h before being quenched with sat. aq. NH₄Cl (25 mL) and the resulting aqueous layer extracted with ethyl acetate (3x60 mL). Organic layers were combined, dried over MgSO₄, and the solvent removed under reduced pressure. Purification by column chromatography (pentane/ethyl acetate 70:30) afforded 2.25 g (6.77 mmol, 37%) of a complex mixture of coupling adducts **4.27/4.28** (*dr* 81:19), engaged in the next step.



Analytical samples of pure diastereoisomers **4.27** and **4.28** were obtained by HPLC (pentane/ethyl acetate 85:15).

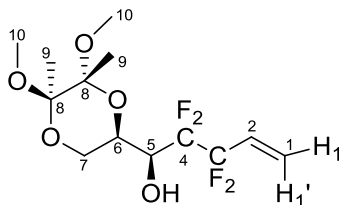
Major isomer: (1R)-1-((2R,5R,6R)-5,6-dimethoxy-5,6-dimethyl-1,4-dioxan-2-yl)-2,2,3,3-tetrafluoropent-4-en-1-ol (**4.27**)



R_f 0.47 (pentane/ethyl acetate 70:30). [α]_D -127.7 (c 1.20, CHCl₃, 21 °C). IR (neat) 3419 (w, br.), 2952 (w), 1376 (w), 1110 (s, br.), 1034 (s) cm⁻¹. ¹H NMR (400 MHz, CDCl₃) δ 6.07 (1H, br. ddt, *J* 17.4, 12.5,

11.2 Hz, H_2), 5.87 (1H, br. dt, J 17.4, 2.0 Hz, $H_{1'}$), 5.67 (1H, d, J 11.0 Hz, H_1), 4.38 (1H, br. ddt, J 11.5, 3.7, 2.2 Hz, H_6), 3.90 (1H, t, J 11.2 Hz, H_7), 3.82 (1H, m, from which could be extracted J 21.0, 9.3 Hz, H_5), 3.45 (1H, dd, J 11.2, 3.4 Hz, H_7), 3.31 (3H, s, H_{10}), 3.27 (3H, s, H_{10}), 3.11 (1H, d, J 9.3 Hz, OH), 1.31 (3H, s, H_9), 1.30 (3H, s, H_9) ppm. ^{13}C NMR (101 MHz, CDCl_3) δ 127.3 (1C, t, J 23.8 Hz, C_2), 123.3 (1C, t, J 9.5 Hz, C_1), 99.6 (1C, s, C_8), 98.0 (1C, s, C_8), 67.8 (1C, dd, J 29.7, 22.4 Hz, C_5), 64.1 (1C, br. s, C_6), 60.0 (1C, d, J 2.2 Hz, C_7), 48.3 (1C, s, C_{10}), 48.1 (1C, s, C_{10}), 17.6 (1C, s, C_9), 17.5 (1C, s, C_9) ppm. ^{19}F NMR (376 MHz, CDCl_3) δ -114.0 (1F, dd, J 261.8, 10.4 Hz), -115.9 (1F, br. ddd, J 261.8, 12.1, 3.5 Hz), -121.3 (1F, br. d, J 272.2 Hz), -129.1 (1F, dd, J 272.2, 20.8 Hz) ppm. $^{19}\text{F}[^1\text{H}]$ NMR (376 MHz, CDCl_3) δ -114.1 (1F, d, J 261.8 Hz), -115.9 (1F, dd, J 263.6, 5.2 Hz), -121.3 (1F, dd, J 272.2, 5.2 Hz), -129.1 (1F, d, J 272.2 Hz) ppm. MS (ESI-) (m/z) 377.8 $[\text{M}+\text{HCO}_2]^-$. HRMS (ESI+) for $\text{C}_{13}\text{H}_{20}\text{F}_4\text{NaO}_5$ $[\text{M}+\text{Na}]^+$ Calcd. 355.1145; Found. 355.1141.

Minor isomer: (1S)-1-((2R,5R,6R)-5,6-dimethoxy-5,6-dimethyl-1,4-dioxan-2-yl)-2,2,3,3-tetrafluoropent-4-en-1-ol (4.28)



4.28

R_f 0.58 (pentane/ethyl acetate 70:30). $[\alpha]_D -136.0$ (c 0.70, CHCl_3 , 21 °C). IR (neat) 3434 (w, br.), 2954 (w), 1380 (m), 1106 (s, br.), 1030 (s) cm^{-1} . ^1H NMR (400 MHz, CDCl_3) δ 6.05 (1H, ddt, J 17.4, 12.0, 11.2 Hz, H_2), 5.89 (1H, m, from which could be extracted J 17.1 Hz, $H_{1'}$), 5.70 (1H, d, J 11.0 Hz, H_1), 4.36-4.23 (2H, m, H_5 and H_6), 3.99 (1H, t, J 11.4 Hz, H_7), 3.62 (1H, m, from which could be extracted J 11.2 Hz, H_7), 3.29 (3H, s, H_{10}), 3.28 (3H, s, H_{10}), 2.59 (1H, br. d, J 3.4 Hz, OH), 1.31 (3H, s, H_9), 1.29 (3H, s, H_9) ppm. ^{13}C NMR (101 MHz, CDCl_3) δ 126.8 (1C, t, J 23.8 Hz, C_2), 123.8 (1C, t, J 9.5 Hz, C_1), 99.7 (1C, s, C_8), 97.8 (1C, s, C_8), 70.0 (1C, dd, J 28.6, 21.3 Hz, C_5), 66.0 (1C, s, C_6), 58.2 (1C, dd, J 5.1, 1.5 Hz, C_7), 48.2 (1C, s, C_{10}), 48.1 (1C, s, C_{10}), 17.6 (1C, s, C_9), 17.5 (1C, s, C_9) ppm. ^{19}F NMR (376 MHz, CDCl_3) δ -113.8 (1F, dd, J 261.8, 12.1 Hz), -115.2 (1F, m, from which could be extracted J 261.8 Hz), -122.2 (1F, br. d, J 275.7 Hz), -125.6 (1F, dd, J 275.7, 20.8 Hz) ppm. $^{19}\text{F}[^1\text{H}]$ NMR (376 MHz, CDCl_3) δ -113.9 (1F, d, J 263.6 Hz), -115.2 (1F, m, from which could be extracted J 263.6, 6.9, 3.5 Hz), -122.2 (1F, m, J 275.7 Hz), -125.6 (1F, dd, J 275.7, 3.5 Hz) ppm. MS (ESI+) (m/z) 355.2 $[\text{M}+\text{Na}]^+$. HRMS (ESI+) for $\text{C}_{13}\text{H}_{20}\text{F}_4\text{NaO}_5$ $[\text{M}+\text{Na}]^+$ Calcd. 355.1145, Found. 355.1141.

7.5.2.3 Deprotection of the coupling adduct mixture 4.27/4.28

To a solution of mixture **4.27/4.28** (4.88 g, 14.7 mmol, 1 equiv) in THF (150 mL) was added HCl aq. (2 M, 180 mL, 360 mmol, 24 equiv). The resulting mixture was stirred for 4 h at 70 °C before being

quenched with sat. aq. K_2CO_3 (60 mL) and extracted with ethyl acetate (3x250 mL). Organic layers were combined, dried over $MgSO_4$, and the solvent removed under reduced pressure. Purification by column chromatography (hexane/acetone 70:30) afforded 2.49 g (11.4 mmol, 78%) of a complex mixture of triols **4.19/4.20** (*dr* 80:20), engaged in the next step.

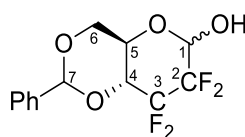
7.5.2.4 Ozonolysis of the triol mixture **4.19/4.20**

Following the same procedure as described in **7.5.1.5**, triol mixture **4.19/4.20** (2.32 g, 10.6 mmol) was converted into a mixture of tetrafluoro glucose and galactose **1.40/4.1** (2.25 g, 10.2 mmol, 96%), engaged in the next step.

7.5.2.5 Separation of tetrafluoro glucose (**1.40**) and galactose (**4.1**)

To a solution of mixture **1.40/4.1** (2.25 g, 10.2 mmol, 1 equiv) in benzaldehyde (18 mL) were added 3 Å activated molecular sieves and activated zinc chloride (1.39 g, 10.2 mmol, 1 equiv). The resulting mixture was stirred overnight at rt before being filtered and quenched with sat. aq. $NaHCO_3$ (20 mL). The layers were separated and the aqueous phase was extracted with ethyl acetate (3x50 mL). Organic layers were combined, dried over $MgSO_4$, and the solvent removed under reduced pressure. Purification by column chromatography (pentane/acetone 90:10 to 70:30) afforded 2.32 g (7.43 mmol, 72%) of pure 4,6-benzylidene tetrafluoro glucose **4.29** as a dense gel, and 0.80 g (2.59 mmol, 24%) of pure 4,6-benzylidene tetrafluoro galactose **4.30** as a white solid.

Data for 4,6-O-benzylidene-2,3-dideoxy-2,2,3,3-tetrafluoro-D-glucopyranose (4.29**):**

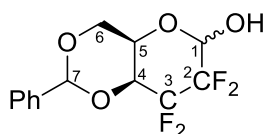


4.29

R_f 0.48 (pentane/acetone 80:20). $[\alpha]_D^{20} +20.8$ for α/β 1.00:0.99 (c 1.10, $CDCl_3$, 21 °C). IR (neat) 3347 (w, br.), 2943 (w), 2914 (w), 1063 (s), 991 (s) cm^{-1} . 1H NMR (500 MHz, $CDCl_3$) δ 5.84 (2H, s, $H_{7\alpha+\beta}$), 5.46 (1H, dd, J 8.0, 5.4 Hz, $H_{1\alpha}$), 5.22 (1H, br. dd, J 14.7, 2.1 Hz, $H_{1\beta}$), 4.46 - 4.32 (3H, m), 4.31 - 4.18 (2H, m), 3.99 - 3.91 (2H, m), 3.87 (1H, br. td, J 10.2, 4.7 Hz, $H_{5\beta}$) ppm. ^{13}C NMR (126 MHz, $CDCl_3$) δ 137.1 (1C, s, C_{Ar}), 137.0 (1C, s, C_{Ar}), 129.2 (1C, s, C_{Ar}), 129.2 (1C, s, C_{Ar}), 128.1 (2C, s, C_{Ar}), 128.1 (2C, s, C_{Ar}), 126.3 (2C, s, C_{Ar}), 126.3 (2C, s, C_{Ar}), 116.0- 109.4 (4C, m, CF_2), 101.6 (1C, s, C_7), 101.5 (1C, s, C_7), 92.4 (1C, dd, J 26.2, 20.5 Hz, $C_{1\beta}$), 92.4 (1C, dd, J 37.7, 26.2 Hz, $C_{1\alpha}$), 76.3 - 75.7 (2C, m, C_4), 67.9 (1C, s, $C_{6\alpha}$), 67.7 (1C, d, J 1.4 Hz, $C_{6\beta}$), 64.3 (1C, d, J 6.7 Hz, $C_{5\beta}$), 60.9 (1C, d, J 6.7 Hz, $C_{5\alpha}$) ppm. ^{19}F NMR (376 MHz, $CDCl_3$) δ -118.7 (1F, m, from which could be extracted J 272.2 Hz, F_α), -130.4 (1F, m, from which could be extracted J 253.2, 24.3, 15.6, 8.7 Hz, F_α), -132.2 (1F, m, from which could be

extracted J 254.9, 12.1, 10.4 Hz, F_β), -132.9 (1F, m, from which could be extracted J 251.4 Hz, F_α), -133.7 (1F, ddd, J 272.2, 15.6, 10.4 Hz, F_α), -134.8 (1F, m, from which could be extracted J 253.2 Hz, F_β), -136.3 (1F, ddd, J 261.8, 13.9, 8.7 Hz, F_β), -138.1 (1F, m, from which could be extracted J 261.8 Hz, F_β) ppm. **$^{19}\text{F}[^1\text{H}]$ NMR** (376 MHz, CDCl_3) δ -118.7 (1F, ddd, J 272.2, 17.3, 8.7 Hz, F_α), -130.4 (1F, ddd, J 251.4, 15.6, 8.7 Hz, F_α), -132.2 (1F, ddd, J 253.2, 13.9, 8.7 Hz, F_β), -132.9 (1F, ddd, J 251.4, 15.6, 8.7 Hz, F_α), -133.7 (1F, ddd, J 272.2, 15.6, 8.7 Hz, F_α), -134.8 (1F, ddd, J 254.9, 17.3, 8.7 Hz, F_β), -136.3 (1F, ddd, J 261.8, 15.6, 8.7 Hz, F_β), -138.1 (1F, ddd, J 261.8, 17.3, 10.4 Hz, F_β) ppm. **MS** (ESI+) (m/z) 309.3 $[\text{M}+\text{H}]^+$. **HRMS** (ESI+) for $\text{C}_{13}\text{H}_{13}\text{F}_4\text{O}_4$ $[\text{M}+\text{H}]^+$ Calcd. 309.0750, Found. 309.0746.

Data for 4,6-*O*-benzylidene-2,3-dideoxy-2,2,3,3-tetrafluoro-D-galactopyranose (4.30):



4.30

R_f 0.27 (pentane/acetone 80:20). **$[\alpha]_D$** +31.2 for α/β 0.93/1.00 (c 1.00, CHCl_3 , 24 °C). **IR** (neat) 3430 (w, br.), 2847 (w), 1683 (m), 1137 (s), 1100 (s) cm^{-1} . **^1H NMR** (500 MHz, CD_3OD) δ 7.53 - 7.45 (4H, m, H_{Ar}), 7.41 - 7.34 (6H, m, H_{Ar}), 5.67 (1H, s, $\text{H}_{7\alpha}$), 5.66 (1H, s, $\text{H}_{7\beta}$), 5.32 (1H, dd, J 8.7, 6.6 Hz, $\text{H}_{1\alpha}$), 5.00 (1H, m, from which could be extracted J 13.0, 3.5 Hz, $\text{H}_{1\beta}$), 4.59 - 4.50 (2H, m, H_4), 4.32 - 4.17 (5H, m, H_6 and $\text{H}_{5\alpha}$), 3.83 (1H, dq, J 3.0, 1.6 Hz, $\text{H}_{5\beta}$) ppm. **^{13}C NMR** (126 MHz, CD_3OD) δ 137.6 (1C, s, C_{Ar}), 137.5 (1C, s, C_{Ar}), 128.8 (1C, s, C_{Ar}), 128.8 (1C, s, C_{Ar}), 127.7 (2C, s, C_{Ar}), 127.7 (2C, s, C_{Ar}), 126.1 (2C, s, C_{Ar}), 126.1 (2C, s, C_{Ar}), 115.0 - 107.4 (4C, m, CF_2), 100.5 (1C, s, C_7), 100.5 (1C, s, C_7), 91.7 (1C, m, from which could be extracted J 36.7, 26.7 Hz, $\text{C}_{1\alpha}$), 91.4 (1C, ddd, J 26.2, 21.0, 3.8 Hz, $\text{C}_{1\beta}$), 74.8 (1C, ddd, J 36.7, 19.5, 2.4 Hz, C_4), 74.5 (1C, ddd, J 35.8, 19.1, 1.9 Hz, C_4), 68.3 (1C, d, J 1.0 Hz, $\text{C}_{6\alpha}$), 68.0 (1C, d, J 1.0 Hz, $\text{C}_{6\beta}$), 65.2 (1C, d, J 5.7 Hz, $\text{C}_{5\beta}$), 60.8 (1C, d, J 5.2 Hz, $\text{C}_{5\alpha}$) ppm. **^{19}F NMR** (471 MHz, CD_3OD) δ -119.7 (1F, m, from which could be extracted J 276.8, 15.7, 9.3 Hz, F_α), -120.9 (1F, ddt, J 266.6, 17.7, 9.1 Hz, F_α), -122.0 (1F, m, from which could be extracted J 277.5 Hz, F_β), -133.3 (1F, m, from which could be extracted J 276.8 Hz, F_α), -135.6 (1F, m, from which could be extracted J 278.2, 12.9 Hz, F_β), -137.1 (1F, dddd, J 266.8, 15.7, 10.7, 5.0 Hz, F_α), -139.5 (1F, m, from which could be extracted J 258.9, 14.3, 5.7 Hz, F_β), -140.3 (1F, m, from which could be extracted J 259.6, 10.7, 3.6 Hz, F_β) ppm. **$^{19}\text{F}[^1\text{H}]$ NMR** (471 MHz, CD_3OD) δ -119.7 (1F, ddd, J 276.8, 15.7, 8.6 Hz, F_α), -120.9 (1F, ddd, J 266.8, 17.2, 8.6 Hz, F_α), -122.0 (1F, ddd, J 277.7, 10.6, 5.0 Hz, F_β), -133.3 (1F, ddd, J 276.8, 17.2, 10.7 Hz, F_α), -135.6 (1F, ddd, J 277.5, 15.0, 11.4 Hz, F_β), -137.1 (1F, ddd, J 266.8, 15.7, 10.7 Hz, F_α), -139.5 (1F, ddd, J 258.9, 15.0, 5.0 Hz, F_β), -140.3 (1F, dt, J 258.9, 10.7 Hz, F_β) ppm. **HRMS** (ESI+) for $\text{C}_{13}\text{H}_{13}\text{F}_4\text{O}_4$ $[\text{M}+\text{H}]^+$, Calcd. 309.0750, Found. 309.0750; for $\text{C}_{13}\text{H}_{12}\text{F}_4\text{NaO}_4$ $[\text{M}+\text{Na}]^+$, Calcd. 331.0569, Found. 331.0570; for $\text{C}_{13}\text{H}_{12}\text{F}_4\text{KO}_4$ $[\text{M}+\text{K}]^+$, Calcd. 347.0309, Found. 347.0303.

7.5.2.6 Deprotection of 4,6-*O*-benzylidene-tetrafluoroglucose (4.29)

To a solution of 4,6-*O*-benzylidene-tetrafluoro glucose **4.29** (297 mg, 0.96 mmol, 1 equiv) in MeOH (30 mL) at 0 °C was added *p*-toluenesulfonic monohydrate (91 mg, 0.48 mmol, 0.5 equiv). The resulting mixture was stirred at rt for 3 h before being quenched with triethylamine (0.7 mL) and the solvent removed under vacuum. Purification by column chromatography (hexane/acetone 70:30 to 50:50) afforded 200 mg (0.91 mmol, 94%) of pure tetrafluoro glucose **1.40** as a dense gel. See **7.5.1.5** for full characterisation data.

Bibliography

- (1) Sears, P.; Wong, C.-H. *Angew. Chem. Int. Ed.* **1999**, *38*, 2300.
- (2) Wu, C.-Y.; Wong, C.-H. *Chem. Commun.* **2011**, *47*, 6201.
- (3) Werz, D. B.; Seeberger, P. H. *Chem. Eur. J.* **2005**, *11*, 3194.
- (4) Cuneo, M. J.; Changela, A.; Warren, J. J.; Beese, L. S.; Hellinga, H. W. *J. Mol. Biol.* **2006**, *362*, 259.
- (5) Quiocho, F. A. *Pure & Appl. Chem.* **1989**, *61*, 1293.
- (6) Davis, A. M.; Teague, S. J. *Angew. Chem. Int. Ed.* **1999**, *38*, 736.
- (7) Vyas, N.; Vyas, M.; Quiocho, F. *Science* **1988**, *242*, 1290.
- (8) Lemieux, R. U. *Acc. Chem. Res.* **1996**, *29*, 373.
- (9) Purser, S.; Moore, P. R.; Swallow, S.; Gouverneur, V. *Chem. Soc. Rev.* **2008**, *37*, 320.
- (10) Wang, J.; Sánchez-Roselló, M.; Aceña, J. L.; del Pozo, C.; Sorochinsky, A. E.; Fustero, S.; Soloshonok, V. A.; Liu, H. *Chem. Rev.* **2014**, *114*, 2432.
- (11) O'Hagan, D. *J. Fluorine Chem.* **2010**, *131*, 1071.
- (12) Gao, J.; Qiao, S.; Whitesides, G. M. *J. Med. Chem.* **1995**, *38*, 2292.
- (13) Mecinović, J.; Snyder, P. W.; Mirica, K. A.; Bai, S.; Mack, E. T.; Kwant, R. L.; Moustakas, D. T.; Héroux, A.; Whitesides, G. M. *J. Am. Chem. Soc.* **2011**, *133*, 14017.
- (14) Olsen, J. A.; Banner, D. W.; Seiler, P.; Obst Sander, U.; D'Arcy, A.; Stihle, M.; Müller, K.; Diederich, F. *Angew. Chem. Int. Ed.* **2003**, *42*, 2507.
- (15) Müller, K.; Faeh, C.; Diederich, F. *Science* **2007**, *317*, 1881.
- (16) Olsen, J.; Seiler, P.; Wagner, B.; Fischer, H.; Tschopp, T.; Obst-Sander, U.; Banner, D. W.; Kansy, M.; Müller, K.; Diederich, F. *Org. Biomol. Chem.* **2004**, *2*, 1339.
- (17) Olsen, J. A.; Banner, D. W.; Seiler, P.; Wagner, B.; Tschopp, T.; Obst-Sander, U.; Kansy, M.; Müller, K.; Diederich, F. *ChemBioChem* **2004**, *5*, 666.
- (18) Kim, H. W.; Rossi, P.; Shoemaker, R. K.; DiMagno, S. G. *J. Am. Chem. Soc.* **1998**, *120*, 9082.
- (19) Biffinger, J. C.; Kim, H. W.; DiMagno, S. G. *ChemBioChem* **2004**, *5*, 622.
- (20) Street, I. P.; Armstrong, C. R.; Withers, S. G. *Biochemistry* **1986**, *25*, 6021.
- (21) McCarter, J. D.; Adam, M. J.; Hartman, N. G.; Withers, S. G. *Biochem. J* **1994**, *301*, 343.
- (22) N'Go, I.; Golten, S.; Ardá, A.; Cañada, J.; Jiménez-Barbero, J.; Linclau, B.; Vincent, S. P. *Chem. Eur. J.* **2014**, *20*, 106.

- (23) Morgenthaler, M.; Schweizer, E.; Hoffmann-Röder, A.; Benini, F.; Martin, R. E.; Jaeschke, G.; Wagner, B.; Fischer, H.; Bendels, S.; Zimmerli, D.; Schneider, J.; Diederich, F.; Kansy, M.; Müller, K. *ChemMedChem* **2007**, *2*, 1100.
- (24) Mukherjee, L. H.; Grunwald, E. *J. Chem. Phys.* **1958**, *62*, 1311.
- (25) Graton, J.; Wang, Z.; Brossard, A.-M.; Gonçalves Monteiro, D.; Le Questel, J.-Y.; Linclau, B. *Angew. Chem. Int. Ed.* **2012**, *51*, 6176.
- (26) Kuhn, B.; Mohr, P.; Stahl, M. *J. Med. Chem.* **2010**, *53*, 2601.
- (27) Elangannan, A.; Gautam, R. D.; Roger, A. K.; Joanna, S.; Steve, S.; Ibon, A.; David, C. C.; Robert, H. C.; Joseph, J. D.; Pavel, H.; Henrik, G. K.; Anthony, C. L.; Benedetta, M.; David, J. N. *Pure Appl. Chem.* **2011**, *83*, 1619.
- (28) Arunan, E.; Desiraju Gautam, R.; Klein Roger, A.; Sadlej, J.; Scheiner, S.; Alkorta, I.; Clary David, C.; Crabtree Robert, H.; Dannenberg Joseph, J.; Hobza, P.; Kjaergaard Henrik, G.; Legon Anthony, C.; Mennucci, B.; Nesbitt David, J. In *Pure Appl. Chem.* 2011; Vol. 83, p 1637.
- (29) Dunitz, J. D.; Taylor, R. *Chem. Eur. J.* **1997**, *3*, 89.
- (30) Carosati, E.; Sciabola, S.; Cruciani, G. *J. Med. Chem.* **2004**, *47*, 5114.
- (31) Pier Alexandre Champagne, J. D., Jean-François Paquin *Synthesis* **2015**, 306.
- (32) Struble, M. D.; Kelly, C.; Siegler, M. A.; Lectka, T. *Angew. Chem. Int. Ed.* **2014**, *53*, 8924.
- (33) Linclau, B.; Peron, F.; Bogdan, E.; Wells, N.; Wang, Z.; Compain, G.; Fontenelle, C. Q.; Galland, N.; Le Questel, J.-Y.; Graton, J. *Chem. Eur. J.* **2015**, *21*, 17808.
- (34) Bernet, B.; Vasella, A. *Helv. Chim. Acta* **2007**, *90*, 1874.
- (35) Fraser, R. R.; Kaufman, M.; Morand, P.; Govil, G. *Can. J. Chem.* **1969**, *47*, 403.
- (36) Zapata, A.; Bernet, B.; Vasella, A. *Helv. Chim. Acta* **1996**, *79*, 1169.
- (37) Biamonte, M. A.; Vasella, A. *Helv. Chim. Acta* **1998**, *81*, 695.
- (38) Potts, J. R.; Hounslow, A. M.; Kuchel, P. W. *Biochem. J* **1990**, *266*, 925.
- (39) Potts, J. R.; Kuchel, P. W. *Biochem. J* **1992**, *281*, 753.
- (40) O'Connell, T. M.; Gabel, S. A.; London, R. E. *Biochemistry* **1994**, *33*, 10985.
- (41) Bresciani, S.; Lebl, T.; Slawin, A. M. Z.; O'Hagan, D. *Chem. Commun.* **2010**, *46*, 5434.
- (42) Percival, M. D.; Withers, S. G. *Biochemistry* **1992**, *31*, 498.
- (43) Mtashobya, L.; Quiquempoix, L.; Linclau, B. *J. Fluorine Chem.* **2015**, *171*, 92.

- (44) Karban, J.; Cisarova, I.; Strasak, T.; Stastna, L. C.; Sykora, J. *Org. Biomol. Chem.* **2012**, *10*, 394.
- (45) Rönöls, J.; Manner, S.; Siegbahn, A.; Ellervik, U.; Widmalm, G. *Org. Biomol. Chem.* **2013**, *11*, 5465.
- (46) Bresciani, S.; Slawin, A. M. Z.; O'Hagan, D. *J. Fluorine Chem.* **2009**, *130*, 537.
- (47) Boukerb, A.; Grée, D.; Laabassi, M.; Grée, R. *J. Fluorine Chem.* **1998**, *88*, 23.
- (48) Adinolfi, M.; Barone, G.; Guariniello, L.; Iadonisi, A. *Tetrahedron Lett.* **1999**, *40*, 8439.
- (49) Corr, M. J.; O'Hagan, D. *J. Fluorine Chem.* **2013**, *155*, 72.
- (50) Pacák, J.; Podešva, J.; Točík, Z.; Černý, M. *Collect. Czech. Chem. Commun.* **1972**, 2589.
- (51) Barford, A. D.; Foster, A. B.; Westwood, J. H.; Hall, L. D.; Johnson, R. N. *Carbohydr. Res.* **1971**, *19*, 49.
- (52) Rasmussen, T. S.; Jensen, H. H. *Org. Biomol. Chem.* **2010**, *8*, 433.
- (53) Sarda, P.; Escribano, F. C.; José Alves, R.; Olesker, A.; Lukacs, G. *J. Carbohydr. Chem.* **1989**, *8*, 115.
- (54) Horník, Š.; Červenková Šťastná, L.; Cuřínová, P.; Sýkora, J.; Káňová, K.; Hrstka, R.; Císařová, I.; Dračínský, M.; Karban, *Beilstein J. Org. Chem.* **2016**, *12*, 750.
- (55) Viuff, A. H.; Hansen, J. C.; Christiansen, A. B.; Jensen, H. H. *Synth. Commun.* **2012**, *43*, 1557.
- (56) Barford, A. D.; Foster, A. B.; Westwood, J. H.; Hall, L. D.; Johnson, R. N. *Carbohydr. Res.* **1971**, *19*, 49.
- (57) Beaulieu, F.; Beauregard, L.-P.; Courchesne, G.; Couturier, M.; LaFlamme, F.; L'Heureux, A. *Org. Lett.* **2009**, *11*, 5050.
- (58) Yin, J.; Zarkowsky, D. S.; Thomas, D. W.; Zhao, M. M.; Huffman, M. A. *Org. Lett.* **2004**, *6*, 1465.
- (59) Zhao, X.; Zhuang, W.; Fang, D.; Xue, X.; Zhou, J. *Synlett* **2009**, *2009*, 779.
- (60) Hunter, L.; Kirsch, P.; Slawin, A. M. Z.; O'Hagan, D. *Angew. Chem. Int. Ed.* **2009**, *48*, 5457.
- (61) Rubira, M.-J.; Jimeno, M.-L.; Balzarini, J.; Camarasa, M.-J.; Pérez-Pérez, M.-J. *Tetrahedron* **1998**, *54*, 8223.
- (62) Keddie, N. S.; Slawin, A. M. Z.; Lebl, T.; Philp, D.; O'Hagan, D. *Nat. Chem.* **2015**, *7*, 483.
- (63) Raffael, V.; Nils, T.; Daniel, Z.; Björn, W.; Holger, F.; A., K. N.; Manfred, K.; M., C. E.; Klaus, M. *ChemMedChem* **2016**, *11*, 2216.

- (64) Ng, S.; Sederholm, C. H. *The Journal of Chemical Physics* **1964**, *40*, 2090.
- (65) Hierso, J.-C. *Chem. Rev.* **2014**, *114*, 4838.
- (66) Quiquempoix, L.; Bogdan, E.; Wells, N.; Le Questel, J.-Y.; Graton, J.; Linclau, B. *Molecules* **2017**, *22*, 518.
- (67) Giuffredi, G. T.; Gouverneur, V.; Bernet, B. *Angew. Chem. Int. Ed.* **2013**, *52*, 10524.
- (68) Timofte, R. S.; Linclau, B. *Org. Lett.* **2008**, *10*, 3673.
- (69) Boydell, A. J.; Vinader, V.; Linclau, B. *Angew. Chem. Int. Ed.* **2004**, *43*, 5677.
- (70) Linclau, B.; Boydell, A. J.; Timofte, R. S.; Brown, K. J.; Vinader, V.; Weymouth-Wilson, A. C. *Org. Biomol. Chem.* **2009**, *7*, 803.
- (71) Golten, S.; Fontenelle, C. Q.; Timofte, R. S.; Bailac, L.; Light, M.; Sebban, M.; Oulyadi, H.; Linclau, B. *J. Org. Chem.* **2016**, *81*, 4434.
- (72) Wu, F.-H.; Huang, W.-Y. *J. Fluorine Chem.* **2001**, *110*, 59.
- (73) Jiang, Z.-X.; Qing, F.-L. *J. Org. Chem.* **2004**, *69*, 5486.
- (74) Gassman, P. G.; O'Reilly, N. J. *Tetrahedron Lett.* **1985**, *26*, 5243.
- (75) Gassman, P. G.; O'Reilly, N. J. *J. Org. Chem.* **1987**, *52*, 2481.
- (76) Konno, T.; Takano, S.; Takahashi, Y.; Konishi, H.; Tanaka, Y.; Ishihara, T. *Synthesis* **2011**, *2011*, 33.
- (77) Konno, T.; Hoshino, T.; Kida, T.; Takano, S.; Ishihara, T. *J. Fluorine Chem.* **2013**, *152*, 106.
- (78) Schmid, C. R.; Bryant, J. D. *Org. Synth.* **1995**, *72*.
- (79) Hertel, L. W.; Grossman, C. S.; Kroin, J. S. *Synth. Commun.* **1991**, *21*, 151.
- (80) Schmid, C. R.; Bradley, D. A. *Synthesis* **1992**, *1992*, 587.
- (81) Ley, S. V.; Woods, M.; Zanotti-Gerosa, A. *Synthesis* **1992**, *1992*, 52.
- (82) Ley, S. V.; Downham, R.; Edwards, P. J.; Innes, J. E.; Woods, M. *Contemp. Org. Synth.* **1995**, *2*, 365.
- (83) Jäger, V.; Wehner, V. *Angew. Chem. Int. Ed.* **1989**, *28*, 469.
- (84) Michel, P.; Ley, S. V. *Angew. Chem. Int. Ed.* **2002**, *41*, 3898.
- (85) Michel, P.; Ley, S. V. *Synthesis* **2003**, *2003*, 1598.
- (86) Bridgwood, K. L.; Tzschucke, C. C.; O'Brien, M.; Wittrock, S.; Goodman, J. M.; Davies, J. E.; Logan, A. W. J.; Hüttel, M. R. M.; Ley, S. V. *Org. Lett.* **2008**, *10*, 4537.
- (87) Fontenelle, C. Q.; Tizzard, G. J.; Linclau, B. *J. Fluorine Chem.* **2015**, *174*, 95.

- (88) Anh, N. T.; Eisenstein, O. *Tetrahedron Lett.* **1976**, *17*, 155.
- (89) Anh, N. T.; Springer Berlin Heidelberg: Berlin, Heidelberg, 1980, p 145.
- (90) Burgi, H. B.; Dunitz, J. D.; Shefter, E. *J. Am. Chem. Soc.* **1973**, *95*, 5065.
- (91) Burgi, H. B.; Dunitz, J. D.; Lehn, J. M.; Wipff, G. *Tetrahedron* **1974**, *30*, 1563.
- (92) Boyer, J.; Allenbach, Y.; Ariza, X.; Garcia, J.; Georges, Y.; Vicente, M. *Synlett* **2006**, *2006*, 1895.
- (93) Ariza, X.; Garcia, J.; Georges, Y.; Vicente, M. *Org. Lett.* **2006**, *8*, 4501.
- (94) Chen, L. S.; Chen, G. J.; Tamborski, C. *J. Organomet. Chem.* **1980**, *193*, 283.
- (95) Drakesmith, F. G.; Stewart, O. J.; Tarrant, P. *J. Org. Chem.* **1968**, *33*, 280.
- (96) Nadano, R.; Fuchibe, K.; Ikeda, M.; Takahashi, H.; Ichikawa, J. *Chem. Asian J.* **2010**, *5*, 1875.
- (97) Pierce, O. R.; McBee, E. T.; Judd, G. F. *J. Am. Chem. Soc.* **1954**, *76*, 474.
- (98) Beel, J. A.; Clark, H. C.; Whyman, D. *J. Chem. Soc (Resumed)* **1962**, 4423.
- (99) Usutani, H.; Tomida, Y.; Nagaki, A.; Okamoto, H.; Nokami, T.; Yoshida, J.-i. *J. Am. Chem. Soc.* **2007**, *129*, 3046.
- (100) Nagaki, A.; Yamada, S.; Doi, M.; Tomida, Y.; Takabayashi, N.; Yoshida, J.-i. *Green Chemistry* **2011**, *13*, 1110.
- (101) Nagaki, A.; Tokuoka, S.; Yoshida, J.-i. *Chem. Commun.* **2014**, *50*, 15079.
- (102) Nagaki, A.; Tokuoka, S.; Yamada, S.; Tomida, Y.; Oshiro, K.; Amii, H.; Yoshida, J.-i. *Org. Biomol. Chem.* **2011**, *9*, 7559.
- (103) Nagaki, A.; Tsuchihashi, Y.; Haraki, S.; Yoshida, J.-i. *Org. Biomol. Chem.* **2015**, *13*, 7140.
- (104) Yoshida, J.-i.; Nagaki, A.; Yamada, T. *Chem. Eur. J.* **2008**, *14*, 7450.
- (105) Yoshida, J.-i.; Takahashi, Y.; Nagaki, A. *Chem. Commun.* **2013**, *49*, 9896.
- (106) Yoshida, J.-i.; Nagaki, A.; Yamada, D. *Drug Discovery Today: Technologies* **2013**, *10*, e53.
- (107) Fanelli, F.; Parisi, G.; Degennaro, L.; Luisi, R. *Beilstein J. Org. Chem.* **2017**, *13*, 520.
- (108) Nagaki, A.; Takahashi, Y.; Yamada, S.; Matsuo, C.; Haraki, S.; Moriwaki, Y.; Kim, S.; Yoshida, J.-i. *J. Flow Chem.* **2012**, *2*, 70.
- (109) Nagaki, A.; Takabayashi, N.; Tomida, Y.; Yoshida, J.-i. *Beilstein Journal of Organic Chemistry* **2009**, *5*, 16.
- (110) Kim, H.; Yonekura, Y.; Yoshida, J. i. *Angew. Chem. Int. Ed.*, *0*.

- (111)Nagaki, A.; Tomida, Y.; Usutani, H.; Kim, H.; Takabayashi, N.; Nokami, T.; Okamoto, H.; Yoshida, J. i. *Chem. Asian J.* **2007**, *2*, 1513.
- (112)Moon, S.-Y.; Jung, S.-H.; Bin Kim, U.; Kim, W.-S. *RSC Advances* **2015**, *5*, 79385.
- (113)Newman, S. G.; Jensen, K. F. *Green Chemistry* **2013**, *15*, 1456.
- (114)Kim, H.; Min, K.-I.; Inoue, K.; Im, D. J.; Kim, D.-P.; Yoshida, J.-i. *Science* **2016**, *352*, 691.
- (115)Nagaki, A.; Imai, K.; Kim, H.; Yoshida, J.-i. *RSC Advances* **2011**, *1*, 758.
- (116)Hafner, A.; Meisenbach, M.; Sedelmeier, J. *Org. Lett.* **2016**, *18*, 3630.
- (117)Pacak, J. P., J.; Tocik, Z.; Cerny, M. *Collect. Czech. Chem. Commun.* **1972**, *37*, 2589.
- (118)Ronnols, J.; Manner, S.; Siegbahn, A.; Ellervik, U.; Widmalm, G. *Org. Biomol. Chem.* **2013**, *11*, 5465.
- (119)Van Rijsbergen, R.; Anteunis, M. J. O.; De Bruyn, A. *Carbohydr. Res.* **1982**, *105*, 269.
- (120)Hori, H.; Nishida, Y.; Ohru, H.; Meguro, H. *J. Org. Chem.* **1989**, *54*, 1346.
- (121)Wollwage, P. C.; Seib, P. A. *Carbohydr. Res.* **1969**, *10*, 589.
- (122)Černý, M.; Černý, I.; Trnka, T. *Carbohydr. Res.* **1978**, *67*, 33.
- (123)Krohn, K.; Gehle, D.; Flörke, U. *Eur. J. Org. Chem.* **2005**, *2005*, 2841.
- (124)J. Pacák, M. B., D. Stropová, M. Černý *Collect. Czech. Chem. Commun.* **1976**, *1977*, 120.
- (125)Grindley, T. B.; Reimer, G. J.; Kralovec, J.; Brown, R. G.; Anderson, M. *Can. J. Chem.* **1987**, *65*, 1065.
- (126)Elbert, T.; Černý, M.; Defaye, J. *Carbohydr. Res.* **1979**, *76*, 109.
- (127)Hesek, D.; Lee, M.; Zhang, W.; Noll, B. C.; Mobashery, S. *J. Am. Chem. Soc.* **2009**, *131*, 5187.
- (128)Carter, C. F.; Baxendale, I. R.; Pavey, J. B. J.; Ley, S. V. *Org. Biomol. Chem.* **2010**, *8*, 1588.